“Quantifying the effect of atmospheric pollution and meteorology on visibility and tropospheric chemistry”

Ajit Singh

A thesis submitted to the University of Birmingham for the degree of

Doctor of Philosophy

School of Geography, Earth and Environmental Sciences

University of Birmingham, Edgbaston, Birmingham

B15 2TT, United Kingdom

May 2017

Abstract

There are two distinct research foci within this thesis; the role of aerosol particle and trace gases on (*i*) visibility and (*ii*) tropospheric chemistry. This work investigates short and long term visibility, by exploring the combined influence of atmospheric aerosol and meteorology. Observations were fitted to a newly developed light extinction model to generate predictions of historic aerosol and gas scattering and absorbing properties, explaining long term visibility trends and their dependence on meteorological conditions. This model incorporates parameterizations of aerosol hygroscopicity, gas absorption and particle concentration, scattering, and absorption. Historical visibility data can therefore be used to assess trends in aerosol particle properties for time periods when observational data are scarce or non-existent.

Short term visibility variations caused by particulate matter from firework and bonfire emissions is presented. It is shown that a reduction in the atmospheric visibility nationwide is ~25%; which is a consequence of increased loading of atmospheric PM, and is found to be dependent upon relative humidity.

Within tropospheric chemistry, HONO is an important source of OH radicals, and daytime HONO sources are poorly constrained. This work explores the abundance of HONO during a solar eclipse as a natural short-term perturbation to atmospheric photochemistry. A chemical kinetic model is employed to predict the concentrations of HONO using different source scenarios. The study provides insights into the variation of HONO with meteorology, traffic emission and other sources.

Dedication

I dedicate this thesis to my guardian

Mr. Brij Nath Singh

and

my parents

Acknowledgments

I express my profound gratitude and indebtedness to my supervisors: Dr. Francis D. Pope and Professor William J. Bloss for their guidance and support during my PhD studies. They gave me genuine and numerous suggestions for improving the quality of my research. I am unable to express, in words the deep understanding shown by them during the entire period of my association with them.

I want to thank the University of Birmingham for supporting through the Elite Scholarship Scheme. I am also thankful to UK Met Office and Department for Environment, Food and Rural Affairs (DEFRA) for the provision of data used in this research. I want to thank Dr James Lee, Dr Leigh Crilley, Dr Lisa Whalley, Dr Sebastian Laufs and and Dr. Jörg Kleffmann for providing York and London measurements data, which are used in Chapter 6. However, Birmingham campaign was performed by me, where gas (O_3, NO_x and HONO) and particle species were measured using number of ground based instruments.

I would also like to acknowledge my colleagues: Dr Leigh Crilley, Dr Louisa Karmar, Dr Pallavi Pant, Dr Salim Alam, Nick Davidson, Dr Indrani Mahapatra and Marliyyah Mahmood, who have gone to great lengths in helping me in this undertaking. The knowledge I have gained and the help I have received during my time at university of Birmingham is much appreciated. No action of mine could repay their kindness. I would like to thank Gretchel Coldicott, Jamie Peart, and Richard for all help and support during my study. I am also thankful to whole staff of School for their help and support.

There were days when I buckled under the pressure, I faced while working on my thesis. There also were days when I felt lost and alone far away from my family.

However, I was fortunate enough to have found a group of friends who were a lot more than that. They became my family. I would like to express my greatest gratitude for my friends: Chandan Aggarwal, Mehul Patel, Tejas A Wagle, Sabah, Aditya Acharya and Manu Sasidharan. They are irreplaceable in every meaning of the word.

Finally, I thank to my family for their support and encouragement. I also thank the almighty God for showering blessing on me.

Declaration

The results and contents of this thesis are original and have not been submitted in part or full to any other university forward of any other degree or qualification. The work presented in this thesis is my own and I have written all of the chapters individually. Most of the materials in this thesis have been published or under process in following journals:

Singh, A., Bloss, W.J. and Pope, F.D., **2017**. 60 years of UK visibility measurements: impact of meteorology and atmospheric pollutants on visibility. *Atmospheric Chemistry and Physics*, 17(3): 2085-2101.

Singh, A., Bloss, W.J. and Pope, F.D., **2015**. Remember, remember the 5th of November; gunpowder, particles and smog. *Weather*, 70(11): 320-324.

Singh, A., Crilley R.L., Bloss, W.J. and Pope, F.D., Measurments of HONO during 2015 solar eclipse: Insight into potential sources and sinks. *Geophysical Reaserch Letters* (under process)

The work has also been presented at the following conferences, meetings and events:

1. Long-term visibility trends in the UK and India, *National Environmental Engineering Research Institute (NEERI), Government of India,* 3 Dec 2016- Invited talk

   Link:http://www.rsc.org/events/download/Document/a21ab3a2-2122-447e-8eaa-faa5de4f0e4c

2. Long-term visibility data in the UK-how does visibility vary with meteorological and pollutant parameters?, *European Geosciences Union,* 17-22 April 2016.

   Link: http://meetingorganizer.copernicus.org/EGU2016/EGU2016-874-3.pdf

3. 60 years of visibility data in the UK-how does visibility vary with meteorological and pollutant parameters?, *American Geophysical Union,* 14-18 Dec 2015.

   Link: https://agu.confex.com/agu/fm15/webprogram/Paper63394.html

4. Are aerosol particles a source of HONO in the atmosphere?, *Aerosol Society Conference,* Birmingham,12 Nov 2015.

   Link:https://aerosol-soc.com/abstracts/aerosol-particles-source-hono-atmosphere

5. Atmospheric photochemical pollution measurement during 2015 solar eclipse, *Royal Meteorological Society,* July 2015.

   Link:https://www.rmets.org/sites/default/files/event_documents/6/Master%20Abstract%20Book%20V3_0.pdf

6. Impact of changing PM concentration on UK visibility, *ACCENT Plus-2014, Urbino-Italy,* 22-29 June 2014.

7. Role of aerosol and metrological parameters in visibility change: A view from the United Kingdom, *Aerosol Society Conference, Birmingham,* 27 Dec 2014.

   Link: http://aerosol-soc.org.uk/files/AjitSingh.PodiumAbstract.AASC14.pdf

8. Long term visibility trends with effects of changing atmospheric particles and meteorological parameters over the UK, *ASCITES networking meeting,* York, 1-3 December 2014

Ajit Singh

May 2017

Supervisor's declaration

I declare that to my Knowledge, the work presented in this thesis has been performed and written by Ajit Singh. The results from chapter 3 and 4 have been published in journals mentioned above and results from chapter 5 are in preparation for publication. All publications have Ajit Singh as first author.

Dr. Francis D. Pope
(Lead supervisor)

Professor William J. Bloss
(Co-supervisor)

Table of Contents

List of Figures

List of Tables

Symbols and abbreviation used

Symbols

β_{ext}	Extinction coefficient
D_p	Particle diameter
km	Kilometer
m	Meter
λ	Wavelength
γ	Gamma
$\beta_{PM,sca}$	PM scattering coefficient
$\beta_{PM,abs}$	PM absorption coefficient
n	Refractive index
r	Correlation coefficient
T	Air temperature
w_d	Wind direction
w_s	Wind speed

Abbreviations

abs	Absorption
BADC	British Atmospheric Data Centre
BC	Black Carbon
CPF	Conditional Probability Function
DEFRA	Department for Environment Food & Rural Affairs
EROS	Elms Road Observing Station
GMT	Greenwich Mean Time
GFN	Guy Fawkes Night
HMSO	Her Majesty's Stationery Office
ICAO	International Civil Aviation Organization
MOR	Meteorological Optical Range
NAPAP	National Acid Precipitation Assessment Program
NSAS	National Smoke Abatement Society
ONS	Office for National Statistics
PM	Particulate Matter
$PM_{2.5}$	Particulate matter with diameter less than 2.5 μm
PM_{10}	Particulate matter with diameter less than 10 μm
PNS	Particle Number Concentration

PR	Present Weather
RAF	Royal Air Force
RH	Relative Humidity
RVP	Runway Visual Path
RVR	Runway Visual Range
sca	Scattering
src	Station Reference Code
SV	Standers Visibility
TSC	Total Surface Area
UK	United Kingdom
UKMO	United Kingdom Meteorological Office
USA	United States of America
VOCs	Volatile Organic Compounds
V	Visibility
VS	Visual Range
WHO	World Health Organization
WMO	World Meteorological Organization

Definitions of terms

Absorption coefficient – Parameter expressing the ability of PM to absorb radiation

Contrast threshold – Smallest difference that the eye can discern between two different stimuli

Extinction coefficient – Sum of the light scattering and absorption coefficient

Inverse distance weighting interpolation – A mathematical technique used to estimate the visibility at locations lying between two different measurement locations

Mass normalized absorption coefficient – Ratio of absorption coefficient to mass concentration of the absorbing material

Scattering coefficient – Parameter expressing the ability of PM to scatter radiation

*All these definitions are from Singh et al. (2015)

Refractive index – The ratio between the phase velocity of light in a vacuum and in a certain medium (Aas, 1996).

Chapter 1.0

Introduction

Some of the material in this chapter has been taken from following papers:

Singh, A., Bloss, W.J. and Pope, F.D., **2017**. 60 years of UK visibility measurements: impact of meteorology and atmospheric pollutants on visibility. *Atmospheric Chemistry and Physics*, 17(3): 2085-2101.

Singh, A., Bloss, W.J. and Pope, F.D., **2015**. Remember, remember the 5th of November; gunpowder, particles and smog. *Weather*, 70(11): 320-324.

Singh, A., Crilley R.L., Bloss, W.J. and Pope, F.D., Measurments of HONO during 2015 solar eclipse: Insight into potential sources and sinks. *Geophysical Reaserch Letters* (under process)

1.1 Chapter Overview

This chapter introduces the concept of atmospheric visibility and the aerosol-visibility-meteorology relationship. An in-depth description of visibility measurements and methods are provided here. An overview of the importance of visibility and its linkage with air quality is also presented. This chapter provides an introduction to aerosols; their significance, sources and influence with regard to visibility and also human health. The influences of meteorological factors such as relative humidity (RH), air temperature and both wind speed and direction are also introduced in this chapter. Influence of pollutants generated from anthropogenic activities such as fireworks and bonfires is explained in this chapter. This chapter also introduces the tropospheric chemistry of nitrous acid (HONO).

1.2 Air pollution in the troposphere

Air pollution introduces many harmful gases and particle species into the Earth's atmosphere and affects human life. The lower region of earth's atmosphere known as the "troposphere" contains the Earth's weather system and convective activities. The region of troposphere extends from the surface of the earth to approximately 12 kms, and this height varies depending upon different seasons and surface latitude. Within ~ 2 km height above the earth's surface, the "boundary layer" is the zone where strong horizontal and vertical mixing occurs (Beer et al., 2001). In the Earth's atmosphere, mixtures of trace gases, aerosol particles and volatile organic compounds (VOCs) exist, where they are involved in various atmospheric processes and influence the Earth's climate both directly (via scattering and

absorbing radiation) and indirectly (by serving as nuclei for cloud condensation) (Charlson and Schwartz, 1992). Human activity as well as natural processes can introduce both gases and particles into the atmosphere and lead to poor air quality. In the last two decades, most of the research has focused on understanding sources of air pollution and their impact on human health. However, our understanding of the impact of the air pollution on visibility is relatively limited, even though visibility is one of the most readily observable climate factors influenced by physical and chemical processes in the atmosphere.

Gas phase chemistry in the troposphere is very complex and includes several precursor gases as well as diverse formation mechanisms. Presence of aerosols can further facilitate reactions since the particle can act as catalytic binding sites for photochemical reactions (Bian and Zender, 2003). In addition, meteorological factors are also important and their effect on these atmospheric processes cannot be neglected. Past research has largely focused on quantifying the levels of gas phase and particle pollutants, but recent scientific and technical advances have allowed for specific analysis of individual gases such as nitrous acid (HONO). As a result, understanding sources and chemistry of HONO is one of the active research questions in the scientific community.

Research presented in this thesis aims to investigate the influences of atmospheric pollution and meteorology on visibility and tropospheric chemistry of HONO. In this study, visibility and HONO chemistry are quite distinct but related research topics. In the troposphere, visibility is an important atmospheric phenomenon and can be a good proxy for air quality. In particular, loss of viability is one of the most apparent impacts of air pollution (Dzubay et al., 1982; Singh et al., 2015). Generally, visibility

depends upon both particles and gaseous (like NO_2) pollutants including meteorological factors such as relative humidity (RH), air temperature and wind conditions. Particles and gases influence visibility via their light scattering and absorbing behaviour, while meteorological factors influence clear sky visibility indirectly, by changing the sources and sinks of particles including their microphysical and optical properties (Bäumer et al., 2008). In particular, RH can change the particles' properties via changes in water content and the sorption nature of particles, although RH depends upon atmospheric air temperature (Barreca, 2012). Over the last few decades, average global air temperature has increased, which has contributed to Earth's climate change. However, greenhouse gas emissions (e.g., NH_4, N_2 and CO_2), together with natural and anthropogenic influences on global air temperature and hence contributing changes in earth's climate system (Sottong John et al., 2015). Long term changes in weather events such as fog, hail, snow, and rainfall due to changes in climatic conditions cause visibility challenges and are also a major concern for the environment (Badri, 2016a; Sullare et al., 2013). In the last three decades, clear sky average visibility has globally reduced over the land, indicative of changes in aerosol loading, trace gases emissions and climatic conditions (Sullare et al., 2013).

As mentioned above, aerosols and trace gases interact in several ways within surface-atmosphere system which involves modifications in direct and indirect radiative budget (Tie et al., 2005). Although some trace gases are precursors of aerosols, they can also alter photolysis rates and act as sites for heterogeneous conversion of trace gases (Pozzoli et al., 2008). However, these interactions influence the tropospheric chemistry via significant impact on ozone (O_3), nitrogen

oxides (NO_x) and OH budgets (Tie et al., 2001; Tie et al., 2005). Changes in climate conditions such as air temperature and general circulation can have significant impact on aerosols and chemical oxidants such as O_3 and OH radical (Tie et al., 2005). In the troposphere, OH radicals are formed primarily from photolysis of ozone by ultraviolet light in the presence of water vapour, while secondly from photolysis of HONO; discussed in detail in Section 1.4. OH is the major oxidant in the troposphere and responsible for the formation of secondary species. In the troposphere, OH radical also acts as a sink for pollutants such as methane and large source of water vapour ($CH_4 + OH \rightarrow CH_3 + H_2O$) where the products of reactions can contribute to climate change. Thus both visibility and HONO chemistry are both closely linked within aerosol-gas interactions, metrological conditions and climate change.

Furthermore, HONO can be influence the measurements of NO_2 (and vice versa), in conventional chemiluminescent NO_x monitors, thus indirectly affecting the estimation of the effects of NO_2 on visibility (Kotchmar et al., 1996). The homogeneous self-reaction of HONO in the atmosphere is slow, but can lead to the formation of additional NO_2, NO and H_2O (Stutz et al., 2002). It is important therefore to accurately measure HONO in order to calculate any possible interference in NO_x measurements in order to calculate the influence on visibility accurately.

1.3 Visibility characteristics and the influences of air pollution and meteorology

1.3.1 Concept of visibility

Poor visibility is an important air quality problem that has drawn the attention of the scientific community and public for a long time. In general, the maximum visible distance along a horizontal line at the Earth's surface is called visibility (V). The meteorological definition of visibility is the "*distance at which the contrast of a given object with respect to its background is just equal to the contrast threshold of an observer*" (WMO, 1992; WMO, 2015). According to Roach (1994), light scattering by particles and air molecules changes the contrast between object and viewer and thus dictates the visibility.

In meteorology, visibility can be represented as Meteorological Optical Range (MOR), where optical range is the maximum visual distance for an observer. A different contrast threshold of 5% is used for MOR measurement in meteorology to reduce the observer psychological and stress effects (Weitkamp, 2006). Usually MOR is used in meteorology and aviation industry mainly during flight take-off and landing. However, measuring methods vary depending upon applications. In the aviation industries, visibility is also represented as Runway Visual Range or Runway Visual Path (RVR or RVP), which can be defined as "*horizontal distance a pilot can see down the runway*" (Prentice, 2010). In the aviation industry, vertical visibility is also used and according to WMO (2008), it is defined as "*the maximum distance at which an observer can see and identify an object on the same vertical as him/her, above or below*". However, it is not as important for landing operations (Gaumet et al., 1998). These definitions (MOR, RVR and vertical visibility) are included for completeness and do not appear further in the text.

Mathematically, horizontal visibility can be represented as a function of the extinction coefficient (β_{ext}) via Equation 1.1, where the constant K is equal to 3.912, which assumes a visibility contrast threshold of 2% (Koschmieder, 1924).

$$V = \mathrm{K}/\beta_{\mathrm{ext}} \tag{1.1}$$

The extinction coefficient is dependent upon both the scattering (sca) and absorption (abs) due to particulate matter (PM) and gases ($\beta_{ext} = \beta_{gas,sca} + \beta_{gas,abs} + \beta_{PM,sca} + \beta_{PM,abs}$). Typically the contribution of PM to the extinction coefficient far outweighs the contribution of gases. Nitrogen dioxide (NO_2) is the only gas with a significant visible absorption coefficient (Groblicki et al., 1981) and may be present with appreciable abundance in urban areas. For PM with a given size distribution and composition, the extinction coefficient is linearly dependent upon the PM number concentration, hence, visibility can be used as a metric of atmospheric pollutant levels.

Horizontal visibility can be measured either manually by eye or automatically using light sensitive instruments (e.g., visiometer sensors). Before the 1990s the traditional method for visibility measurement was manually by eye; however visibility sensors were adopted later in the 1990s for purposeful, accurate measurements and to save labour. These visibility instruments measure the scattering and absorption of visible light to calculate the extinction coefficient and thus visibility (Bennett, 2012). Manual visibility measurements are imprecise by nature since results can vary according to the contrast and illuminance thresholds (ability to discern and sensitivity to light, respectively) of the observer's eyes (WMO, 2008).

Therefore, automated measurements are more objective and reproducible. Automated visibility measuring instruments are composed of a transmitter and receiver, with a local display unit (Jebson, 2008). The automatic sensor calculates the extinction coefficient generated by the transmitter using a light scattering method and thus visibility. More details, including the limitations of the instruments, are given in Chapter 3, section 3.4.1.

Another way of measuring horizontal visibility is using digital photography. The method is based on the determination of the contrast (*C*) between a dark target and background (Horvath, 1996; Janeiro et al., 2007). According to Janeiro et al. (2007), contrast "*C*" between target and background can be expressed as:

$$C = \frac{I_B - I_X}{I_B} \tag{1.2}$$

Where, I_B and I_X are intensities of background and target respectively. Due to light scattering and absorption effects, the change in intensity can be represented by the Beer-Lambert Law (Seinfeld and Pandis, 1998):

$$C = C_0 \exp(-\beta_{ext} X) \tag{1.3}$$

Where C_0 is a calibrating constant due to scattering and absorption effects and depends upon the medium, condition and type of target and background and "*X*" is the distance between observer and selected target (Janeiro et al., 2007). Measured extinction coefficient (β_{ext}) from Equation 1.3 can be applied in Equation 1.1 to calculate the visibility. The contrast threshold may vary from 1 % to 20 % depending

upon light conditions (Middleton, 1957). The benefit of a digital photography method is that during measurements, multiple targets can be set to obtain visibility (Janeiro et al., 2007). Factors such as the colour of an object and day and night conditions can also affect visibility measurements.

Visibility is generally measured in units of distance, e.g. miles, kilometers, meters or decameters depending upon method and instrument. Typically in a cloud free sky, visibility can vary from ca. 5 - 100 kilometres depending on atmospheric composition and conditions. Visibility is reduced by the interaction of light with atmospheric gases and aerosol particles which can absorb or scatter the light (Equation 1.1); consequently, visibility is greatest within non-polluted pristine atmospheres, other factors (e.g., meteorology) being equal. Reduced visibility is attributed mainly to high concentrations of aerosol particles, and in general, scattering effects are the dominant visibility reducing mechanism within the atmosphere. For example, during the 1952 London smog event, visibility declined to a few metres due to high air pollution (caused by a rise in smoke and other pollutant concentrations in the atmosphere (Wilkins, 1954)) as discussed in detail by Brimblecombe (1987). More recently, a study by Sati and Mohan (2014) also found sharp decreases in visibility due to increased particulate matter (PM) and NO_2 concentrations during a smog event in Delhi in November 2012. Similarly, Zhang et al. (2006) described the influence of PM upon visibility reduction in Beijing, China. Other natural phenomena (such as fog, mist, haze, snow, cloud, and rain, etc.) and anthropogenic activities (fireworks, bonfires, and crop fires, etc.) under specific weather conditions also contribute in visibility degradation.

According to Vautard et al. (2009), atmospheric factors like fog (V ≤ 1 km), mist (V ≤ 2 km) and haze (V ≤ 5 km) can be defined by local visibility (V) range. However, specific humidity conditions are required for fog (nearly 100% RH), mist (95 % ≤ RH < 100 %) and haze (RH < 95 %) (UKMO, 1994). In general, under high humidity conditions, a high particle loading in the lower atmosphere can increase fog formation and thus severely reduce visibility (Tiwari et al., 2011). Fog contains water droplets suspended in the air in the size range of ~10 to 50 microns (Day, 2005) along with pollutants like dust, smoke particles, sodium chloride and ammonium sulphate etc. (Roach, 1994). Usually visibility drops to below 1000 meters in normal fog conditions, however, under high RH and a polluted atmosphere, visibility can drop below 100 meters. In general, mist contains microscopic sized droplets of ~10 micron with particle range in ~50 to 500 microns in size (Day, 2005). In the lower atmosphere, smog can be defined as the effect of air pollution on visibility (Hyslop, 2009). In a polluted environment, smog is generated from a mixture of fog and smoke (Middleton et al., 1950). Usually, smog is a more critical phenomenon compared to fog, since it directly affects atmospheric visibility (i.e., loss of visibility) as well as human health. For example, during the 1952 London smog event, visibility was reduced to 10 meters and many people died due to exposure to the smog (Laskin, 2006).

Photochemical smog differs from regular smog events. Photochemical smog is not directly formed from primary pollutants; rather it is produced from chemical reactions among these primary pollutants in the presence of high ultraviolet radiation (Tiao et al., 1975). Such smog can be even more hazardous to the environment and human health due to high concentrations of ozone (O_3) and photochemical oxidants; for

example Los Angeles type photochemical smog (Finlayson-Pitts and Pitts, 1997). Photochemical smog events result in atmospheric visibility reduction due to increases in airborne particle (such as secondary organics and nitrates) concentrations in the atmosphere (White and Roberts, 1977; White, 1976).

1.3.2 Importance of visibility

Poor visibility (<2.0 km, (Founda et al., 2016)) can affect the transportation of goods and people, whether it is by rail, road, sea or air. Low visibility can lead to accidents and thus is a concern for public safety (Singh et al., 2017). Tourism is often dependent on good visibility for appreciation of the tourist attractions (Singh and Dey, 2012), For example, an Office for National Statistics (ONS) report from 2014, states that in 2013 the tourism industry in the UK earned £56 billion from foreigner visitors (ONS, 2014), which is also mentioned in the House of Commons Library 2016 report (Rhodes, 2016). It is very clear that tourism in the UK contributes greatly to the country's economy and cannot be neglected. Poor visibility can negatively influence the experiences of visitors and thus impact the tourism industry. For example; a study at Grand Canyon Park in United States of America (USA) has shown that visitor frequency in the park had reduced as visibility decreased (NAPAP, 1990). As mentioned above, visibility can disturb transportation, in particular rail and road, and air flights. Every year millions of pounds are lost in cancelation of flights, trains and through accidents due to poor weather and visibility. A study in the USA reported doubling of traffic/road accidents due to visibility related problems from natural hazards; such as floods, hurricanes, tornadoes, etc. during 1982 to 1991 (Clark et al., 2008; Rosenfeld, 1996). In various parts of the USA, fog

related visibility problems are a big issue, with over 700 deaths in a year due associated specifically with visibility related road accidents (Whiffen et al., 2004). It has also been found that in European countries, such as France, the annual death percentage due to accidents that occur as a result of poor visibility (less than 400 meters) is approximately same as North America (Hautière et al., 2013). Particularly, the combined presence of fog and smoke on the motorways are of significant concern. For example 8 people died and 40 people were injured due to very low visibility on the A10 motorway near Coulomiers, France in 2012 (Hautière et al., 2013). In 2006, London-Heathrow airport was completely closed due to heavy fog related visibility problems (Hautière et al., 2013). The incident occurred during the Christmas holidays and resulted in huge economic loss due to the shutdown of the airport and cancelation of fights. In 1974 approximately £120 million (at 2010 prices) loss occurred in the UK economic due to poor visibility impact. This loss included costs associated with police, medical, insurance property damage, etc. (Perry and Symons, 1991). Visibility conditions can get worse during smog events, which occur with high humidity in the presence of fog. In those conditions the chances of an accident are increased and can result in human death and economic loss. Poor visibility is not only a problem for drivers, but also affects the pedestrian's ability to judge the vehicle speed and distance (Badri, 2016b; Siddiqui et al., 2006). A road study by WHO found that one third of pedestrian road traffic accidents happen as a result of poor visibility (WHO, 2004). To reduce loss in terms of human life, economic loss and transportation inconvenience due to degradation in visibility, accurate visibility and hence pollutant predictions are needed.

1.3.3 Effects of atmospheric aerosols on air quality including associated human impacts

Air quality can have an important role in human life by affecting their health and local weather. Air quality is primarily influenced by particles and gases, generated through traffic emission, power plants, factories, forest-fires, bio-mass burning, vegetation, cooking, etc. In general, shape, size, concentration, and composition of aerosols and gases directly influence the atmospheric air quality. Any particle or trace gas sources in the earth's atmosphere that can affect the air quality are termed air pollutants. The source of air pollutants can be natural or anthropogenic; however, both can have an impact on the atmosphere. Natural sources of pollutants include dust, soil, sea spray, volcanic eruption, forest fires, biological activities, and bio-aerosols such as pollen and fungal spores. On the other hand, anthropogenic sources include fossil fuel combustion, power plants, transport and industries, cooking, agriculture, construction, biomass burning, fireworks, etc. Both natural and anthropogenic pollutants can also be generated from chemical processes via interaction between gas-to-gas and gas-to-particle, gas-to-liquid or a combination of all. In general, two types of particles (primary and secondary) exist in the environment. Primary particles are emitted directly into the atmosphere as solids or liquids by the process of biomass burning, volcanic eruptions, traffic related suspension on road, soil, mineral dust, sea salt, biological activities etc., while secondary particles are generated from gas-to-particle conversion by nucleation and condensation of gaseous species (Pöschl, 2005). Particles can be categorize into three modes based on their size distribution: nucleation mode (0.001 > 0.1 μm size), accumulation mode (0.1 > 2.5 μm size), and coarse mode (2.5 > 100 μm size). Nucleation mode particles are mainly generated from condensation and coagulation

of vapour during combustion, while coarse mode particles originate from natural and anthropogenic mechanical process (Morawska et al., 1999). Once the particle is formed in the atmosphere from these various processes they are removed through precipitation or wet deposition (Koch et al., 2007) or dry deposition (Haywood and Boucher, 2000) within a few days (average lifetime ca. 7 days) depending upon particle type.

In the past few years, developing countries, mainly from the Asian continent, are facing poor air quality problems. The rising migration from rural areas to urban cities and industrialization are dominant factors in changing air quality at these countries. Climate change is also influencing air quality in these countries via changing weather conditions. In Asia, China and India are the fastest growing countries in terms of the economy and development. Pollution levels along with degradation in visibility have increased in these areas (Chan and Yao, 2008). Concentrations of pollutants in megacities of these developing countries are very high and regularly exceed air quality standards (WHO, 2016). Particularly, cities in northern India are facing poor air quality, where annual concentrations of $PM_{2.5}$ and PM_{10} are greater than the Indian National Ambient Air Quality Standards (40 μgm^{-3} and 60 μgm^{-3} respectively) (Tiwari et al., 2009). Similarly, annual concentrations of $PM_{2.5}$ and PM_{10} in major Chinese cities like Beijing and Shanghai are about 10 fold and 6 fold respectively higher than World Health Organization Air Quality Standards (10 μgm^{-3} and 20 μgm^{-3} respectively) (He et al., 2001; Ye et al., 2003). Developed countries such as those in western Europe have also endured major long term air pollution problems (Brunekreef and Holgate, 2002).

As introduced in section 1.3.1, particles emitted from various natural and anthropogenic sources can influence the atmospheric visibility by their light scattering and absorbing nature (Appel et al., 1985), where ability of PM to scatter and absorb light is dependent upon the size and composition (refractive index) of the particles. Absorption, to a first order approximation, increases with increasing PM volume. The amount of scattering for a given PM ensemble is much more finely tuned to the given particle size and composition distribution. In general, the closer the PM size matches with the wavelength of the light, the greater the scattering (Mie, 1908).

In addition to their impact on visibility, atmospheric aerosols can also affect the earth's energy balance through modification in the global radiation budget via radiative forcing (RF) (Han et al., 2012; Penner et al., 2004; Stier et al., 2007; Xiaoye, 2007). Radiative forcing has been defined by Myhre et al. (2013) as "*The change in net downward radiative flux at the tropopause after allowing for stratospheric temperatures to readjust to radiative equilibrium, while holding surface and tropospheric temperatures and state variables such as water vapour and cloud cover fixed at the unperturbed values*". The aerosol radiative forcing (ARF) can be defined as *"the differences between radiative fluxes with aerosol and those without aerosols"* (Satheesh and Srinivasan, 2006). Generally, ARF is classified as direct radiative forcing (DRF) and indirect radiative forcing (IRF), where DRF involves scattering and absorbing the solar radiations by aerosols in the cloud free sky, (Pope et al., 2010; Satheesh and Srinivasan, 2006; Stier et al., 2007) while indirect radiative forcing (IRF) can change the microphysical and cloud properties via aerosol-cloud interaction (Haywood and Boucher, 2000).

Aerosol particles also affect human health, and both indoor and outdoor sources of air pollution have been reported to contribute to specific health outcomes. Indoor air pollutants (mainly fine particles and biological particles) usually come from cooking, tobacco smoke, air conditioning system, printer machines, construction etc. In general, people in developed countries spend >90% of their time in indoor environments, whether it could be home, office, shop, schools etc. (Jones, 1999; Li et al., 2007; Roberts and Dickey, 1995). Outdoor air pollution sources are vehicles, power plants, forest fires, construction, factories, bio-aerosol activities, etc. The major effects of PM exposure from indoor and outdoor air pollution include cardiopulmonary diseases, respiratory illnesses and eye and skin allergies. Pollutants such as SO_x (sulphur oxides), NO_x (nitrogen oxides), surface O_3, VOCs, metals and PM contribute to morbidity and mortality (Holgate et al., 1999; Kampa and Castanas, 2008; Künzli et al., 2000) via impact on human cardiovascular and respiratory system (Dominici et al., 2006).

The concentration and size of emitted particles mainly depend upon the type of engine and fuel used for power consumption. In general, the size range of emitted particles can vary from sub-micrometre to micrometre and are composed of various organic and inorganic species (Ramanathan et al., 2001). Particles with very small sizes such as ultrafine particles (diameter < 100 nm) have a greater potential influence on human health (Kumar et al., 2014). In the environment, ultrafine particles are complex and largely insoluble (Donaldson et al., 2001). Typically, airborne ultrafine particles are very small and have a large surface area and high toxic hydrocarbon content (Nel, 2005) with very high potential for lung deposition (HEI, 2013; Kumar et al., 2014).

Further details of aerosol particles and air quality are presented in chapter 2.

1.3.4 Influence of meteorology

Meteorology plays a key role in the atmospheric and climatological studies via changes in global or local environment. Visibility is mainly influenced by aerosols and gases; however, meteorological components such as wind speed, wind direction, RH, rain, hail, snow, fog, solar radiation, cloud cover and air temperature can also have direct or indirect impacts on visibility. These meteorological components can have either long-term or short-term effects on weather condition and thus visibility. High RH with high aerosol loading, in particular can have an adverse impact on visibility (Sloane, 1983). Under specific meteorological conditions, high particle loads in the lower atmosphere can increase fog formation and thus reduce visibility (Tiwari et al., 2011). It must also be noted that mean monthly humidity shows a strong influence on visibility (Singh and Dey, 2012). A recent study had shown that hygroscopic growth of aerosol particles at high RH are able to change overall visibility (Liu et al., 2012). Thus, both aerosol loading and meteorological factors such as RH are important for the assessment of visibility. Further discussion of these interactions is documented in Chapter 2 (section 2.2.3). In addition, parameters such as wind speed and wind direction are also able to change the pollution level and thus visibility depends upon the emission sources in the surrounding area. Various studies have shown a connection between meteorology and air pollution and climate change (Arya, 1999; Comrie, 1990; Davis, 1991; Eder et al., 1994; Seinfeld et al., 1998). However, a limited number of studies in the literature have focused on the meteorology-visibility relationship (Dayan and

Levy, 2005; Doyle and Dorling, 2002; Sequeira and Lai, 1998). These relationships are described further in Chapter 2 (section 2.2.4).

1.3.5 Short-term effects of air pollution generated from fireworks

Over the past few years the concern for the effects of both long term and short term air pollution has increased (Cesaroni et al., 2014; Pope III and Dockery, 2006; Singh et al., 2015; Singh et al., 2017; Vecchi et al., 2008; Wang et al., 2014). Fireworks and bonfires are one possible source of pollutants in the atmosphere and typically influence short term air quality. Festivals and other celebrations involving fireworks, which release aerosol particles upon detonation, are a good example of how spatially and temporally localised pollution events can lead to reduced visibility (Kong et al., 2015; Seidel and Birnbaum, 2015; Singh et al., 2015). Fireworks are often used to celebrate festivals and special days, for example, Bastille Day in France, Independence Day in USA, New Year's Eve on a worldwide level, Diwali in India, Chinese New Year in China and large sporting events. Within the UK, the biggest fireworks event is Guy Fawkes Night (GFN) which is celebrated around the 5 November every year. It commemorates the events of that day in the year 1605 when the Gunpowder Plot, involving the eponymous Mr Fawkes, failed to blow up the Houses of Parliament. Typically the celebrations involve both bonfires and fireworks (ground and air detonating). Fireworks and bonfires have tremendous and enduring appeal, however, some of their effects are not always beneficial. Incorrect handling and use of fireworks can lead to injury (Vernon, 1988) and allergy (Becker et al., 2000), which can be deadly sometimes. They can also be distracting through various human senses (sight, sound and smell). In the UK, a number of incidents

have been recorded around the Guy Fawkes Night celebrations. For example; In 2005, approximately a thousand injuries were recorded in the UK due to use of fireworks during October and November, in the occasion of Guy Fawkes Night celebrations (DTI, 2005; Flynn, 2008; Galea and Powles, 2010). Similarly, Knox et al. (2008) observed that in the UK, between 2004 to 2006 approximately 81% fireworks injuries occurred during October and November. Careless handlings of fireworks during storage also have serious concern. In a major incident, 22 people died and approximately 1000 injured due to an explosion at a fireworks storage site in the Netherlands in 2000 (Soeteman, 2009). Similarly, in December 2006 two people died after an explosion in a fireworks store at Lewes, UK (Cathcart et al., 2007). For public safety, the UK government has legislation surrounding the purchase and use of fireworks during the celebration period which limits the dates on which fireworks displays can occur. Under the UK "Fireworks Act 2003", British Standards Regulations are made for their control and handling, where additional Standards Regulations were introduced in 2004 under "Fireworks Regulations 2004" (HMSO, 2004). Under Regulation 7, at any occasion the use of fireworks are restricted between 11:00 pm GMT to 07:00 am GMT, except for a few special events such as Guy Fawkes Night, New year's Eve, Diwali and Chinese New Year (HMSO, 2004). For these special events fireworks are permitted until 01:00 pm GMT for New year's Eve, Diwali and Chinese New Year, and 12:00 am GMT for Guy Fawkes Night (HMSO, 2004). However, purchase and use of fireworks are highly restricted for a person below the age of 18 under Regulation 4, Fireworks Act 2003 (HMSO, 2004). Usually, fireworks can be divided into four specific categories by their use; such as (1) Indoor fireworks, (2) Garden fireworks, (3) Display fireworks, and (4) Professional fireworks only for trained people (Galea and Powles,

2010; HMSO, 1997; HMSO, 2004). Normally, UK imports all kinds of fireworks mainly from Asian countries, where the UK has set safety standards for its import (British Standard 7114) under the Fireworks Act 2003, Regulation 3 (Galea and Powles, 2010). In the UK, fireworks can be bought from any licenced shop at any time of the year, while during Guy Fawkes Night, New Year's Eve, Diwali and Chinese New Year they can be bought from any registered seller (HMSO, 2004). Any illegal fireworks activities can result in a fine and jail according to the "Fireworks Act 2003".

Fireworks can generate dense clouds of smoke in the lower atmosphere (Drewnick et al., 2006) and are sources of pollution including gas phase species (e.g. sulphur dioxide, ozone, etc.) and particulate species including black carbon and metals (Ravindra et al., 2003; Seidel and Birnbaum, 2015), some of which have negative health effects (Ravindra et al., 2001). In particular, one of the key impacts of fireworks is visibility loss due to formation of PM and other polluting components in the environment (Shi et al., 2011; Singh et al., 2015). Other meteorological parameters such as RH and temperature can contribute to visibility change during fireworks and bonfire events via changes in PM properties. The effect of RH on visibility from an air parcel moving from a fire could be higher than under normal conditions. In particular, surrounding RH is likely to increase fast under the conditions of fireworks and bonfires and thus contributes to sudden changes in physical characteristics of particles and influences visibility. Temperature variation with presence of moisture content in wood directly ties to the RH (Simpson, 2007; Vidal Bastías and Cloutier, 2005), which affects behaviour of particle emissions during bonfires. In general, wood burning emits various harmful pollutants such as

CO, CH_4, SO_x, NO_x and fine particles (Dasch, 1982; McDonald et al., 2000; Paulrud and Nilsson, 2004). These pollutants contains highly toxic organic compounds (Gaeggeler et al., 2008). However, during a fire, the type of wood and moisture condition may completely change the emitted particle type and concentrations in the atmosphere (Dasch, 1982). Therefore, meteorology, in particular RH and temperature cannot be neglected for visibility analysis during fireworks and bonfire.

1.4 Tropospheric chemistry and the role of nitrous acid (HONO)

1.4.1 Introduction of HONO in the troposphere

In the troposphere, trace gases such as ozone (O_3) and nitrogen oxides ($NO_x = NO_2 + NO$) play a key role in the tropospheric chemistry by controlling the chemical composition in the troposphere (Logan, 1985; Zhang et al., 2003). In a polluted atmosphere, high concentrations of NO_x and surface O_3 operate synergistically to build a complex air pollution event. In the troposphere, ozone is produced by photochemical oxidation through formation of hydroxyl radical (OH) (Lelieveld and Dentener, 2000). OH radical is the detergent of the atmosphere, and is responsible for removal of various natural and anthropogenic gases. In particular, OH radical is the dominant oxidant in troposphere and drives the formation of secondary species like peroxyacetyl nitrate (PAN) and secondary organic aerosols alongside O_3 (LaFranchi et al., 2009; Ren et al., 2010). In general, chemistry of surface O_3 can be explained through the following sketch diagram:

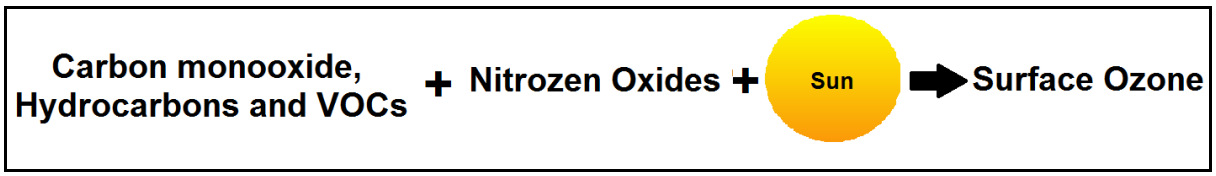

Moreover, the reaction cycle of surface ozone can be represented as (Lal et al., 2000):

$$CO + OH \longrightarrow CO_2 + H \quad \text{(R1.1)}$$

$$H + O_2 + M \longrightarrow HO_2 + M \quad \text{(R1.2)}$$

$$HO_2 + NO \longrightarrow NO_2 + OH \quad \text{(R1.3)}$$

$$NO_2 + h\nu \longrightarrow NO + O \quad \text{(R1.4)}$$

$$O_2 + O \longrightarrow O_3 \quad \text{(R1.5)}$$

However, NO_x controls the oxidation and biogeochemical reactions linked with OH radical (Navarro-González et al., 2001; Zhang et al., 2003). To understand the oxidative processes in the troposphere, identification and observation of OH radical source is critically important (Villena et al., 2011a). In the troposphere, HONO is one of the key sources of the OH radical via Reaction 1.6 (Kleffmann, 2007; Spataro and Ianniello, 2014), where it contributes in chemistry of nitrogen oxides and hydrogen oxides cycle (Finlayson-Pitts and Pitts Jr, 2000). In the urban environment, HONO contributes up to 80% of daytime OH production in winter and 50% in summer (Elshorbany et al., 2009; Kleffmann, 2007). However, the contribution of HONO to OH production changes by altitude (Spataro and Ianniello, 2014), while HONO contribution to HO_x production is more relevant to near surfaces (Rappenglück et al., 2014).

$$HONO + h\nu\ (\lambda < 440\ nm) \longrightarrow NO + OH \quad \text{(R1.6)}$$

1.4.2 Sources of HONO in the troposphere

In the troposphere, sources of HONO are either chemical formation or direct emissions (Kleffmann, 2007; Spataro and Ianniello, 2014). HONO is formed in the gas phase, through reaction of OH and NO (Reaction 1.7), where M is any third body (Calvert et al., 1994; Lee et al., 2016). It can also be formed via heterogeneous chemistry through reaction of NO_2 on wet surfaces (Baergen et al., 2015; Gherman et al., 2007) via Reaction 1.8.

$$OH + NO + M \longrightarrow HONO + M \qquad (R1.7)$$

$$2NO_2 + H_2O \longrightarrow HONO + HNO_3 \qquad (R1.8)$$

NO_2, typically generated from anthropogenic activities such as vehicular emission, power plants, and domestic cooking etc., plays a key role in the troposphere due to highly reactivity and contribution in HONO chemistry.

The other possible source of HONO can be direct emission. Direct emissions of HONO generally come from traffic via vehicular exhaust (Kurtenbach et al., 2001; Rappenglück et al., 2013), biomass burning (Roberts et al., 2010; Yokelson et al., 2009) and microbial activities of soil surface (Oswald et al., 2013; Su et al., 2011).

In general, a possible HONO cycle and its chemistry are shown in Figure 1.1, where heterogeneous, gas phase and direct emission processes are illustrated. However, the sources of HONO and formation processes are still not completely understood (Brumby et al., 2016; Kleffmann et al., 2006; Kurtenbach et al., 2001), which illustrate the need for improving understanding of HONO sources and sinks and their variations.

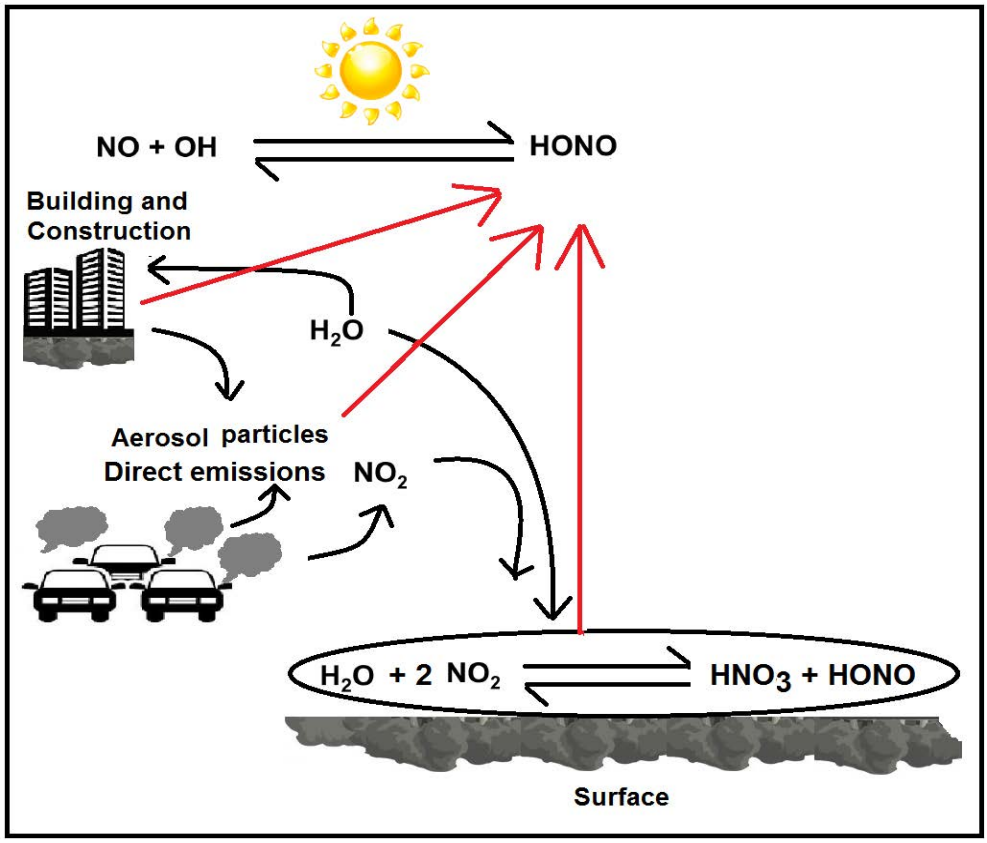

Figure 1.1 A possible HONO cycle in the troposphere using different sources and sinks.

1.5 Research objectives and structure of the thesis

1.5.1 Objectives

The overall objective of this research is to explore the long-term and short-term influences of atmospheric aerosol particles and gases along with meteorology on visibility and tropospheric chemistry. Based on the review of the literature, the following objectives were finalized:

1. To quantify the combined influence of atmospheric particles and gas characteristics, and meteorology, on long-term visibility in the UK focusing on eight meteorological sites.

2. To investigate the dependence of visibility on meteorological parameters, such as RH, air temperature, precipitation, and wind speed and direction.
3. To develop a light extinction model using historical aerosol data to explain the long-term visibility trends and their dependence on meteorological conditions.
4. To analyse the short term visibility variations caused by the PM generated from the combination of fireworks and bonfires in the UK on Guy Fawkes Night.
5. To characterise the influence of meteorology such as RH in short term visibility variations.
6. To quantify the variations in HONO concentration as a result of meteorological factors (temperature, RH, wind speed and direction), traffic emission and other sources using measured data form three urban background sites.
7. To analyse the relationship between tropospheric HONO and other air pollutants (NO_x, O_3, and PM) in response to sudden changes in solar intensity during a solar eclipse.
8. Develop chemical kinetic models to understand the observed trends in HONO during the eclipse by exploring the influence of different possible sources

1.5.2 Thesis overview

This thesis is a culmination of six subsequent chapters:

Chapter 2 explores the existing literature in the field of atmospheric visibility as it relates to air pollution and meteorology. This chapter also includes the literature of tropospheric HONO chemistry.

Chapter 3 discusses the combined influences of aerosol concentration and composition and meteorology on long-term visibility in the UK using historical data.

Chapter 4 discusses the role of firework generated pollution and meteorology on observed variations in short-term visibility.

Chapter 5 explores daytime tropospheric HONO variations and presents potential source scenarios under different light conditions that occur during a solar eclipse.

Chapter 6 compares and contrasts the concentrations of HONO at different geographical locations and seasons in order to investigate HONO variation in relation to meteorology, traffic emission and other sources.

Finally chapter 7 presents an overall summary of the research, and outlines ideas for future work.

Chapter 2.0

Literature Review

Some of the material in this chapter has been taken from following papers:

Singh, A., Bloss, W.J. and Pope, F.D., **2017**. 60 years of UK visibility measurements: impact of meteorology and atmospheric pollutants on visibility. *Atmospheric Chemistry and Physics*, 17(3): 2085-2101.

Singh, A., Bloss, W.J. and Pope, F.D., **2015**. Remember, remember the 5th of November; gunpowder, particles and smog. *Weather*, 70(11): 320-324.

Singh, A., Crilley R.L., Bloss, W.J. and Pope, F.D., Measurments of HONO during 2015 solar eclipse: Insight into potential sources and sinks. *Geophysical Reaserch Letters* (under process)

2.1 Chapter Overview

This chapter presents a detailed literature review on existing knowledge in the field of visibility, aerosols and meteorology. In particular, the relationship between fireworks and their impacts on visibility and human health is discussed here. In addition, literature concerning the tropospheric chemistry of HONO is discussed here. The chapter concludes with a discussion of the gaps in knowledge of these topics, and the motivation for the present study.

2.2 Characteristics of visibility and the role of aerosols and meteorology in determining visibility

2.2.1 Introduction

Visibility is an important atmospheric phenomenon, and serves as a practical index for the air quality (Kuo et al., 2013). Influences of air quality on various fields such as environment, health and society have been studied for a long time. Aerosols, in particular, play a key role in influencing physical and chemical processes in the lower atmosphere, and changes in aerosol properties can change their impact on air quality. Past studies have shown that changes in aerosol properties not only affect the air quality but also influence the atmospheric visibility (Malm and Pitchford, 1997; Yang et al., 2012; Yuan et al., 2006). Over the years, many studies have presented results that connect visibility with aerosol particles (Bäumer et al., 2008; Dzubay et al., 1982; Jinhuan and Liquan, 2000; Majewski et al., 2014; Noll et al., 1968; Schichtel et al., 2001; Singh and Dey, 2012; Tiwari et al., 2011; Wu et al.,

2005). These investigations demonstrate that visibility is markedly influenced by the size, chemical composition, and concentration of airborne particles. Reduced visibility is attributed mainly to high concentrations of aerosols.

There have been very few studies, however, for the UK that show long-term changes in visibility trends (Doyle and Dorling, 2002; Gomez and Smith, 1987; Lee, 1990). Additional long and short term visibility studies, therefore, have the potential to contribute to improved understanding of the interactions between different aspects of air quality. Overall, such analyses can help generate higher quality advice to legislators and contribute to improvement of the environment in the UK. At present, most cities in UK are heavily polluted (DEFRA, 2016) compared to rural locations, where the major sources of pollutants are vehicular emissions, fossil fuel burning (Allan et al., 2010; Colvile et al., 2001; Kumar et al., 2014), domestic heating and wood burning (Briggs, 2003; Crilley et al., 2015; Lohmann et al., 2000). Despite significant improvements in air quality in the UK since the 1956 Clean Air Act, different types of emissions are still creating negative effects on air quality as well as human health (DEFRA, 2016). Other studies have also demonstrated the influence of PM and trace gases in the smog condition over different countries (Baik et al., 1996; Sati and Mohan, 2014; Zhang et al., 2006).

After the 1952 London Smog event, many air quality policies were introduced in the UK. The first Clean Air Act was introduced in 1956 by the UK Government directly in response to December 1952 London Smog, which was applicable until 1964. The National Smoke Abatement Society (NSAS) estimated more than 4000 deaths in the 1952 smog event (Sanderson, 1961) and a great loss to the economy due to transportation disturbances. The 1956 act was introduced to reduce concentrations

of smog, smoke and sulphur dioxide (SO_2) in the environment. In particular, the policy was focused on industrial emission sources and its reduction (Williams, 2004). At the time, coal burning was the major energy source, and as per the 1956 Act, coal could be used for only approved energy equipment and the equipment had to be in the category of low emission production (Williams, 2004). A recent study by Harrison et al. (2015) showed that trends in air pollutant emissions (such as $PM_{2.5}$, PM_{10}, NO_x SO_2 and black smoke) significantly decreased in the UK between 1970-2014. Similarly, Brimblecombe (2006), also found that the concentration of SO_2, coal smoke and NO_2 were significantly reduced over six decades in London (Figure 2.1) as a result of the act. The other effect of this policy was exploration of other fuel sources for energy consumption. Indeed, use of coal for transportation and domestic heating largely stopped after the 1956 Clean Air Act, and it was replaced by other fuels such as diesel, petrol (Brimblecombe, 2006) and natural gas (Fenger, 1999; Semb, 2001). Between 196 5 and 1999, the use of petrol increased by 43% and diesel by 175% (Williams, 2004). However, diesel and petrol related emissions can also have an impact on present air quality through emitting particles and trace gases. In particular, the changes in fuel pattern and consumption have had a major influence on environment and air quality policies. Furthermore, growing urbanization and industrialization in the UK are important factors in air pollution and require consideration in air quality legislations.

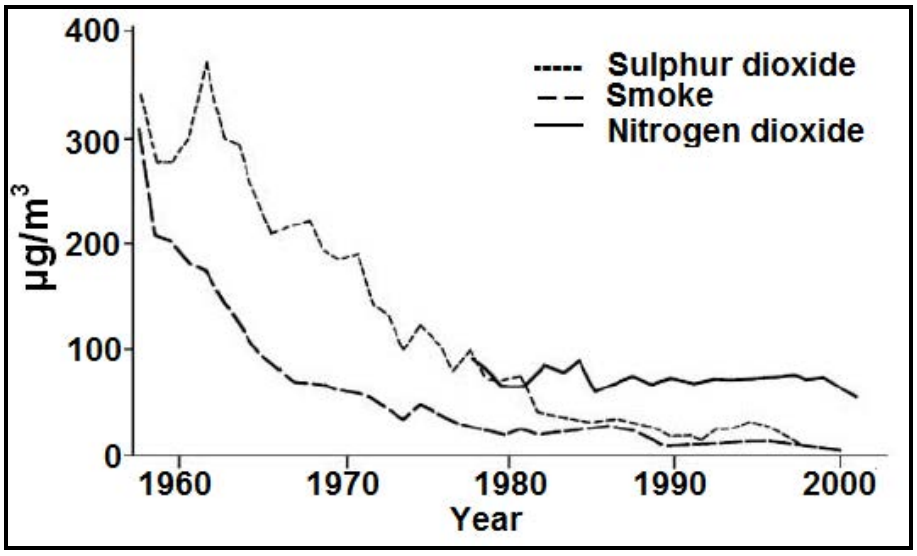

Figure 2.1 50 years of London air pollutants' concentrations. Source: Brimblecombe (2006).

2.2.2 Influence of aerosol on visibility

In a polluted environment, visibility impairment is one of the most obvious effects of air pollution (Dzubay et al., 1982; Kim et al., 2006b). Air pollutants, mainly PM and light absorbing gases (such as NO_2) can influence the visible range (VR) via the absorption and scattering of radiation at specific wavelengths (Huang et al., 2009). At present, visibility loss is a major concern all around the world, primarily in urban cities, due to a heavily polluted atmosphere (Kim et al., 2006b). Over the past few decades, both developed and developing countries, mainly in Asia and North and South America, are facing visibility degradation due to increased pollution levels. Analysis of 35 years (1973-2007) of aerosol data has shown that Asia, the USA, Australia and Africa have experienced visibility reductions, while visibility significantly improved in Europe during the same period (Wang et al., 2009). Examples from different continents are given below;

India: In the Asian continent, a rapid decline in visibility trends (0.11 km/year) from 1980s due to high aerosol loading has been reported for Delhi, India (Singh and Dey, 2012), and 90% of the visibility loss was attributed to aerosols, while the other 10% was linked to gas species and fog. In particular, anthropogenic sources like water soluble particles and soot particles had a greater contribution compared to other aerosol species in this area (Singh and Dey, 2012). Another study found that 41% of visibility loss in Delhi was due to an increase in carbonaceous particles (Singh et al., 2008). However, visibility was found to always be better during rainy days (monsoon season) when compared to other days (Goyal et al., 2014), when particles were washed out of the atmosphere (Singh et al., 2008). In recent years, urban areas in India, mainly northern parts adjoining the Indo-Gangetic Plain, are facing a rising fog occurrence problem (Mohan and Payra, 2009). A recent study by Tiwari et al. (2011) quantified the visibility changes during foggy and non-foggy conditions. Increased PM in Delhi is liable for frequent fog formation and the associated visibility loss in this area (Tiwari et al., 2011). Mohan and Payra (2009) found that in the Delhi region, the fog frequency has increased about 10 times in the last 50 years because of rising PM concentrations due to increased urbanization, industrialization and population level.

China: Most of the megacities (Beijing, Chengdu, Guangzhou, Shanghai, and Xi'an) in China are also dealing with poor visibility since the 1980s due to increased PM concentrations (Chang et al., 2009). In particular, Chang et al. (2009) found that the main sources of PM in these cities are coal power plants, industries, vehicular emission and dust storms. From the 1980s, most of the Chinese urban cities, which are mainly in the eastern part of China, have shown a significant loss in visibility of

2.1 km/decade and an increase in the extinction coefficient (a metric for visibility loss- see page xxiii and Equation 1.1) by 25% over the last twenty five years (in response to 75th percentile) (Che et al., 2007). Zhao et al. (2011) studied 29 years (1980-2008) of visibility data, including meteorology at Beijing, Tianjin, and Hebei, for 100 sites and found visibility was far better in non-urban sites compared to urban sites. A negative correlation between horizontal visibility and $PM_{2.5}$ was also found at these study areas (Zhao et al., 2011) and shows the influence of secondary aerosol on visibility. Variation in visibility due to aerosol composition at Xi'an city was also examined by Cao et al. (2012), and they attributed visibility loss below 5km to secondary inorganic aerosol species (e.g., SO_4^{2-} and NO_3^-). In another study, temporal and spatial visibility during sunny days was analysed for 543 stations in China, and annual averaged sunny visibility was found to be higher in Northwest China compared to other areas, while lower visibility was reported for southeast China (Wu et al., 2012). Furthermore, Wu et al. (2012) examined the relationship between visibility and energy consumption during sunny days and found a good correlation between visibility and energy consumption, mainly in southeast China. Another example of the link between PM and visibility is the Pearl River Delta study by Dui et al. (2007), where the authors observed a good correlation between atmospheric visibility and fine particles. Zhao et al. (2013) also mentioned that fine particles are the key element of pollutant in the Northeast China, which is responsible for significant visibility loss in urban areas of this region.

United States of America (USA): Many studies, connecting visibility with atmospheric pollutant species have been conducted in the USA. Visibility, along with particle and meteorology data, was analysed for Eastern USA by Mathai and

Tombach (1987), and they reported a decreasing visibility trend between 1950s to 1970s after a gradual improvement, due to significant changes in particle concentrations and meteorology. A large study called Big Bend Regional Aerosol and Visibility Observational Study (BRAVO) performed in Big Bend National Park, Texas (USA) from July through October month in 1999 to determine and identify the pollution sources, which influence the Park air quality and visibility (Hand et al., 2002; Pitchford et al., 2004; Schichtel et al., 2005). In particular, the study found that particulate sulphate aerosols were the major pollutant at Big Bend National Park and was responsible for visibility loss (Hand et al., 2002; Schichtel et al., 2005). A study by Sisler and Malm (1994) linked the seasonal variations in sulphate aerosol with seasonal changes in relative humidity (RH), and this was reported to have a significant influence on visibility. In a similar study, Malm et al. (1994) stated that high concentrations of hygroscopic sulphate aerosol with high RH leads to a bigger impact on visibility in Eastern USA compared to Western USA. Another study over Mid-Eastern USA noted huge changes in visibility in response to changes in air quality and meteorology after 1940 (Sloane, 1984). Many more studies have been performed for this region to examine visibility in response to suspended air pollutants (Abbey et al., 1994; Barone et al., 1978; Cahill et al., 1977; Wise, 2008).

Europe: A recent report for 39 different European countries from the European Environmental Agency (EEA, 2015) has shown that in the past few years, air quality polices were implemented successfully with the result of improved air quality over most of Europe. The effect of improved air quality can be seen in the form of improved visibility. For example, a study by Stjern et al. (2011) at 48 different European weather stations (30 from central Europe; known as Black Triangle area

(BT) and 18 from west coast of Europe) mentioned that visibility has significantly improved at BT from 1980s to 2000s due to reduction in pollutants emission level. The term “Black Triangle” area is pollution hot spot region covering Northern Bohemia, Southern Saxony and part of Lower Silesia (Renner et al., 2004). In a recent study in Hungary, data from 23 weather sites (for the period 1996 to 2002) showed that visibility increased at most of the study sites due to reduction in sulphur dioxide emission and light attenuation (Molnár et al., 2008). Furthermore, a study that analysed the solar radiation and visibility at eight different sites over Germany during 1964 to 1990 reported improved visibility linked with decreased solar radiation and increased solar extinction (Liepert and Kukla, 1997) and decreased sulphur aerosol concentration (Arends et al., 1997). Bäumer et al. (2008), in a field campaign in southwest Germany (49°06′N, 8°26′E), found significant decline in visibility (45 km to 25 km) due to increased PM_{10} concentrations (from 17.3 μg/m^3 to 41.2 μg/m^3) and aerosol optical depth (a measure of light extinction by aerosol in the atmosphere- Van Donkelaar et al. (2006)) (from 0.1 to 0.6) over a monitoring period of five consecutive days. The authors also discussed particle hygroscopic effects on visibility change by comparing calculated and observed visibility. Population density can also have an indirect influence on visibility change; for example, a study over central Europe showed considerably poorer visibility in the populated area of the central Europe compared to the outside of the population centre, due to high pollutant emissions through various human activities (Horvath, 1995).

United Kingdom: In the field of visibility-particle relationships, very few studies have been conducted in the United Kingdom on historical trends. One such study was a long-term trend analysis of visibility using different statistical methods,

performed at eight UK weather stations between 1950 and 1997 by Doyle and Dorling (2002). In this study, improved visibility was identified at most of the stations, mainly after 1973, and this was attributed to the oil crisis which led to rising fuel prices and ultimately, lower fuel consumption. In another study, summer visibility trends for five different sites in London and southern England for the period of 1962 to 1979 were analysed by Lee (1983), and a dramatic rise in visibility at all sites was reported. The improvement was linked to the reduction in oil consumption in energy industries from 1970s. A study in the late 1980s quantified the seasonal visibility trends at Oxford during 1926 to 1985 (Gomez and Smith, 1987). They observed a clear reduction in visibility from 1926 to 1944, a notable rise after World War II from 1944 to 1952, and another reduction from 1952 to 1966 (mainly in the summer season). The visibility improved again after 1966 in all seasons at Oxford due to reduction in aerosol concentration (Gomez and Smith, 1987). It was also found that after the 1956 Clean Air Act, fog occurrence declined at Oxford and nearby rural areas due to a drop in smoke concentration, and the urban heat island effect (Gomez and Smith, 1984). Analyses by Lee (1985) at four meteorological sites (Glasgow, Leuchars, Prestwick, and Turnhouse) in central Scotland for the period of 1962 to 1982, mentioned about the effect of 1973 oil crises on visibility and air quality, where a significant increase in visibility was shown primarily in urban areas due to a major reduction in sulphate aerosol concentration. After the 1973 oil crisis, total annual UK oil consumption reduced from 96.6 Mt to 80 Mt until late 1970s followed by a further reduction of 10-15 Mt up to 1982 (Lee, 1985). A similar study on historical visibility trends at 22 different UK meteorological stations (including urban, rural and marine areas) during 1962 to 1990 was performed by Lee (1994), and similar to other analyses, a clear rise in visibility was identified at most of the

sites due to reduction in coal and smoke emissions. Furthermore, a steady reduction in fog frequency with improved visibility correlated with decreased smoke pollution at Glasgow airport was noted (Harris and Smith, 1982). The correlation between various air pollutants (ammonium ion (NH_4^+), and non-marine pollutants such as SO_4^{2-} and NO_3^- and visibility at northwest England, UK was also performed in the 1980s, where strong negative correlations were found between visibility and these pollutants (Colbeck and Harrison, 1984).

2.2.3 Aerosol particles and their hygroscopic nature

According to Hueglin et al. (2005) in the atmosphere, PM is the "*mixture of elemental and organic carbon, ammonium, nitrates, sulphates, mineral dust, trace elements, and water droplets*". In the past few decades, research on atmospheric particles has significantly increased due to its direct effect on human health, atmospheric energy balance and climate change (Ackermann-Liebrich et al., 1997; Charlson and Pilat, 1969; Kulmala et al., 2004; Pope III et al., 2002). The role of PM on visibility has described previously in Chapter 1. However, variation in particle physical properties can change their contribution to visibility, for example; particle hygroscopic effect. Nearly all atmospheric aerosol particles are hygroscopic to some degree; hence, their size is dependent upon the local RH. As RH increases, hygroscopic particles take up water, through absorption and adsorption, and grow in size, volume and weight. The addition of water can also change the overall particle composition. This typically lowers the mean refractive index (*n*) (see page xxiii) of the particle since the refractive index of water is lower than other common aerosol components, such as minerals, organics, sulphates and nitrates (Harrison et al.,

2004). Numerous studies have attempted to explain aerosol particles and changes in their properties due to atmospheric processes. This section provides a summary of particle properties and the effects of atmospheric processes.

In general, an emitted particle undergoes transformation through various aging processes (Weingartner et al., 1997) for example particle interaction with water vapour (Raes et al., 2000). The amount and ability of the water absorption by any single particle depends upon the type of particle and its size, along with the atmospheric conditions like temperature and humidity. In particular, the hygroscopicity properties of particles not only influence the atmospheric aqueous phase chemistry due to reactive dependency (Pandis et al., 1995) but also make changes in particle optical properties, which may then influence the radiative forcing (Sloane and Wolff, 1985), cloud droplets (Kulmala et al., 1996; Svenningsson et al., 2006) and fog droplet formation (Jiusto, 1969).

A study was performed during a fog event in 1989 in the Po Valley to understand variation in particle hygroscopicity using a particle hygroscopicity parameter, PGF (Particle Growth Factor - **"***ratio of the particle diameter at a given relative humidity to that of the dry particle"* (Alshawa et al., 2009; Meier et al., 2009)). The authors reported separate particle growth for two different modes of particles (PGF= 1.44 and 1.1) for size of 0.030 µm < $D_p(dry)$ < 0.020 µm at the same RH (85%) (Svenningsson et al., 1992). In the 1990s, a study by McInnes et al. (1998) at Sable Island Climate Monitoring Diagnostics Laboratory, Canada aimed to understand the light scattering behaviour for different types of aerosols (influenced by marine, continental and anthropogenic air masses) including hygroscopicity evaluation. In conclusion, they found that the hygroscopic growth factor of aerosol light scattering

was the lead factor during the estimation of the aerosol radiative forcing (McInnes et al., 1998). Aerosol hygroscopic properties were examined in Gosan, Korea and compared with results during different pollution events at different sites worldwide (Kim et al., 2006a). This study reported a much higher (2.75) mean hygroscopic growth factor in the Chinese sector (due to a lot of sulphate aerosol) compared to European anthropogenic aerosol (1.46). In particular, a negative correlation was identified between hygroscopic growth factor and organic carbon aerosol (Kim et al., 2006a). In a recent study, Carrico et al. (2005) analysed the hygroscopic behaviour of two different sizes (dry size = 100 and 200nm) of aerosol particles in response to changes in RH. Negligible hygroscopic growth was found below 40% RH, however, a significant particle hygroscopic growth was observed in response to changes in RH above 40% (Carrico et al., 2005). A constant growth of particles above 80% RH was also observed. Another study was performed by Pope et al. (2010) to evaluate the hygroscopicity of mixed organic-inorganic aerosols at varying RH, where mass growth factors (growth factor as a function of particle mass - Mikhailov et al. (2013)) of the mixed organic-inorganic aerosol were found to be dependent upon the RH and mole fraction of individual components. Several other studies have connected particle hygroscopicity with meteorological components, such as RH and temperature ((Fitzgerald, 1975; Sorooshian et al., 2010) and references therein). Fitzgerald (1975) analysed the RH dependence of the size and scattering coefficients of the aerosol particles, where they observed a smooth variation of scattering coefficient with RH and the average scattering coefficient changed by a factor of 3.5 between 39-95% RH (Fitzgerald, 1975). RH is therefore a strong indicator of potential particle growth of atmospheric aerosols.

Changes in the particle properties can also have an influence on human health. For example; the interactions between particles and water droplets change the particle wet and dry deposition in the atmosphere as well as in the lungs during inhalation (Chan et al., 2002; Schroeter et al., 2001). Schroeter et al. (2001) found that during inhalation, secondary cigarette smoke particles may interact and absorb the water vapour in the presence of warm and high humidity conditions, which are responsible for significant changes in particle physicochemical properties and affects the dynamics of inhaled secondary cigarette smoke particles. Chan et al. (2002) examined the particle deposition in the human lung using different particle conditions and sizes, where they found a significant difference in particle deposition in the lung for wet and dry particles.

2.2.4 Meteorological influences

In addition to particle and gas concentrations and composition, specific meteorological conditions can also affect visibility (Sloane, 1983). There exists a body of literature on visibility studies, which attempt to connect visibility with meteorological parameters (e.g. (Clarke et al., 1978; Hänel, 1972; Haywood and Boucher, 2000; Lee, 1983; Lee, 1990)). Whilst temperature (T), RH, wind speed (w_s) and wind direction (w_d) do not affect clear sky visibility directly, they can influence the sources and sinks of the trace gases and aerosol particles in the atmosphere. For example, high wind speeds can re-suspend dust particles and generate sea spray aerosol particles. Windy conditions can also lead to a cleaning effect by replacing polluted air with cleaner air. Temperature can influence the production of secondary organic aerosol (SOA) particles, for example, via the chemical formation

and partitioning between the gas and particle phase. RH not only affects the sources and sinks of gases and aerosols, it also directly influences the size and composition of aerosol particles, which is discussed in the previous section.

Previous studies confirm these meteorology effects on aerosol-visibility (Charlson et al., 1991; Dayan and Levy, 2005; Sequeira and Lai, 1998; Zhang et al., 2015). A study over Hong Kong has shown that visibility was usually highest in summer months and lowest in winter months, where atmospheric mixing height (a fundamental parameters characterising the structure of the lower atmosphere - Seibert et al. (2000)) and concentrations of chemical species within aerosol like sulphate, nitrate, ammonium and trace elements like K and Zn had considerable influence on visibility (Sequeira and Lai, 1998). Another study was performed over 60 Korean meteorological sites during 1980s to 2000s to see the spatial and temporal visibility trends including meteorology effect (Ghim et al., 2005). In particular, they observed a negative correlation between RH and visibility during study period. Poirot and Wishinski (1986) also found an inverse correlation between visibility and the combined effect of sulphate aerosol and RH at Northern Vermont study in 1980s. The variation in summertime visibility due to meteorology was analysed during two specific eras (1950s and 1980s) in Mideastern USA (Sloane, 1983). A clear influence of meteorological parameters such as RH and air masses on visual air quality and hence visibility was observed in the study. In Beijing, it was found that visibility decreased from 1970 to 1979 due to an increase in sulphate aerosols, PM and RH, where the authors noted that sulphate aerosols (with the RH dependent hygroscopic effect) were responsible for visibility degradation (Weihanl et al., 1990). Trijonis (1982) found that the loss in visibility in California during 1949 to 1976 was mainly due to anthropogenic impacts and changes in meteorology like

RH. In a study in Jinan, China a combined effect of PM and meteorological conditions on visibility was observed, where $PM_{2.5}$ and PM_{10} showed an exponential relationship with visual range (Yang et al., 2007). Another analysis in Nanjing, China to characterize the visibility, where they found that PM, RH, wind, air temperature and air pressure directly or indirectly contribute in visibility variation (Deng et al., 2011). In this study, a negative correlation between extinction coefficient and wind, during all seasons was observed. Aerosol mixing state and composition can also vary due to changes in meteorology, a study has shown that significant variation in mixing state is due to meteorology during hazy periods (Whiteaker et al., 2002).

2.2.5 Air pollution caused by fireworks and bonfires and their associated impacts

Human activities such as fireworks and bonfires during celebrations and festivals can have adverse effect on visibility, air quality and human health (Godri et al., 2010; Hamad et al., 2016; Singh et al., 2015). All over the world, during different occasions, people celebrate their festivals using fireworks, firecrackers and bonfires. During these events, smoke plumes are produced due to the burning effect of fireworks and bonfires, which can raise the PM concentration level (Joly et al., 2008) and influence the short-term air quality within the local environment (Mandal et al., 1997; Singh et al., 2015; Zhang et al., 2010).

The influence of fireworks and bonfires used in these events has previously been connected to a change in visibility, air quality and health hazards in many studies (Becker et al., 2000; Kong et al., 2015; Kulshrestha et al., 2004; Nasir and Brahmaiah, 2015; Pathak et al., 2013; Singh et al., 2005; Van Kamp et al., 2006;

Witsaman et al., 2006; Yerramsetti et al., 2013). In this context, a recent study in Delhi has shown that PM_{10} concentration increased about 23-33% due to fireworks during a Diwali event in 2010 (Sarkar et al., 2010). Furthermore, firework effects during the Indian traditional festival "Vishu" was analysed at Kannur, India in 2010, where they observed that levels of pollutants like ozone, NO_2 and PM_{10} increased by 200%, 100% and 100%, respectively (Nishanth et al., 2012). Chatterjee et al. (2013) also reported higher levels of PM (about 5 times more PM_{10} in concentration than in the day) during Diwali festival at Kolkata in 2010. A significant rise in surface ozone was also found in New Delhi during Diwali festival (Ganguly, 2009). In a similar study in Dibrugarh (eastern India), Pathak et al. (2013) observed a notable increment in concentrations of trace gases (such as SO_2, NO_X, CO) . Fireworks and bonfires are also responsible for emissions of harmful trace metals (mainly; Sr, Ba, Pb, Mg, K, Ti, S and Cu) with particles and organics in the atmosphere (Kulshrestha et al., 2004; Moreno et al., 2007; Steinhauser et al., 2008; Vecchi et al., 2008). In general, fine metals such as K and S are produced from black powder combustion during fireworks and burning of firecrackers (Perry, 1999). In a previous study at Kaohsiung Harbor, during 2009 Taiwan's Lantern festival, the concentrations of trace metals like Mg, K, Pb, and Sr in $PM_{2.5}$ were found to be 10 fold higher during the fireworks display period as compared to the normal days (Tsai et al., 2012). Sarkar et al. (2010) also reported high loading of metal elements; in particular, Ba, K, Mg, Al, and EC with 16.8 $\mu g/m^3$, 46.8 $\mu g/m^3$, 21.3 $\mu g/m^3$, 38.4 $\mu g/m^3$, and 40.5 $\mu g/m^3$ in mean concentrations respectively at Delhi during a fireworks event. Moreover, a study performed by Dyke et al. (1997) revealed the short-term effect of bonfires during Guy Fawkes Night in Oxford, UK, where they found a sharp rise in organic pollutants; dioxin and furan concentrations. A study performed in

Switzerland during a fireworks display for Swiss National Day in 2011, showed about a 10 fold increase in organic elements; pentachlorophenol and polychlorinated dibenzo-*p*-dioxins and dibenzofurans concentrations compared to normal days (Schmid et al., 2014). The sudden rise in these metals, particles and organics during fireworks, bonfire and firecrackers events can increase chances of asthmatic attacks, lung infection, eye allergies, cough, fever and cardiovascular disease (Barman et al., 2008; Becker et al., 2000; Beig et al., 2013; Hirai et al., 2000). For example; one study reported a statistically significant increment of 113% in treated respiratory illness during fireworks events (Bach et al., 1975). Similarly, Gouder and Montefort (2014) found a clear adverse effect of fireworks on respiratory health. Moreover, the use of fireworks, bonfires, and crackers can be responsible for serious injuries (D'Argenio et al., 1996; McFarland et al., 1984; Vassilia et al., 2004). In particular, burning and eye injuries are more likely in the occasion of fireworks and crackers fire (Fogarty and Gordon, 1999; Kuhn et al., 2000). Another side-effect of fireworks is often noise pollution. In general, an increased noise level during fireworks event was observed in previous literature, and high noise levels can trigger psychological stress (Ising et al., 1980; Verma and Deshmukh, 2014). The unwanted noise pollution during fireworks events can affect the hearing function (Björkman and Rylander, 1997; Gjaevenes et al., 1974) and also increase the chances of cardiovascular disease (Babisch, 2000).

In the UK, several studies have linked the use of fireworks with changes in air quality (Godri et al., 2010; Knox et al., 2008). Over the past few years, several studies have connected fireworks to visibility issues (for example; (Kong et al., 2015; Saha et al., 2014; Vecchi et al., 2008; Wang et al., 2007)). Local scale and short-

term pollution episodes can cause large decreases in visibility, with potentially devastating consequences. For example, in 2011, a tragic incident occurred on the M5 motorway near Taunton, Somerset, where seven people died and 57 were injured due to a car crash. The resulting investigation found that a local fireworks display near the road might have contributed to the poor visibility on an already foggy night albeit no blame was assigned to the organizer of the fireworks event (Rose, 2014).

2.3 Tropospheric chemistry of HONO

In the troposphere, HONO is one of the key trace species which directly influences the chemistry of the polluted atmosphere via its involvement in the chemistry of NO_x and HO_x (Li et al., 2012; Xu et al., 2015). Additionally, HONO may also impact directly on human health (Kirchstetter et al., 1996). HONO was discovered for the first time in 1979 by Perner and Platt (1979), using a long path differential absorption spectrometer. Since HONO was first detected in the atmosphere, many in situ techniques have been developed for HONO measurements such as Differential Optical Absorption Spectroscopy (DOAS) (Febo et al., 1996), Negative-Ion Proton-Transfer Chemical Ionisation Mass Spectrometer (NI-PT-CIMS) (Roberts et al., 2010), Tuneable Infrared Laser Differential Absorption Spectrometry (TILDAS) (Lee et al., 2011), Stripping Coil–Visible Absorption Photometry (SC-AP) (Ren et al., 2011), Incoherent Broadband Cavity-Enhanced Absorption Spectroscopy (IBBCEAS) (Pusede et al., 2014), and Long Path Absorption Photometer (LOPAP) (Heland et al., 2001).

Numerous studies have shown that HONO is the dominant source of OH radicals in the early morning and remains a significant source over the rest of the day (Michoud et al., 2014; Michoud et al., 2012; Ren et al., 2003; Villena et al., 2011a). In general, it was believed that HONO is mainly formed from heterogeneous conversion of NO_2 on humid surfaces (Bröske et al., 2003; Kleffmann, 2007), however this formation mechanism is not clear, especially during daytime (Qin et al., 2009). Heterogeneous conversion of NO_2 to HONO depends upon the volume and physical properties of the surfaces (Acker et al., 2006b). Many studies have suggested that in the atmosphere, HONO can also be formed from heterogeneous conversion of NO_2 on carbonaceous surfaces such as suspended soot particles (Arens et al., 2000; Kalberer et al., 1999; Kleffmann et al., 1999). However, reactive sites on soot particles rapidly become saturated so this mechanism may not be significant in a polluted atmosphere (Kalberer et al., 1999; Longfellow et al., 1999; Prince et al., 2002). In a recent study, Cazoir et al. (2014) examined HONO production from photolytic conversion of NO2 gas on polycyclic Aromatic Hydrocarbon (PAH) films, where they found that the proposed reaction clearly depends upon irradiance. They observed a slow reaction under dark conditions, but the rate was greatly enhanced by the presence of UV light (Cazoir et al., 2014).

In the last two decades, many measurements and analyses were carried out to investigate HONO formation by different sources such as heterogeneous reactions on surfaces, gas phase reactions and direction emission (Crilley et al., 2016; Finlayson-Pitts et al., 2003; Kleffmann, 2007; Liang et al., 2017; Su et al., 2011; Vecera and Dasgupta, 1994). However, these sources do not fully account for observed daytime HONO (Elshorbany et al., 2010; Su et al., 2011). These formation

mechanisms were introduced in Chapter 1 (section 1.4.2). Primarily, in the urban environment, HONO is directly emitted by combustion processes, where HONO/NO_x ratio is commonly used as a proxy parameter to evaluate HONO emission from vehicles (Elshorbany et al., 2012; Kleffmann, 2007; Liang et al., 2017). Previous empirically determined emission ratios of HONO/NO_x based on tunnel and car exhaust studies were significantly lower (0.3% to 0.8%) (Kirchstetter et al., 1996; Kurtenbach et al., 2001) than ratios observed in the atmosphere, suggesting a number of secondary sources of HONO in addition to vehicular emissions (Liang et al., 2017; Sörgel et al., 2011; Spataro and Ianniello, 2014). Typically, during the daytime, the homogenous gas phase reaction ($OH + NO \xrightarrow{M} HONO$) is significant for HONO formation when OH and NO are high (Alicke et al., 2003). In addition, Stockwell and Calvert (1983) introduced a further gas phase reaction (Reaction 2.1) that can only have a small contribution to daytime HONO production (Kleffmann, 2007).

$$NO_2 + HO_2 \longrightarrow HONO + O_2 \qquad (R2.1)$$

However, Bejan et al. (2006) found that under urban conditions, daytime HONO formation (100 pptv h^{-1}) from photolysis of different ortho-nitrophenols cannot be neglected. These homogenous gas phase reactions, which are too slow, and direct vehicular emissions, which are too small, are not sufficient to explain high observed HONO concentrations (Acker et al., 2006a). Furthermore, Su et al. (2011) found that soil nitrate which is formed from biological soil activities can be a major source of HONO and can explain the missing HONO source in the troposphere. They observed that fertilized soils with low pH (Potential of hydrogen) tend to be strong sources of HONO and OH radicals (Su et al., 2011). In recent years, a number of

laboratory and field studies (in urban, rural and remote areas) were carried out to understand HONO variation and HONO chemistry (Acker et al., 2006a; Kurtenbach et al., 2001; Li et al., 2012; Meusel et al., 2016; Michoud et al., 2014; Stutz et al., 2004; Villena et al., 2011b). Nonetheless, tropospheric sources of HONO are poorly constrained and uncertainties persist in understanding sources and variations in HONO in the urban environment.

In addition, very few field and laboratory studies were performed to evaluate the influence of meteorology on tropospheric HONO chemistry (Harrison and Collins, 1998; Sörgel et al., 2011; Wojtal et al., 2011). For example; Yu et al. (2009) performed a study to investigate the relationship between HONO and RH. They found that in early mornings under high RH (above 95%) conditions hygroscopic aerosol particles deliquesce to form water droplets which appear to absorb and remove HONO from the air. Similarly, Stutz et al. (2004) observed a significant influence of RH on heterogeneous HONO formation, where lower $HONO/NO_2$ ratios were observed in high RH (above 95%) conditions as compared to average (70-95%) or low RH (10-30%). However, the role of other meteorological parameters (such as temperature and wind speed and direction, precipitation and solar radiation) on tropospheric HONO chemistry cannot be neglected (Gandolfo et al., 2017; Meusel et al., 2016).

Chapter 3.0

60 years of UK visibility measurements: impact of meteorology and atmospheric pollutants on visibility

Most of the material in this chapter has been taken from following paper:

Singh, A., Bloss, W.J. and Pope, F.D., **2017**. 60 years of UK visibility measurements: impact of meteorology and atmospheric pollutants on visibility. *Atmospheric Chemistry and Physics*, 17(3): 2085-2101.

3.1 Chapter overview

The purpose of this chapter is to examine the combined impacts of atmospheric pollutants and meteorology on long-term UK visibility. This chapter describes the historical data collection of visibility and meteorological parameters, including pollutant species at different sites over the United Kingdom. It also includes discussion of data availability, measurement and processing procedures. Detailed geographical and economic descriptions of each site are also presented in this chapter. Finally, methods and procedures including a detailed description of the model developed utilising these datasets are stated in this chapter.

3.2 Abstract

Reduced visibility is an indicator of poor air quality. Moreover, degradation in visibility can be hazardous to human safety; for example, low visibility can lead to road, rail, sea and air accidents. This work explores the combined influence of atmospheric aerosol particle and gas characteristics, and meteorology, on long-term visibility. Visibility data was used from eight meteorological stations, situated in the UK, which have been running since the 1950s. The site locations include urban, rural and marine environments.

Most stations show a long term trend of increasing visibility which is indicative of reductions in air pollution, especially in urban areas. Additionally, the visibility at all sites show a very clear dependence on relative humidity indicating the importance of aerosol hygroscopicity on the ability of aerosol particles to scatter radiation. The dependence of visibility on other meteorological parameters, such as wind speed and wind direction is also investigated. Most stations show long term increases in

temperature which can be ascribed to either climate change, land-use changes (e.g. urban heat island effects) or a combination of both; the observed effect is greatest in urban areas. The impact of this temperature change upon local relative humidity is discussed.

To explain the long term visibility trends and their dependence on meteorological conditions, the measured data were fitted to a newly developed light extinction model to generate predictions of historic aerosol and gas scattering and absorbing properties. In general, an excellent fit was achieved between measured and modelled visibility for all 8 sites. The model incorporates parameterizations of aerosol hygroscopicity, particle concentration, particle scattering, and particle and gas absorption. This new model should be applicable and is easily transferrable to other data sets worldwide. Hence, historical visibility data can be used to assess trends in aerosol particle properties. This approach may help constrain global model simulations which attempt to generate aerosol fields for time periods when observational data are scarce or non-existent. Both the measured visibility and the modelled aerosol properties reported in this work highlight the success of the UK's Clean Air Act, which was passed in 1956, in cleaning the atmosphere of visibility reducing pollutants.

3.3 Introduction and objectives

Over the last few decades air pollution has become a critical environmental issue across the world, although early industrial countries like the UK began to act as early as the 1950s. In the present day, enhanced urbanisation, industrialisation and growing population are affecting the air quality within the troposphere (Tie and Cao,

2009), via processes associated with development such as large scale construction projects, increasing vehicular emissions, and industrial agriculture. In the troposphere, poor visibility can be a useful indicator with regard to air quality (Tsai and Cheng, 1999), since air pollution can cause a reduction in visibility (Doyle and Dorling, 2002). In the polluted atmosphere visibility mainly depends upon the optical and microphysical properties of aerosol particles (Bäumer et al., 2008; Singh and Dey, 2012), however meteorological conditions cannot be neglected (Lee, 1994; Sloane, 1983).

This study focusses on the analysis of historical visibility, specifically as it relates to aerosol composition and concentration along with meteorology in different geographical areas (urban, rural and marine). There have been a few studies which attempt to connect visibility with aerosol and meteorological parameters, however, very few for the United Kingdom region. This study investigates visibility in the United Kingdom focusing on 8 specific meteorological station sites. The same sites were previously investigated by Doyle and Dorling (2002) who presented long term UK visibility trends for 1950-1997 and the dependence of the measured visibility on meteorological conditions. This work builds upon the work of Doyle and Dorling to analyse UK visibility trends from 1950-2013. Furthermore, the analysis was extended by investigating causes of the observed visibility trends; in particular the role of air pollutant concentrations upon UK visibility. The outputs from this work help to explain historic visibility trends in the UK. A new model is also presented which can aid in future visibility prediction under different climate and pollution scenarios.

Based on the past literature and gaps in our knowledge of historical trends and visibility-aerosol-meteorology relationships in the United Kingdom, the key objectives of this study are:

1. To quantify the annual and seasonal variations in visibility and its temporal trends over the past 60 years in the UK for different geographical sites (urban, rural and marine).
2. To examine the sensitivity of visibility in response to changes in RH.
3. To develop a light extinction model using parameterised data of aerosols to deduce visibility-aerosol-RH relationships and predict historical aerosol and gas scattering and absorption properties.
4. To investigate the influence of changes in historical aerosol composition and concentration on present visibility by using the model developed in Objective 3.
5. To characterise the potential effects of meteorological parameters on visibility variations.

3.4 Data

3.4.1 Data Collection

Daily archived horizontal visibility data, defined as the visibility distance along a horizontal line at the earth's surface, were obtained from the British Atmospheric Data Centre (BADC) which is run by the UK's Natural Environment Research Council (www.badc.nerc.ac.uk). All data were stored in the Met Office Integrated Data Archive System (MIDAS), where each meteorology station can be identified by their given Unique Source Identifier ID (src id) and name. The archive contains visibility data, in addition to other relevant meteorological parameters, archived at an

hourly time resolution. In addition to visibility, the following meteorological parameters were also utilised: RH, wind speed, wind direction, air temperature, rainfall and present weather (PR) code which provides further qualitative detail about the weather conditions. A description of the present weather codes is provided in the table (www.badc.nerc.ac.uk/data/ukmo-midas/WH_Table.html) at www.badc.nerc.ac.uk. Unfortunately the use of present weather codes largely ceased with the introduction of automated meteorological stations and insufficient PR codes were available after the year 1997. It is noted, that if the present weather codes were available they would have been useful to screen the data for rain or other precipitation events. Due to unavailability of present weather codes during required study period (1950-2012), data filtration was done on the bases of RH limits instead of PR codes. Data were removed when the relative humidity reading was > 99 % which is highly suggestive of rain or other precipitation events. Removal of data with RH > 99% removes between 0.91 – 3.44 % of the data dependent on site location. Since the ability of visibility observers is affected by light levels, with greater difficulty encountered in night time measurements (Lee, 1990) the daily data used for this study were all measured at 12 noon for all sites.

Meteorological data were collected for the eight UK stations which possess near continuous time series data starting in the 1950s and continuing to present day. The eight stations are Aldergrove, Heathrow, Ringway, Nottingham, Plymouth, Tiree, Leuchars, and Waddington, and details of the stations are given in Table 3.1 and Fig. 3.1 and section 3.4.2. It is noted that visibility data are available from over 2438 meteorological stations within the UK (encompassing 154 counties) but the majority of the sites have much shorter time series than the eight stations chosen.

The visibility data sets are based on ground based measurement using a variety of techniques. More details of visibility observations method are found in UK Met Office Surface Data Users guidelines (https://badc.nerc.ac.uk/data/ukmo-midas/ukmo_guide.html). Until the late 1990s all visibility measurements were performed by human observer. Subsequently data collection was automated using visibility sensors (visiometers). See Table 3.2 for detail on measurement type used and dates of service.

There are advantages and disadvantages with both human observation and visiometers. Clearly from a manpower perspective, visiometers are preferred. Human observation provides a true measure of visibility since the observer is looking for objects located at a known distances away from their location, however, the visibility measurements are imprecise by nature since results can vary according to the contrast and illuminance thresholds (ability to discern and sensitivity to light, respectively) of the observer's eyes (WMO, 2008). Since human observation requires objects to observe the measurement is quantized by the geographical spread of available objects i.e. there is not a continuum of measurement locations. Consequently, human observations provide a lower limit to the actual visibility. Distances between objects to observe can be large especially at the longer distances measured (> 10 km) which leads to reductions in accuracy at high visibility. At high elevation the visibility calculation can be different from that at the surface (Malm et al., 1981). Visiometers automatically measure the extinction of light over a small distance (typically ca. 1 m) and from the measured extinction can estimate visibility. In particular automatic visibility measuring instruments consist of a light transmitter and receiver, the light extinction observed between the transmitter

and receiver is then used to estimate the visibility (Jebson, 2008). These automated estimates of visibility are more objective and reproducible compared to than human observation. However, since the visiometer only measures air local to the device it can be much more affected by variations in local air quality. This is likely to be a more important consideration at urban meteorological sites where air composition is more heterogeneous, compared to rural sites, due to the greater number of pollutant sources in urban areas.

The change from human to automatic measurement occurred at different times for the different sites (see Table 3.2). It is clear for most sites investigated, that the changeover from manually observed to automatically measured data leads to step changes in the visibility reported, see Fig. 3.10.1 (Section 3.6.1) and further discussion in methodology section. This is unsurprising given the discussion above. In particular, clear deviations away from the long term trend measured under human observation are observed at Aldergrove, Plymouth and Tiree stations once automation was introduced (see Table 3.2). After consultation with the UK Met Office it was noted that automated sensors can be unreliable during high visibility events when compared to human readings. In particular automatic sensors perform sub-optimally at coastal sites unless the sensor is cleaned regularly, due to accumulation of sea salt residue. Unfortunately, the Tiree station was reported to fall into this category.

To assess the effects of the gaseous pollutant nitrogen dioxide (NO_2) on visibility, daily ground based measured data of NO_2 was obtained from the Department of Environment Food and Rural Affairs (Defra) (https://uk-air.defra.gov.uk/) for one observing station (Harlington), closely co-located to the Heathrow meteorological

station (ca. 1.3 miles distant). NO_2 data were only available for 9 years (2004-2012) of the visibility study period.

Table 3.1 Study stations with area and length of data description

No.	Station Name	Station code (src id)	Area	Period	Length of Data (in Year)
1	Aldergrove	1450	Urban (Airport)	1950-2012	63
2	Heathrow	708	Urban (Airport)	1950-2012	63
3	Ringway	1135	Urban (Airport)	1950-2004	55
4	Nottingham	556	Urban	1957-2012	56
5	Plymouth	1336	Urban (near coastal area)	1950-2012	63
6	Tiree	18974	Rural (Airport, near Coastal area)	1957-2012	56
7	Leuchars	235	Rural (RAF, near coastal area)	1957-2012	56
8	Waddington	384	Rural (RAF, Airport)	1950-2012	63

* RAF stands for Royal Air Force

Table 3.2 Method of visibility measurement at different station with its used time period, where present indicates the sensor is still installed and being used.

	Method/ Sensor/ Equipment Type Name with their working period					
Station Name	**Manually**		**Sensor 1**		**Sensor 2**	
Aldergrove	01/01/1926	24/01/2003	**VISMETER -BELFORT 6230A** 24/01/2003	28/08/2012	**PRESENT WEATHER SENSOR - FD12P** 28/08/2012	Present
Heathrow	01/01/1947	01/01/2000	**VISMETER -BELFORT 6230A** 01/01/2000	15/06/2005	**VISMETER - BELFORT (Replaced with new one)** 15/06/2005	Present
Ringway	01/01/1941	01/01/2000	**VISIBILITY: VISIOMETER** 01/01/2000	01/11/2004	**Manually** 01/11/2004	Present
Nottingham	01/01/1941	01/01/2000	**VISMETER -BELFORT 6230A** 01/01/2000	Present	----------	
Plymouth	01/01/1920	23/01/1997	**VISMETER -BELFORT 6230A** 23/01/1997	16/12/2010	**PRESENT WEATHER SENSOR - FD12P** 16/12/2010	Present
Tiree	01/01/1926	16/12/2010	**VISMETER -BELFORT 6230A** 16/12/2010	Present	----------	
Leuchars	01/01/1921	16/12/2010	**VISMETER -BELFORT 6230A** 16/12/2010	Present	----------	
Waddington	01/01/1946	01/01/2000	**VISMETER -BELFORT 6230A** 01/01/2000	Present	----------	

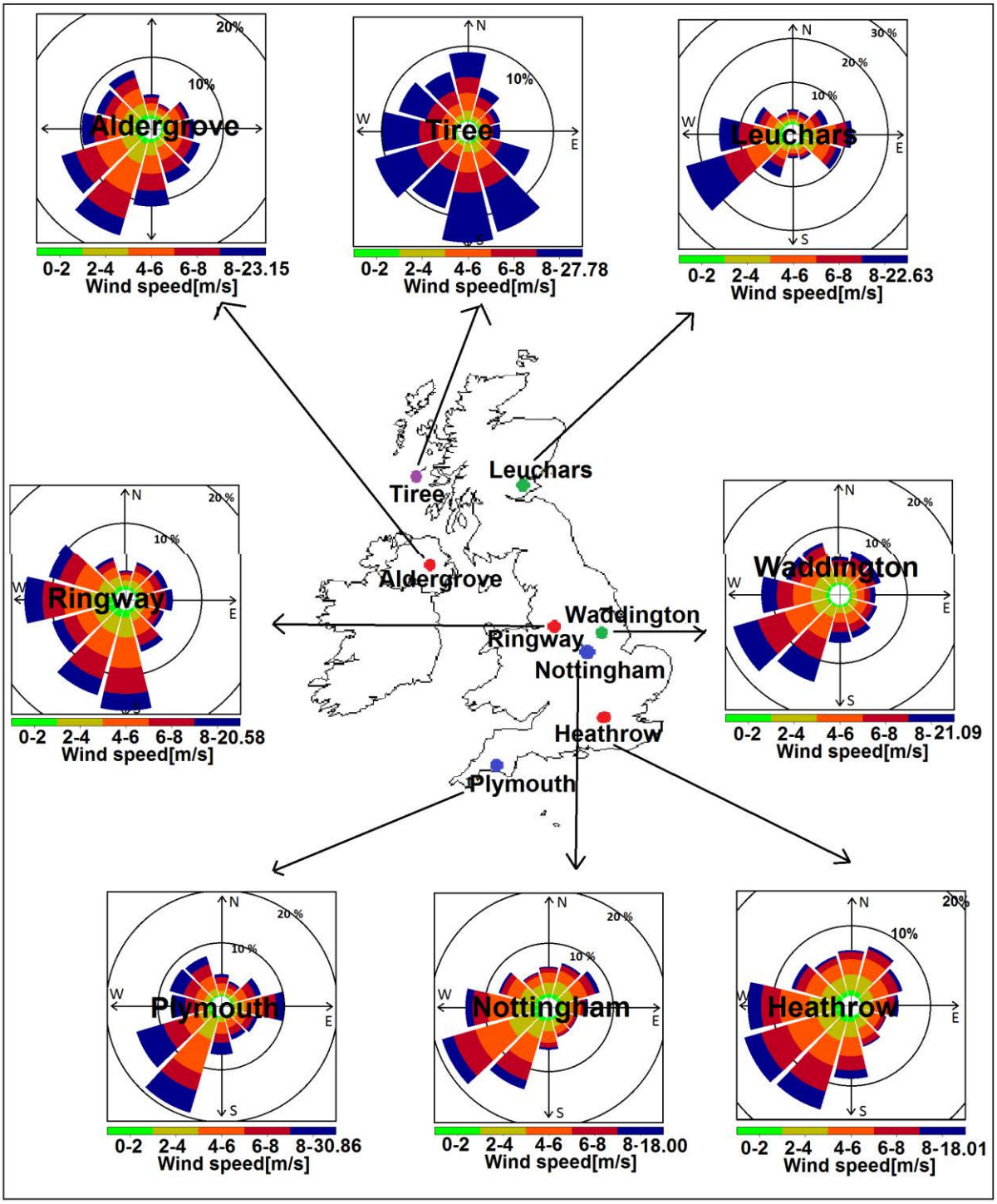

Figure 3.1 Geographical location of measurement stations used. Location point colours describe location type: red - urban airport; blue - urban; purple - rural/remote and green - rural airport. Also presented are mean wind rose statistics whole time period (approximately 60 years) for all eight stations.

3.4.2 Geographical description of study sites

About 60 years of a large visibility dataset, which includes meteorology (RH, air temperature, wind speed and wind direction, rainfall) were collected at eight different geographical locations (Figure 3.1). All eight meteorological stations measure various weather parameters (wind speed, wind direction, air temperature, dew point temperature, wet bulb temperature, soil temperature, atmospheric pressure, relative humidity, solar intensity, cloud cover, fog, and precipitation including horizontal and vertical visibility) continuously over the year. Details of the measurement approaches applied to different weather parameters can be found at http://cedadocs.badc.rl.ac.uk/270/1/factsheet17.pdf. Geographical descriptions of the eight meteorological study sites are given below. Details of the meteorology at each station are discussed in the results section 3.6.2.2.

(a) Aldergrove, Belfast, Northern Ireland

63 years (1950-2012) of dataset were collected at Aldergrove airport site (src id 1450), which is currently the Belfast International Airport. The airport is situated northwest of Belfast (54.40^{o} N, 6.13^{o} W) (see Figure 3.1 and 3.2), which is approximately 15 miles from Belfast city centre. Belfast is the capital of Northern Ireland and also one of the most populous cities in the United Kingdom. Moreover, Belfast International Airport is the second largest and busiest airport in Northern Ireland, where over 2.6 million passengers travel every year (Barrett, 2000). At the Airport site (Figure 3.2), meteorological observations run continuously, where their data is stored in the Met Office Integrated Data Archive System.

Figure 3.2 Map of meteorology observatory site at Belfast International airport (Aldergrove airport). Image source: Google Earth

(b) Heathrow Airport, London, England.

The weather station (51.48^{o} N, 0.45^{o} W) (see Figure 3.1 and 3.3) was established in May 1946 at Heathrow Airport, London, and became fully functional in the late 1940s, (Ogden, 1998; Webster, 1984). Historical visibility and meteorology data was collected at Heathrow weather station (src id 708) during the period from 1950 to 2012. The weather station monitors meteorology and air pollutants using various instruments. These instruments were updated over time to improve the quality of observations (Webster, 1984).

Heathrow Airport ranks as one of the busiest and largest airports in the world (Atkin et al., 2007). It is approximately 14 miles west of central London. Over 70 million passengers travel every year through Heathrow airport as per record of 2012

(Butcher, 2012), which was increased by 75 million in 2015 (Heathrow, 2016). The airport is located nearby to one of London's busiest motorways, the M25, which influences the local air quality (Hadjimitsis et al., 2002; Stebbings et al., 1999). Moreover, the airport lies in one of the highest NO_x emission zones in London; mainly due to emissions from aircraft, supporting ground vehicles and equipment at the airport (Farias and ApSimon, 2006; Hadjimitsis et al., 2002). In addition, surrounding road traffic emissions and residential pollution also influence the air quality of Heathrow (Parker, 1971).

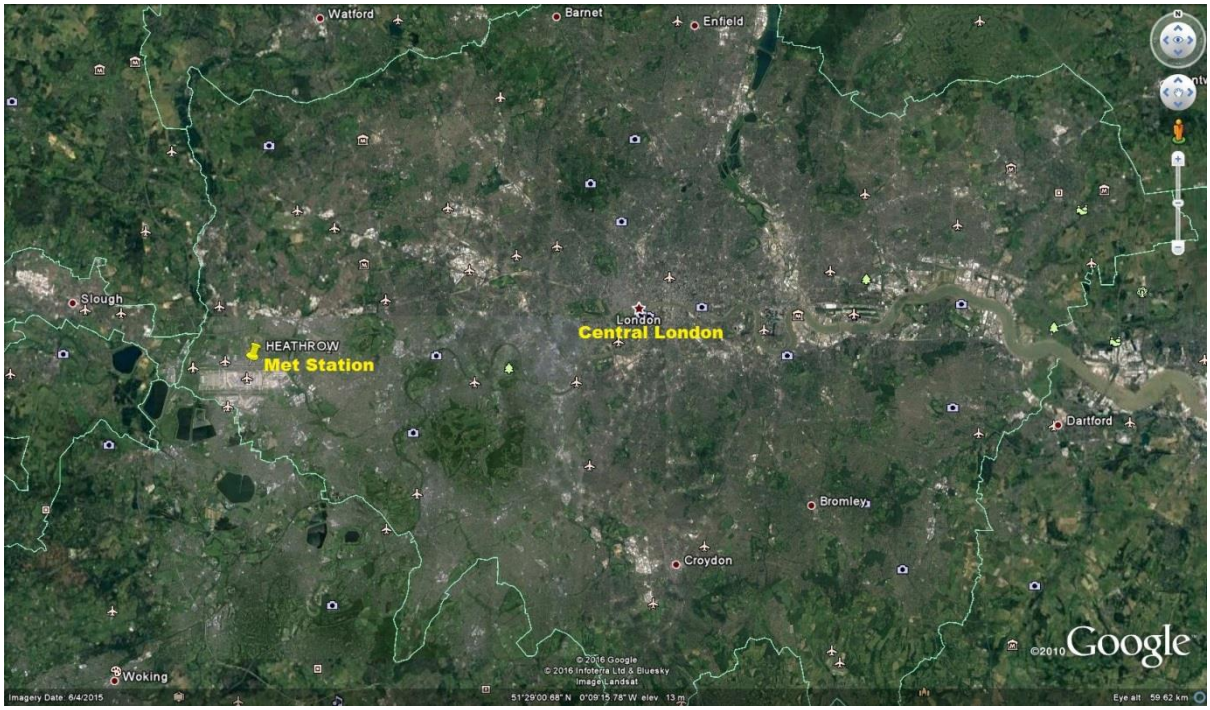

Figure 3.3 Map of meteorology observatory site at Heathrow airport. Image source: Google Earth

(c) Ringway, Manchester, England.

Ringway meteorological station (src id 1135) is based at Ringway International Airport (Manchester International Airport), Greater Manchester, UK (53.35^{o} N, 2.27^{o} W), which is about 8 miles south of Manchester city centre (Figure 3.4). The weather station was opened in 1939 and started recording observations in the early 1940s. For the current station, 55 years (1950-2004) of data was collected, i.e. the required study data was only available from 1950 to 2004 for this site. Manchester airport is the 3rd busiest airport in the UK, which handles more than 18 million people every year (Miyoshi and Mason, 2013; UKCAA, 2011). The airport area is surrounded by motorways, industry and residential areas (Gill et al., 2007), which influences the air quality of the area.

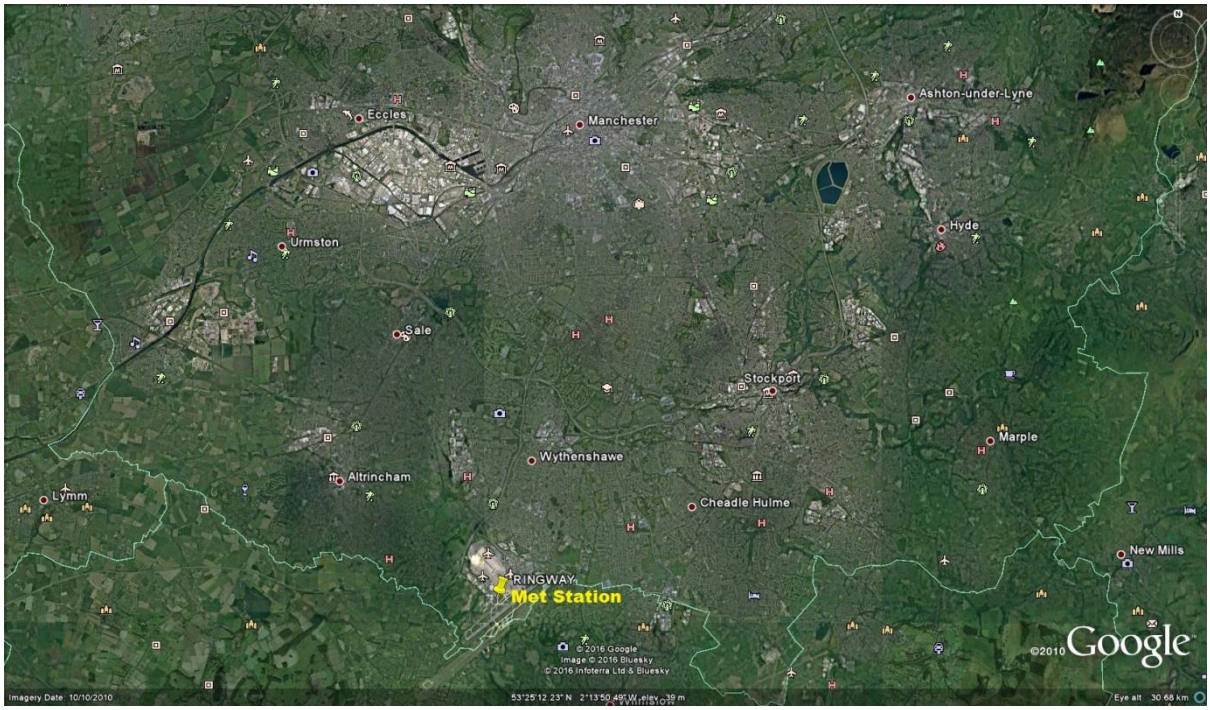

Figure 3.4 Map of weather station at Ringway (Manchester International airport). Image source: Google Earth

(d) Watnall, Nottingham, England

Nottingham Watnall (src id 556) meteorological station is located in Nottinghamshire, UK (53.01^{o} N, 1.25^{o} W), which is very close to the city centre of Nottingham (approximately 5 miles). Watnall weather station (Figure 3.1 and 3.5) started functioning in 1941; however due to the unavailability of required data before 1957, only the archived hourly dataset during the period of 1957-2012 was used.

Nottingham is one of the largest cities in the UK, with a population of more than three million as of 2013 (Lawton, 2014). The primarily sources of pollution in Nottingham are mainly residential emissions, surrounding industry, and traffic emissions, which directly influences the air quality of Nottingham (Pyatt and Haywood, 1989). Nottingham is also influenced by pollutants transported from Ratcliffe-on-Soar coal power station in the southwest (Pyatt and Haywood, 1989).

Figure 3.5 Map of Nottingham Watnall weather station. Image source: Google Earth

(e) Plymouth, Devon, England

Plymouth Mountbatten weather station (src id 1336) is situated at Plymouth Sound on the south west cost of Devon, UK (50.35^{o} N, 4.12^{o} W). For the Plymouth site (Figure 3.1 and 3.6) an hourly visibility and meteorology dataset is available from 1950 to 2012. Plymouth is the highest populated city within Devon County in the UK, where more than 2.5 million inhabitants live in Plymouth (Public Health, 2014). The major pollution sources in Plymouth are marine aerosol, road traffic emissions and port activities including prevailing wind from continental Europe (Estellés et al., 2012). However, domestic residential emission also contributes to changes in the pollution level at Plymouth.

Figure 3.6 Map of Plymouth Mountbatten meteorological observatory at Plymouth. Image source: Google Earth

(f) Tiree, Inner Hebrides, Scotland

Tiree meteorological station (src id 18974) is based at Tiree Airport (56.49^{o} N, 6.87^{o} W), which is located at Isle of Tiree (follow Figure 3.1 and 3.7), Scotland. Tiree meteorological station was established in early 1920s at Cornaig school, which was overtaken by Air Ministry in 1942 during the second world war and later handed over to the meteorology office in 1946 for weather observations (Holliday, 2004). However, hourly visibility and meteorology data were available from 1957 (see Table 3.1). Tiree's unique geography distinguishes it from the other sites, which is covered in detail in section 3.6.3.

Figure 3.7 Geographical view of Tiree weather station. Image source: Google Earth

(g) Leuchars, Fife, Scotland.

Leuchars weather station (src id 235) is positioned at Leuchars Royal Air Force (RAF) base, which is located on the northeast coast of the county of Fife in Scotland (56.37^{o} N, 2.86^{o} W). For this study site 56 years of hourly visibility and meteorology data were collected (see Table 3.1). The RAF based weather site lies in a rural area, which is surrounded by small villages (RAF, 2014), agricultural fields and trees (see Figure 3.1 and 3.8). According to Scotland's Census (http://www.scotlandscensus.gov.uk/), the current population of the town of Leuchars (located 1 mile from the base) is approximately 2000.

Figure 3.8 Map showing the Leuchars meteorology station at leuchars. Image source: Google Earth

(h) Waddington, Lincolnshire, England.

Hourly visibility data including meteorology was measured at Waddington station (src id 384) for the period 1950-2012 (see Table 3.1). The site (Figure 3.1 and 3.9) is located at the base of the RAF station in Lincolnshire in the east of the UK (53.17^{o} N, 0.52^{o} W). The observatory is surrounded mostly by agricultural fields and villages. The weather station was established in the late 1940s; however, the station started to store recorded observation data in early 1950s. According to the UK's Office for National Statistics (https://www.ons.gov.uk/), the population of Waddington in 2011 was approximately 6000. The air quality of Waddington is mainly influenced by pollution from industrial activity in the East (Dick van Steenis, 1997).

Figure 3.9 Map of study site, Waddington Lincolnshire station located at of Royal Air Force base. Image source: Google Earth

3.5 Methodology

3.5.1 Trend analysis of visibility and other meteorological parameters

60 year trend analyses have been performed on the visibility dataset described in Data section 3.4. For long term trend analysis each days value was averaged (simple mean) to determine trends over decadal, annual and seasonal cycles. The seasonal periods were defined, as is typical, as winter (Dec-Feb), spring (Mar-May), summer (Jun-Aug), and autumn (Sep-Nov). Diurnal, day of the week and monthly averaged trends of visibility and RH were determined at each site using the 60 years of dataset, where weekdays and weekend are categorised as Monday-Friday and Saturday-Sunday respectively.

To examine the hygroscopic growth effect of aerosol particles upon visibility, the decadal data sets were disaggregated into RH bins. The aerosol hygroscopic growth effect on visibility was examined by using decadal mean visibility within specific relative humidity bins with the following boundaries: 52.5-57.5 %, 57.5-62.5 %, 62.5-67.5 %, 67.5-72.5 %, 72.5-77.5 %, 77.5-82.5 %, 82.5-87.5 %, 87.5-92.5 %, 92.5-97.5 %. The data with RH > 97.5 % due to likely presence of fog and mist at RH greater than this threshold was excluded.

To highlight the daily variation in RH, histograms of daily RH (at 12 noon) were generated using the following boundaries (0-10 %, 10-20 %, 20-30 %, 30-40 %, 40-50 %, 50-60 %, 60-70 %, 70-80 %, 80-90 %, and 90-100 %).

To evaluate the dominant meteorology at each site several meteorological analyses were conducted. Wind rose plots using the complete dataset time series were generated to highlight the dominant wind speed and direction for all sites. Decadal-seasonal bivariate polar plots of visibility using wind direction and wind speed allow

for spatial analysis of likely pollution sources (Carslaw and Ropkins, 2012). Finally time series plots of the following meteorological parameters were generated, RH, wind speed, wind direction and air temperature. These calculations were performed using the timePlot function in the openair package for R statistical program, which works on vector functions for wind direction averaging.

3.5.2 Estimation of aerosol and gas phase properties through analysis of RH dependent visibility

In this section the contribution of aerosol particles and gases upon visibility is estimated via mathematical modelling. In general horizontal visibility (V) can be defined via Koschmieder equation Eq. (3.1), where, horizontal visibility shows an inverse relationship with the extinction coefficient (β_{ext}). In the Eq. 3.1, constant (k) is equal to 3.912 which assumes a contrast threshold of 2 % (Koschmieder, 1924). The constant (k) is a measured by the threshold sensitivity of the observer's eye (Chang et al., 2009; Schichtel et al., 2001), which can vary from 2 to 5 % (Appel et al., 1985).

$$V = \mathrm{k}/\beta_{ext} \tag{3.1}$$

The extinction coefficient depends upon (β_{ext}) is the sum of the scattering (β_{sca}) and absorption coefficients (β_{abs}) as shown in Eq. (3.2).

$$\beta_{ext} = \beta_{sca} + \beta_{abs} \quad (3.2)$$

In the atmosphere, aerosol particles and gas phase species can both contribute to light scattering and absorption. However, the contribution of gas phase scattering to the total extinction is negligible except in the most pristine environments. Hence under UK conditions, the scattering component of the extinction coefficient can be assumed to be completely dominated by the presence of aerosol particles.

The ability of an individual particle to scatter radiation is dependent on its size, shape, morphology and refractive index (Appel et al., 1985; Liu and Daum, 2000). The particle scattering coefficient (β_{sca}) can be estimated by Mie theory as shown in Eq. (3.3) (Tang, 1996);

$$\beta_{scat} = \int_0^\infty \pi \left(\frac{D}{2}\right)^2 Q_{scat}(\alpha, \lambda, n) N f(D) dD \quad (3.3)$$

Where, *D* represents particle diameter, the aerosol size distribution is given by N*f(D)* and α is the size parameter (α = πD/λ). N is particle number concentration and $Q_{scat}(\alpha, \lambda, n)$ is single-particle scattering cross section, which depends upon size parameter (α), wavelength (λ) and refractive index (*n,* which is composition dependent). All these particle characteristics can change as the particle undergoes water uptake or loss which is dependent on the local RH. To parameterise the aerosol scattering enhancement due to water uptake an approach, similar to Titos et

al. (2014), is taken. The scattering enhancement is parameterised using a single hygroscopicity parameter (γ) using Eq. (3.4), where $\beta_{sca}(RH)$ and $\beta_{sca}(dry)$ are the aerosol scattering coefficients under a specified RH condition and completely dry conditions, respectively.

$$\frac{\beta sca(RH)}{\beta sca(dry)} = (1 - \frac{\mathrm{RH}}{100})^{-\gamma} \tag{3.4}$$

Rearranging Eq. (3.1), Eq. (3.2), and Eq. (3.4) allows for the relationship in Eq. (3.5) to be derived, where $\beta_{abs}(RH)$ and $\beta_{abs}(dry)$ are the combined aerosol and gas absorption coefficients under a specified RH condition and completely dry conditions, respectively.

$$Vis(RH) = \frac{3.912}{(1-\frac{\mathrm{RH}}{100})^{-\gamma} \times (\frac{3.912}{Vis\,(dry)} - \beta_{abs(dry)}) + \beta_{abs(RH)}} \tag{3.5}$$

To reduce the number of parameters within Eq. (3.5), it is assumed that $\beta_{abs}(RH) = \beta_{abs}(dry)$. This assumption always holds for gas absorption; and it is largely true for aerosol particles as well, although it is noted that particle absorption can increase due to lensing effects in mixed phase aerosol, and this lensing effect will be affected by aerosol water content e.g. (Lack and Cappa, 2010). After applying stated assumption in Equation 3.5, it can be now represented as in Eq. (3.6)

$$Vis(RH) = \frac{3.912}{(1-\frac{RH}{100})^{-\gamma} \times (\frac{3.912}{Vis\,(dry)} - \beta_{abs(RH)}) + \beta_{abs(RH)}} \quad (3.6)$$

To examine the contribution of the absorption coefficient to the total extinction coefficient, Eq. (3.5) can be further simplified by assuming that all absorption due to both gases and particles is negligible compared to the RH dependent aerosol scattering, leading to the two parameter Eq. (3.7).

$$\log\,[Vis(RH)] = \gamma \log\left[1 - \left(\frac{RH}{100}\right)\right] + \log\,[Vis(dry)] \quad (3.7)$$

Equations (3.6) and (3.7) can be used to obtain information about aerosol scattering and gas and aerosol absorption, with associated assumptions, through fitting of the measured visibility at a given RH. Equation (3.7) is linear and so can be fitted using the linear least squares fitting algorithm, whereas Eq. (3.6) requires non-linear least squares fitting algorithm. The statistical program R was used for all fittings (Version 0.99.489). The 'lm' algorithm was used for linear fitting, and the 'nls' fitting algorithm was used for the non-linear fitting. The 'nls' algorithm was always initially run with no lower or upper boundaries for the 3 fitting parameters (*Vis(dry)*, β_{abs} and γ) specified. However, when fits produced negative values for β_{abs}, which are physically impossible, a lower boundary for β_{abs} was specified to be zero.

3.5.3 Gas absorption

All gases scatter radiation via Rayleigh scattering but the effect is negligible in all but the most pristine visibility conditions (which are not observed in this study). The only atmospheric gas present at levels that lead to significant absorption of visible light is NO_2 (Ferman et al., 1981; Groblicki et al., 1981). The contribution of NO_2 to visibility can be quantified by its absorption coefficient ($\beta_{NO_2 abs}$). The effect of the NO_2, absorption coefficient, at 550 nm wavelength, was calculated using the relationship from Groblicki et al. (1981), shown in Eq. (3.7), where [NO_2] is the NO_2 in ppm.

$$\beta_{NO_2 abs} = 3.3\times10^{-4}[NO_2] \quad (3.7)$$

3.6 Results and Discussion

3.6.1 Historical trend of annual and seasonal visibility

The annual and seasonal mean visibility at 12 noon have been calculated for all eight stations, see Fig. 3.10.1 and Fig. 3.10.2. The effect of changing the visibility observation technique from human observation to automatic observation via visiometers (which is highlighted by different shading in Fig. 3.10.1) is very clear at some sites. In particular, two stations, Tiree and Aldergrove, do not show realistic values after the changeover from human to automated measurement, with the changeovers coinciding with large and sustained drops in recorded visibility. The effect of human to automated changeovers at Heathrow, Leuchars, Nottingham, Ringway and Waddington sites appears to be minimal, with the pre-changeover long

term trends being continued after the changeover. Furthermore the annual data from these sites exhibit similar year to year variance before and after changeover. The long term trend at the Plymouth site is similar before and after changeover but the year to year variance is much reduced once measurement automation is installed. This likely indicates strong localised sources (ship and traffic emissions from nearby ports and roads) close to the visiometer at the Plymouth site. Henceforth it is assumed that all stations, except Aldergrove and Tiree, are performing adequately for both human and automated visibility measurement. Therefore the time series, as shown in Fig. 3.10.1, are used in their entirety for the analysis of these six stations. The time series data for the Aldergrove and Tiree stations are used up until automation occurs.

A similar variation in visibility trends is observed for the period of 1950-1997, comparing with Doyle and Dorling (2002). However, this study reports overall lower visibility values when compared to Doyle and Dorling (2002). These differences are due to slightly different data filtering methodologies. Doyle and Dorling (2002) filtered data for 12 noon, relative humidity > 90% and PR codes of 00-05 in their statistical analysis for the period of 1950-1997. However, due to uncertainty and unavailability of PR code after 1997, these codes were not used. Furthermore, mean averaging for statistical analysis, where data is filtered for 12 noon and relative humidity > 99 %, was performed. The filtered data accounts for 0.91 – 3.44 % of the total data dependent upon site location. Number of data points removed due to the filtering of data with RH > 99 % is very low. Therefore removing these points does not make any significant difference. The details of uncertainty and

unavailability of PR codes and used data filtration method are given in data and methodology sections.

Clear trends of increasing annual visibility are observed for four sites: Ringway, Waddington, Nottingham, and Heathrow with the rate of visibility increase being 0.339±0.016 km year^{-1}, 0.293±0.010 km year^{-1}, 0.235±0.023 km year^{-1} and 0.201±0.018 km year^{-1}, respectively, where standard errors were determined at the 95 % confidence interval. A, more gradual increasing trend was observed at the Leuchars site (0.157±0.019 km year^{-1}). The Plymouth site shows a more variable trend with increases from ca. 1950-1990 followed by decreases from ca. 1990-2006 which is then followed by more increases in the most recent measurements. The long term trend for Plymouth 1950-2013 is near constant (0.040±0.021 km year^{-1}). Both the Aldergrove and Tiree sites, with the automated data omitted, show near constant long term visibility with long term rates of visibility change calculated to be 0.0562±0.021 km year^{-1} and -0.0892±0.014 km year^{-1}, respectively.

The seasonal trends for the 8 sites are detailed in Table 3.3. Poorest visibility was observed in the winter season compared to other seasons mostly due to the seasonal rise in RH (discussed in section 3.6.3). Another reason is the greater concentration of particles in the environment due to lower mixing layer height in the winter season (Jayamurugan et al., 2013). Furthermore, the long term rate of visibility change in the winter season is significantly higher as compared to spring, summer and autumn seasons for all stations apart from the Ringway station. At Ringway station the rate of change of visibility is higher in spring (0.363±0.018 km year^{-1}) as compared to winter (0.330±0.020 km year^{-1}). All stations show positive rates of visibility change in winter season except for Tiree (-0.186±0.012 km year^{-1}).

It is also observed that Aldergrove station shows negative rate of visibility change in the summer season (-0.417±0.036 km year^{-1}).

The improvement in median visibility at most of the sites can be seen in Fig. 3.11. Moreover, Boxplots of the decadal visibility are also produced showing the median, interquartile range, outliers etc. (see Figure 3.12).

Improved visibility at most of the sites is due to reduction in air pollution and the likely changes in fuel use and consumption that took place after 1956 Clean Air Act. The Clean Air Act was introduced with the aims of reducing smog, smoke and sulphur dioxide concentrations in the environment. In particular, the policy focused on industrial emission sources and its reduction (Williams, 2004). Recently, Harrison et al. (2015) have shown that concentration of sulphur dioxide, coal smoke, nitrogen dioxide, suspended matter (black smoke) and PM were significantly reduced in the UK over last five decades as the result of switching to cleaner fuels after 1956 Clean Air Act.

Rainfall data has been used to investigate the impact on visibility for all 8 study stations. Daily rainfall data from 12 noon averaged over each year is shown in Fig. 3.13. Figure 3.14 shows a comparison between annual average visibility that has been filtered for when rainfall is present (hourly rainfall > 0 mm) and non-filtered data. The percentage of data removed by filtering for rain accounts for 8 - 13% of the total data dependent upon the site location, with the Tiree and Aldergrove sites having the highest percentage of rainfall. It is observed that filtering for rainfall only results in very small visibility increases for some stations. Overall the effect is negligible in most circumstances. Therefore the non-filtered data is used in this study.

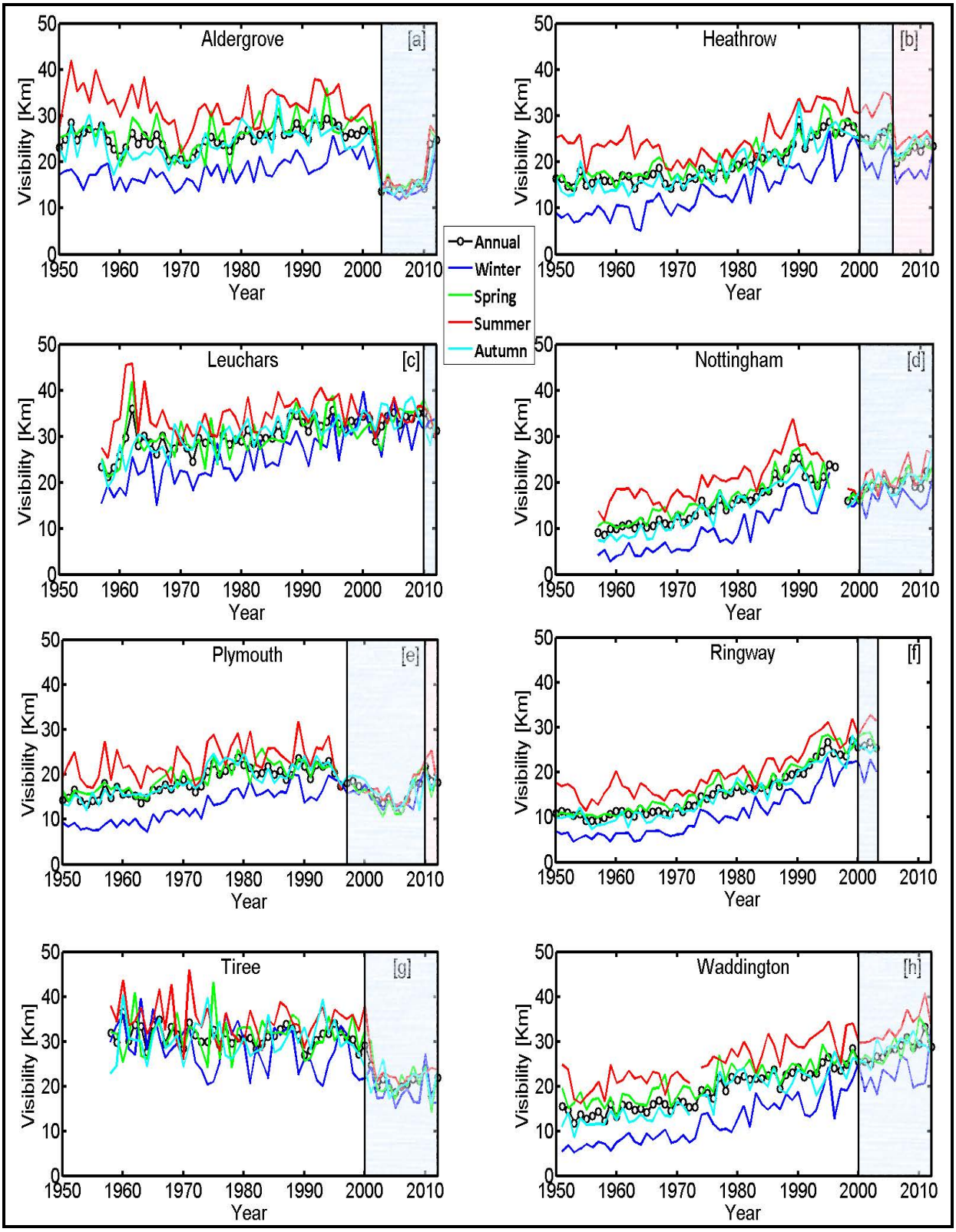

Figure 3.10.1 Historical trend of annual and seasonal visibility derived from daily (12 noon) observations by station: **a)** Aldergrove **b)** Heathrow, **c)** Leuchars, **d)** Nottingham, **e)** Plymouth, **f)** Ringway, **g)** Tiree, **h)** Waddington. Shading indicates changes in measurement methodology, where white is human observation, while blue and red are automated observation using different instruments. For further details see the Table 3.2

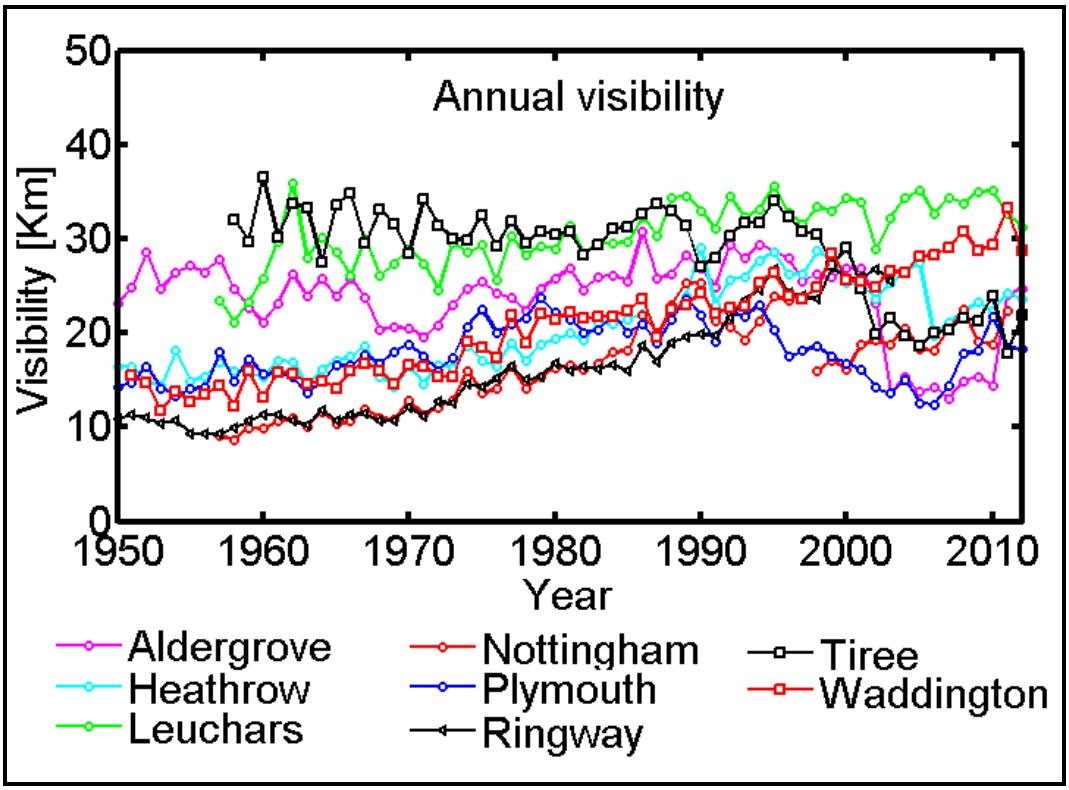

Figure 3.10.2 Historical trend of annual visibility derived from daily (12 noon) observations by all 8 sites.

Table 3.3 Rate of change of visibility (in km year^{-1}) with their standard error at 95% confidence interval

Satiation	Year	Annual	Winter	Spring	Summer	Autumn
Plymouth	1950-2012	0.040 ± 0.021	0.152 ± 0.017	0.006 ± 0.025	-0.043 ±0.031	0.049 ± 0.022
Aldergrove	1950-2002	0.056 ± 0.021	0.110 ± 0.019	0.831 ± 0.030	-0.417 ±0.036	0.074 ± 0.029
Heathrow	1950-2011	0.201 ± 0.018	0.231 ± 0.021	0.181 ± 0.020	0.145 ± 0.028	0.226 ± 0.020
Ringway	1950-2004	0.339 ± 0.016	0.331 ± 0.020	0.363 ± 0.018	0.316 ± 0.025	0.343 ± 0.018
Waddington	1950-2012	0.293 ± 0.010	0.331 ± 0.019	0.245 ± 0.016	0.270 ± 0.018	0.325 ± 0.016
Leuchars	1957-2012	0.157 ± 0.019	0.286 ± 0.027	0.140 ± 0.030	0.030 ± 0.034	0.180 ± 0.025
Tiree	1957-2002	-0.089 ± 0.014	-0.186 ± 0.014	-0.035 ± 0.015	-0.098 ±0.015	-0.046 ± 0.015
Nottingham	1957-2012	0.235 ± 0.023	0.293 ± 0.022	0.214 ± 0.024	0.149 ± 0.033	0.270 ± 0.022

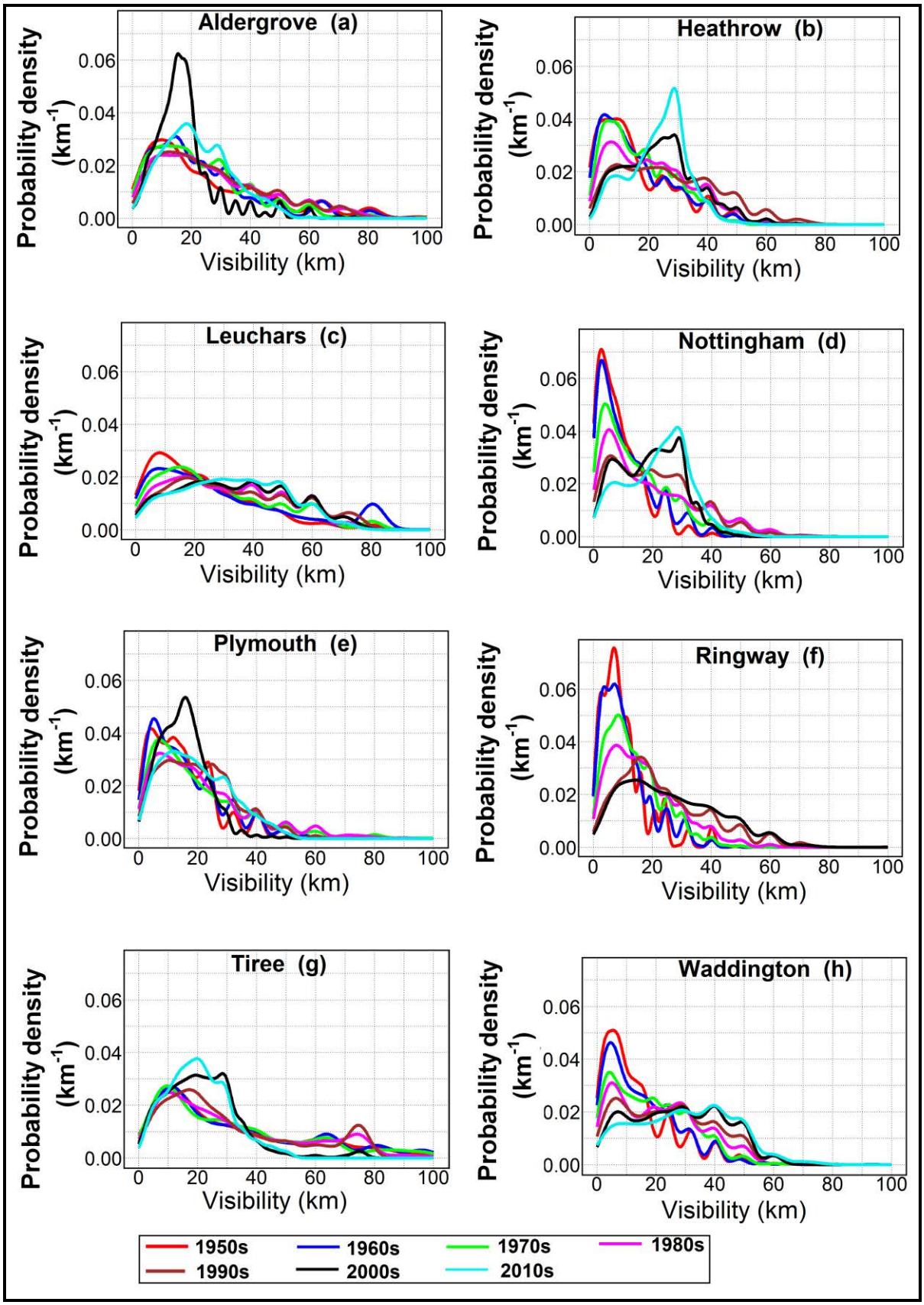

Figure 3.11 Occurrence of different visibility range for eight UK study sites during different decades.

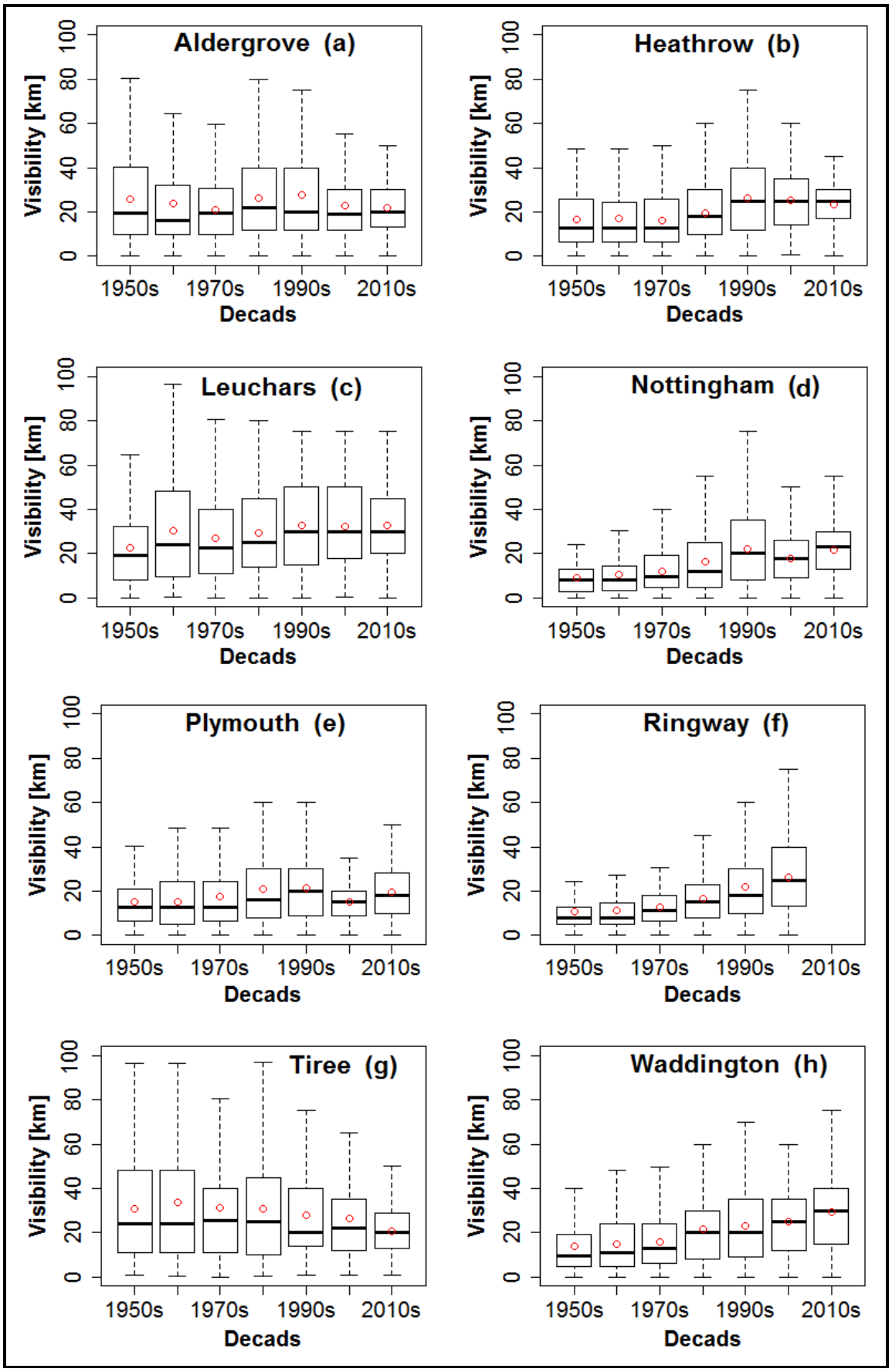

Figure 3.12 Boxplot of decadal visibility at eight different study sites, where red circle denotes mean value of decadal visibility

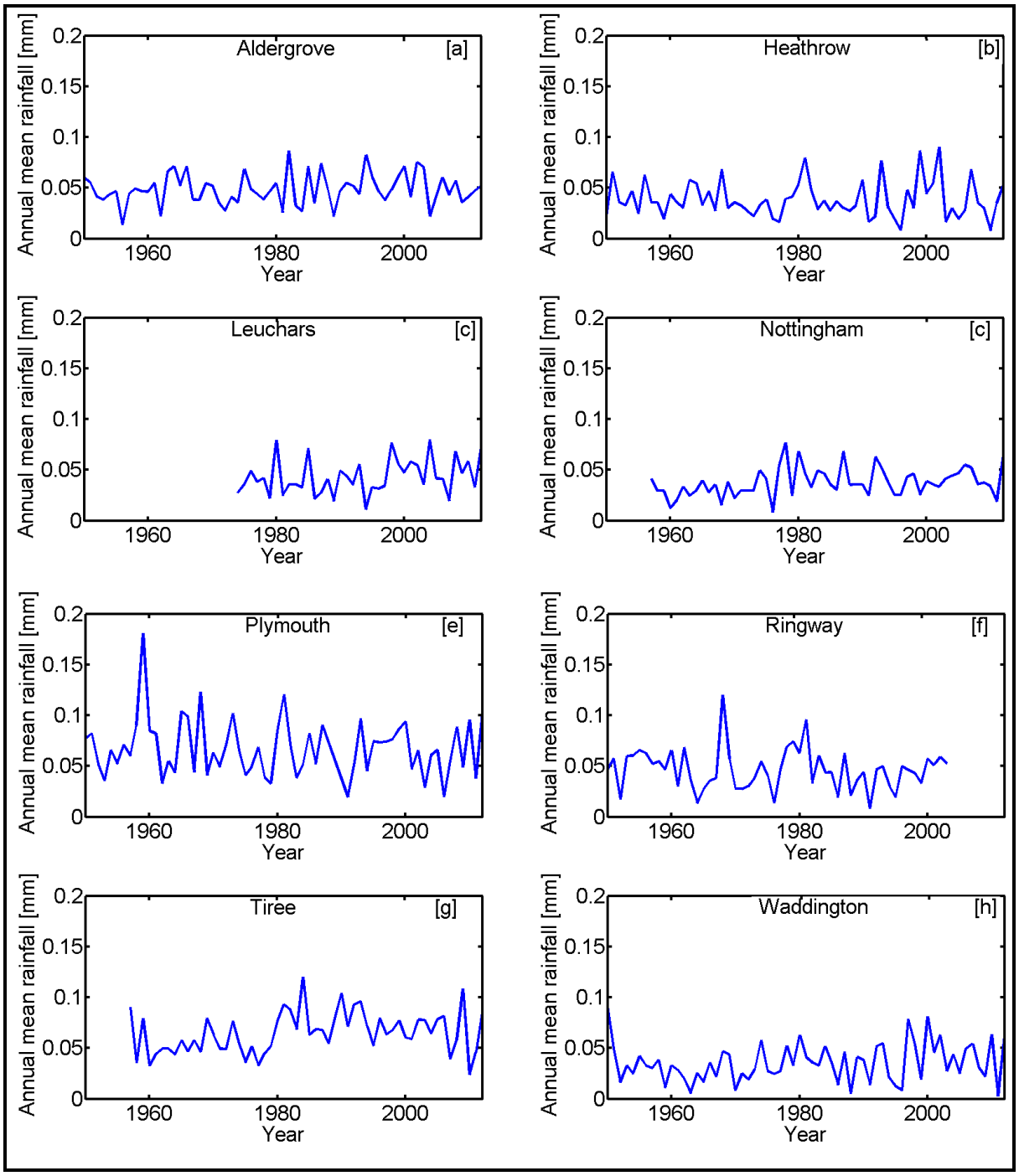

Figure 3.13 Historical trend of annual mean rainfall derived from daily (12 noon) observations by station: **a)** Aldergrove **b)** Heathrow, **c)** Leuchars, **d)** Nottingham, **e)** Plymouth, **f)** Ringway, **g)** Tiree, **h)** Waddington.

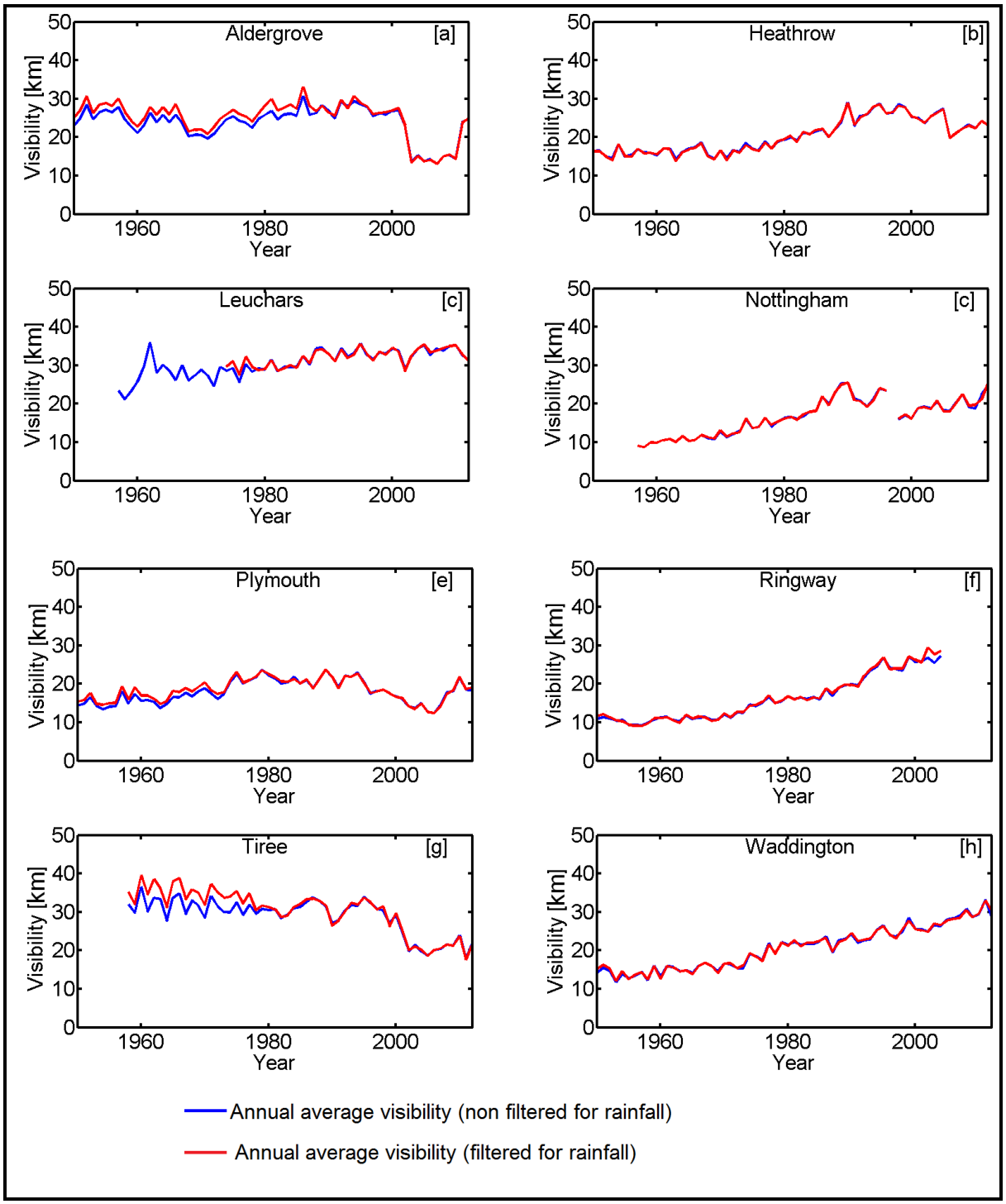

Figure 3.14 Historical trends of annual mean visibilities (with and without filtering for precipitation) derived from daily (12 noon) observations by station: **a)** Aldergrove **b)** Heathrow, **c)** Leuchars, **d)** Nottingham, **e)** Plymouth, **f)** Ringway, **g)** Tiree, and **h)** Waddington.

3.6.2 Evaluation of historical wind-data

3.6.2.1 Wind Roses for the 8 study stations

A graphical representation of historical wind speed and direction at the eight chosen stations is shown in Fig. 3.1 using the wind rose polar co-ordinate representation. These graphs describe the most probable wind speeds and directions over the whole time series (Carslaw and Ropkins, 2012). As expected, the graphs show that the predominant wind directions in the UK are from the southwest. However, there are clear variations between the different stations. The range of wind speed varies from 0-35 m s^{-1} dependent upon location, with the more coastal sites experiencing greater average wind speeds.

3.6.2.2 Analysis of influence of wind speed and wind direction on visibility

Decadal-seasonal bivariate polar plots are presented for all eight stations in Fig. 3.15.1 and Fig. 3.15.2; these diagrams provide information on the variation of visibility with wind speed and direction and can suggest locations for visibility degrading sources. The detailed analyses of each site are given below:

(a) Aldergrove: Overall, lower values of visibility were observed when the wind was from the south to east, while above average values were collected when the wind was from the north to west direction. Intermediate visibility was generally observed when the wind came from the south to west or north to east quadrants. Distinct differences are observed between the different seasons. In particular, in the summer visibility with wind from the north to west direction was higher compared to other seasons in every decade. It is clearly seen that visibility has improved the most when wind comes from the south to east direction which covers mainland urban

areas such as Belfast, the major regional city. It is noted that the seasonal and polar trends are similar between the visiometer (2000s–2010s) and human derived (1950s–1990s) data sets even though the absolute magnitudes are different as noted above.

(b) Heathrow: Low visibility was observed whenever wind speeds were lower than 5 m s^{-1} in any direction which implies a significant local source of visibility degrading pollutants. Since Heathrow is the site of major international airport, with commensurate road and other transport infrastructure, this is not surprising. Overall, lower visibility is also seen when the wind direction comes from the northeast to southeast direction which is consistent with visibility reducing pollution arriving from the Greater London area. The highest visibilities are typically observed when the wind direction is from the north to southwest which is consistent with less densely populated surrounding areas. In particular during summer visibility in the northwest wind direction was highest compared to other seasons in every decade. It is identified that visibility has improved in all wind directions, but most significantly in the easterly direction which covers the London urban centre. The change in visibility illustrates the dramatic improvement of air quality in London since the introduction of the Clean Air Act in 1950s (Brimblecombe, 2006).

(c) Leuchars: Two distinct spatial groupings of visibility are clearly observed. When the wind direction comes from the northeast to southwest (clockwise) visibility is generally lower, and it is generally higher when the wind direction is from the northeast to southwest (anti-clockwise). The lowest visibilities are from the southeast direction in all seasons. The spatial pattern of low visibility suggests a maritime aerosol source as the major source of visibility reduction whilst high

visibility was associated with air which had passed over the predominantly rural Scotland. Visibility in the northwesterly wind direction was highest in the summer months, as expected see Fig. 3.10.1 and 3.16, compared to other seasons in every decade.

(d) Nottingham: Like Heathrow, the poorest visibility conditions occurred when wind speed was below 10 m s^{-1} suggesting local sources of visibility degrading pollutants. Visibility is often lowest when the wind comes from the southeast direction consistent with the relative placement of Nottingham city centre to this direction (the meteorological station is actually located in Watnall just about 5 miles of Nottingham city centre). Visibility is generally highest when the wind comes from the west and southwest directions which is largely consistent with air masses passing over less urban areas compared to the other wind directions. During the summer months, visibility in southwest direction was highest compared to other seasons in every decade. It is clear from Fig. 3.10.1 that visibility has increased in all seasons, and the strongest improvement is seen in air from the southeast as seen in Fig. 3.15.2.

(e) Plymouth: In general, the lowest visibility was observed when the wind comes from southeast to southwest direction which is consistent with maritime air causing the lowest visibility which suggests a maritime source of aerosol causing visibility degradation. The highest visibilities are observed when wind comes from the northwest to northeast directions, and in particular the northeast, this is consistent with airmasses passing over relatively rural areas. Regardless of the direction of wind, the summer months showed higher visibility than all other seasons. It is identified that visibility has improved over time for all wind directions.

(f) Ringway: Overall visibility was poor at low wind speeds and when the wind direction was from the northeast to southeast. Ringway is the location of Manchester International Airport so, like Heathrow, there is likely to be a significant local source of visibility degrading pollutants arising from the airport and its associated infrastructure. The wind directions associated with higher visibility are a lot more variable in time and space when compared to other locations. However, in general, high wind speeds from either the northwest or south west directions are often associated with higher visibility. Since the 1960s visibility has improved for all wind directions. In particular, visibility associated with air masses coming from the direction of the Greater Manchester Area to the north has shown a marked increase since the 1970s.

(g) Tiree: The island of Tiree has by far the highest visibility at low wind speeds. Overall low visibility was observed when wind came from the west to southeast, while highest visibility occurred with wind from the northeast. The spatial variation of low visibility is consistent with a maritime source of visibility impairing aerosols. The higher the wind speed typically the lower the visibility which is consistent with greater aerosol production from greater wave activity (Venkataraman et al., 2002). The higher visibility from the northeast is consistent with air masses passing over the larger rural highlands of Scotland. Visibility was relatively stable for all wind directions for all decades of the human observation data series which is consistent with this rural maritime site being largely unperturbed by anthropogenic pollution.

(h) Waddington: In general, lower visibility is observed when wind speeds are lower than 10 m s^{-1} which is consistent with local pollution sources. Low visibility is also observed when the wind direction is from the east to southeast which

potentially indicates a maritime source. Higher visibility is observed from the west at high wind speeds. Visibility has improved for wind from all directions since the 1970s.

Overall it is clear that visibility has improved at most of the sites for most local wind directions. The most marked improvements in visibility are seen in directions when air masses pass over major metropolitan areas such as Greater London and Greater Manchester. Whilst most of the visibility changes can be ascribed to the location of the meteorological stations with respect to either urban or maritime sources, it is noted that for most sites the wind direction with the lowest visibility overall is often from the East, i.e. continental Europe and hence synoptic scale pollution events which affect visibility. Poor air quality, in the UK, is often associated with synoptic scale events originating in continental Europe (Charron et al., 2007a; Charron et al., 2013; Charron et al., 2007b; Lee et al., 2006)

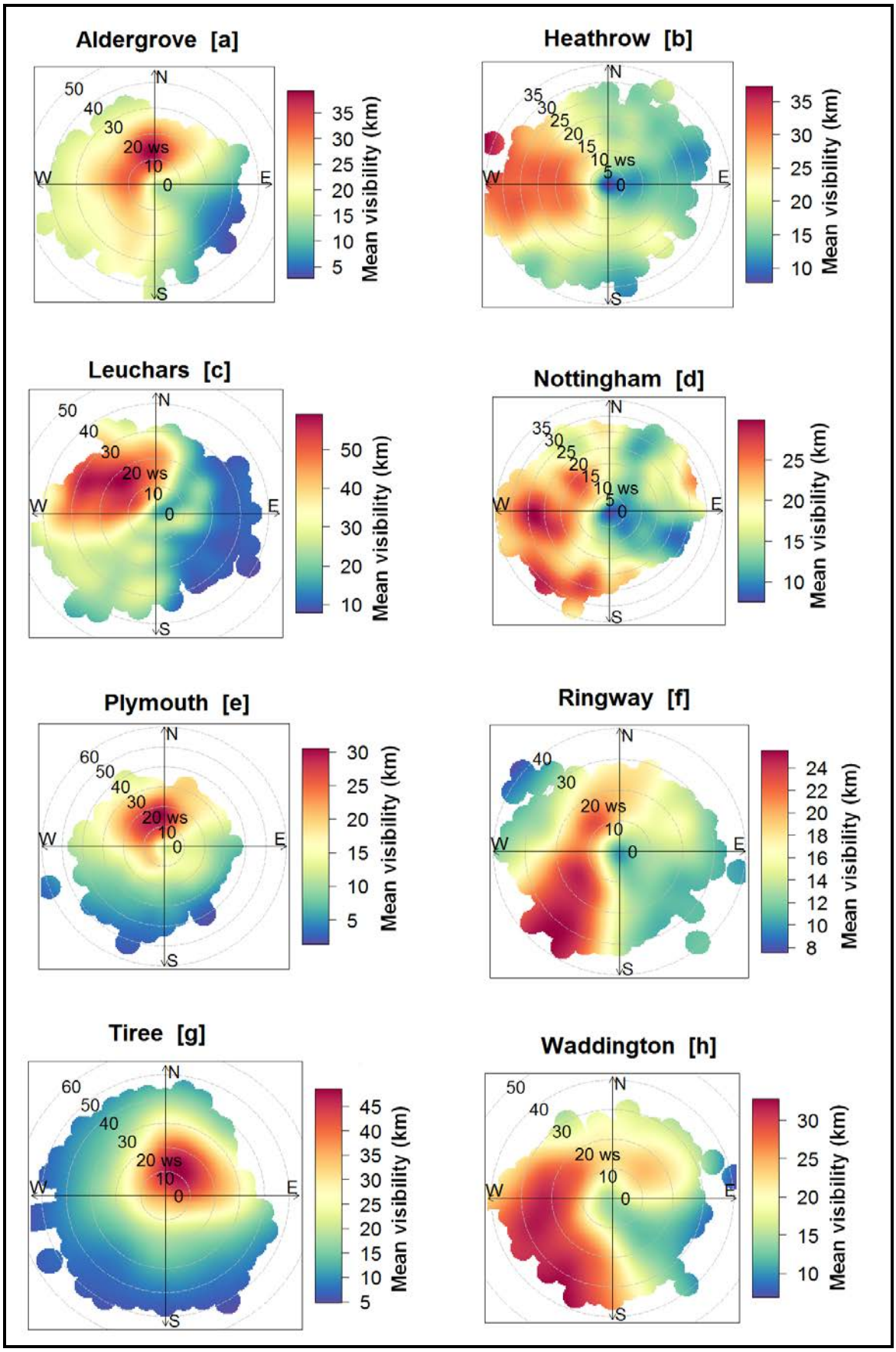

Figure 3.15.1 Overall polar plots for all eight stations, derived from observation between1950s to 2010s.

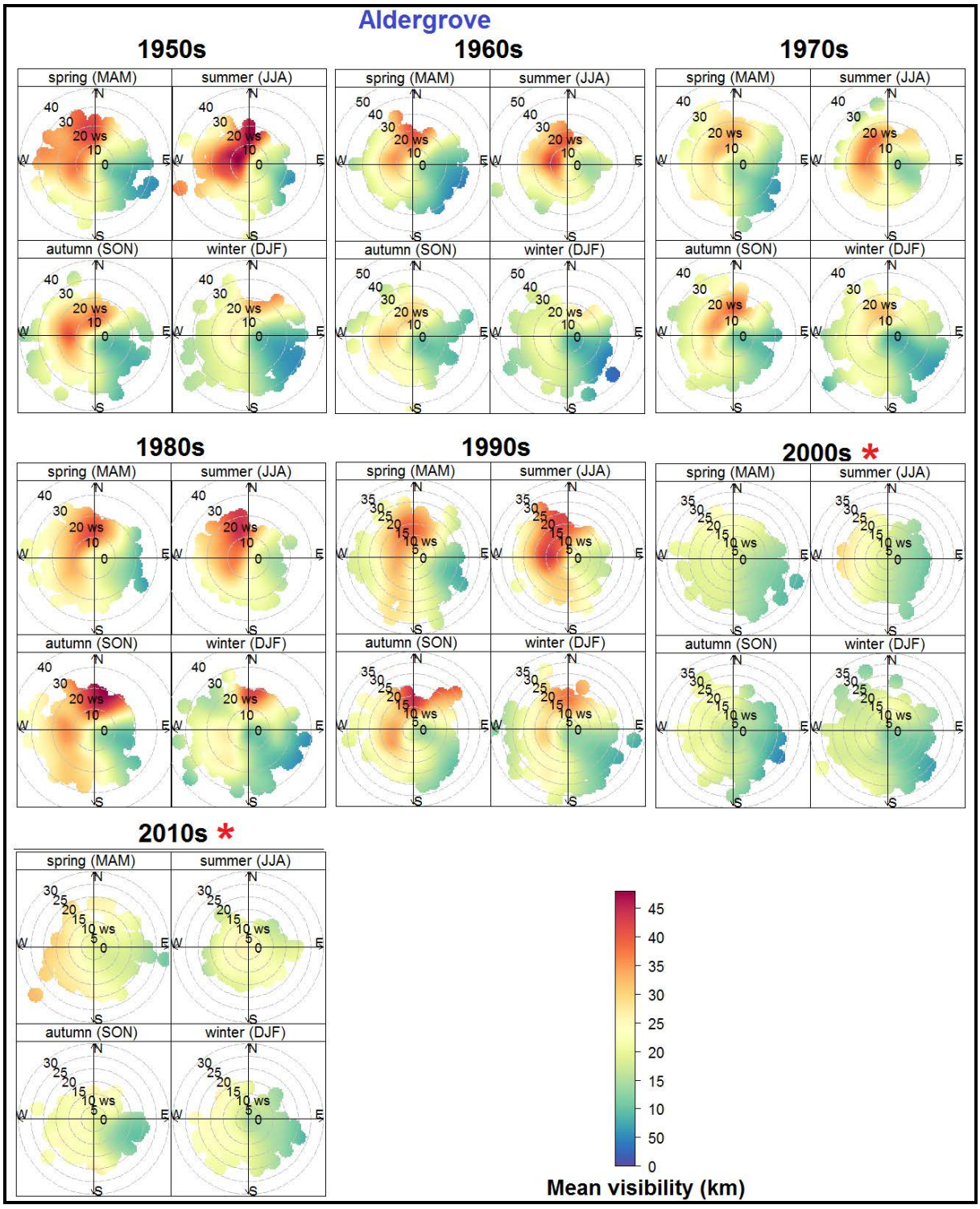
Aldergrove
1950s
1960s
1970s
1980s
1990s
2000s *
2010s *
spring (MAM)
summer (JJA)
autumn (SON)
winter (DJF)
N
E
S
W
ws
Mean visibility (km)
0
10
50
15
20
25
30
35
40
45

Continue…

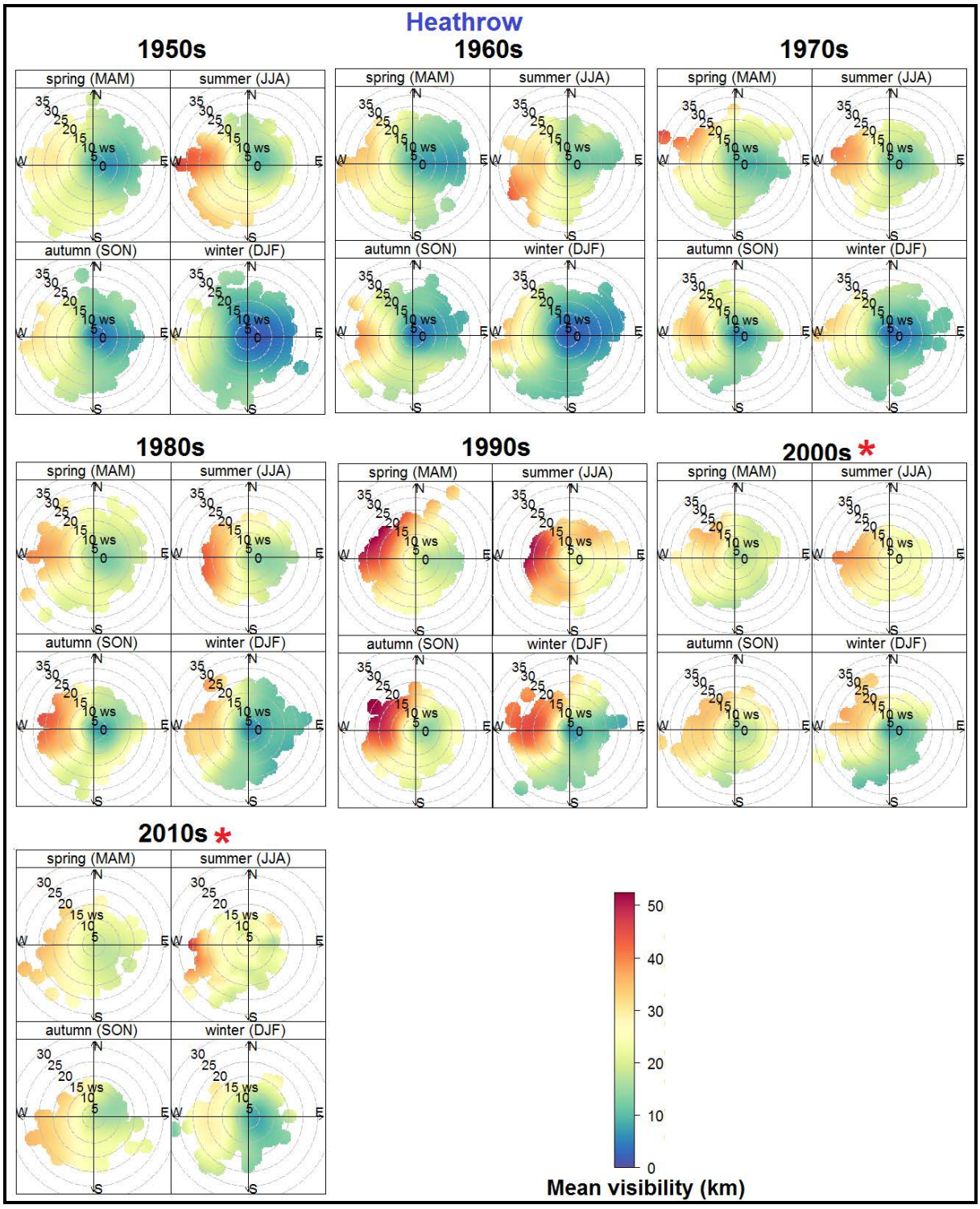
Heathrow
1950s
1960s
1970s
1980s
1990s
2000s *
2010s *
spring (MAM)
summer (JJA)
autumn (SON)
winter (DJF)
N
E
S
W
ws
Mean visibility (km)
0
10
20
30
40
50

Continue…

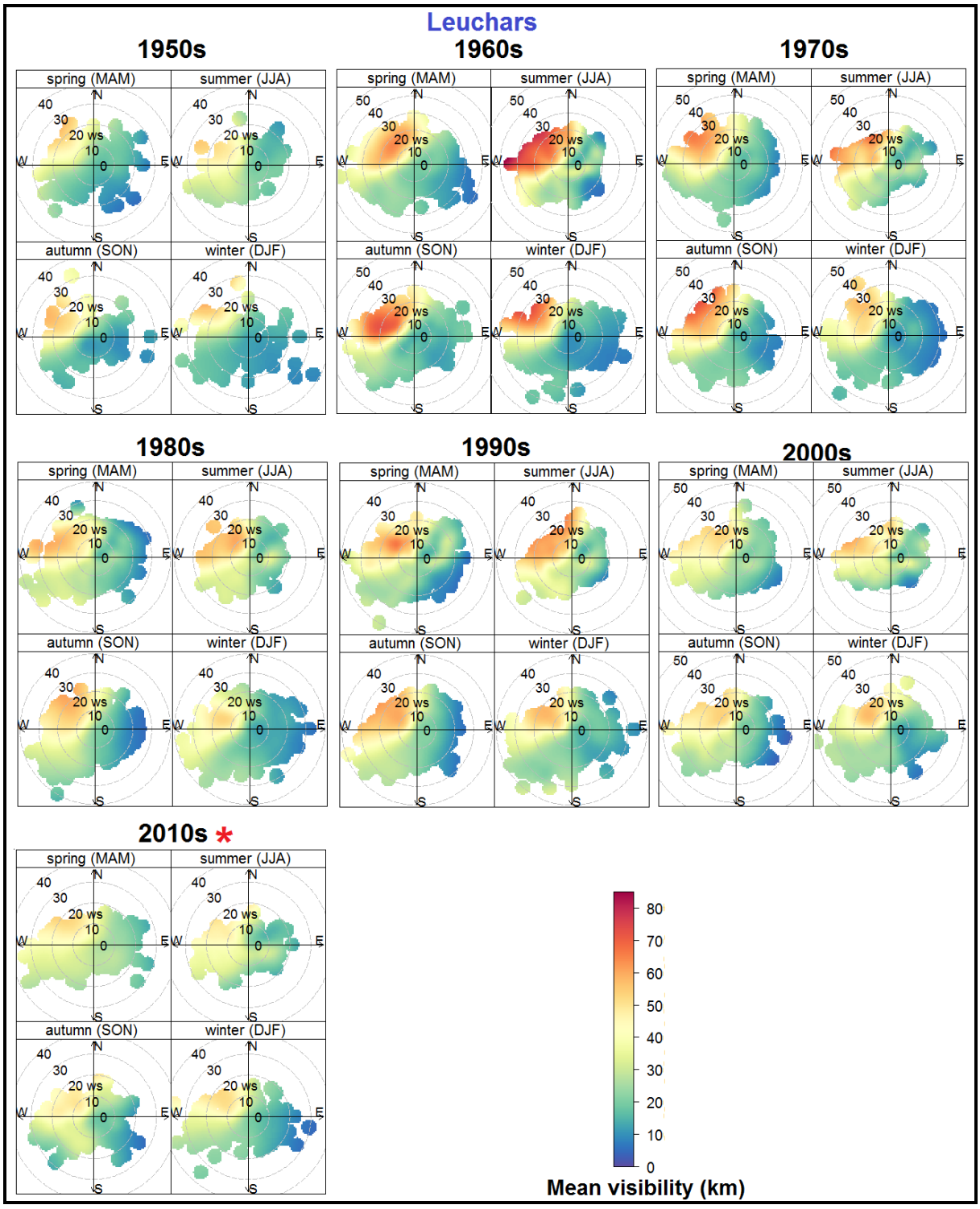
Leuchars
1950s
1960s
1970s
1980s
1990s
2000s
2010s *
spring (MAM)
summer (JJA)
autumn (SON)
winter (DJF)
N
E
S
W
20 ws
10
0
30
40
50
80
70
60
50
40
30
20
10
0
Mean visibility (km)

Continue…

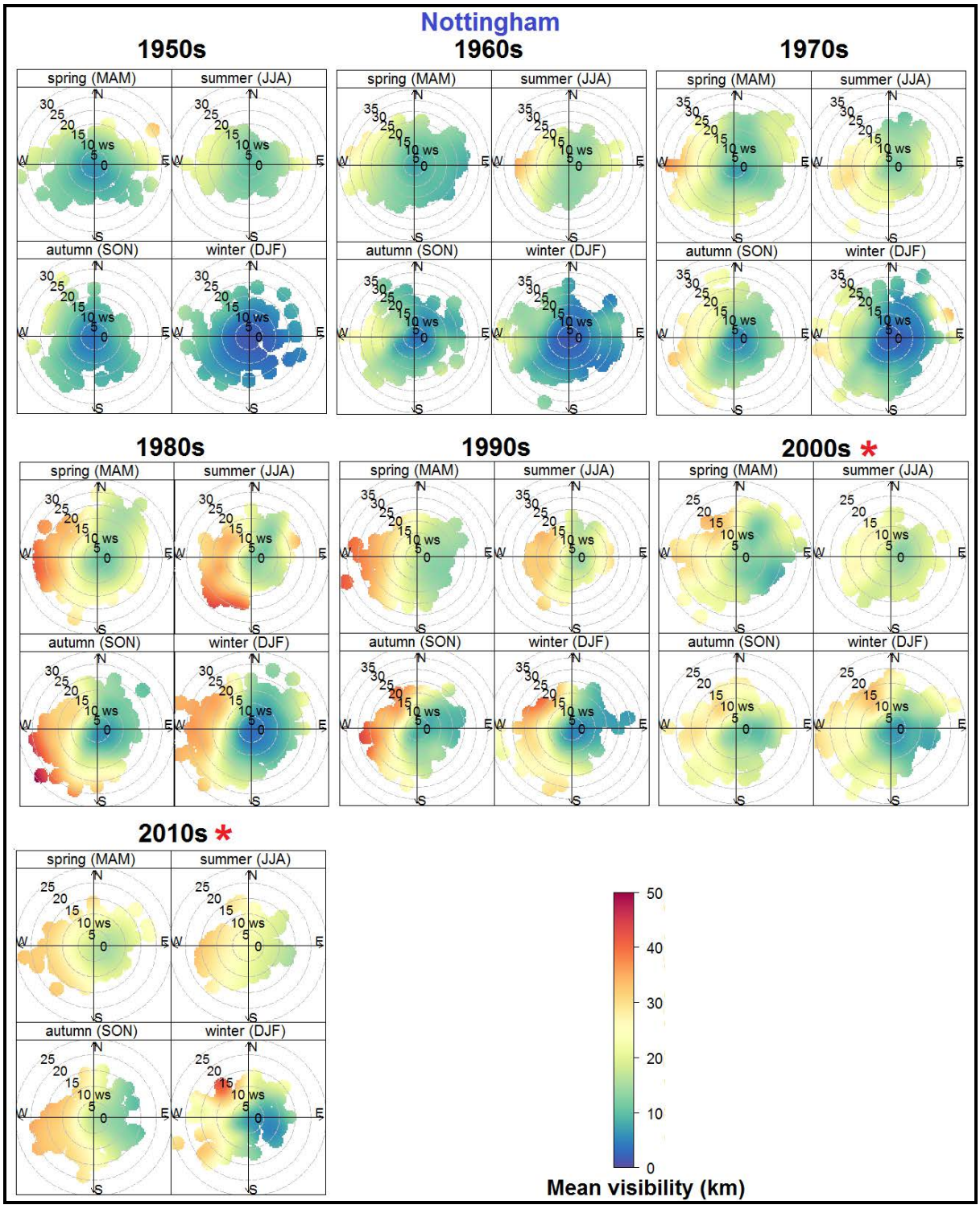
Nottingham
1950s
1960s
1970s
1980s
1990s
2000s *
2010s *
spring (MAM)
summer (JJA)
autumn (SON)
winter (DJF)
ws
N
E
S
W
0
10
40
50
Mean visibility (km)

Continue…

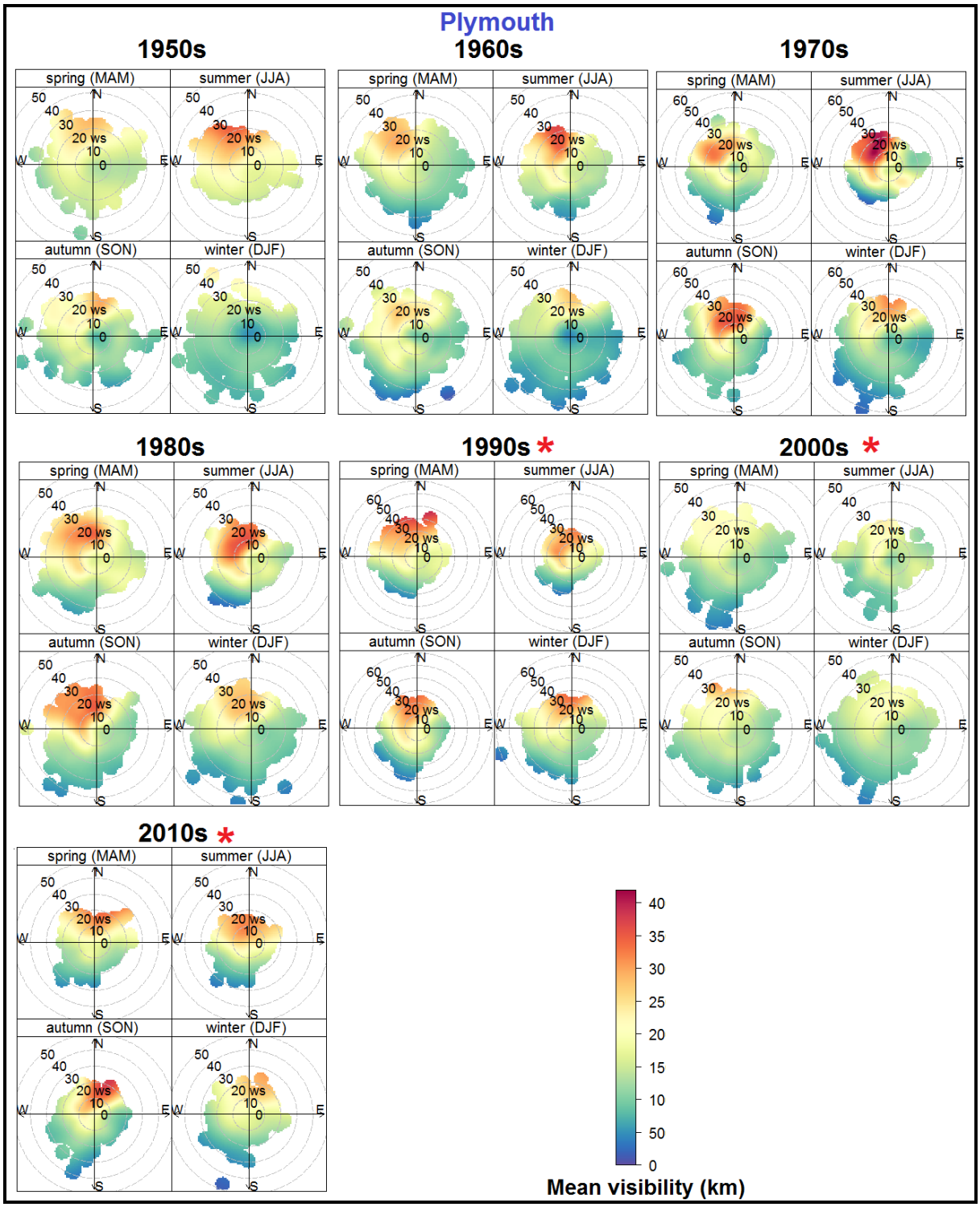
Plymouth
1950s
1960s
1970s
1980s
1990s *
2000s *
2010s *
spring (MAM)
summer (JJA)
autumn (SON)
winter (DJF)
Mean visibility (km)

Continue…

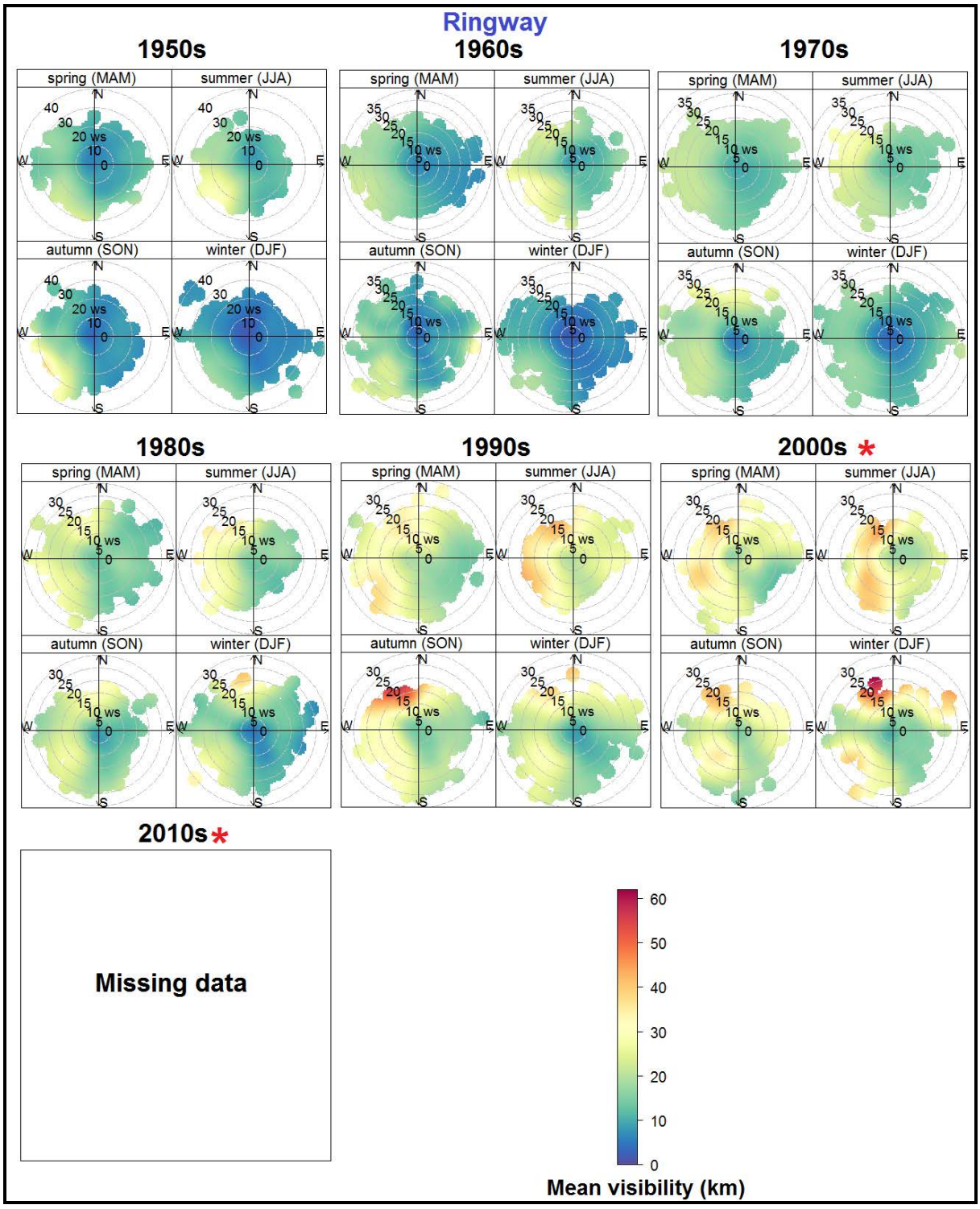
Ringway
1950s
1960s
1970s
1980s
1990s
2000s *
2010s *
spring (MAM)
summer (JJA)
autumn (SON)
winter (DJF)
Missing data
Mean visibility (km)

Continue…

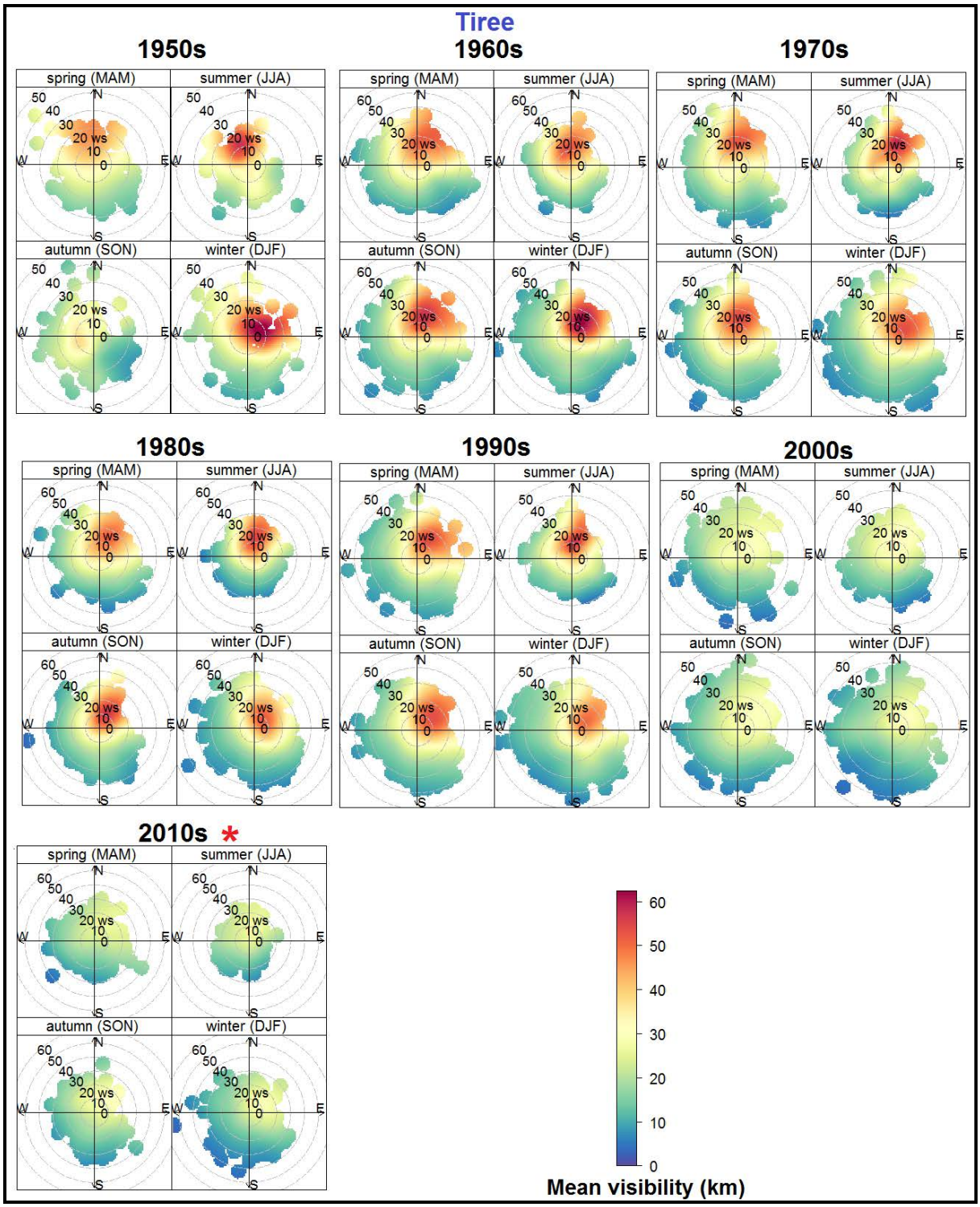
Tiree
1950s
1960s
1970s
1980s
1990s
2000s
2010s *
spring (MAM)
summer (JJA)
autumn (SON)
winter (DJF)
Mean visibility (km)

Continue…

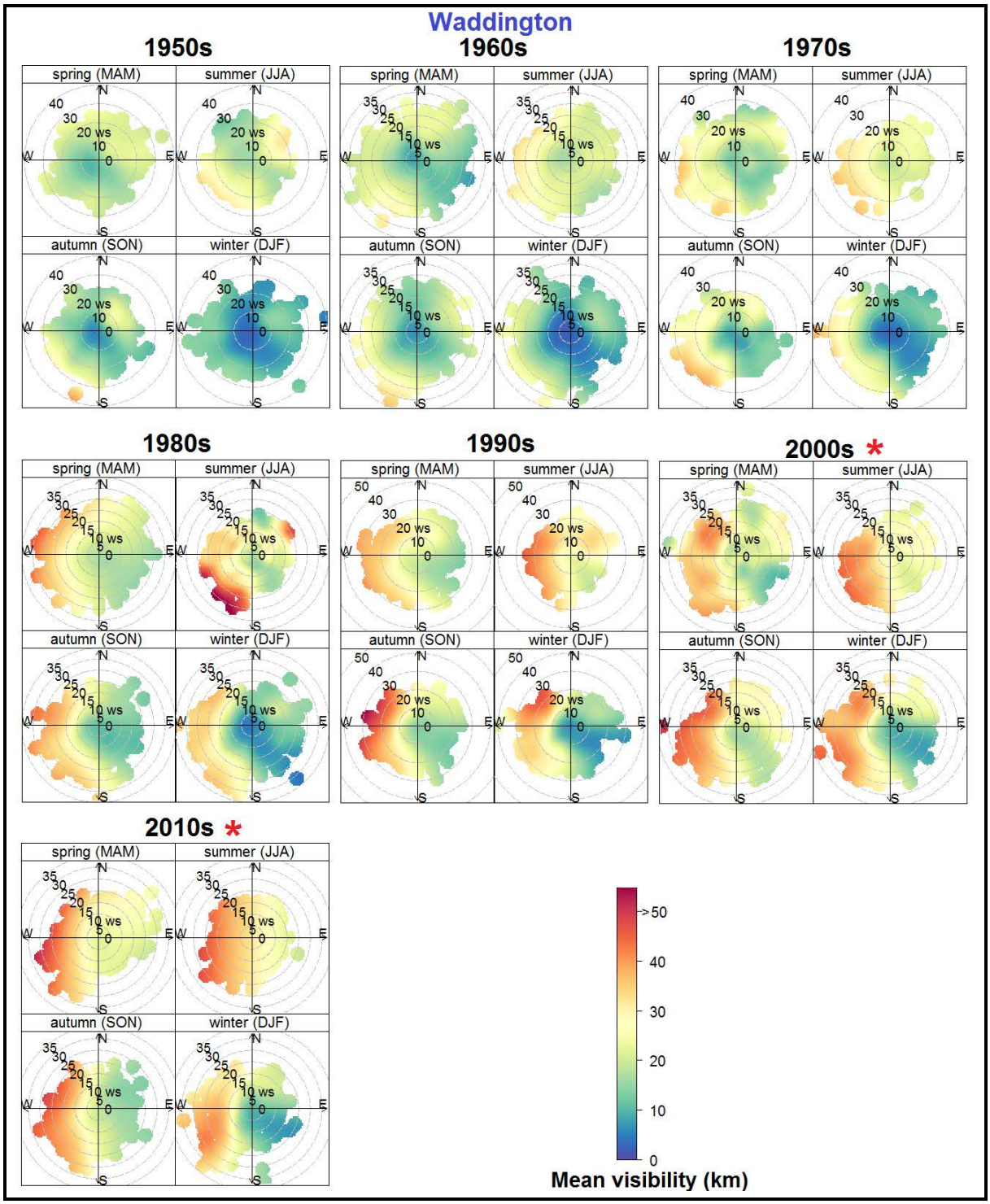

Figure 3.15.2 Decadal seasonal polar plots for all eight stations for 1950s, 1960s, 1970s, 1980s, 1990s, 2000s and 2010s (left to right). * represents years where visiometer measured data is included.

3.6.3 Correlation between RH and visibility: seasonal, day of the week and decadal effects

Figure 3.16 provides monthly values for visibility and RH, averaged over the whole time series, for each station. This figure clearly illustrates that visibility shows a strong seasonal cycle which is anti-correlated with RH at all stations. The relationship at Tiree is less strong compared to the other seven sites. The geographical location of Tiree, which is a maritime island, is the likely reason for the RH trend being different to the other stations. Tiree Island has a very flat landscape, which does not provide shelter from wind in any direction; this directly affects the local meteorology (Holliday, 2004). Overall, the monthly trends indicate that visibility is lowest in winter and highest in summer with spring and autumn being intermediate in visibility values.

In addition to the seasonal cycle, there is a clear day of the week effect on visibility changes at most sites (Fig. 3.16), where visibility improves sharply at the weekend with Sunday showing the highest visibility. It is observed that visibility improves at Sunday from 5 % to 12.5 % (depending upon area) as compared to other week days (Mon-Fri). Lower traffic and industrial emissions at the weekend are the likely reasons for better visibility at the weekend due to less pollutant emissions. The inherent assumption in this analysis is that traffic is higher during week days compared to the weekend. It is noted that visibility tends to peak on Sunday (rather than both Saturday and Sunday) and this may reflect the non-negligible timescale required for pollutant removal by wind driven dispersion, i.e. the build-up of pollution during weekdays is not fully dispersed until Sunday. The same argument explains

why visibility is typically higher on Mondays compared to the other weekdays later in the week.

The long term decadal (1950s–2010s) variation in visibility with RH is shown in Fig. 3.17, for all 8 stations, where the visibility is averaged within RH bins. A qualitatively similar pattern has been observed for all stations: Visibility is observed to vary strongly with relative humidity, which clearly indicates a significant particle hygroscopicity effect on visibility. It is noted that very high RH can also be indicative of precipitation which also decreases visibility.

To further highlight the effect of RH on visibility, the mean monthly visibility trend is compared to RH for the 60 years of data recorded at the Waddington station, see Fig. 3.18. A scatter plot of visibility versus RH reveals a clear near-linear relationship (linear fit R^2 = 0.60) between the variables. Removal of the long term trend in the visibility data was achieved by fitting the visibility to a quadratic function and subtracting the quadratic function from the time series. A scatter plot of the long term detrended visibility data versus RH reveals a more linear relationship (R^2 = 0.66) where every rise in RH of 10 % results in a reduction of approximately 5 km of visibility.

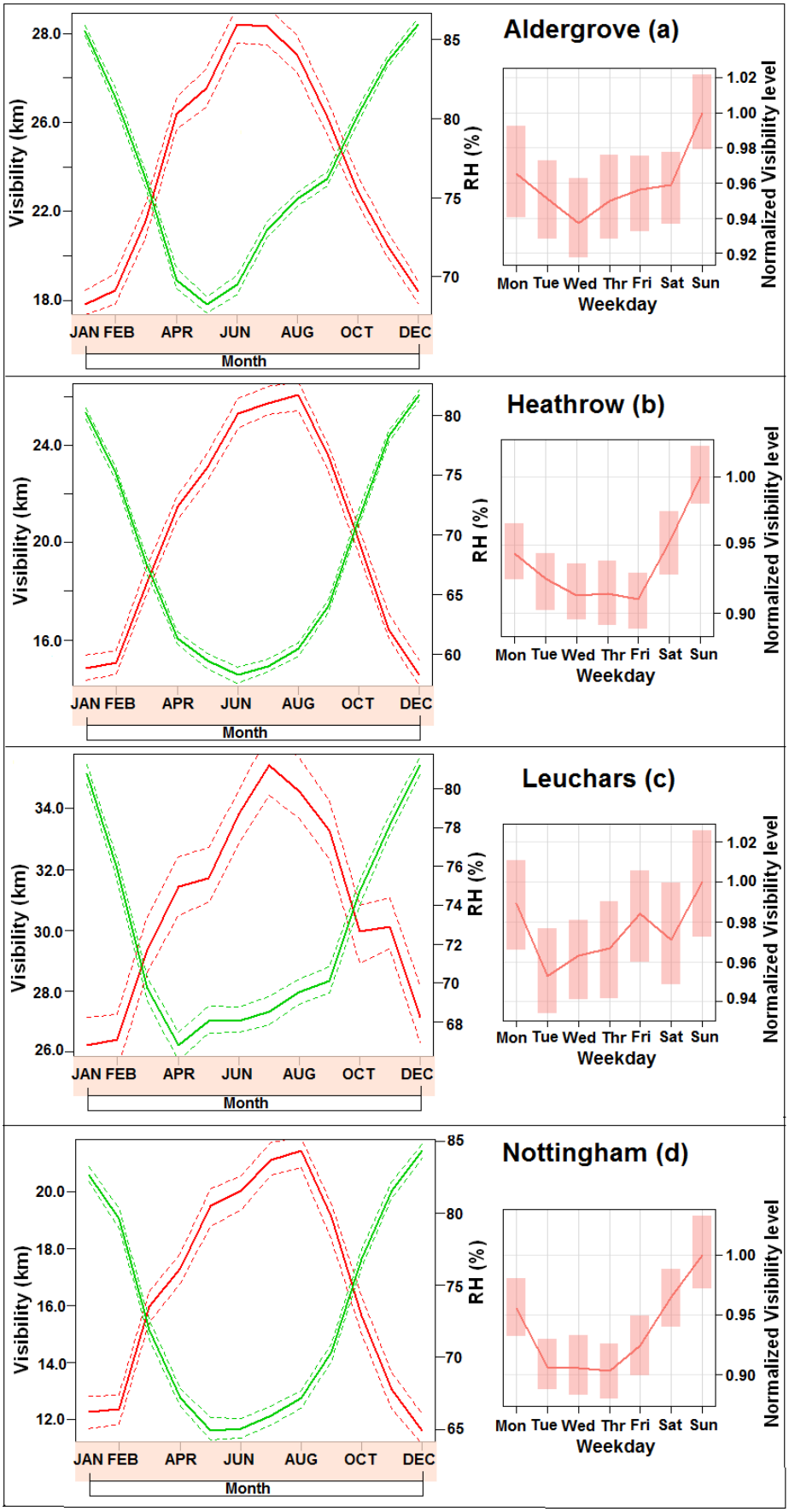
Aldergrove (a)
Visibility (km)
RH (%)
Normalized Visibility level
JAN FEB APR JUN AUG OCT DEC
Month
Mon Tue Wed Thr Fri Sat Sun
Weekday
Heathrow (b)
Visibility (km)
RH (%)
Normalized Visibility level
JAN FEB APR JUN AUG OCT DEC
Month
Mon Tue Wed Thr Fri Sat Sun
Weekday
Leuchars (c)
Visibility (km)
RH (%)
Normalized Visibility level
JAN FEB APR JUN AUG OCT DEC
Month
Mon Tue Wed Thr Fri Sat Sun
Weekday
Nottingham (d)
Visibility (km)
RH (%)
Normalized Visibility level
JAN FEB APR JUN AUG OCT DEC
Month
Mon Tue Wed Thr Fri Sat Sun
Weekday

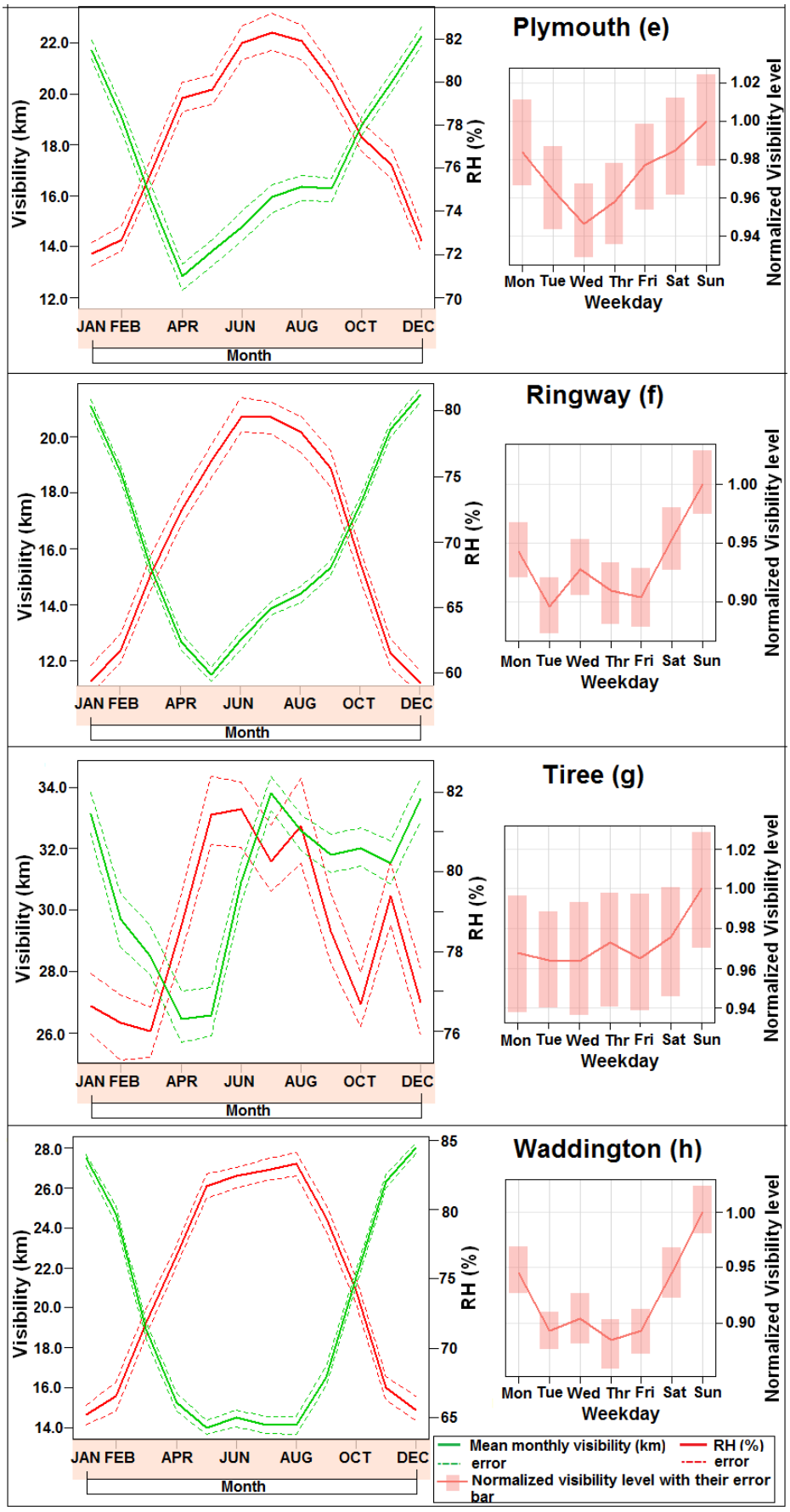

Figure 3.16 Mean monthly visibility and RH (Left-side) and average weekday visibility normalized to Sunday mean values (Right-side) at all eight sites: **a)** Aldergrove **b)** Heathrow **c)** Leuchars **d)** Nottingham **e)** Plymouth **f)** Ringway **g)** Tiree **h)** Waddington.

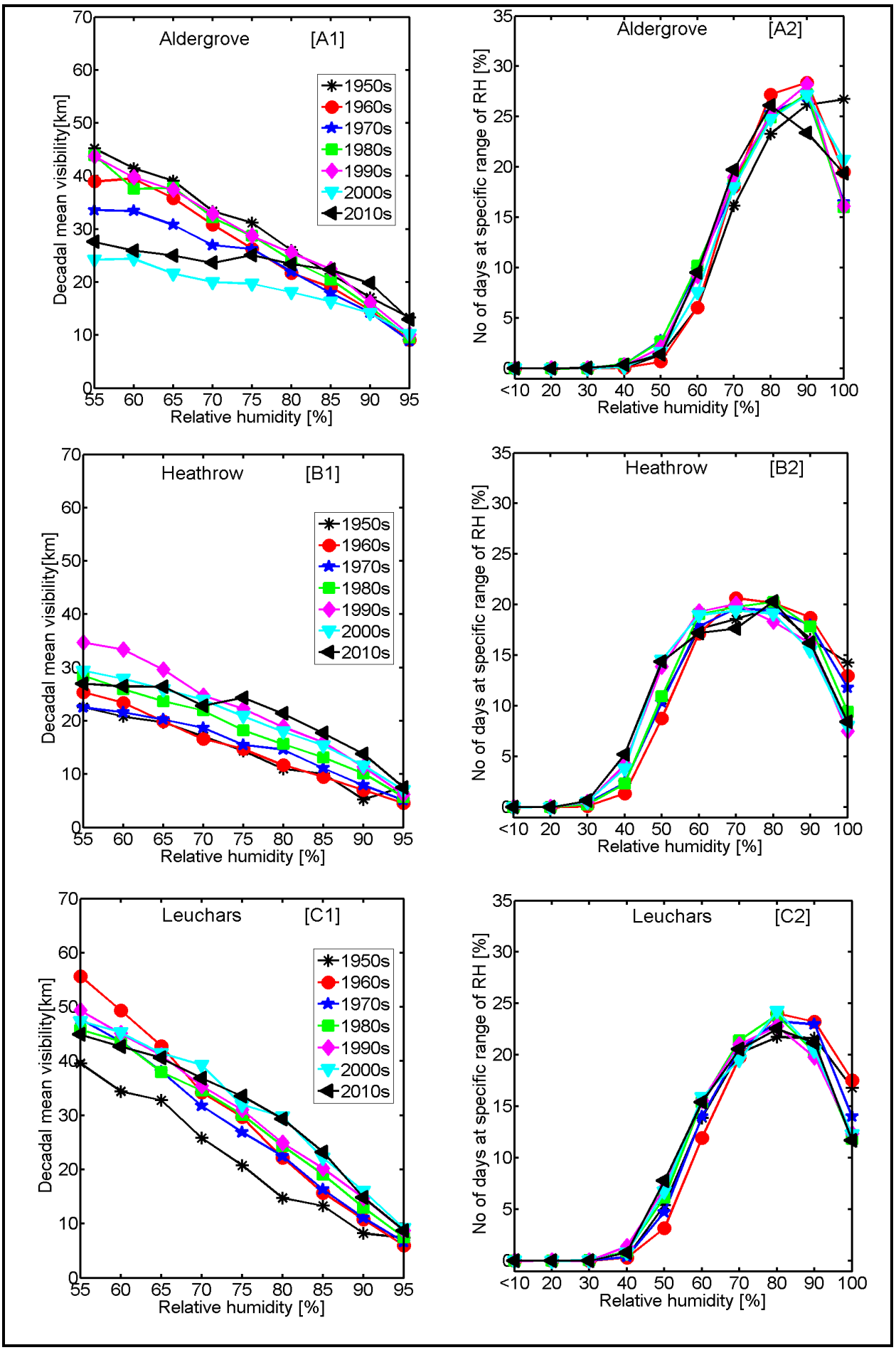
Aldergrove [A1]
Decadal mean visibility[km]
Relative humidity [%]
1950s
1960s
1970s
1980s
1990s
2000s
2010s
Aldergrove [A2]
No of days at specific range of RH [%]
Relative humidity [%]
Heathrow [B1]
Decadal mean visibility[km]
Relative humidity [%]
Heathrow [B2]
No of days at specific range of RH [%]
Relative humidity [%]
Leuchars [C1]
Decadal mean visibility[km]
Relative humidity [%]
Leuchars [C2]
No of days at specific range of RH [%]
Relative humidity [%]

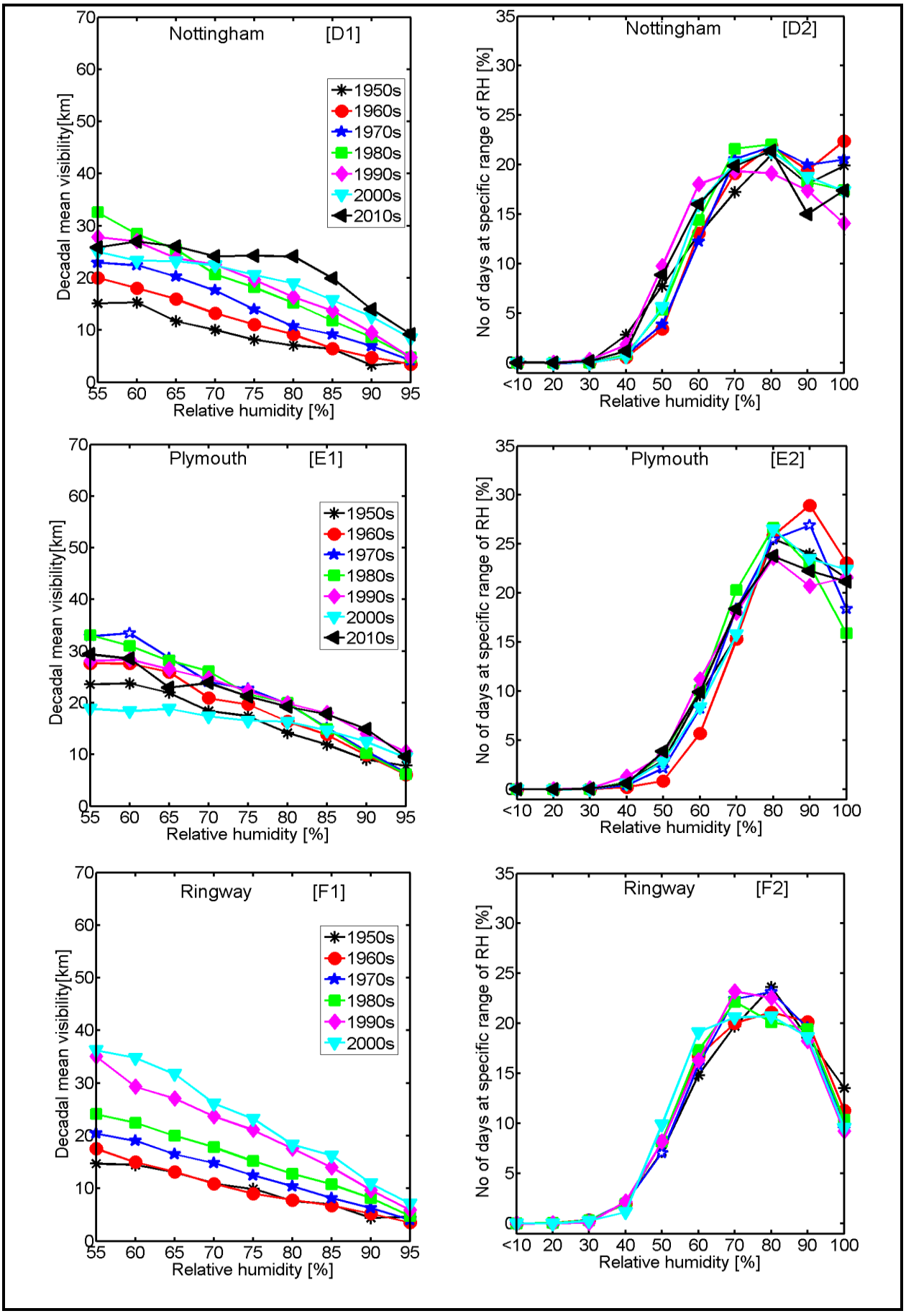
Nottingham [D1]
Decadal mean visibility[km]
Relative humidity [%]
1950s
1960s
1970s
1980s
1990s
2000s
2010s
Nottingham [D2]
No of days at specific range of RH [%]
Relative humidity [%]
Plymouth [E1]
Decadal mean visibility[km]
Relative humidity [%]
Plymouth [E2]
No of days at specific range of RH [%]
Relative humidity [%]
Ringway [F1]
Decadal mean visibility[km]
Relative humidity [%]
Ringway [F2]
No of days at specific range of RH [%]
Relative humidity [%]

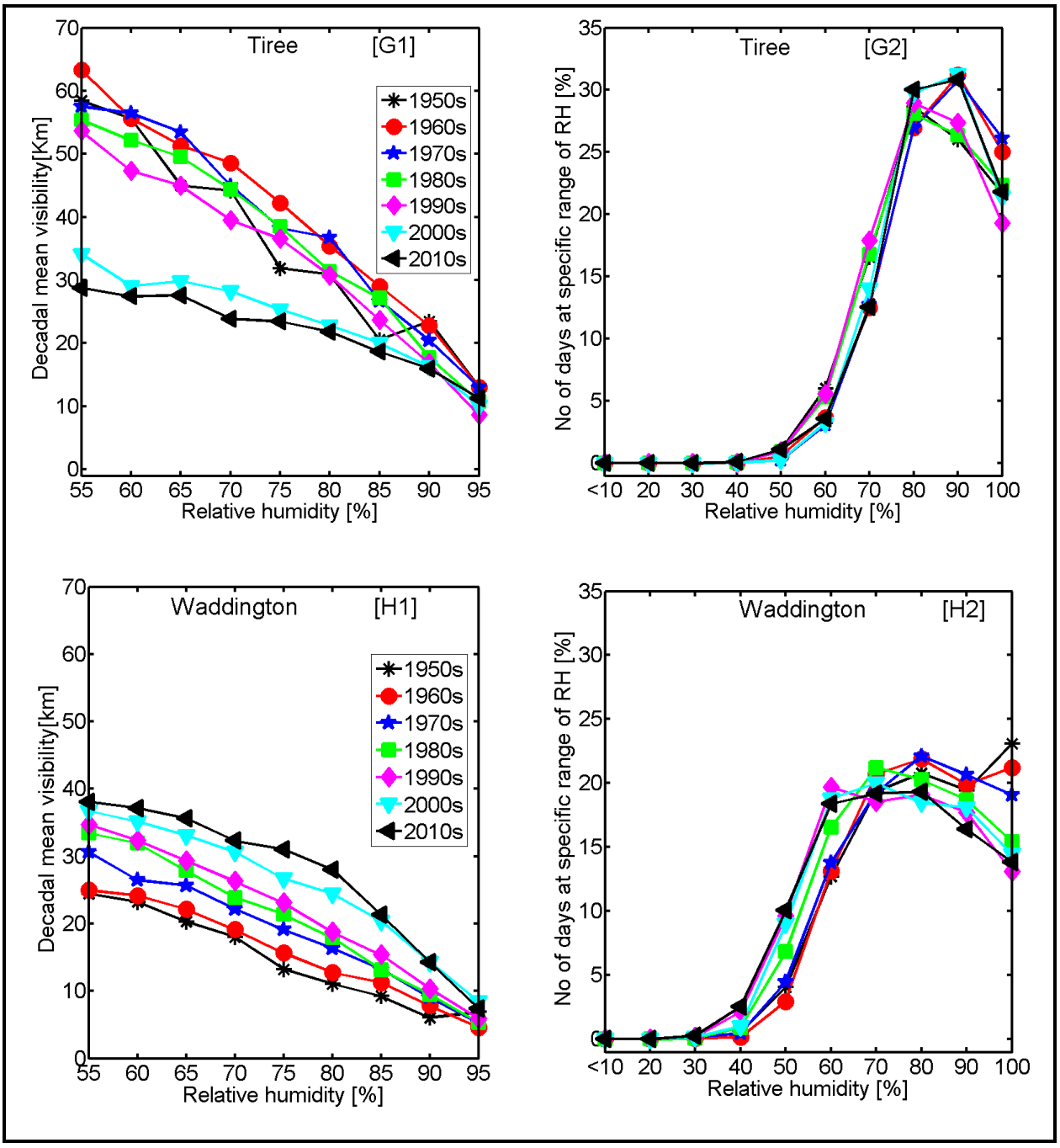

Figure 3.17 Decadal visibility at specific range of relative humidity (left side) and number of days in % during different relative humidity (right side)

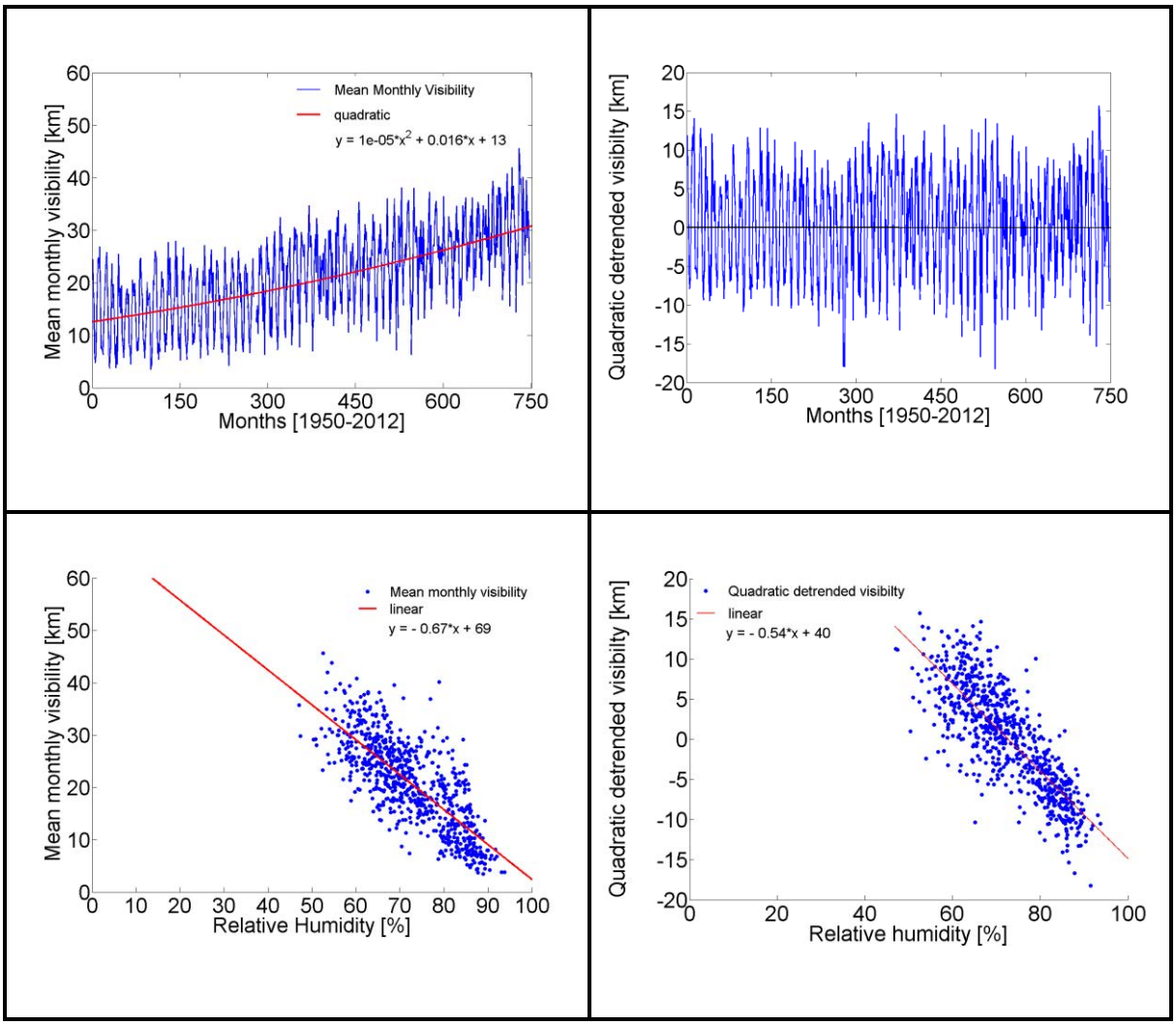

Figure 3.18 Mean monthly visibility at different RH conditions at Waddington

3.6.4 Effect of long term changes in meteorological parameters upon visibility

The long term trends in visibility are compared to the other recorded meteorological parameters: RH, air temperature, and wind speed and direction (Fig. 3.19). It is observed that at most of the stations RH decreases as average air temperature increases. Previous literature observed that the UK mean air temperature and sea surface temperature have increased by about 1^{o}C and 0.7^{o}C respectively between the early 1970s and mid 2000s (Jenkins, 2007). However, overall UK mean RH

decreased about 2.7 % between the 1961 and 2006 (Jenkins, 2007). This reduction in RH is also seen more widely in the mid-latitudes (Willett et al., 2014). The temperature change is likely due to climate change, land-use (urban heat island) effects or a combination of both. Clearly, urban heat island effects can only affect stations that are located in urban areas (Fig. 3.19). However, as Fig. 319 shows, visibility is strongly related to relative humidity and hence to the air temperature of a given location, highlighting a possible indirect effect of climate change and urban heat island effects on regional visibility. The correlation statistics between visibility, relative humidity, air temperature and wind speed are provided for all stations in Table 3.4.

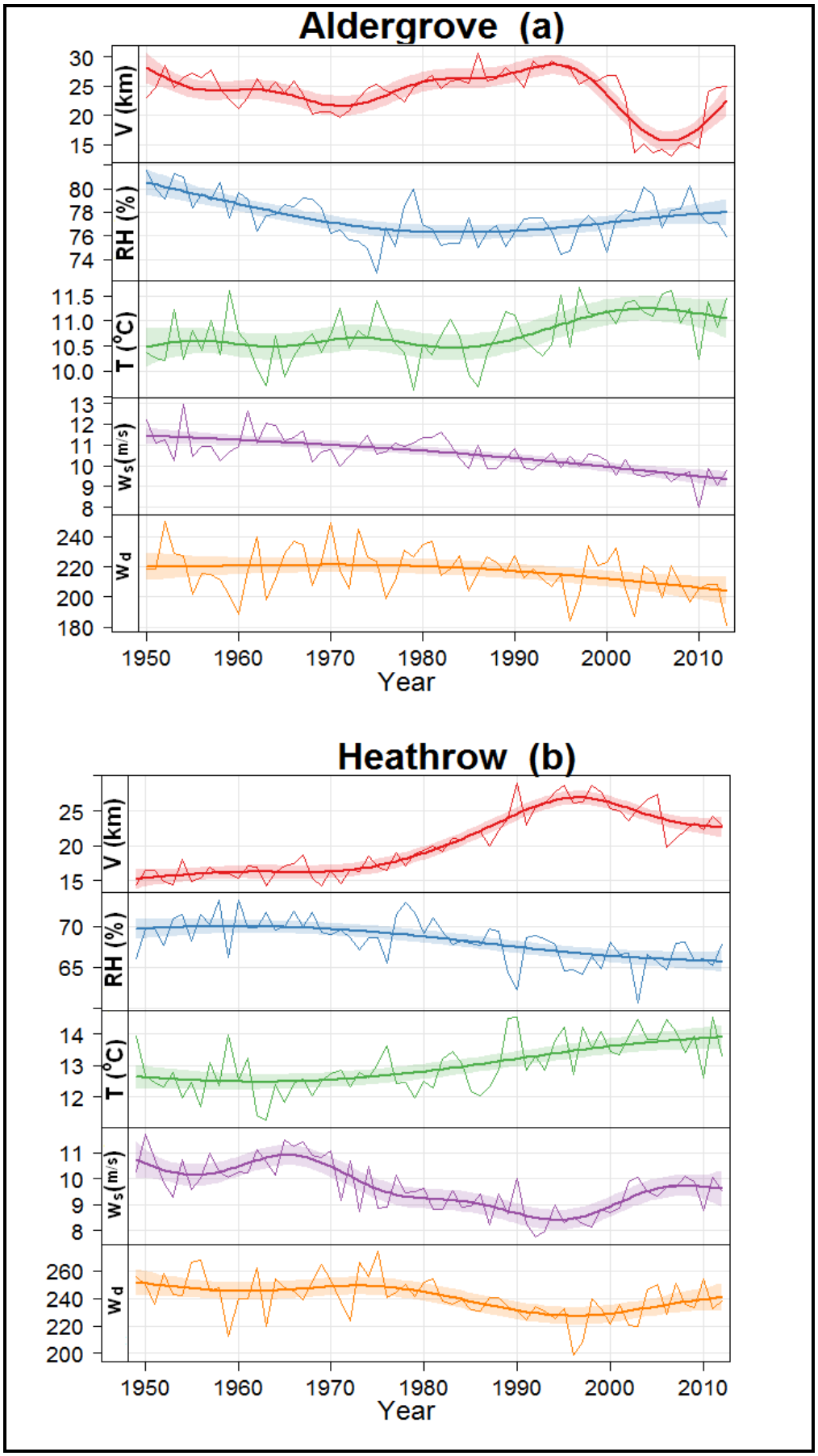
Aldergrove (a)
V (km)
RH (%)
T (°C)
Ws(m/s)
Wd
Year
Heathrow (b)
V (km)
RH (%)
T (°C)
Ws(m/s)
Wd
Year

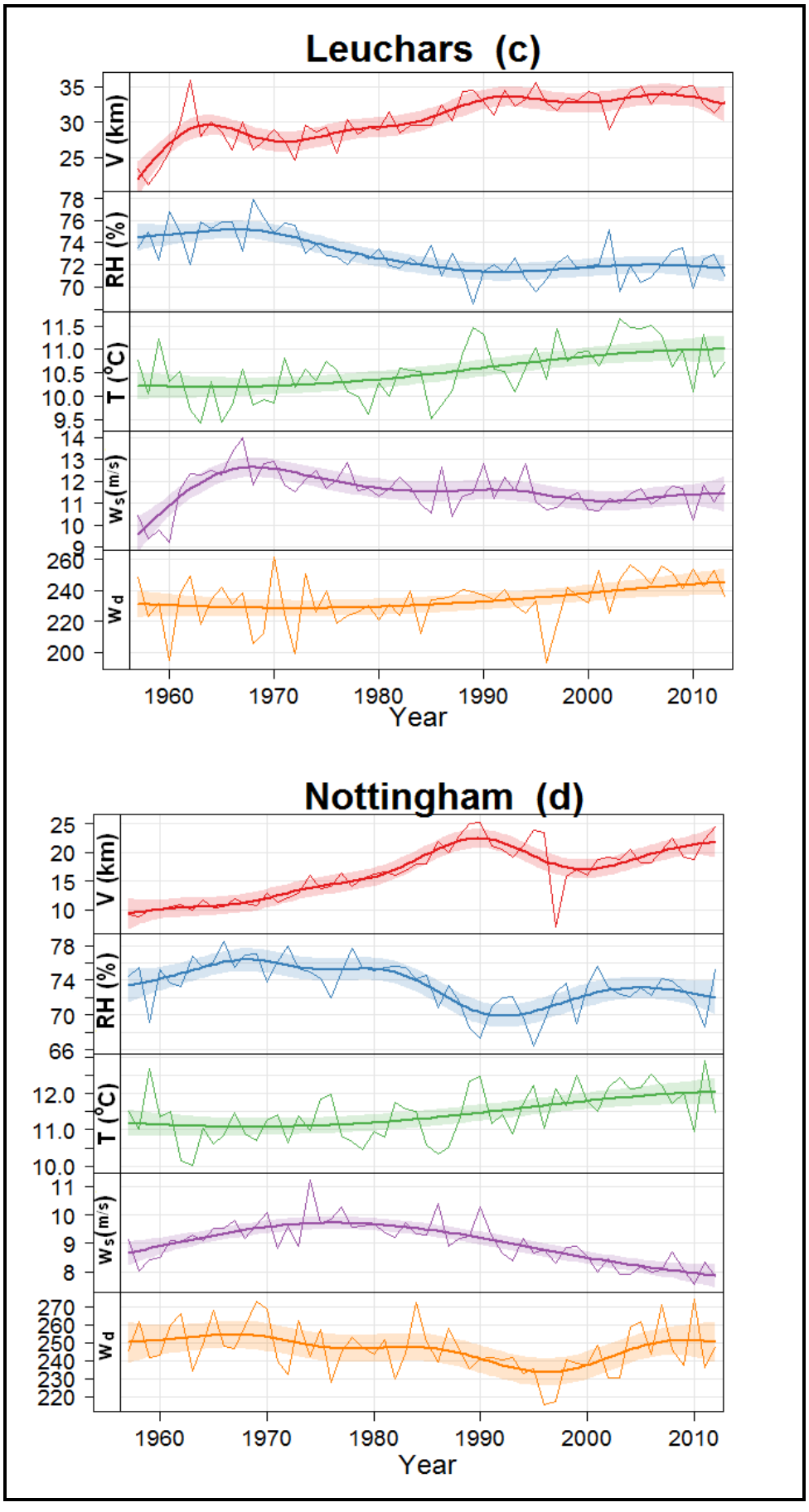
Leuchars (c)
V (km)
RH (%)
T (°C)
Ws(m/s)
Wd
Year
Nottingham (d)
V (km)
RH (%)
T (°C)
Ws(m/s)
Wd
Year

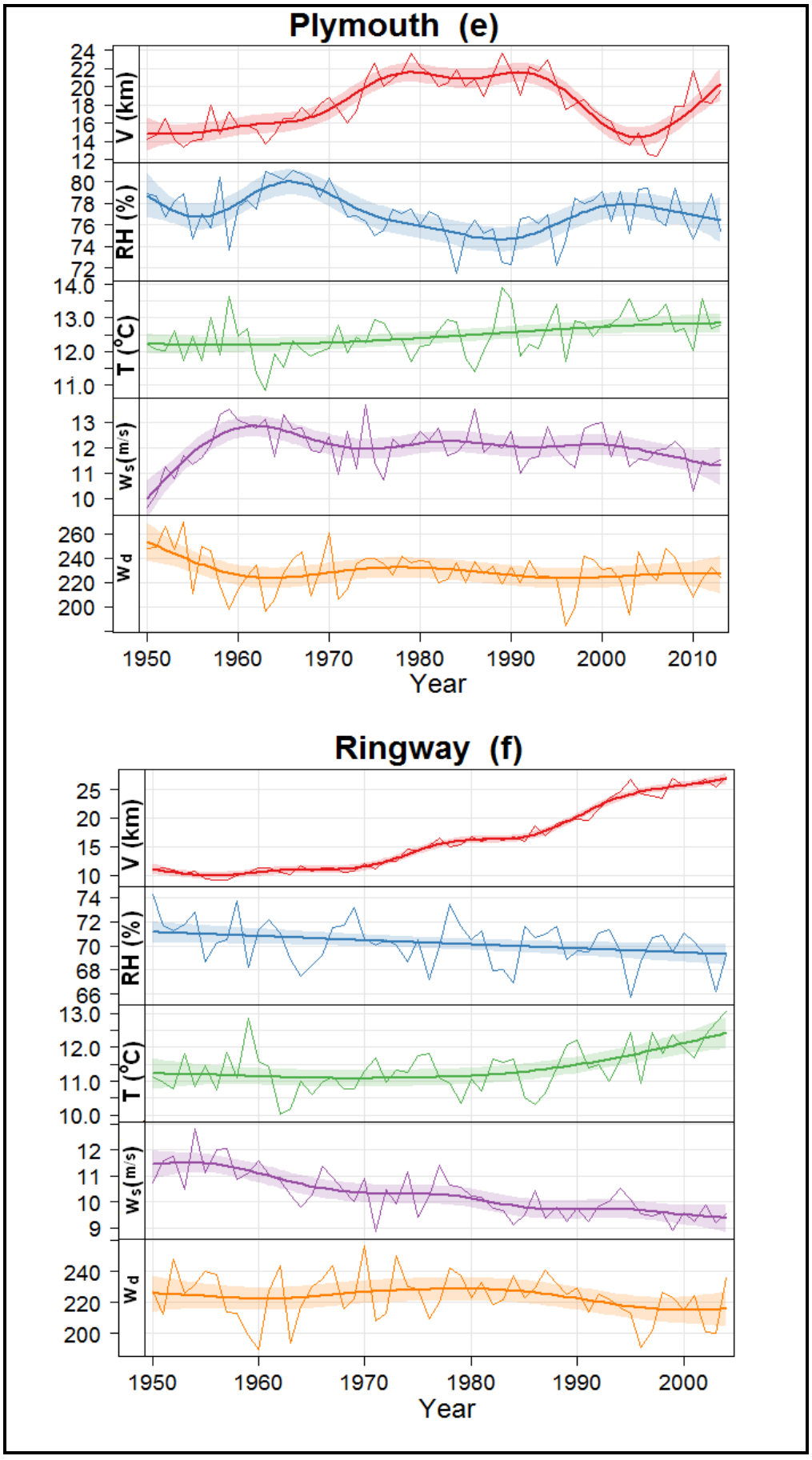
Plymouth (e)
V (km)
RH (%)
T (°C)
Ws (m/s)
Wd
Year
Ringway (f)
V (km)
RH (%)
T (°C)
Ws (m/s)
Wd
Year

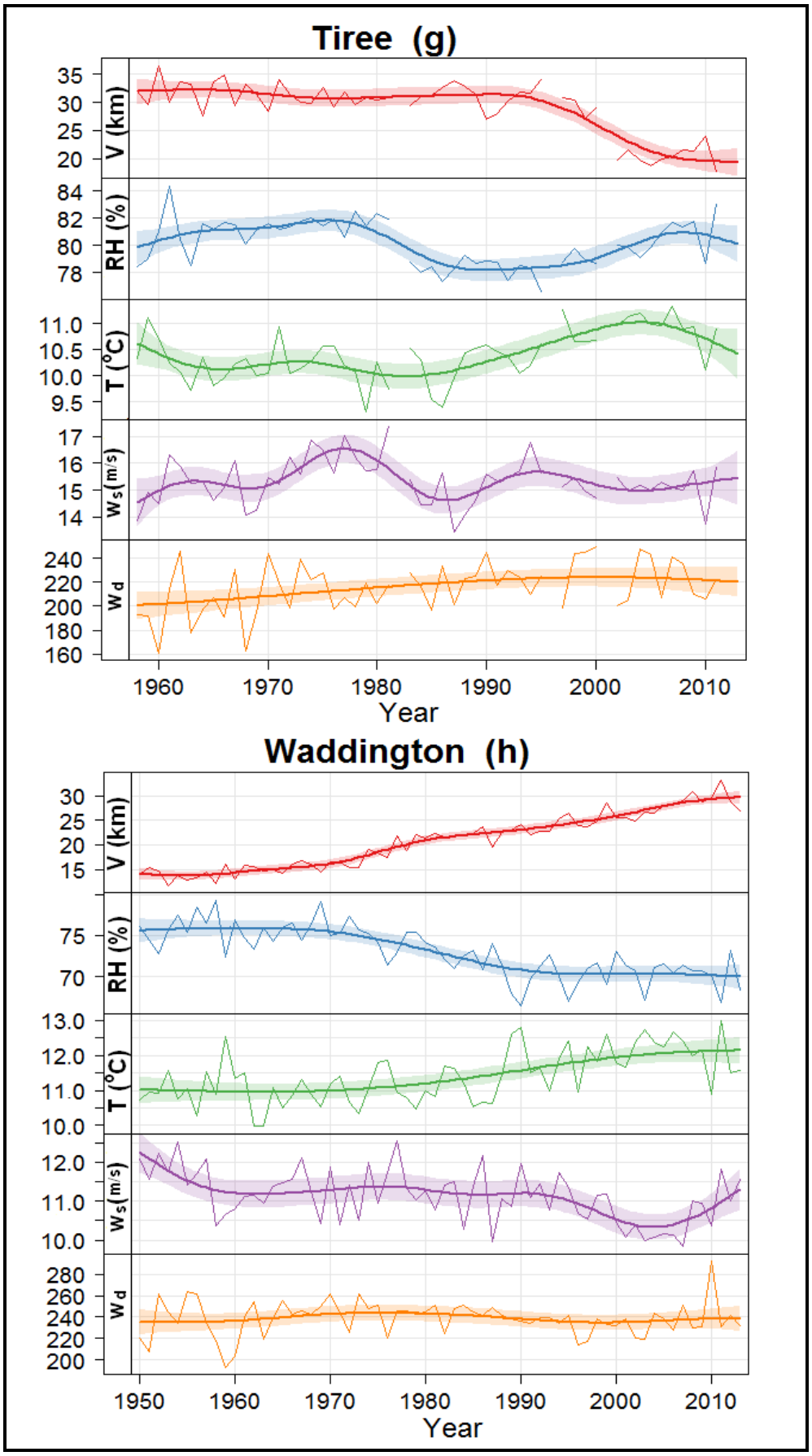

Figure 3.19 Time-series of meteorological components relative humidity (RH), air temperature (T), wind speed (w_s), and prevailing wind direction (w_d) including visibility (V), where all variables are averaged at 12 noon. Shaded lines show smooth fit line at 95 % confidence interval.

Table 3.4 Correlation coefficient (r) values between different variables, where daily data at 12 noon was used for calculation for last six decades

Aldergrove

	Visibility	RH	Temp	Wind speed
Visibility	1			
RH	-.519**	1		
Temp	.199**	-.373**	1	
Wind speed	.095**	-.028**	-.050**	1

Heathrow

	Visibility	RH	Temp	Wind speed
Visibility	1			
RH	-.542**	1		
Temp	.322**	-.540**	1	
Wind speed	.261**	-.084**	-0.008	1

Leuchars

	Visibility	RH	Temp	Wind speed
Visibility	1			
RH	-.688**	1		
Temp	.179**	-.353**	1	
Wind speed	.124**	-.208**	-.084**	1

Norringham

	Visibility	RH	Temp	Wind speed
Visibility	1			
RH	-.583**	1		
Temp	.299**	-.511**	1	
Wind speed	.272**	-.072**	-.054**	1

Plymouth

	Visibility	RH	Temp	Wind speed
Visibility	1			
RH	-.589**	1		
Temp	.185**	-.186**	1	
Wind speed	.220**	-.059**	-.073**	1

Ringway

	Visibility	RH	Temp	Wind speed
Visibility	1			
RH	-.549**	1		
Temp	.342**	-.423**	1	
Wind speed	.269**	-.070**	-.018**	1

Tiree

	Visibility	RH	Temp	Wind speed
Visibility	1			
RH	-.612**	1		
Temp	.041**	-.389**	1	
Wind speed	.331**	-.099**	-.226**	1

Waddington

	Visibility	RH	Temp	Wind speed
Visibility	1			
RH	-.633**	1		
Temp	.340**	-.550**	1	
Wind speed	.232**	-.091**	-.015*	1

* **Statistically significant value ($p < 0.05$)**

** **Statistically significant value ($p < 0.01$)**

Temp- Air Temperature **RH- Relative Humidity**

3.6.5 Mathematical fitting of measured visibility

In section 3.6.1, it was quantified that the decadal observed visibility has improved at most of the stations, which is a direct indicator of change in the combination of aerosol concentration, aerosol composition, gas concentration and RH. To better understand these changes in visibility, the absorption coefficient (β_{abs}), scattering coefficient (β_{sca}), particle hygroscopicity parameter (γ), and dry visibility (*Vis(dry)*) have all been calculated via constructed model (Eq. (3.5)) using assumptions described in section 3.5.2 (Methodology section).

Equations 3.6 and 3.7 were fit to the decadal visibility data subset into distinct RH bins using nonlinear and linear fitting respectively, as detailed in section 3.5.2. The fitted data is able to match the observed visibility extremely well ($R^2 > 0.98$) for all stations when Eq. (3.6) used; for example see Fig. 3.20 for Heathrow station. The last decade, starting in 2010, has the poorest fit, albeit still with an $R^2 = 0.95$, but only comprises 3 years of data. The results reported in this study are from nonlinear fitting of Eq. (3.6) using assumption $\beta_{abs}(RH) = \beta_{abs}(dry)$

The determined model output parameters (*Vis(dry)*, γ, β_{sca}, and β_{abs}) are presented in Fig. 3.21, where analysis has been carried out for all sites within each decade; however, the following discussion only considers data that was measured manually, due to the impacts of measurement methodology changes noted above. A clear improvement in calculated dry visibility was observed for Plymouth, Heathrow, Ringway, Nottingham and Waddington, while only minor changes were observed at Aldergrove, Leuchars and Tiree (Fig. 3.21a and Appendix A). Broadly, the 5 sites in England are similar with all showing an upwards trend in visibility, whereas the

Scottish and Northern Irish sites have greater dry visibilities but less discernible trend with time.

The derived value for γ has decreased slightly at Heathrow, Leuchars and Ringway sites over those decades (Fig. 3.21b and Appendix A), which indicates a decrease in hygroscopicity over the time (and a concomitant improvement in visibility). Tiree is the only station which showed increased hygroscopicity parameter values, implying a rise in aerosol particle hygroscopicity which results in a drop in visibility. The other stations like Aldergrove, Ringway, Plymouth, and Waddington show very little change in hygroscopicity parameter values.

Reductions in scattering coefficient are observed at all sites except Aldergrove. The scattering coefficients calculated at RH = 75 % is shown in Fig. 3.21d. Larger decreases in the scattering coefficient are observed at the urban sites compared to the rural sites. Reductions are also observed in the absorption coefficient at most sites but there is much more variability compared to the scattering coefficient. It is interesting to note that the two most remote sites, both in Scotland, have increasing absorption coefficients, which is potentially indicative of episodes of long range transport of absorbing aerosol to these pristine sites becoming more frequent. As expected, both the absorption and scattering coefficients show an inverse relationship with the observed visibility (Fig. 3.21a and 3.21c).

The change in the fitted values for dry visibility and scattering coefficient are not significantly affected by the change in visibility measurement from manual observation to visiometers. Contrastingly, the absorption coefficient and gamma values are much more influenced by measurement technique. This likely indicates that local sources have markedly different absorption and hygroscopicity parameters

compared to more regional sources; whereas their local and regional scattering properties are relatively similar.

The modelled scattering coefficient, at 75 % RH, is always higher than the absorption coefficient for all sites and times. However, at lower RH the two values become more comparable, see Fig. 3.22 which examines the contribution of the scattering coefficient to the total extinction coefficient at Heathrow. The non-negligible contribution of the absorption coefficient to the total extinction coefficient indicates that the model shown in Eq. (3.7) is not appropriate for the data reported in this study. However, for other locations with lower concentrations of absorbing species, gas or aerosol, the model may be valid and the benefit of a linear fitting algorithm, compared to a non-linear algorithm, could be exploited. It is shown the contribution of aerosol scattering to total extinction has remained relatively constant over time which indicates that the reduction in particulate matter has decreased both the absorbing and scattering fractions in equal measure.

Seasonal decadal changes in aerosol parameters were calculated for the Heathrow station (Fig. 3.23). In general, an improved dry visibility with reduced β_{abs} and γ values was observed for all seasons over time. However, during winter months the greatest improvement in dry visibility with a reduction in β_{abs} was noted.

Trends in visibility for those data acquired at a single RH value of 70 % (67.5-72.5 %) during the period of 1950s to 1990s were investigated for the Heathrow site to demonstrate the disaggregation of the RH effect on visibility from aerosol concentration effect upon visibility. At constant RH, a clear improved visibility was determined for the study period (Fig. 3.24). The result implies significant changes in

aerosol composition/concentration are driving the visibility trend. Hence improving air quality contributes significantly to better visibility.

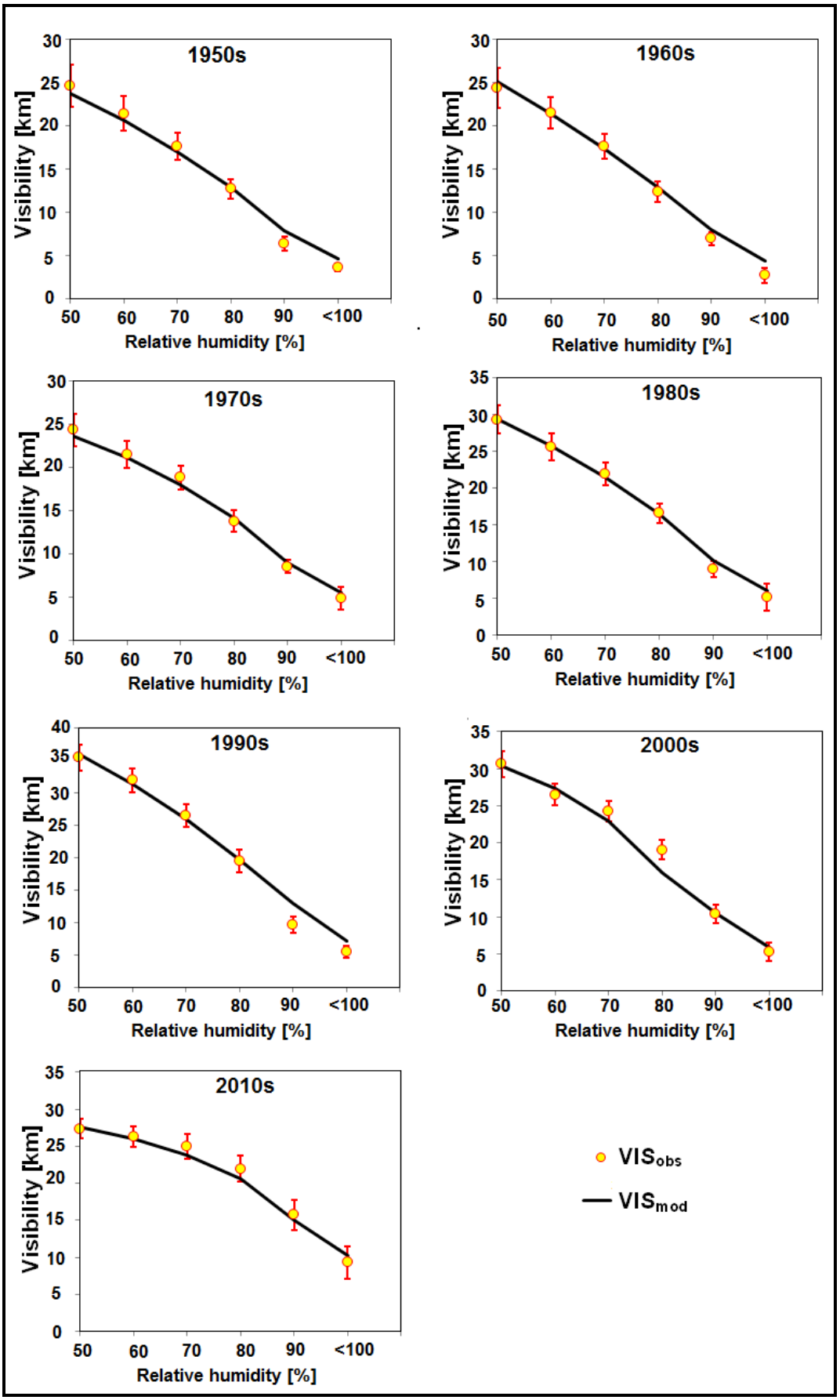

Figure 3.20 Comparisons of modelled and observed visibility at specific range of RH using Eq. (3.5) at Heathrow station. The observed visibility is presented with standard error bars at 95 % confidence interval.

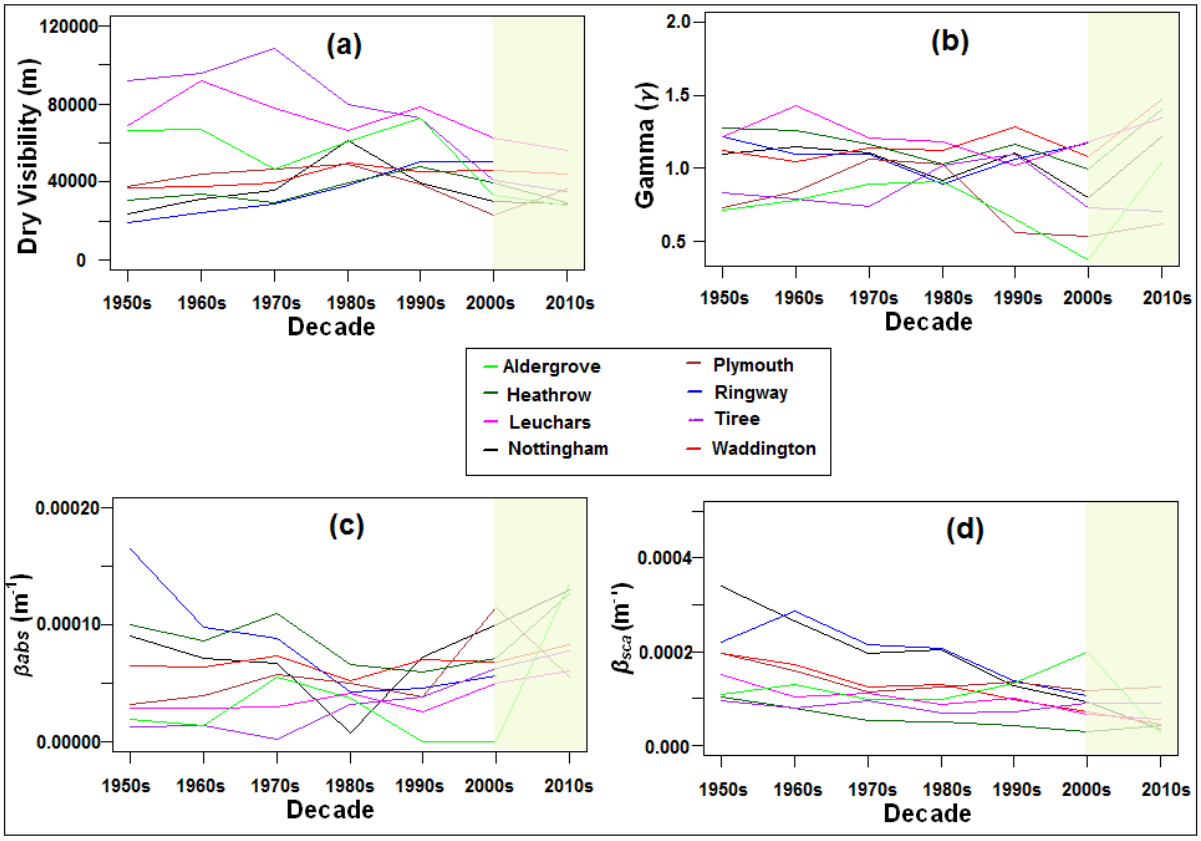

Figure 3.21 Model output parameters **a)** Dry visibility, **b)** gamma and **c)** absorption coefficient and **d)** scattering coefficient at 75 % n.b. from 1950s to 2010s. The green shaded region shows the start of visiometer era at most of the stations (see Table 3.2 to see the starting year of visiometer measurement).

* See Appendix A for model output parameter values including their uncertainties

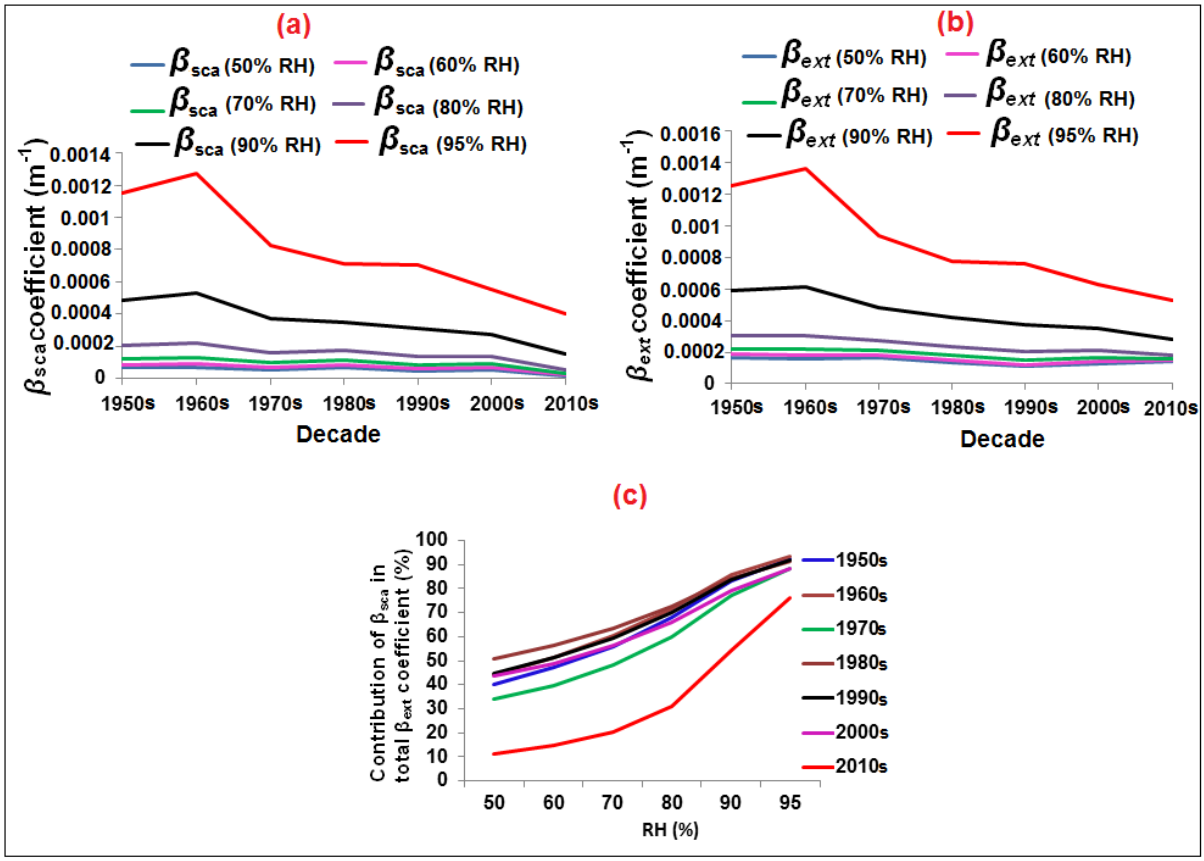

Figure 3.22 (a) Scattering coefficient (*βsca*), **(b)** total extinction coefficient (*βext*) and **(c)** contribution of scattering coefficient in total extinction coefficient at Heathrow. Estimates of error are not included here to improve clarity.

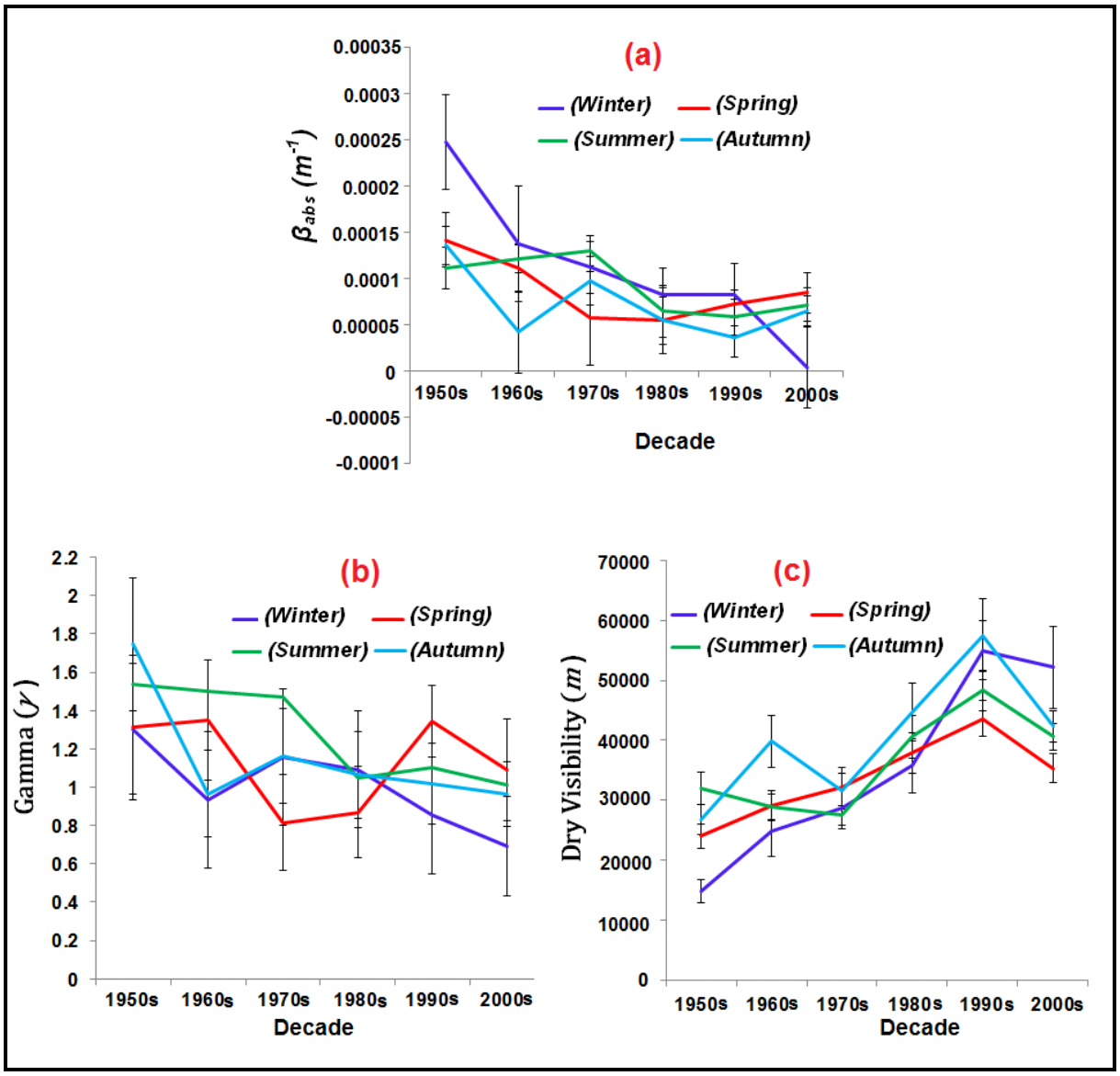

Figure 3.23 Model output parameters **a)** absorption coefficient **(β_{abs}), b)** Gamma (γ), and **c)** dry visibility at different seasons for Heathrow site.

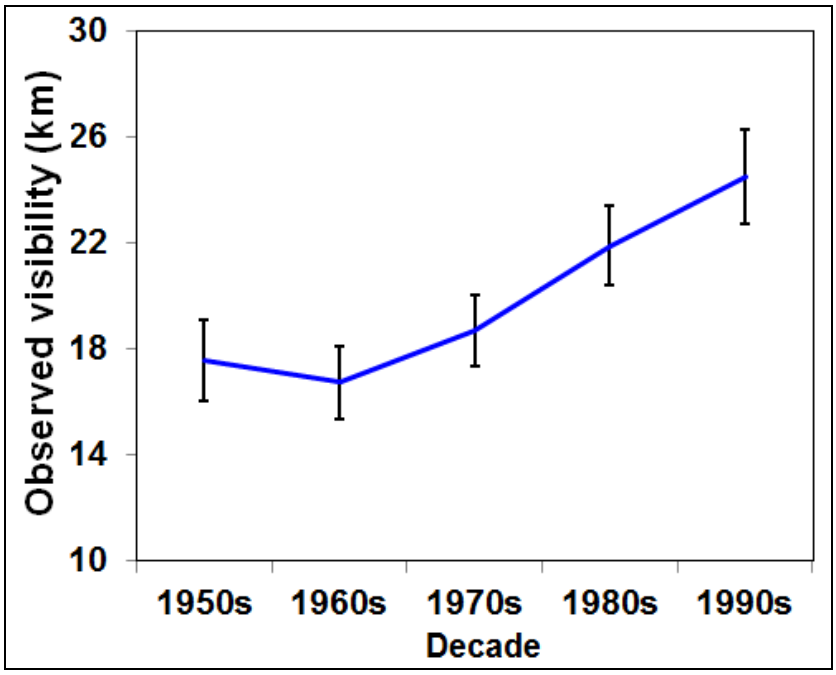

Figure 3.24 Decadal observed visibility at 70 % RH (range 67.5 -72.5 %) for Heathrow site. Error bars represent standard error at 95 % confidence interval.

3.6.6 Effect of nitrogen dioxide gas upon visibility at Heathrow

The potential influence of NO_2 levels upon visibility was analysed using data from the Harlington station (proximate to the Heathrow site), for the period 2004 - 2012. The annual mean concentration of NO_2 varied from 33.6 μg m^{-3} to 38.5 μg m^{-3}, peaking in 2005 (Table 3.5). The NO_2 influence on observed visibility (in the RH bin centred at 75 % (72.5-77.5 %)) was greatest in the year of 2005 (where it contributed 4.7 ± 1.6 % in total extinction) and lowest for 2012 (3.3 ± 1.5 % in total extinction) with the remaining visibility reduction being caused by aerosol extinction. Overall, during 2004 to 2012 NO_2 contributed approximately 4 % to the observed visibility change, while the remaining 96 % contributed arose from aerosol particles and fog. However it is worth considering the contribution of NO_2 towards the total extinction coefficient during the 1970s when visibility was very low (16.5 km) as

compared to 2012 (25.24 km) and NO_2 levels higher. Unfortunately NO_2 data is not available before 2004 at nearby Heathrow site, but a recent study shows that, NO_x emission in UK has almost doubled in the time period 1970 to 2012 (Harrison et al., 2015). Using the UK NO_x record for 1970 from Harrison et al. (2015), it was assumed that the annual mean NO_2 concentration in 1970 is double of what is measured in the year 2012 (34.6 µg m^{-3}) as emission estimates are approximately related to concentration. This assumption does not take into account the changing vehicle fleet with corresponding changing emissions of NO and NO_2 (Carslaw and Rhys-Tyler, 2013). Using this data the absorption coefficient for NO_2 was calculated. In particular, a higher absorption coefficient (β_{NO2abs}) in 1970 (0.0121 km^{-1}) as compared to 2012 (0.00507 km^{-1}) was identified. However, the contribution of NO_2 to the total extinction coefficient remained at 5.2 % in 1970, only about 2 % higher than in 2012.

Table 3.5 Gases contribution in visibility change over Heathrow airport

Year	NO_2 concentration ($\mu g\ m^{-3}$)	NO_2 (ppm)	Total Extinction coefficient (km^{-1}) by all effects	Absorption coefficient in km^{-1} (β_{NO2abs}) by NO_2	% contribution of NO_2 in total extinction coefficient
2004	38.3	0.0203	0.1475	0.00671 ± 0.0023	4.5 ± 1.5
2005	38.5	0.0204	0.1425	0.00675 ± 0.0023	4.7 ± 1.6
2006	36.9	0.0196	0.1978	0.00648 ± 0.0022	3.3 ± 1.1
2007	36.9	0.0197	0.1855	0.00649 ± 0.0029	3.5 ± 1.4
2008	34.7	0.0185	0.1759	0.00600 ± 0.0026	3.4 ± 1.4
2009	36.3	0.0193	0.1681	0.00636 ± 0.0023	3.8 ± 1.2
2010	34.4	0.0183	0.1755	0.00604 ± 0.0023	3.4 ± 1.3
2011	33.6	0.0179	0.1614	0.00589 ± 0.0025	3.6 ± 1.5
2012	34.6	0.0184	0.1550	0.00507 ± 0.0024	3.5 ± 1.5
1970*	69.2	0.0368	0.2370	0.0121	5.12

*estimated values given for 1970 (see main text for details)

3.7 Conclusions

Long term trends in visibility for 8 meteorological stations situated in the UK have been investigated. In general, visibility has improved at most of the stations through time. The improvements are greatest in urban areas, and are attributed to

reductions in aerosol particle loadings and decreases in atmospheric RH. Visibility was found to be lowest during winter and highest in the summer due to seasonal variations in RH and likely changes in the mixing layer height. The rate of change of visibility was higher in winter for all stations, with the exception of Ringway. A sharp positive increment (5-12.5 %) in visibility was observed on Sundays, as compared to other days of the week (Mon-Sat), which is most likely due to weekend reductions in traffic and other particulate matter emission sources.

Bivariate polar plots of visibility, which account for both the influence of wind speed and wind direction, explained the influence of wind on likely source areas of visibility reducing aerosols. These bivariate polar plots identified likely locations for visibility reducing pollutants sources and their variation over time. Overall, an improved visibility at most of the stations in almost all directions was observed with notable improvements when the air masses moved over metropolitan areas, for example, Greater Manchester and Greater London Areas. At most sites, low visibility was observed when the winds came from the direction of continental Europe which may indicate an influence of regional pollution events leading to visibility reductions. Significant changes in visibility were observed with changes in relative humidity, which indicates a strong dependency of visibility on aerosol hygroscopicity. The measured RH at all sites was typically in the range of 60-80% and variations of a few percent in this RH range can have significant effects on visibility. Many sites showed long term decreases in RH which correlated with increases in air temperature, and had the effect of improving visibility. If the trend of increasing RH continues, the UK can expect further improvements in visibility for the same pollutant loading.

Calculations indicate that the majority of visibility reduction is caused by PM, however, a non-negligible contribution of light absorption is due to NO_2 gas. For the Heathrow station, over the time period 2004-2012, light absorption by NO_2 was calculated to contribute approximately 4% to the total visibility reduction, with the remainder caused by PM absorption and scattering. The NO_2 contribution was likely to have been significantly higher in prior decades due to the higher NO_x emissions and hence atmospheric concentrations.

A light extinction model was developed to explain the dependency of visibility upon meteorology and aerosol characteristics. The agreement between the modelled and measured visibility is excellent. The model suggests that there have been significant changes in aerosol concentration over the last 60 years. The model incorporates parameterizations of aerosol hygroscopicity, particle concentration, particle scattering, and particle and gas absorption. The developed model is easily transferrable and applicable to other data sets worldwide.

Visibility can be used as a proxy for aspects of air quality, in particular particulate matter and nitrogen dioxide. Since visibility measurements can extend back for hundreds of years whilst air quality measurements typically only go back decades albeit with a few sparse datasets going back longer in time. The approach demonstrated in this work has potential for generating historical air quality indications for locations with visibility records.

Chapter 4.0

Short term impacts of firework generated aerosols and meteorology on the UK visibility

Most of the material in this chapter has been taken from following paper:

Singh, A., Bloss, W.J. and Pope, F.D., **2015**. Remember, remember the 5th of November; gunpowder, particles and smog. *Weather*, 70(11): 320-324.

4.1 Chapter overview

This chapter details the short term effects of firework and bonfire emissions in conjunction with meteorology on visibility during Guy Fawkes Night celebrations in the UK. Collection methods and processing of datasets, which include visibility, particulate, and other meteorological parameters are described in this chapter. Programming methods, which are used in the processing and analysis of archived datasets, are described in addition to the results and conclusions using different analytical approaches.

4.2 Abstract

The effects of emitted aerosol particles and meteorological conditions on visibility during Guy Fawkes Night festival are assessed using hourly data collected across13 years (2000-2012) at 34 UK based meteorological stations. In the UK on the 5th November every year, Guy Fawkes Night is celebrated with bonfires and fireworks. An undesirable consequence of these activities is a statistically significant reduction (~25%) in atmospheric visibility nationwide. This reduction is caused by increased loading of atmospheric particulate matter generated by bonfires and fireworks. However, it is found that the impact of emitted pollutants on visibility is short-lived, with visibility returning to the normal range for each site within two days, due to the dispersal of the additional PM loading. The effect of increased loading on visibility is investigated in greater detail for the city of Nottingham (urban background area) where larger visibility decreases (~64%) compared to the national average (~25%) was observed. Visibility reduction is more significant when the background particulate, i.e. that which is not associated with Guy Fawkes's Night) matter loading

and/or the atmospheric relative humidity are high. In particular, a clear anti-correlation between fireworks/bonfires generated PM with diameter less than 10 μm (PM_{10}), or less than 2.5 μm ($PM_{2.5}$) and black carbon (BC) on PM and visibility is found. The concentrations of pollutants $PM_{10,}$ $PM_{2.5,}$ and BC increase from 7 pm to midnight on November 5th by 62%, 253%, and 201%, respectively. No significant variations in gas pollutants such as SO_2 and NO_2 are observed during the celebration period.

4.3 Introduction and objectives

Air pollution caused by suspended particles and trace gases are a major concern, especially in urban areas due to its significant impact on human health and air quality parameters (Chan and Yao, 2008; Hamad et al., 2016; Jiang et al., 2015; Pathak et al., 2013; Samoli et al., 2016) such as atmospheric visibility (Lee et al., 2005; Singh et al., 2015). The sources of these suspended pollutants can be natural or anthropogenic via various activities. Fireworks on the occasion of different cultural, national and personal celebrations is a major local anthropogenic source, which affects both short-term and long-term air quality (Galea and Powles, 2010; Pathak et al., 2013). Guy Fawkes Night is the biggest traditional event in the UK involving fireworks displays and bonfires, and is celebrated every year on 5th November. Fireworks and bonfires produce a mixture of hazardous pollutants such as fine particles, trace metals (Al, Mn, Cd) and gases like sulphur dioxide, nitrogen oxides, ozone, carbon dioxide, carbon monoxide (Attri et al., 2001; Ravindra et al., 2003; Wang et al., 2007) that can have direct impacts on human health (Hamad et al., 2016; Ravindra et al., 2001) and local visibility (Sarkar et al., 2010). Serious

injuries such as skin burns, eye damage, and hearing loss can also occur via incorrect handling of fireworks and bonfires (Maglieri and Henderson, 1973; Vernon, 1988). Moreover, in the event of fireworks, present meteorological condition, especially RH can change the water content of particle in line with the particle hygroscopicity and thus contribution to visibility changes (more detail is given in Chapters 1 and 2). Over the last few decades, there has been an emergence of growing concern over attenuation in visibility associated with suspended air pollutants mainly from anthropogenic activities such as fireworks and bonfires (Camilleri and Vella, 2010; Gomez and Smith, 1987; Kulshrestha et al., 2004; Sati and Mohan, 2014; Wang et al., 2007). Of particular interest to this study is the effect of the firework and bonfire smoke on visibility.

The work described in this chapter is focused on short term visibility variations caused by the PM generated from the combination of fireworks and bonfires in the UK on Guy Fawkes Night. In addition, associated changes in pollutant concentrations caused by fireworks and bonfires during Guy Fawkes Night are investigated. This work also provides an improved understanding of the influence of local meteorology on visibility changes during the Guy Fawkes event at specific UK sites.

4.4 Data

The hourly values of horizontal visibility and relative humidity data were obtained from the British Atmospheric Data Centre (BADC), (www.badc.nerc.ac.uk), for 34 stations situated throughout the United Kingdom. For the locations of the study stations see Figure 4.1 (shown by red stars) and Table 4.1. Due to limited

availability of visibility stations which co-located with pollution sensors and limited data-sets, Watnall-Nottingham station (src id 556) has been selected for detailed study. Daily mean pollutant data were obtained 5 miles away from the Watnall site in the centre of Nottingham city. Geographical description of Nottingham site is presented in Chapter 3 section 3.4.2 (follow Figure 3.5). In particular, data for the gas phase species nitrogen dioxide (NO_2) and sulphur dioxide (SO_2) were obtained in addition to three PM metrics: PM_{10}, $PM_{2.5}$, and black carbon PM. These data were obtained from the DEFRA Automatic Urban and Rural Monitoring Network (AURN) (http://uk-air.defra.gov.uk/).

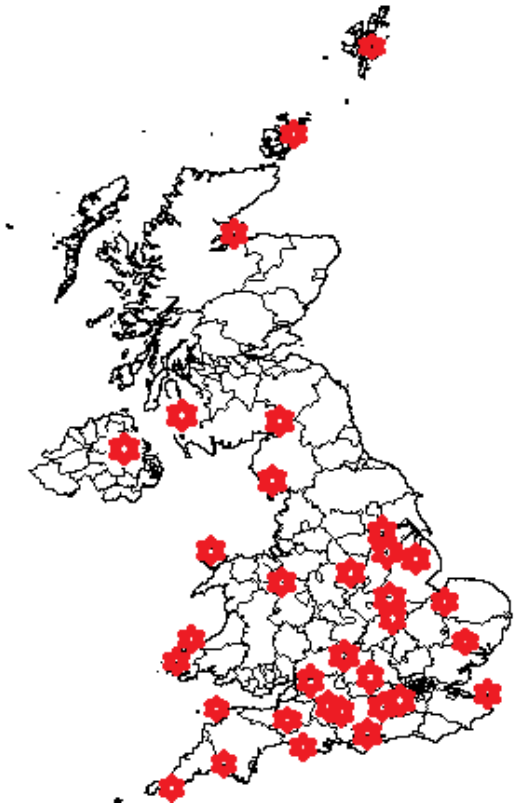

Figure 4.1 Map showing study locations in the UK, where red star represents used weather sites.

Table 4.1 List of used UK meteorological sites with their unique identification code and locations

Station Name	Station code (src id)	Latitude	Longitude
CULDROSE	1393	50.0838	-5.25609
PLYMOUTH: MOUNTBATTEN	1336	50.3544	-4.11986
ISLE OF PORTLAND	1319	50.5216	-2.45431
SOLENT	858	50.8075	-1.20942
YEOVILTON	1302	51.0059	-2.64148
CHIVENOR	1356	51.0886	-4.14743
MIDDLE WALLOP	847	51.1493	-1.56851
BOSCOMBE DOWN	889	51.1613	-1.75317
ODIHAM	862	51.2385	-0.94346
SOUTH FARNBOROUGH	869	51.2794	-0.77107
MANSTON	775	51.346	1.33716
HEATHROW-LONDON	708	51.4787	-0.44904
LYNEHAM	886	51.5028	-1.99094
MILFORD HAVEN CONSERVANCY BOARD	1215	51.7084	-5.05229
BRIZE NORTON	605	51.758	-1.57649
WATTISHAM	440	52.1234	0.9591
ABERPORTH	1198	52.1391	-4.56999
BEDFORD	461	52.2265	-0.46376
WITTERING	583	52.611	-0.45963
MARHAM	409	52.651	0.56772
SHAWBURY	643	52.7943	-2.66329

NOTTINGHAM: WATNALL	556	53.0053	-1.24969
CONINGSBY	393	53.0935	-0.17119
WADDINGTON	384	53.1751	-0.52173
VALLEY	1145	53.2524	-4.53524
SCAMPTON	381	53.3066	-0.54649
WALNEY ISLAND	1078	54.1247	-3.25657
ALDERGROVE	1450	54.6636	-6.22436
WEST FREUGH	1039	54.859	-4.93414
CARLISLE	1070	54.9342	-2.96223
LEUCHARS	235	56.3774	-2.86051
INVERNESS-SHIRE	116	57.542	-4.06096
ORKNEY	23	58.9539	-2.89988
LERWICK	9	60.1395	-1.18299

4.5 Methods and analysis approaches

Two distinct data series were generated for the present study: 1. UK average visibility maps for the dates of the 2 - 8 November inclusive, and 2. Average visibility time series for Nottingham in the months of October and November. The visibility maps allow for the detection of regional changes in visibility associated with Guy Fawkes Night, while the longer time series of the Nottingham data allows for the attribution of the change in visibility on Guy Fawkes Night to the change in atmospheric composition.

Both the meteorological and pollutant data sets were obtained for a 13 year period encompassing the years 2000-2012. The length of the time period investigated was constrained by the availability of the AURN data. The $PM_{2.5}$ data are only available for the period 2009-2012. As official fireworks displays typically start after 1900 h, visibility and humidity data-set are selected for 2100 h for study. Whilst many fireworks displays occur on the 5th November not all do; often official displays will be performed on the weekend preceding or subsequent to the 5th. Within our 13 year data set, the number of days that 5th November fell on a given day of the week was: Monday (3), Tuesday (1), Wednesday (2), Thursday (1), Friday (2), Saturday (2) and Sunday (2). Hourly visibility trends were plotted on a day-to-day basis during October and November, in order to monitor the abrupt and sharp changes in visibility or lack thereof in response to fireworks and bonfire emissions. Hourly values of the visibility measurements were used to emphasise the variations that occurred before, during and after the use of fireworks.

The available visibility data network is not sufficiently dense to allow for the visibility mapping of the whole of the UK. The maps were produced by assuming that the measurement at each station was reliable until the distance exceeded 32 km, which represents a typical upper limit to visibility for the UK measured in November (albeit not for Guy Fawkes Night). Where two measurements overlap, the visibility is approximated by inverse distance weighting interpolation (Lu and Wong, 2008; Shepard, 1968) of the multiple measurements. A more detailed description of visibility mapping is provided in section 4.6.1.

Data processing was carried out using R software, where the ggplot package (Wickham and Wickham, 2007) was used for spatial mapping. The meteorology and pollution data were analysed using Matlab (2014a) software.

4.6 Results

4.6.1 Spatial trends of the UK visibility during Guy Fawkes Night

The variation in the UK visibility over Guy Fawkes Night and the surrounding days is shown in Figure 4.2. The spatial trend analysis is presented using 34 stations with 0.29^{o} x 0.29^{o} distance resolution. This is a latitude equivalent to 32 km and a longitude equivalent to 20.3 km. In Figure 4.2, a dramatic dip in visibility can clearly be seen for 5th November compared with preceding and subsequent days. The average visibilities observed at the 34 stations on the 2nd, 3rd, 4th, 5th, 6th, 7th, and 8th November are 20.0±4.6, 17.8±4.0, 17.6±5.1, 14.8±5.2, 16.9±4.4, 18.3±3.8 and 20.5±4.1 km respectively, with a mean reduction of ~25 % on 5th November compared with other days (2nd, 3rd, 4th, 6th, 7th, and 8th November). It can be seen that the 6th November has the next lowest visibility after the 5th which may be due to higher atmospheric PM loading persisting following Guy Fawkes Night. The effect of the fireworks on visibility is observed at all sites. Typically, urban locations show the greatest visibility loss. It is noted, 82 % of the UK population lives within urban locations (http://data.worldbank.org) and hence poor visibility in these regions has greater potential for disruption.

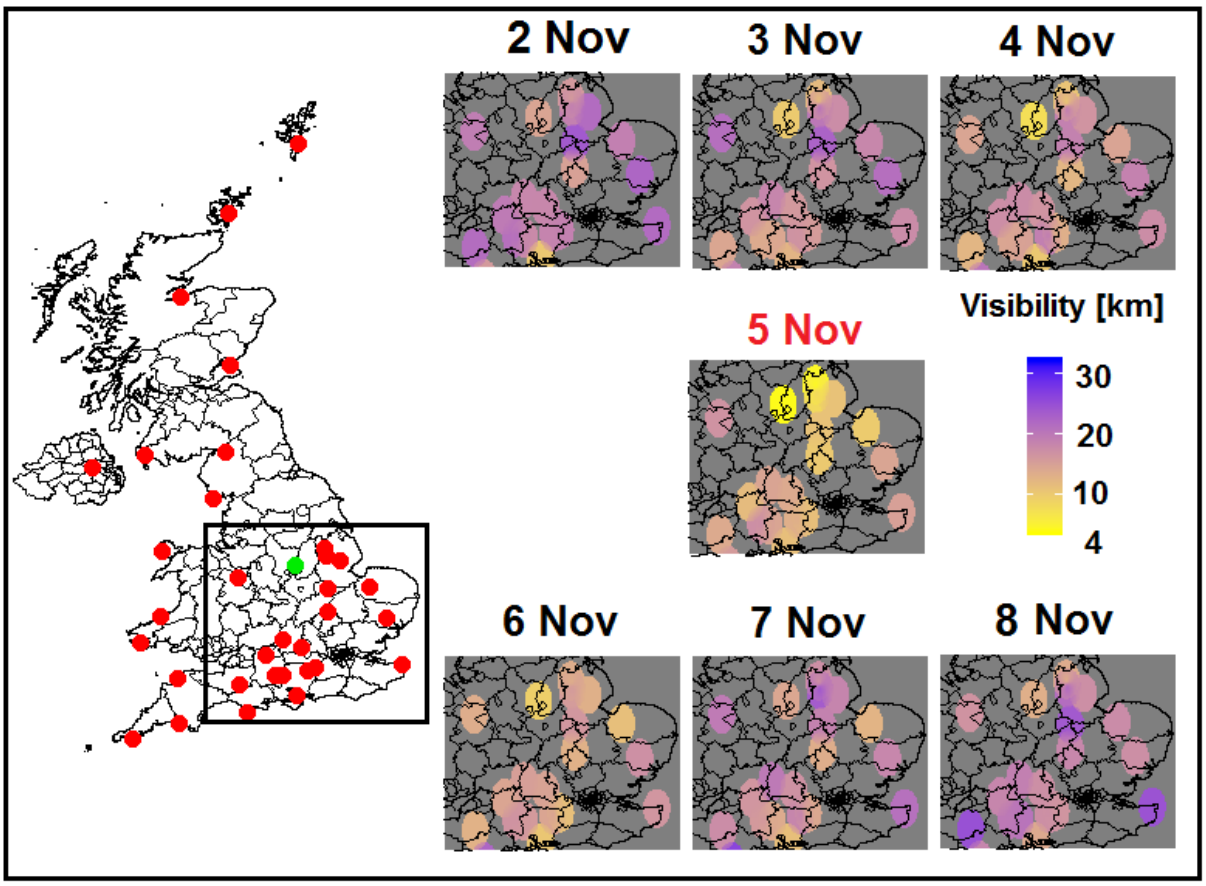

Figure 4.2 Visibility mapping of the UK before (2nd, 3rd, and 4th Nov), during (5th Nov), and after (6th, 7th and 8th Nov) the Guy Fawkes Night using 13 years (2000-2012) data. The colour dots in the UK map represent the available meteorological stations (=34) measuring visibility, where light green colour indicates Watnall station (Nottingham). The meteorological stations (=20) used for the spatial mapping are indicated within the black box. The scale bar provides the visibility range.

4.6.2 Temporal trends analysis of visibility and characterization of RH and particle hygroscopicity on visibility change during fireworks night

To better understand the change in visibility caused by Guy Fawkes Night, this study investigated the 13 year average 2100 h visibility values for a single site (Nottingham-Watnall, SYNOP code number = 3354, station source ID = 556) for the months of October and November (see Figure 4.2 And 4.3). Again there is a clear

dip in visibility occurring on the 5th November showing the effect of Guy Fawkes Night (a reduction of more than 55% compared to the 2nd, 3rd, 4th, 6th, 7th, and 8th November) (Figure 4.3). Investigation of the 24 hourly data over Nottingham also indicates that visibility starts decreasing from 1900 h on the 5th November and stabilises at a lower than average level after 0100 h on the 6th November (for example refer Figure 4.4), due to changes in the loading of firework-derived PM.

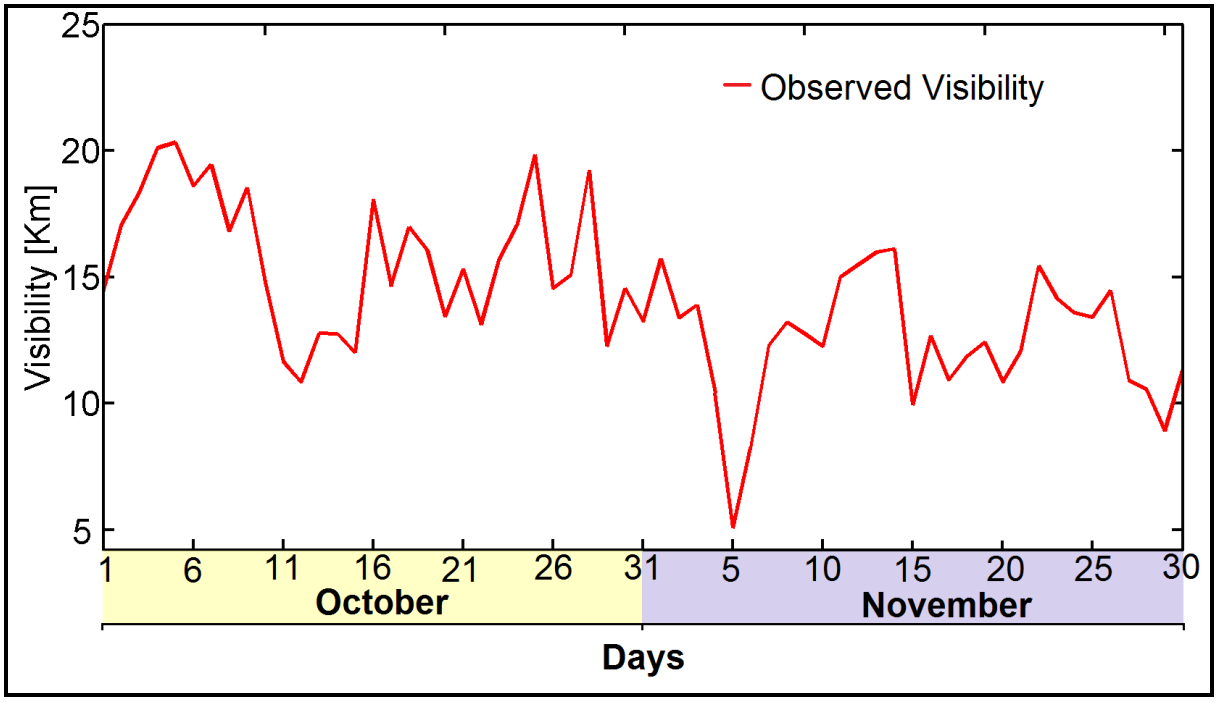

Figure 4.3 13 year averaged observed visibility at 2100 h, during October and November month

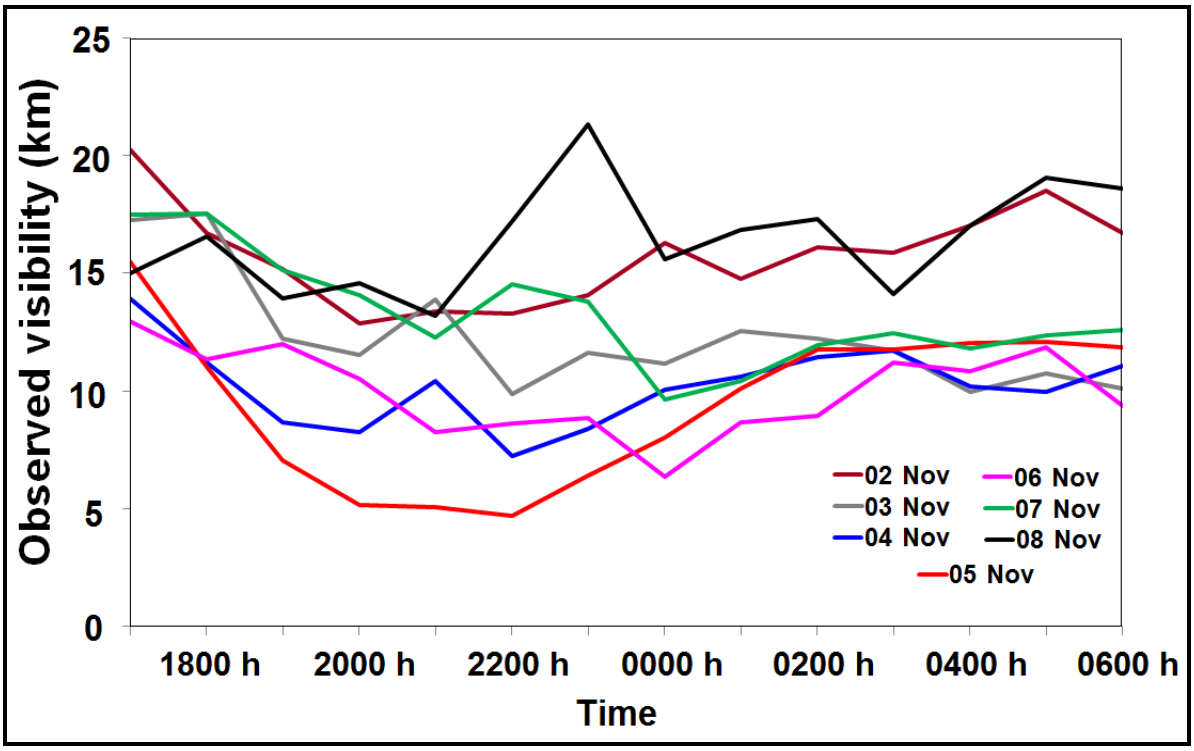

Figure 4.4 13 year (2000-2012) hourly averaged observed visibility for 2nd, 3rd, 4th, 5th, 6th, 7th and 8th November

This Guy Fawkes driven dip in visibility becomes even more pronounced when the effect of RH is taken into account. The daily relative humidity (measured at 2100 h) shows the expected seasonal increase as the date progresses from the start of October to the end of November, see Figure 4.5 panel (a). The relative humidity increases from ~85 to 90 % over the course of the two months, with significant variability. Whilst this represents only a modest increase in relative humidity, such a change of 5 % in this region of a PM hygroscopicity growth curve can be significant (e.g.(Pope et al., 2010)). As discussed in the Chapter 1 and 2, as RH increases so does particle water content with the corresponding changes in size, composition, refractive index and hence extinction coefficient. Since the composition and size distribution of the PM is unknown, the effect of RH cannot be explicitly calculated

but a simple correlation curve between visibility and relative humidity can be generated. The relationship between visibility (V) and RH can be reasonably approximated using a linear relationship, V = m×RH + c, where the fitting constants m and c are best described by -1.19 % and 119.42 km, respectively, with a R^2 value of 0.60. This approach assumes that the non-water component of the PM loading, composition and size stays constant over the time period analysed; clearly this necessitates the exclusion of the data from Guy Fawkes Night.

Using the relationship between visibility and RH, the visibility anticipated for the 5th November in the absence of Guy Fawkes Night can be predicted, see Figure 4.5 panel (b). It is discernible that the predicted visibility shows reasonable agreement with the observed visibility except on the 5th Nov. Panel (c) in Figure 4.5 shows the difference between observed visibility and predicted visibility and the effect of Guy Fawkes Night on visibility is even more apparent. This analysis suggests that Guy Fawkes Night in Nottingham reduces visibility by approximately 10 km which corresponds to a 64% reduction in visibility. This reduction in visibility is highly significant as it lies below four standard deviations (± 8.88 km) of the average visibility, see Figure 4.5 panel (c).

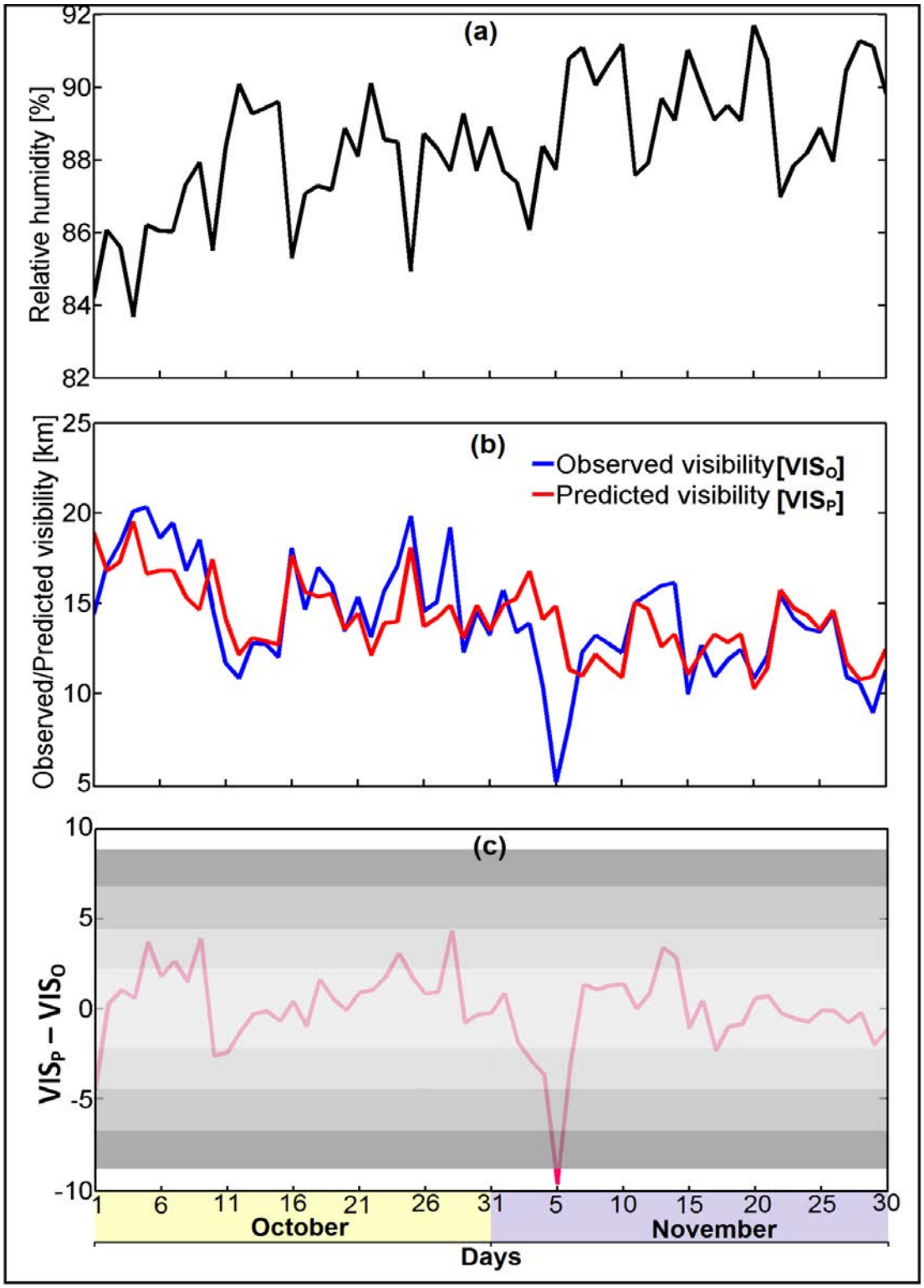

Figure 4.5 Dependency of relative humidity on visibility with 13 years (2000-1012) data-set, where panel **a)** Average relative humidity **b)** Comparison of observed (VIS_O) and predicted visibility (VIS_P) and **c)** Difference between observed and predicted visibility, where grey shading strata represent standard deviations (σ) from the mean. Lightest grey = 1σ and darkest grey = 4σ.

4.6.3 Pollutants alteration during Guy Fawkes Night

The change in visibility due to Guy Fawkes Night is compared with atmospheric pollutant concentrations in Figure 4.6. There are clear spikes in the $PM_{2.5,}$ PM_{10} and black carbon PM matter on Guy Fawkes Night which suggest that these pollutants are, at least in part, responsible for the reduction in visibility for this night. $PM_{2.5,}$ PM_{10} and black carbon PM concentrations were ~253%, ~62% and ~201% greater, respectively. It is emphasized again that the $PM_{2.5,}$ data set only contains 4 years of data whereas the PM_{10}, black carbon and visibility data sets encompass 13 years. The corresponding reduction in visibility for the time period of the $PM_{2.5}$ measurements is 63%. As expected, the $PM_{2.5,}$ data are noisier compared with the other PM data streams. This is due to shorter measurement period which introduces more statistical noise in addition to a greater 'day of the week' effect on the average data. Over longer averaging periods, the likelihood of the 5th November falling preferentially on specific days of the week becomes less likely. The data suggest that the average concentration of $PM_{2.5}$ was higher on both 5th (31.25 μg m^{-3}) and 6th November (38.75 μg m^{-3}) compared with rest of the investigated dates, see Figure 4.6, panel c. In 2010 there was an exceptionally large signal on the 6th November (Saturday) which explains the Guy Fawkes Night $PM_{2.5}$ peak occurring on both the 5th and 6th November.

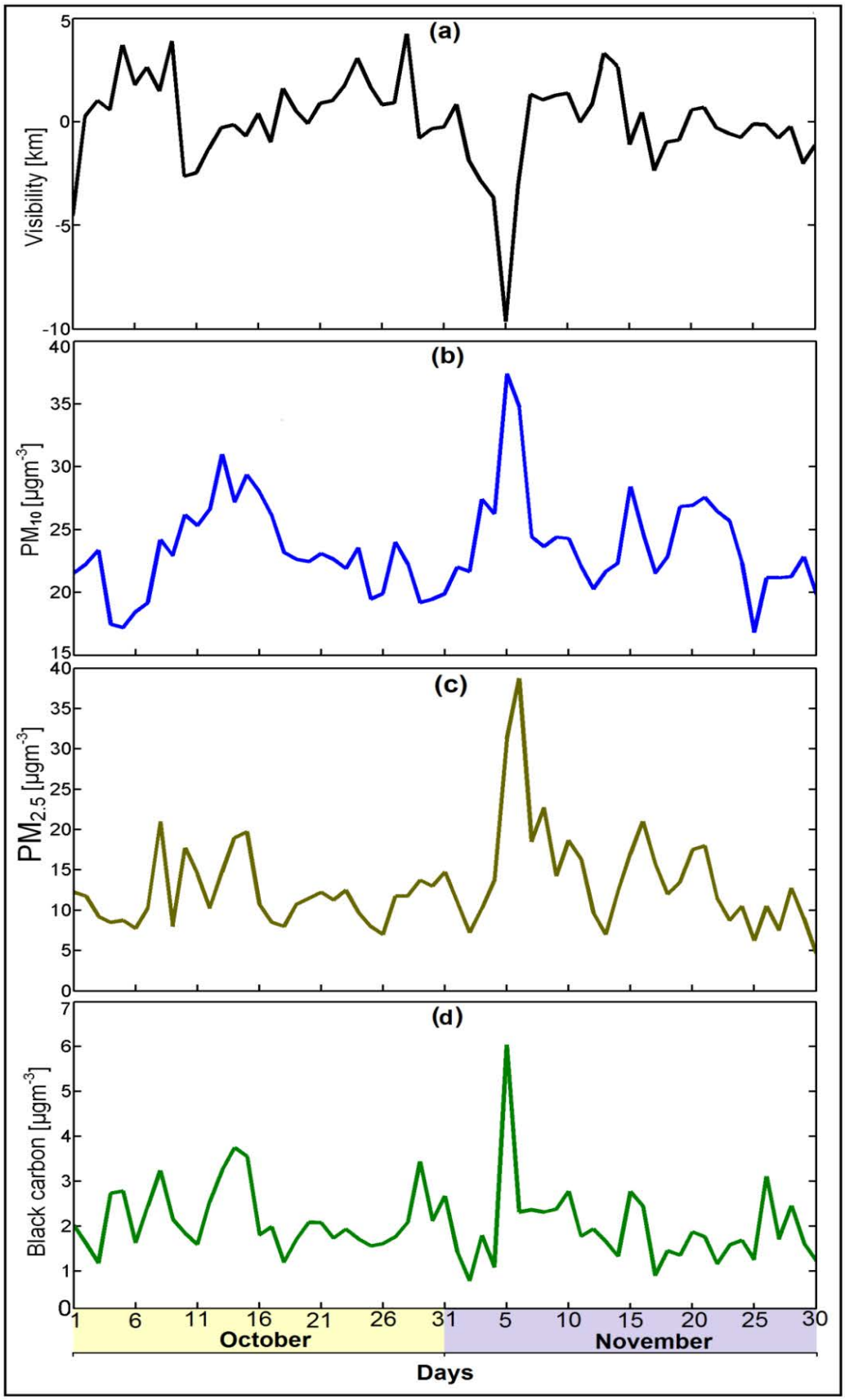

Figure 4.6 Comparison of pollutant concentrations with visibility measurement (predicted – observed). The visibility, PM_{10} and black carbon data sets represent 13 year averages (2000-2012), whereas the $PM_{2.5}$ data set represents a 4 year average (2009-2012).

The influence of NO_2 on visibility was also investigated. The NO_2 concentration did not show any significant change over the Guy Fawkes Night period. Hence none of the additional visibility loss, associated with GFN, can be ascribed to gas phase absorption of light. Likewise gas phase scattering will not be affected by GFN. Therefore the change in the extinction coefficient over the celebration period must be due to changes in PM absorption and scattering. This is expected because the contribution of gases to the extinction coefficient is typically negligible except in pristine conditions or conditions with exceptionally high NO_2.

The most significant component of PM that absorbs light is black carbon. The incremental loading of black carbon on Guy Fawkes night can be directly converted into an PM absorption coefficient ($\beta_{PM,abs}$) through use of the recommended value of the mass-normalized absorption cross section (σ), 7.5 $m^2\ g^{-1}$ (Bond and Bergstrom, 2006) and Equation 4.1, where BC is the black carbon mass concentration.

$$\beta_{PM,abs} = \sigma \times BC \qquad (4.1)$$

The average observed visibility for Guy Fawkes Night (2000-2012) is 5.1 km and the predicted visibility in the absence of celebrations is 14.8 km which correspond to extinction coefficients of 0.77 and 0.26 km^{-1}, respectively. The average black carbon concentration on Guy Fawkes Night was 6.04μgm^{-3}. The average non Guy Fawkes Night background black carbon concentration was 2.00μgm^{-3}. The corresponding average PM absorption coefficients for Guy Fawkes Night and non-Guy Fawkes Night period are 0.045 and 0.015 km^{-1}, respectively. Hence the PM absorption

coefficient only accounts for 5.9 and 5.8 % of the total extinction coefficient for the two different time periods. Even though the absolute loadings are very different on Guy Fawkes Night compared with the normal background conditions, the percentage contribution of black carbon to total visibility reduction is largely independent of Guy Fawkes Night which is surprising.

In contrast to the PM absorption coefficient, it is more difficult to estimate the enhancement in the PM scattering coefficient ($\beta_{PM,sca}$) due to Guy Fawkes Night, because key parameters are unknown, including the distribution in the particle size and composition and how these differ from the background PM. Nevertheless the increment in $PM_{2.5}$ loading over the Guy Fawkes Night period can be used to estimate the effect if several assumptions are made: 1) the distributions of aerosol size and composition are the same as the background PM; 2) the only difference between the PM distributions is the number concentration of PM, i.e. Guy Fawkes Night introduces an additional source of PM which has identical properties to the background aerosol; 3) $PM_{2.5}$ is a good proxy for light scattering PM which are largely sub-micron in size; 4) the component of the extinction coefficient due to gas phase species is negligible. With these assumptions the scattering coefficient can be calculated through knowledge of the extinction and absorption coefficients using Equation 4.2.

$$\beta_{PM,sca} = \beta_{ext} - \beta_{PM,abs} \quad (4.2)$$

The validity of these assumptions can be tested by comparing the scaling constant (δ) required to convert the $PM_{2.5}$ concentration into a scattering coefficient, i.e. $\beta_{PM,sca} = \delta \times PM_{2.5}$. The calculated scattering coefficients for Guy Fawkes Night and non-Guy Fawkes Night period are 0.67 and 0.25 km^{-1}. The corresponding values for

δ are 0.021 and 0.020 m^3 μg^{-1} km^{-1}. Given the assumptions used in deriving the scattering coefficients, the two derived values of δ are in remarkably good agreement. The contribution of the scattering coefficient to the total extinction coefficient for Guy Fawkes Night and non-Guy Fawkes Night is 94.4 and 96.1 %.

In addition to visibility altering pollutants, the gas phase concentration of SO_2 was also investigated. No significant changes in SO_2 were observed over the celebration period. Therefore for the site investigated, SO_2 is not a good chemical marker for Guy Fawkes Night. This is surprising since enhanced SO_2 has previously been shown to be associated with fireworks (Ravindra et al., 2003). One possible reason for the lack of significant changes in SO_2 concentrations during Guy Fawkes Night events may be UK regulations on firework compositions that set limits on sulphur content (Galea and Powles, 2010).

4.7 Conclusions

In the present study, the role and influence of firework and bonfire emissions on visibility and short term air quality has been quantified. Although Guy Fawkes Night only occurs once a year, the associated celebrations occur over a wider time range (on the order of a week). Using data from 34 meteorological stations, sharp reductions in nationwide visibility were clearly observed on Guy Fawkes Night. However, the effect is short-lived, with average visibility returning to normal within two days due to the dispersal of the additional PM loading. More detailed analysis on the data from a single urban area (Nottingham) showed that the effect of Guy

Fawkes Night is even more pronounced when the effect of relative humidity, through its influence on the extinction coefficient of PM, is taken into account.

The reduction in visibility on Guy Fawkes Night is caused by increases in atmospheric PM loading which is generated through bonfires and fireworks. In particular there is clear anti-correlation between the $PM_{2.5}$, PM_{10} and black carbon PM with the observed visibility. It is interesting to note that as the UK becomes ever more multicultural and might expect the frequency and magnitude of festivals/celebrations that use fireworks (such as Diwali and Chinese new year etc.) to increase with corresponding visibility reduction hotspots.

The data and analysis shown through this research, indicates that the public should be made aware of the possibility of low visibility on Guy Fawkes Night which can be very localized. In particular, care should be taken when RH is predicted to be high and the atmosphere already has a high PM loading. Since firework displays are planned months in advance, weather and pollution forecasts of sufficient skill are unavailable to help in their planning. However, if forecasts subsequently suggest that the planned display will coincide with conditions likely to exacerbate poor visibility then the organizers and local authorities should be prepared to issue poor visibility warnings in advance. This precautionary step can help to increase enjoyment, or at least prevent unnecessary accidents, during Guy Fawkes Night which is a much loved and highly anticipated celebration.

Chapter 5.0

Measurements of HONO during 2015 solar eclipse: Insight into potential sources and sinks

Most of the material in this chapter has been taken from following paper:

Singh, A., Crilley R.L., Bloss, W.J. and Pope, F.D., Measurments of HONO during 2015 solar eclipse: Insight into potential sources and sinks. *Geophysical Reaserch Letters* (under process)

5.1 Chapter overview

This chapter explores daytime HONO variations along with other gas and particle pollutants during the 2015 solar eclipse. It also examines the potential source scenarios of HONO under different light conditions that occur during a solar eclipse. Chemical kinetic modelling of the scenarios is employed to explain the HONO trends and the influence of different sources on HONO concentration during the solar eclipse.

5.2 Abstract

Nitrous acid (HONO) is an important source of the OH radical in the troposphere. However, the daytime sources of HONO are poorly constrained. In the UK, a near total solar eclipse occurred on the 20th March 2015 thereby providing a unique opportunity to explore the response of HONO to a short-term (non-diurnal) perturbation in solar intensity. The present work explores the daytime HONO variation and compares the observed variation with that expected for different potential source scenarios across the eclipse period. Little variation in HONO concentration was observed in response to the changing light levels, pointing to relatively balanced photochemical source and sink dominating HONO abundance. To explain the HONO trends and the influence of different sources on HONO concentration during the eclipse, chemical kinetic modelling of the scenarios was employed. The simulations suggest that no single source is able to explain daytime HONO profile during solar eclipse. A clear influence of traffic source on HONO

concentration was observed; however, sources related to photolysis and NO_2 cannot be neglected in daytime HONO chemistry.

5.3 Introduction and objectives

In the last three decades many studies have been conducted to understand the atmospheric sources of HONO and their relationship with different gas and particle species (e.g. (Ammann et al., 1998; Chang et al., 1981; Harrison and Kitto, 1994; Kalberer et al., 1999; Lee et al., 2016; Lee et al., 2002; Su et al., 2008; Tong et al., 2015; Zhou et al., 2002)). High daytime HONO concentrations which are found in many urban environments cannot be explained by its known sources, which clearly suggest one or more unknown HONO sources exist (Michoud et al., 2014). HONO can be formed directly or indirectly from various natural and anthropogenic sources; where, traffic emission is a major source of HONO in the urban environment (e.g. (Crilley et al., 2016; Tong et al., 2015)).

Many field and laboratory studies suggest the photolysis of nitric acid absorbed on the ground as a possible missing daytime HONO source (Michoud et al., 2014; Zhou et al., 2002; Zhou et al., 2003). Su et al. (2011) observed that biological activities in soil can generate nitrates, which can photolyse to HONO and proposed this as a missing daytime source. However, changes in daytime HONO concentration and sources are still unknown and unclear.

Here, a near-total solar eclipse (~ 90 % attenuation) was used as a natural short-term perturbation to atmospheric photochemistry to explore the chemical processes affecting HONO abundance. The reduction in photolysis frequencies due to cloud cover is not as large as the reduction in photolysis frequencies due to an eclipse. In

particular, the light attenuation from cloud is lower (Bohn et al., 2008) than what would occur in a ~ 90 % eclipse situation. The temporal variation of HONO, NO_x and related species (O_3, PM), was reported and used to explore which potential HONO formation mechanisms are, in isolation, consistent with the observed behaviour and the findings are reported in Section 5.5.

5.4 Method

5.4.1 Data measurements and site description

HONO, NO_x, O_3 and particulate matter (PM) were measured at the Elms Road Observing Station (EROS), an urban background monitoring station situated on the University of Birmingham campus (Figure 5.1) (Alam et al., 2015). The eclipse measurements were part of larger field campaign (18th March – 1st April 2015); however our focus here is upon the solar eclipse (20th March 2015). Possible emission sources located near EROS include a suburban rail line (north), roads (east) and a field (west and south).

Figure 5.1 Map of Elms road observatory site at University of Birmingham. Image source: Google Earth

5.4.2 Measurement of HONO

HONO was measured using a Long-path Absorption Photometer (LOPAP) - Heland et al. (2001) / Kleffmann et al. (2002). Briefly, the LOPAP is a wet chemical technique, where gas phase HONO is sampled using a stripping coil into an acidic solution and is derivatived into an azo dye. The light absorption at 550 nm of the azo dye is then measured with a spectrometer using an optical path length of 2.4 m. The LOPAP was operated and calibrated according to the standard procedures described in (Kleffmann and Wiesen, 2008), with a sampling height of 3m above ground level, and data obtained at 5 minute time resolution. Baseline (zero) measurements were taken at frequent intervals (8 hours). The detection limit was determined to be 6 pptV.

In addition to the LOPAP, co-located measurements of NO, NO_2 and NO_x (Thermo Scientific 42c - Mo convertor for NO_2 measurement, hence potentially susceptible to NOy interferences), and ozone (Thermo Scientific 49i) were performed. An optical particle spectrophotometer (TSI 3330) measured the particulate matter number size distribution, and converted from particle number concentration (PNC) to total aerosoal surface area (TSC) via the TSI AIM software, assuming all the particles are spherical. NO_x, O_3 and particle analysers sampled at a 1 min time resolution. Meteorological data (relative humidity, solar intensity, air temperature, and wind speed and direction) was obtained at 1 min time resolution from a nearby weather station.

5.4.3 Description of simulations of HONO production and loss during the solar eclipse

To understand the variation in HONO concentration in response to rapid changes in light conditions (with and without solar eclipse conditions) and to investigate the influence of different generic sources, a number of simulations were performed, in which the forward evolution of in situ HONO abundance over the eclipse timeframe (ca. 2 hours) was simulated using a simple set of differential equations representing different scenarios for processes forming and removing HONO.

At the University of Birmingham site, the eclipse lasted from 08:25 to 10:40 (first / last contact) with the maximum occultation (89 % of the sun's face) occurring at 9:31 (Hanna et al., 2016). The attenuation of photolysis frequencies was approximated using values obtained from the TUV model (Madronich et al., 2003) for clear-sky conditions, with the reduction in *j* values modelled as a 1-π sine wave. It is noted

that this is an approximation, both to the actual photolysis frequencies and the geometric coverage of the solar disk, but one which is not dominant in the context of the analysis which follows. The calculated j_{NO2} values prior to and subsequent to the eclipse were in agreement with those determined by photostationary steady state to within 5.6±1.5 % (before eclipse), 21±1.9 % (during eclipse) and 6.4±2.0 % (after eclipse). A number of cases were simulated (Table 5.1). In each case the simulation was initiated at 07:30, prior to the eclipse start, with the observed HONO level of 0.86ppb, and subsequent evolution of HONO calculated according to the mechanisms presented below. In general, each case may be represented via Equation (5.1), below, where S_x is the source term for HONO formation in each scenario:

$$d[HONO]/dt = S_x - j_{HONO}\,[HONO] \qquad (5.1)$$

Constant C in Table 5.1 was determined from the measured values of $j_{NO2,}$ NO_2 and TSA using equation 5.1 assuming sources and sinks are balanced (d[HONO]/dt = 0) at 8:25 am. This assumption is made on the basis of the measured HONO trend described in section 5.5.1. Each simulation was performed using the actual (eclipse influence) reduction in solar intensity (photolysis frequencies), and via a hypothetical scenario where no eclipse occurred and clear-sky photolysis applied throughout the x hour time period. The resulting predicted and observed HONO are shown in Figure 5.3.

Table 5.1 Summery of HONO simulations in different scenarios

	Potential sources	**Source strength (S)**	**Constant scale factor (C)**
Case 1	No source, only photolytic loss	$S_1 = 0$	------
Case 2	A source related to photolysis	$S_2 = C \times j_{NO2}$	1.2×10^{-1} ppb
Case 3	A source related $[NO_2]$	$S_3=C\times[NO_2]$	1.67×10^{-5} s^{-1}
Case 4	A source related to particle (TSA)	$S_4=C\times$ [TSA]	1.81×10^{-6} ppb $s^{-1}(\mu m^2 cm^{-3})^{-1}$
Case 5	Source(s) related to $[NO_2]$ and TSA	$S_5=C\times [NO_2] \times$ [TSA]	$7.07 \times 10^{-8\,6}$ s^{-1} $(\mu m^2 cm^{-3})^{-1}$
Case 6	Source(s) related to photolysis, $[NO_2]$ and TSA	$S_6=C\times j_{NO2} \times [NO_2] \times$ [TSA]	2.1×10^{-5} $(\mu m^2 cm^{-3})^{-1}$

5.5 Results and Discussion

5.5.1 Measurements during the solar eclipse

During the eclipse, a calm wind was observed (wind speed of 0.5±0.4 m/s) with the average relative humidity of 76 ± 6 % and temperature of 6.7 ± 1.7 ^oC, which are typical for the time of year in the UK. Ozone and NO_x were observed to be tightly coupled during eclipse period (08:25 am to 10:40 am GMT, Figure 5.2b). This behaviour of ozone and NO_x during the eclipse are expected and based upon

known photochemistry. Relatively little change in HONO concentration was observed in response to changing solar intensity, potentially pointing to relatively balanced photochemical source and sink dominating HONO abundance (Figure 5.2a). During the eclipse, the little variation was observed in the particle TSA (Figure 5.2c), and TSA was found to be fairly good correlated with HONO concentration ($r=0.82$, $p<0.0001$). Moreover, high $HONO/NO_2$ ratio (> 1.9 %) suggests additional sources of HONO in the environment in addition to vehicular emissions during measurements (Figure 5.2 c) (Liang et al., 2017).

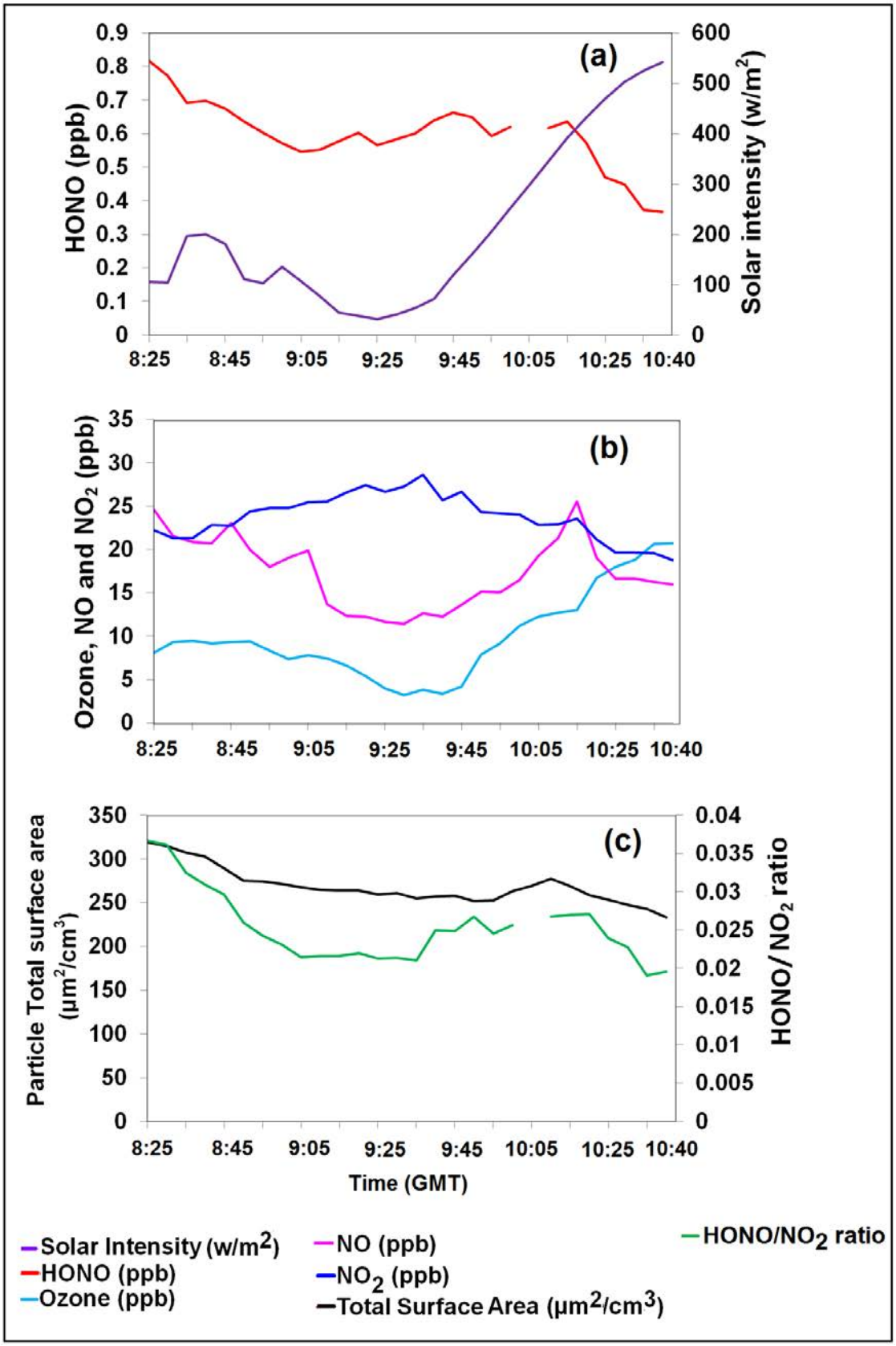

Figure 5.2 Time series of **(a)** measured HONO and solar intensity, **(b)** NO_x and Ozone, **(c)** Particle total surface area (TSA) and HONO/NO_2 ratio.

5.5.2 Simulated HONO production and loss during the solar eclipse

Variation in HONO concentration could be expected due to changing photolysis rates during the eclipse, however this was not observed. Therefore a combination of different sources and their effects on HONO production were simulated compared to measured HONO concentration, which described in section 5.4.3 and Table 5.1, with the results shown in Figure 5.3. Despite the rapid photolytic loss of HONO in the atmosphere, high concentration of daytime HONO are often observed in urban environments, pointing to a strong daytime production of HONO (Michoud et al., 2014). In Figure 5.3a, HONO was simulated with no source and photolysis as the only sink, this does not reflect the observed significant (non-zero) daytime HONO concentration so there must be a source.

During the day previous work has suggested a source of HONO related to photolysis (j_{NO2}) (Lee et al., 2016; Wong et al., 2012). However, when the source was scaled to j_{NO2} (Figure 5.3b), the simulated HONO during the eclipse did not match the measured HONO concentration; therefore a source only related to photolysis cannot explain the observation during the eclipse and points to other daytime source(s) of HONO. The source strength also scaled to j_{NO2} along with NO to predict HONO concentration, which is closely related to OH ×NO and demonstrated gas phase OH + NO process. Unfortunately, this did not work and suggested HONO is not then dominant source.

In the urban environment, photosensitized conversion of NO_2 on aerosol and surface containing organics can also be a daytime HONO source (George et al., 2005; Lee et al., 2016; Stemmler et al., 2006). In Figure 5.3c, a source scaled to NO_2 mixing ratio as scaled as a potential HONO source, and under eclipse

conditions the simulated HONO levels were peaked and consequently did not match the measured HONO concentrations. This implies that this source profile is not complete and NO_2 only cannot explain source during eclipse measurement.

Direct emission of HONO from vehicles is another potential source (Crilley et al., 2016; Kurtenbach et al., 2001). In an urban area, TSA can be used as tracer for vehicles emissions (Lv et al., 2014). In Figure 5.3d, TSA was scaled as a potential source to predict the HONO. No match was found between simulated HONO and measured HONO concentration under eclipse conditions, when considering TSA as the sole HONO source (Figure 5.3d). In addition, similar results were observed, when particle number concentration was used as source strength scale to predict the HONO concentration during the eclipse. This implies that a source scaled to TSA cannot explain the observed trends in HONO concentration during the eclipse.

Furthermore, HONO was simulated using two combined possible sources from traffic emission, where TSA and NO_2 (via NO_2 conversion on particle surface) may better represent traffic emission. This is because HONO forms on surfaces of freshly emitted particles (Kurtenbach et al., 2001) and therefore the particle total surface area (TSA) and NO_2 may be a good proxy for a direct emission source. From simulation a closer match was observed between simulated HONO and measured HONO concentration under eclipse conditions (Figure 5.3e) as compared to cases 1 to 4. NO_2 and TSA could be a better proxy of traffic emissions but still not enough to explain daytime HONO source.

In the next case, the combined contribution of traffic source and source related to photolysis (j_{NO2}) and NO_2 in HONO production and losses from photolysis are seen in case 6. In both eclipse and without eclipse conditions a clear match was observed

between simulated HONO and measured HONO (Figure 5.3f). From Figure 5.3, a single source was not able to explain the trends in measured HONO concentration during the solar eclipse, but once a source was considered which was proportional to the product of these factors in the simulation (TSA, j_{NO2} and NO_2), a better match was observed (Figure 5.3f). However, case 6 had the most parameters, which increased the chances for better prediction. Overall, Case 6 also showed a balanced HONO sources and sinks during eclipse as observed in measured HONO concentration as well as a clear influence of traffic related emissions. However, sources related to photolysis and NO_2 cannot be neglected in HONO formation. Lee et al. (2016) and other papers (Michoud et al., 2014; Tong et al., 2015; Xu et al., 2015) also find similar sources as used in present study, which is needed to explain daytime HONO.

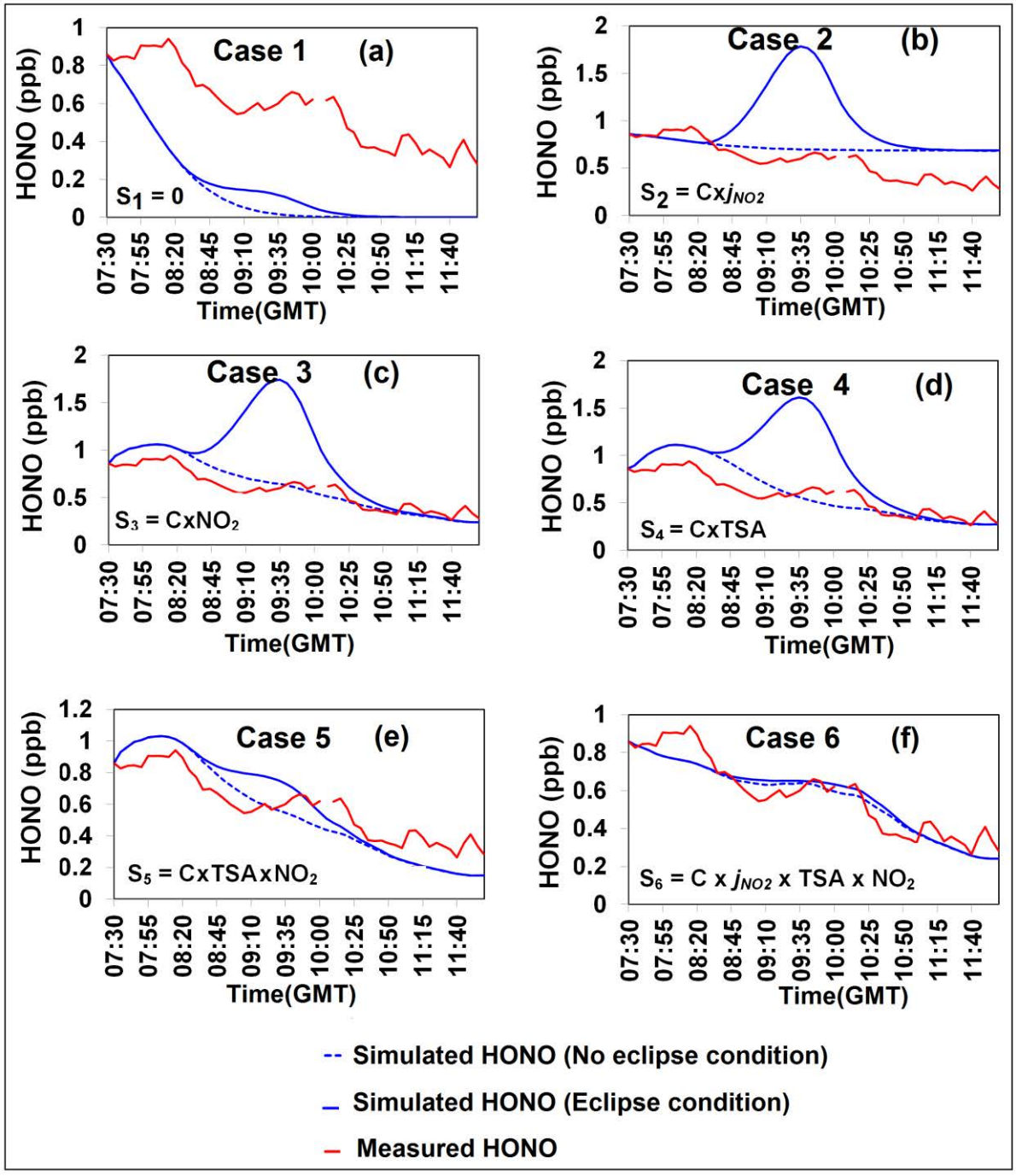

Figure 5.3 Comparison between simulated HONO and measured HONO concentrations during the solar eclipse, for different scenarios, explained in section 5.4.3 and Table 5.1.

5.6 Conclusions

A total solar eclipse on the 20th March 2015 provided a unique natural experiment to understand how HONO and other gaseous species (NO_x and O_3) and airborne PM varied in response to rapid changes in the solar intensity. In general, the observed behaviour of O_3 and NO_x during the eclipse was as expected based upon known photochemistry. However, relatively little variation in HONO concentration was observed during the solar eclipse indicating that photochemical source and sink terms were closely matched. To identify the changes in daytime HONO concentrations and investigate its potential sources, chemical kinetic modelling of various scenarios was employed. No match was observed between simulated HONO concentrations with measured HONO from Case 1 to Case 4 during eclipse condition. While a source scaled to both TSA and NO_2 was partly able to replicate the observed trends in HONO concentration during the eclipse, the closest match was found using a source scaled to the product of TSA, NO_2 and j_{NO2}. Therefore, the simulations have clearly shown that a single source cannot explain the daytime HONO profile during solar eclipse. From the simulations it is found that traffic related emissions during the eclipse influenced the measured HONO concentration, however sources related to photolysis and NO_2 cannot be neglected.

Chapter 6.0

Intercomparison of atmospheric HONO at a number of urban background sites: insights into sources

6.1 Chapter overview

The purpose of this chapter is: to first, perform an intercomparison of HONO concentrations at different UK urban sites; second, to analyse the variation in HONO with meteorology, traffic emissions / abundance of traffic derived species and other potential sources. This chapter includes a description of gas and particle phase measurements and findings in different urban background locations along with site descriptions.

6.2 Abstract

Over the past few years research effort in the field of HONO chemistry has increased, however there are limited studies devoted to field measurements of HONO along with other pollutants in the UK urban environment (Spataro and Ianniello, 2014). Here measurements of gas (HONO, O_3 and NO_x) and particle species made at different urban background sites, during four different campaigns in the UK are analysed to investigate HONO variation and sources in different environments. Overall the highest HONO mixing ratio was observed in London during the winter season (1.18 ± 0.96 ppb), while the lowest was reported in York during the summer season (0.19 ± 0.15 ppb). The results from the relationship between HONO and wind speed show that HONO decreases with increasing wind speed, down to a lower limit (non-zero) that varies by locations and seasons. The relationship between HONO and wind suggests a primary emission source into the atmosphere. An influence from vehicular emissions upon the concentration of HONO, mainly during rush hours in both morning and evening, was observed in Birmingham and London during both winter and summer. In contrast, at the York

site an influence from vehicular emissions was only observed during the mornings. In York, high HONO concentrations along with low NO_2 and NO_x concentrations were found when wind direction was from the south-east direction, where agricultural fields are located. An additional HONO source was inferred for York compared with the other sites, with biological soil activities being postulated as a possible source of HONO. Furthermore, a detailed study at the Birmingham site confirmed three different types of air masses and a pollution event early in the measurement period which appears to correlate with elevated HONO concentrations.

6.3 Introduction and objectives

Because of the importance of nitrous acid (HONO) as a source of the OH radical, its direct contribution to the nitrogen cycle and its role in formation of secondary pollutants (Lee et al., 2016; Tong et al., 2015), a detailed knowledge of its sources and spatial/temporal variation are needed. Typically, tropospheric HONO is generated from direct exhaust emission sources, heterogeneous chemistry at surfaces and homogeneous gas reactions, which are discussed in chapters 1 and 2. The contributions of these sources to the production of HONO are varied and depend upon the surrounding environment, boundary layer height and meteorology. Many field and laboratory studies have been carried out to understand and investigate the HONO sources in different environments such as urban, rural, coastal, forest and tunnels etc. (Acker et al., 2006a; Kleffmann et al., 2005; Kleffmann et al., 2003; Kurtenbach et al., 2001; Li et al., 2012; Meusel et al., 2016; Michoud et al., 2014; Stutz et al., 2004). In a recent study, Tong et al. (2015)

performed measurements at urban and suburban environments in Beijing during winter, and observed that direct emission and homogenous gas phase sources have a larger contribution in urban environments, while heterogeneous sources via gas-surface process are more efficient in suburban environments. A study at a rural site in Southern China found a significant contribution to the HONO concentration from the surface reaction of NO_2 (Li et al., 2012). Acker and Möller (2007) measured HONO and other atmospheric pollutants at different suburban and rural environments in Europe to improve understanding of HONO chemistry. They found that the photolysis of HONO was not only an important source of OH radicals in the morning but also throughout the entire day. Acker and Möller (2007) also observed a higher mixing ratio of HONO with several isolated peaks at hills during the day time. Many more experiments and analyses have been performed to explore tropospheric HONO chemistry and its sources (Crilley et al., 2016; George et al., 2005; Spataro and Ianniello, 2014; Stemmler et al., 2006; Su et al., 2011), but limited literature exists in understanding the variation in HONO concentrations with different geographical, seasonal and meteorological conditions.

In this study, measurements of HONO were performed along with other atmospheric trace gases (O_3, and NO_x) and PM across three urban locations (Birmingham, York and London) in different seasons. The study explores the correlation, or lack thereof of HONO with other measured pollutants at different urban background locations. The study also provides insights into the variation of HONO with meteorology, traffic emission and other sources. The influence of meteorological conditions and air masses on the concentration of HONO is discussed in detail for the Birmingham site.

6.4 Data

This chapter analyses HONO concentrations measured at three urban background sites (Birmingham, York and London) in the UK that were performed as part of different studies. During all studies, HONO was measured using the same technique (LOPAP), and the method is described in chapter 5 (section 5.4.2). Further details of the three urban background sites follow, along with a description of the supporting measurements at each site.

6.4.1 Sampling locations

6.4.1.1 Birmingham measurement site description:

The two week field campaign was performed from 17th March to 1st April in 2015 at the University of Birmingham campus. Details of this site can be found in chapter 5 (section 5.4.1).

6.4.1.2 York measurement site description

These measurements were conducted as part of a campaign investigating the missing OH reactivity from VOCs. The campaign was conducted for a month from 20th May to 16th June 2012, where measurements of HONO, NO_x and O_3 and PM were taken. The LOPAP was housed within a shipping container next to the Wolfson Atmospheric Chemistry Laboratory on the University of York campus and sampled at a height of 3 m. The sampling location is surrounded by the university road (west) and fields (south east) (Figure 6.1). Measurements with the LOPAP were taken from 20th May until the 16th of June 2014 with 5 min time resolution. In addition, co-located measurements of every 5 min interval time resolution of NO_x concentrations

were obtained. Hourly meteorological data was obtained from Met Office for the Linton-upon-Ouse site, the closest site (13 miles away) with wind speed and direction measurements.

Figure 6.1 Map of measurement site at York, where red mark denotes agriculture sources. Image source: Google Earth

6.4.1.3 London measurement site description

Measurements were conducted at Sion Manning School, North Kensington (NK) (Figure 6.2) as part of the Clean Air for London (ClearfLo) project (Bohnenstengel et al., 2015), with sampling occurring over two intensive campaigns; summer (20th July

– 17th Aug 2012) and winter (12th Jan – 10th Feb 2012). During the measurements of HONO, the sampling height was 5 m. The site is adjacent to the Automatic Urban and Rural Network (AURN) (http://uk-air.defra.gov.uk/) and concentrations of NO_x, particle mass (PM) and CO with 15 min time resolution were obtained from this network. More details of the measurements during both summer and winter campaigns can be found in Lee et al. (2016). The air quality and climate at NK has been described in detail by Bigi and Harrison (2010) and are considered as representative of much of London urban background. Hourly meteorological data was obtained from the UK Met Office for Heathrow, which has been shown previously to be representative of air mass movement across London (Beddows et al., 2015). Lee et al. (2016) previously reported the HONO measurements during the ClearfLo summer campaign and where further details can be found. This work explores direct emission sources, and therefore differs from Lee et al. (2016) who focused on modelling HONO chemistry and it implications for the atmospheric radical budget.

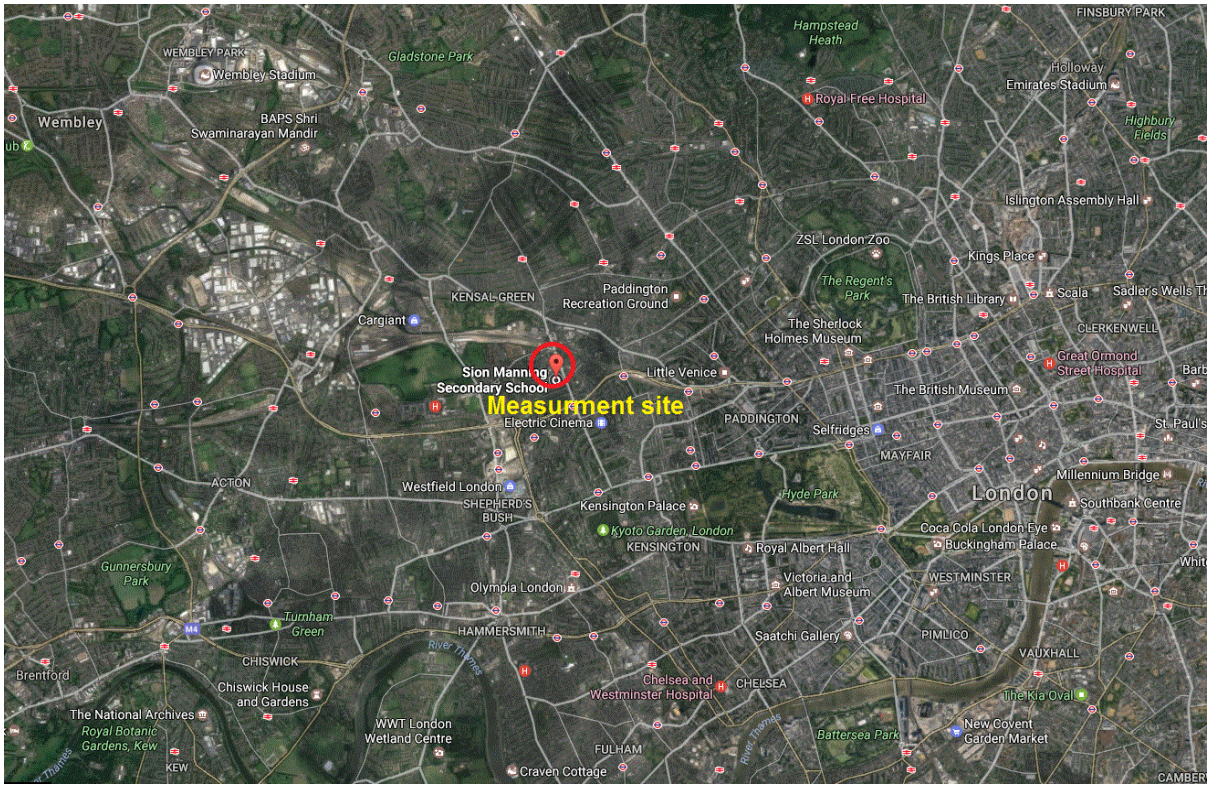

Figure 6.2 Map of measurement site at London. Image source: Google Earth

6.5 Analysis approaches

Analysis of the variations in mean diurnal concentration patterns of gas and particles have been determined from measured data. RStudio (version 0.99.489) was used for all analysis and generation of plots in the present study. Mean diurnal profiles were obtained from the 5 min time resolution datasets at Birmingham and York, however, the 15 min time resolution dataset was used for London site. The variation in the ratios of HONO/NO_x and HONO/NO_2 were also measured to explain the HONO emission sources in different urban environments and conditions using raw data of 5 min time resolution at Birmingham and York, while 15 min time resolution was used for London site.

Conditional Probability Function (CPF) analysis is performed in the form of polar plots to find the dominant source direction of pollutants (HONO, NO_x, and NO_2) using their concentrations and wind direction at the York site. CPF is a data analysis tool, which is able to explain which wind directions are dominated by high or low pollutant concentrations and also present the probability of doing so (Carslaw, 2015; Crilley et al., 2015). In particular, CPF estimates the probability of source contribution at a given wind direction and predetermined threshold (Crilley et al., 2015; Kim and Hopke, 2004; Squizzato et al., 2014). Mathematically, CPF can be explained as:

$$= \frac{m_\theta}{n_\theta} \quad (6.1)$$

Where m_θ is defined as the number of times a source contribution exceeds the predetermined threshold from direction θ, and n_θ is the total number of data points reporting wind from direction θ (Bressi et al., 2014). In this study, CPF - polar plots were performed using the Openair tool (Carslaw and Ropkins, 2012) in RStudio programming at 75th percentile threshold.

6.6 Results and Discussion

6.6.1 Comparison between different urban sites

6.6.1.1 Meteorology during campaigns

During the measurements conditions in Birmingham and London (summer and winter) were characterised by largely south westerly and northerly winds

respectively; however there was no dominant wind direction at York (Figure 6.3). During the campaigns at Birmingham, York, London-summer and London-winter the average relative humidity was 77.8±14.0 %, 76.7±15.6 %, 69.0±16.6 %, and 78.8±13.3% respectively. Average air temperatures were 6.6±2.9 ^{o}C, 14.6±3.3 ^{o}C, 18.6±3.9 ^{o}C, and 5.0±4.3 ^{o}C respectively. Here, uncertainties are at 1 standard deviation.

To determine the influence of wind on the variation in HONO concentrations, here HONO concentration are analysed the as a function of wind speed for all sites (Figure 6.4). Significant changes in HONO concentration with respect to wind speed were observed in Birmingham and London (winter and summer). However, the York observations were different from other sites. The distinct behaviour of York is more discussed in further section 6.6.1.4. In general, it is found that HONO decreases with increasing wind speed, down to a lower limit (non-zero) that varies by locations and seasons. It clearly suggests that HONO is emitted into the atmosphere rather than forming in the atmosphere. High HONO concentration at low wind speed clearly implies the local emission source. In general, wind speed can affect the relocation of pollutants (Wang and Ogawa, 2015). At lower wind speeds pollutants tend to get carried away within a certain geographical range, however, if the wind speed is high it can actually transport pollutants from other geographical locations over a large distance (Wang and Ogawa, 2015).

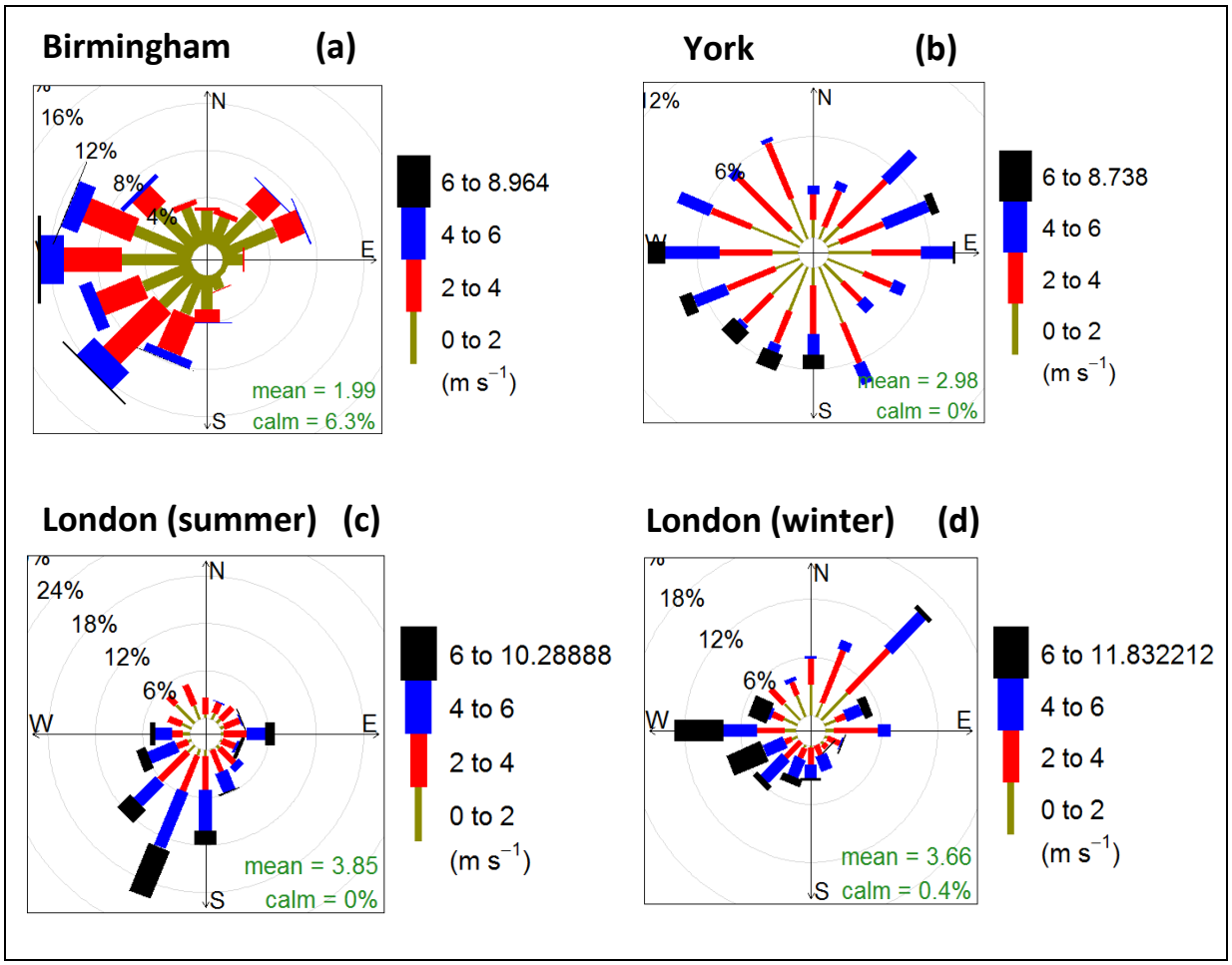

Figure 6.3 Mean windrose statistics for the measurment time period for all four campaigns.

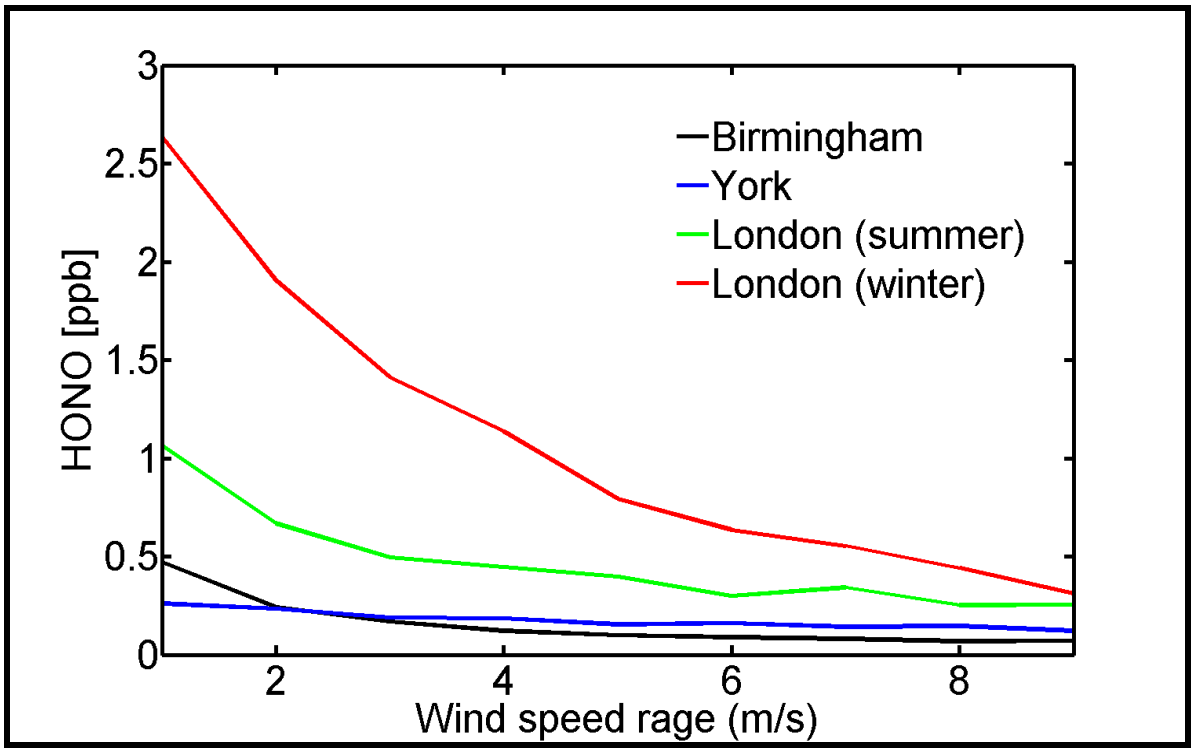

Figure 6.4 Effect of wind speed on variation in HONO concentrations for all four campaigns

6.6.1.2 HONO, NO_x, and NO_2 diurnal profiles during campaigns

Summary statistics of the measured concentrations of HONO and NO_x during all four campaigns is provided in Table 6.1. Overall, the mean HONO concentration (1.18±0.96 ppb) was highest at London during winter, in common with other pollutants like NO_x, and NO_2, compared to all sites. York had the lowest mean HONO concentration (0.19±0.15 ppb) along with NO_x, and NO_2 (Table 6.1). The mean HONO concentration in Birmingham (0.29± 0.26 ppb) was lower than London and higher than York, which is expected because London is a larger city than Birmingham which in turn is larger than York therefore has more cumulative emission.

The mean diurnal profiles of HONO, NO_x, and NO_2 are shown in Figures 6.5. Data have been normalised in order to cross compare easily. It is observed that HONO builds up during the night. In the early morning it is photolysed into OH radical and NO (HONO+ $h\nu \rightarrow$ OH + NO) and its concentration drops. Two peaks in concentration, one in the morning and another in the evening, were identified for HONO, NO_x and NO_2 in Birmingham and London (summer and winter). The morning peak is typically correlated with rush hour traffic (Table 6.2). York is notably different from the other sites, in that a HONO concentration peak was only observed during the morning hours, while NO_x peak was observed during both morning and evening hours (Table 6.2). The York NO_x diurnal profile follows that expected for traffic emissions, unlike that observed for HONO (Figure 6.5). It is also observed that morning peaks of HONO were one to two hours earlier from NO_x peaks due to the onset of HONO photolysis at sunrise. In figure 6.5, the diurnal cycle of NO_2 is a reflection of the balance between primarily traffic-based sources and photochemistry-based sinks (Wang et al., 2017). It is observed that NO_2 concentrations peak during morning rush hour, and then decrease during the day. NO_2 falls primarily due to photolysis during the day, repartitioning NO_x to NO. This can be also as a result of dilution by the deepening boundary layer (Lee et al., 2016) and photochemical oxidation driven by OH radicals (Wang et al., 2017). NO_2 remains at a low level at all locations until sundown when the concentration begins to rise again.

Furthermore, it is observed that the mean concentrations of pollutants: HONO, NO_x, and NO_2 were higher during morning hours as compared to evening time. In London during winter, the concentrations of these pollutants were larger compared to other

locations, which is most likely due to the boundary layer height being lower in winter months, and due to traffic emissions constituting a higher proportion of total nitrogen-based pollution at the London site. In addition, a variation in the timing of the peak HONO concentration was observed in London: earlier in summers, while later in winters. HONO production may be comparable, but longer dark mornings allow HONO to build up for a longer period before sunrise leading to higher overall concentrations and later peaks.

Variations in HONO and NO_x across specific days of the week are analysed. The data sets from all four campaigns (York, Birmingham and London summer & winter) did not show significant changes in HONO and NO_x concentrations between weekdays and weekends. This may be due to the limited number of readings collected in each campaign and relatively high inter day variability. Longer term campaigns may allow for more accurate mean concentration measurements and could potentially record more significant differences between days to be observed.

Table 6.1 Summary statistics of measured HONO NO, NO_x and NO_2 concentrations for the four campaigns, where uncertainties are at 1 standard deviation

Site	Sampling period	Average HONO (ppb)	Average NO_x (ppb)	Average NO_2 (ppb)	HONO/NO_x ratio (%)
Birmingham	18th March – 1st April 2015	0.29±0.26	13.60±12.20	10.30±6.40	2.0±1.0
York	20th May – 16th June 2014	0.19±0.15	6.00±4.96	4.77±3.10	3.9±2.7
London (summer)	20th July – 17th Aug 2012	0.44±0.24	19.43±15.66	14.87±8.96	2.6±0.9
London (winter)	12th Jan – 10th Feb 2012	1.18±0.96	53.61±31.41	26.70±14.05	2.5±0.8

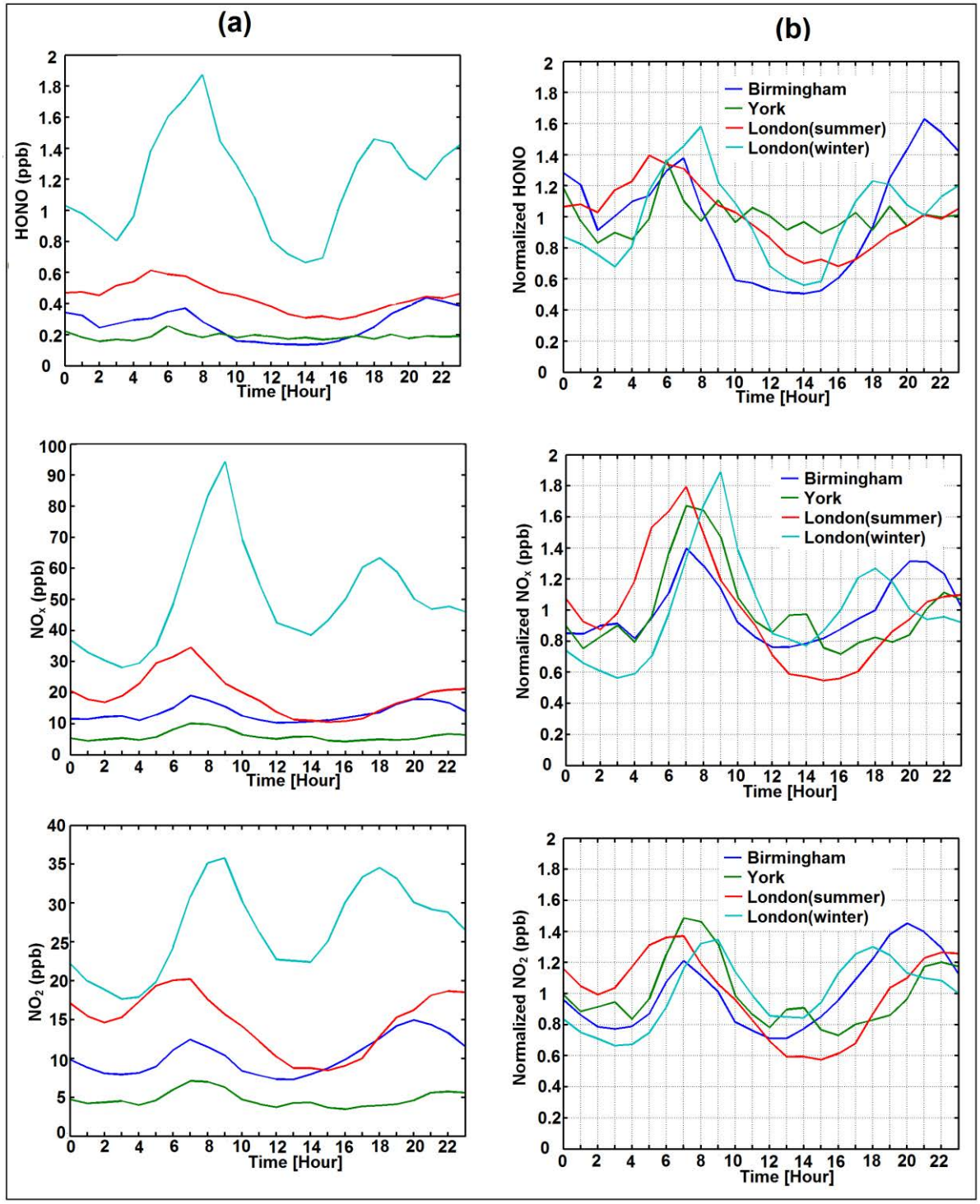

Figure 6.5 Normal (left panel) and normalized diurnal profile (right panel) of HONO, NO_x, and NO_2, at different urban sites.

Table 6.2 Peak pollutant concentrations of the four sites

Pollutants	Locations	Morning peak time	Concentration (ppb)	Evening peak time	Concentration (ppb)
HONO	Birmingham	7:00 am	0.35	21:00 pm	0.42
	York	6:00 am	0.25	17:30 pm	0.2
	London (summer)	5:00 am	0.60	18:00 pm	0.43
	London (winter)	8:00 am	1.80	18:00 pm	1.45
NO_x	Birmingham	7:00 am	19	20:00 pm	18
	York	7:00 am	10	22:00 pm	5
	London (summer)	7:00 am	35	21:00 pm	20
	London (winter)	9:00 am	94	18:00 pm	63
NO_2	Birmingham	7:00 am	12.5	19:00 pm	21
	York	7:00 am	7.5	21:00 pm	5
	London (summer)	5:00 am	20	21:00 pm	18
	London (winter)	8:00 am	35	18:00 pm	34

6.6.1.3 HONO/NO_x and HONO/NO_2 ratios

Analysis of the HONO/NO_x and HONO/NO_2 ratios can be helpful in explaining HONO sources (Kleffmann, 2007). The ratio of HONO/NO_x can be a good proxy to evaluate HONO emission sources during the day-time, while HONO/NO_2 is more suitable during the night-time (Elshorbany et al., 2012; Liang et al., 2017; Sörgel et al., 2011). It has been observed that in Birmingham and London (winter) HONO/NO_x ratios were higher between midnight and dawn when sunlight was absent and hence photolysis was also absent (Figure 6.6). There is large decrease in HONO/NO_x ratio as the morning traffic begins and remains stable during the morning rush period. However, the measurements observed vary in York and London (summer) as there are additional peaks in concentrations that occurred during the day. Previous studies suggest that if HONO/NO_x ratio is below 0.01 then

vehicular emissions are the primary source of HONO (Kirchstetter et al., 1996; Kurtenbach et al., 2001; Liang et al., 2017; Michoud et al., 2014). In this study, the higher HONO/NO_x ratio suggests additional sources of HONO in the environment in addition to vehicular emissions (Liang et al., 2017).

The daytime peak of HONO/NO_x ratio at York and London (summer) suggests strong presence of additional HONO source in the atmosphere (Elshorbany et al., 2012; Kleffmann et al., 2003). It is also found that the average concentration of HONO and NO_x in London during summer and winter were different (Table 6.1), while HONO/NO_x ratios were similar, which suggests similar sources with different levels of influence, potentially affected by changes in boundary layer height. Furthermore, the highest HONO/NO_2 ratio was determined at night time, which is assumed to be due to high conversion of NO_2 on the humid surface in the dark (Figure 6.6) (Elshorbany et al., 2012).

A positive and similar correlation between HONO and NO_x & HONO and NO_2 was also observed at Birmingham and London during summer and winter (Table 6.3). However, the York site does not show a strong correlation between either HONO and NO_x (r= 0.29) or HONO and NO_2 (r= 0.30) compared to other sites. The poor correlation between HONO and NO_x suggests a different source mix of HONO at York compared to other sites. To understand the potential HONO source at the York site CPF analysis was carried out as documented in the following section.

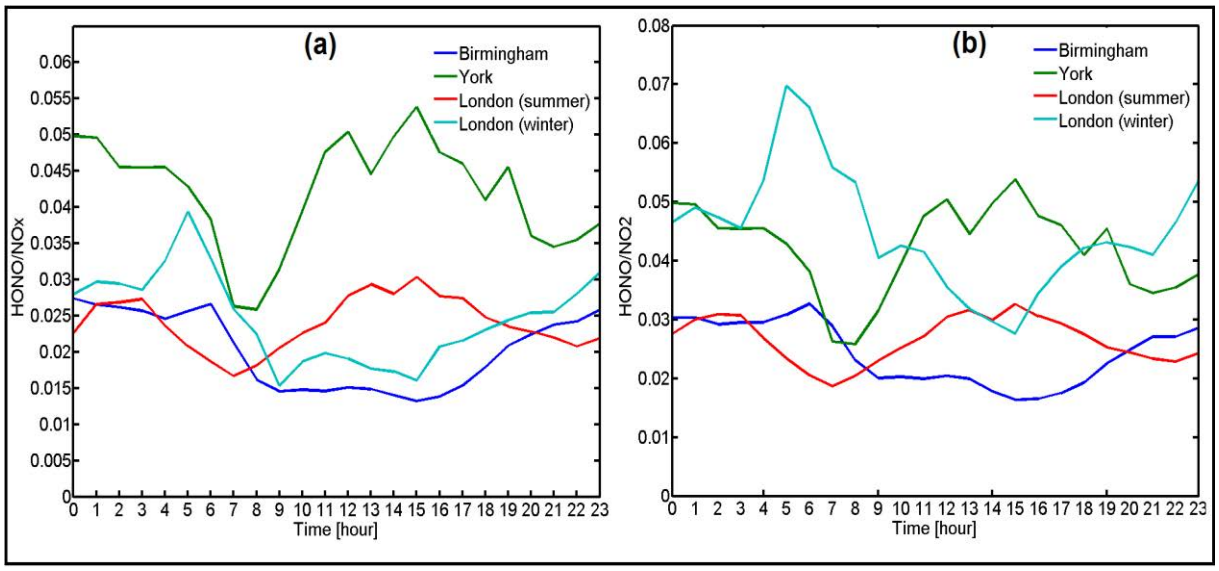

Figure 6.6 (a) HONO/NO_x and **(b)** HONO/NO_2 ratios for all four compaigns

Table 6.3 Correlation coefficient (r) values between specific gas pollutants for all measurement sites

	Correlations (r)	**Correlations (r)**
Site	**Between HONO and NO_x**	**Between HONO and NO_2**
Birmingham	0.68	0.69
York	0.29	0.30
London (S)	0.69	0.70
London (W)	0.73	0.72
statistically significant value at p<0.0001		

6.6.1.4 Other potential sources of HONO at York site

Polar plots of HONO, NO_x and NO_2 have been generated using CPF analysis (Figure 6.7). It is observed that high HONO concentrations at low wind conditions in

south-east direction, while high NO_x and NO_2 were in west-north direction. It is identified that in the south-east direction agricultural fields are located, where biological soil activities are likely a source of HONO (Oswald et al., 2013; Su et al., 2011). Indeed there is influence of traffic emission as well, major contribution in HONO formation can be from biological soil activities in this direction as additional sources of HONO in the environment in addition to vehicular emissions was determined at the York site in section 6.6.1.3.

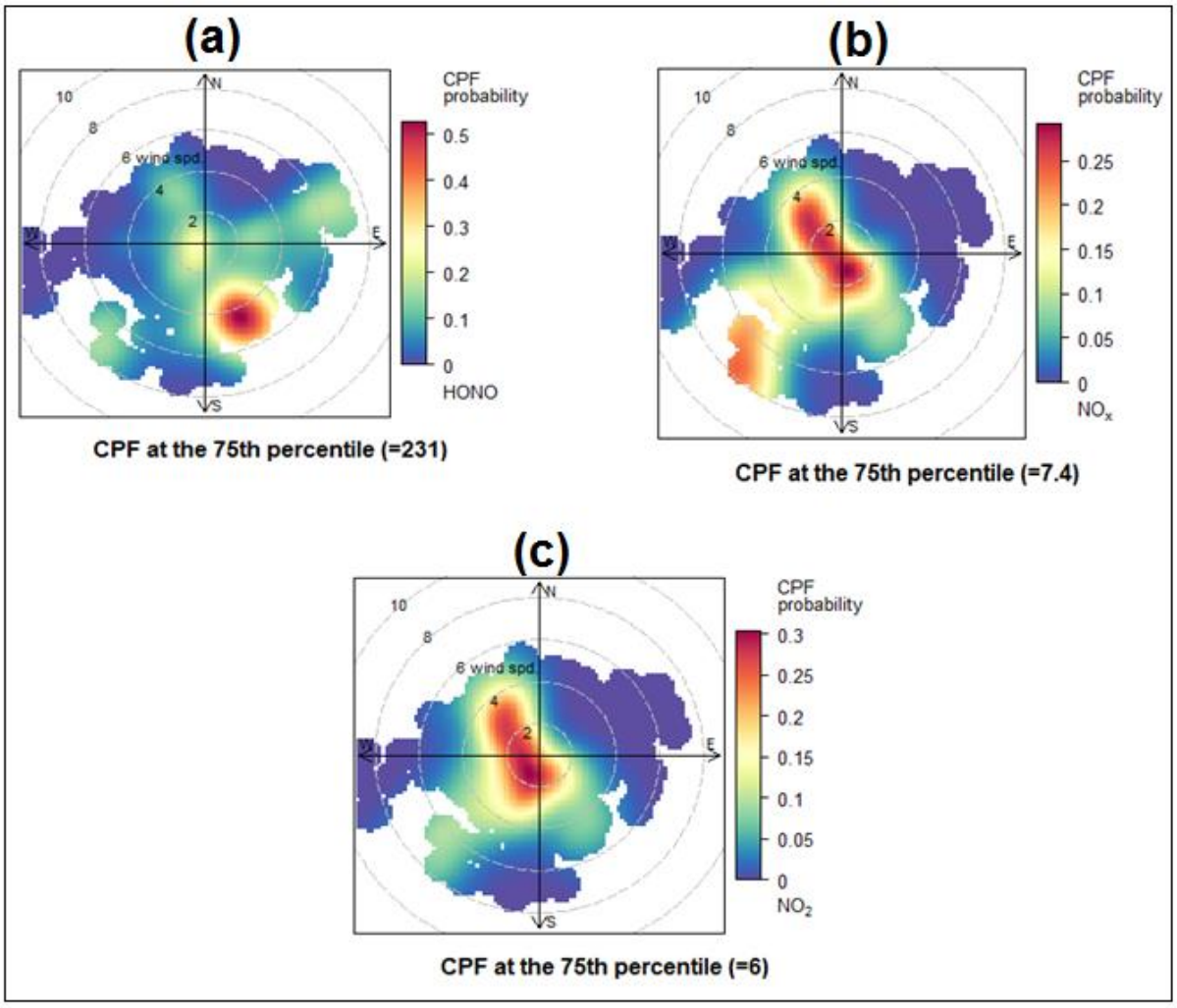

Figure 6.7 Polar plots of **a)** HONO, **b)** NO_x and **c)** NO_2 using CPF analysis at the 75th percentile threshold level at York.

6.6.1.5 Influence of particles on HONO variation at Birmingham and London

The variation in the diurnal concentration of particulate matter such as $PM_{2.5}$, PM_{10}, and Black Carbon (BC) were analysed at London during the summer (Figure 6.8, panel a) and the winter campaigns (Figure 6.8, panel b), and compared with HONO concentrations over the same time periods. Due to unavailability of BC data during the measurement period, only $PM_{2.5}$ and PM_{10} particulates were analysed at the Birmingham site along with HONO (Figure 6.8, panel c).

During the measurement period, the concentration of HONO increased and decreased with $PM_{2.5}$, PM_{10} and BC at London (both summer and winter) (Figure 6.8). In particular, a good correlation was observed between HONO-$PM_{2.5,}$ HONO-PM_{10} and HONO-BC at London. Particularly, correlations with BC were good, however BC is the marker of traffic related pollution. It clearly shows the influence of traffic related sources on variations in HONO concentration. The correlation was similar for summer and winter seasons (see Table 6.4). It was also observed that correlation between HONO-$PM_{2.5}$ and HONO-PM_{10} at Birmingham was similar to the London measurements across both seasons.

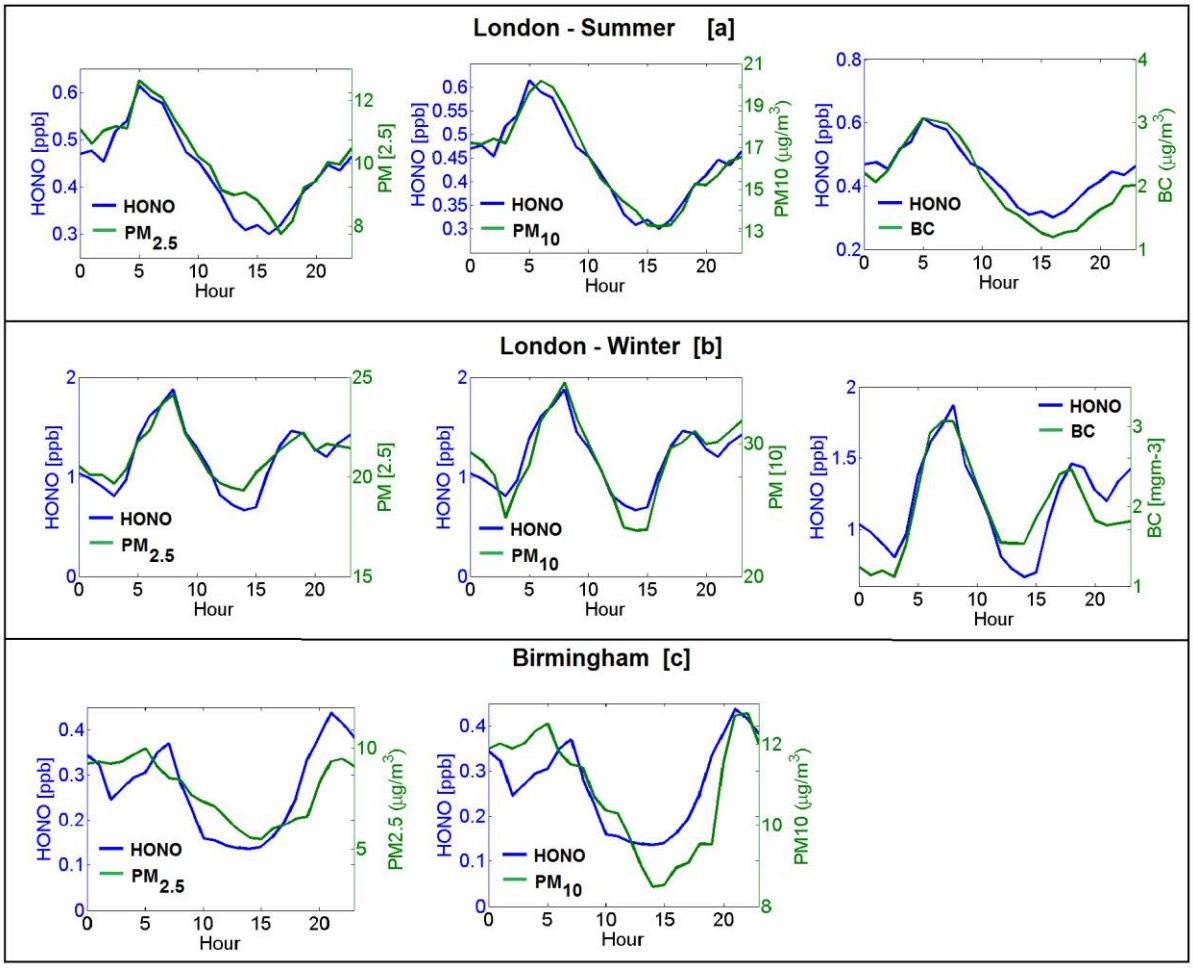

Figure 6.8 Diurnal profiles of $PM_{2.5}$, PM_{10} and Black Carbon (BC) along with HONO at **a)** London during summer, **b)** London during winter and **c)** Birmingham

Table 6.4 Correlation coefficient (r) values between HONO and particle pollutants

	London (Summer) (r)	**London (Winter) (r)**	**Birmingham (r)**
HONO to $PM_{2.5}$	0.50	0.47	0.42
HONO to PM_{10}	0.45	0.46	0.44
HONO to BC	0.72	0.73	----
Statistically significant value at p<0.0001			

6.6.2 Detailed analysis at Birmingham site

6.6.2.1 Influence of air mass origin on HONO at Birmingham

Figure 6.9 shows a time series of HONO, particle total surface area (TSA), $PM_{2.5}$, PM_{10}, NO_x, NO_2, NO, O3 and wind speed. During the campaign the maximum HONO mixing ratio observed was 1.64 ppb, while the minimum mixing ratio was 0.03 ppb. A pollution event was observed during the first few days of the campaign, owing to very low wind speeds (Figure 6.9).

A good correlation (r=0.69) was observed between HONO and NO_2 at the Birmingham site (Table 6.3). However, there was a period when HONO concentrations were largely independent of NO_2 concentration (circled area in Figure 6.10 a). To further explore the relationship between HONO and NO_2, with a series of potential third variables (RH, total surface area and date), a series of scatter plots are presented in Figure 6.10 b, c, and d. During this period, high HONO concentrations occurred at high RH and high total surface area (Figure 6.10 b and c). Figure 6.10 d illustrates this occurrence across one particular time period, which was noted as a high pollution event.

A correlation between HONO and particle total surface area (TSA) is shown in Figure 6.11. Two distinct clusters were observed: one at low TSA and one at higher TSA which suggests the possibility of at least two distinct air masses being present over the course of the campaign. To support this hypothesis, pollutants within different air masses were analysed and is discussed in the following section.

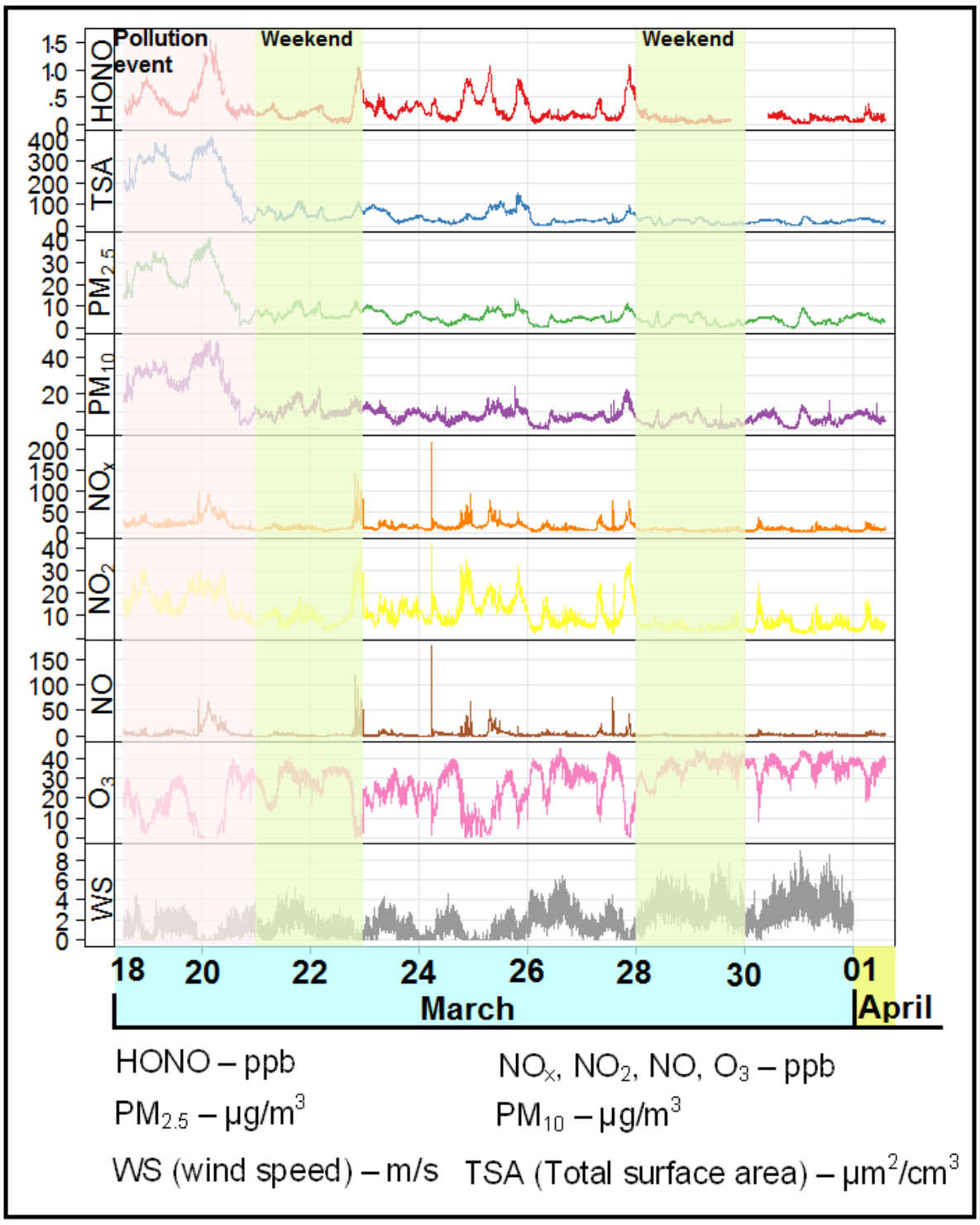

Figure 6.9 Time series of atmospheric pollutants and meteorology. Shadings indicate pollution period (light pink colour) and weekend (green colour).

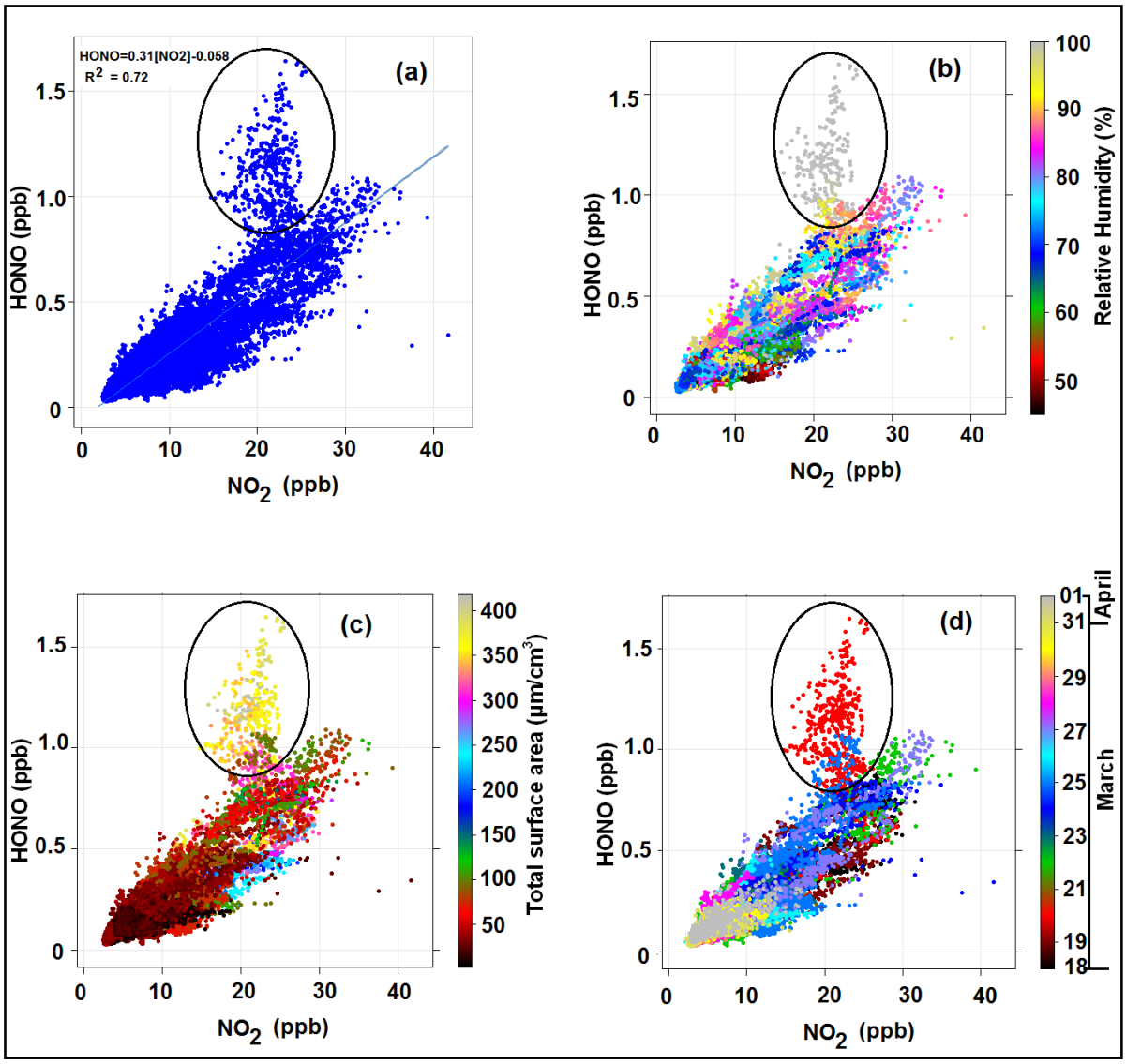

Figure 6.10 Investigate the relationship of HONO and NO_2 with different meteorological and pollution condition. The black circles indicate population appoints deviating from the relationship of HONO and NO_2 due to influence of different factors (such as meteorological and pollution condition).

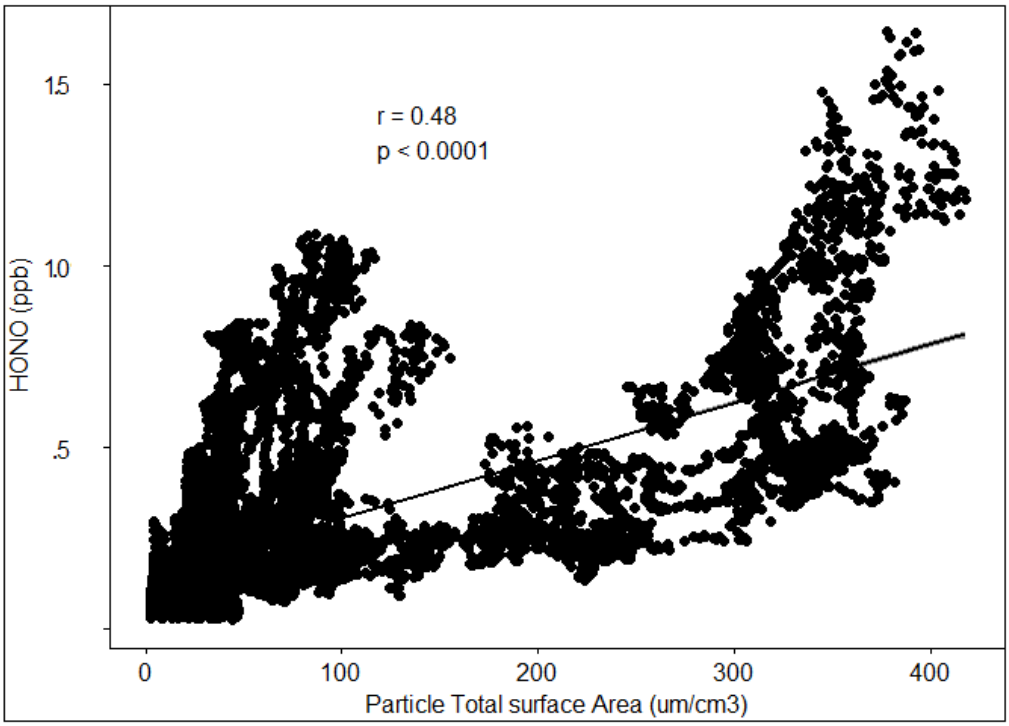

Figure 6.11 Correlation between HONO and particle total surface area during campaign

6.6.2.2 Influence of meteorology at Birmingham

It is found that three broad types of air masses were present during the campaign (Figure 6.12). The time series plots are also shown in Figure 6.13. The descriptions of the three types of existing air masses (1, 2 and 3) are below:

Air Mass 1 is characterised by low wind speed conditions (see Table 6.5) with high HONO concentrations and has a predominantly north-easterly wind direction. Average HONO concentration (0.52 ppb) was highest in this air mass when compared to the other two air masses. The pollution event occurred during Air Mass 1, which may be responsible for the larger HONO concentration owing to the low

wind speed. As discussed previously, HONO concentration increases as wind speed decreases (see Figure 6.4).

Air Mass 2 is characterised by a moderate wind condition (1.38 m/s, predominantly west direction) and it was observed that average HONO concentrations of 0.27 ppb occurred when this air mass was present.

Air Mass 3 is characterised by higher wind speed conditions (3.23 m/s, predominantly south westerly direction). Lower average HONO concentration (0.10 ppb) was observed during Air Mass 3.

Overall, this result indicates that higher wind speed decreases HONO concentration, though wind direction could also have an impact on HONO concentrations depending on the location of the sources which contribute to HONO emissions.

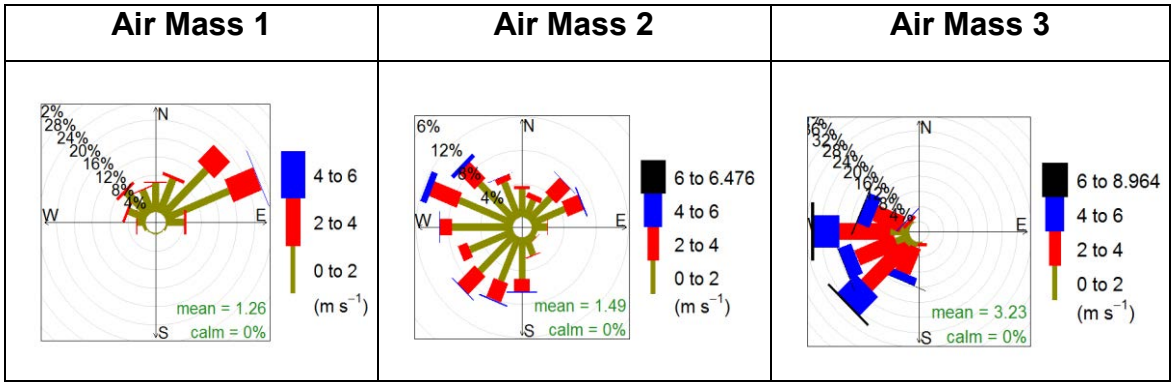

Figure 6.12 Wind pattern in different air masses condition

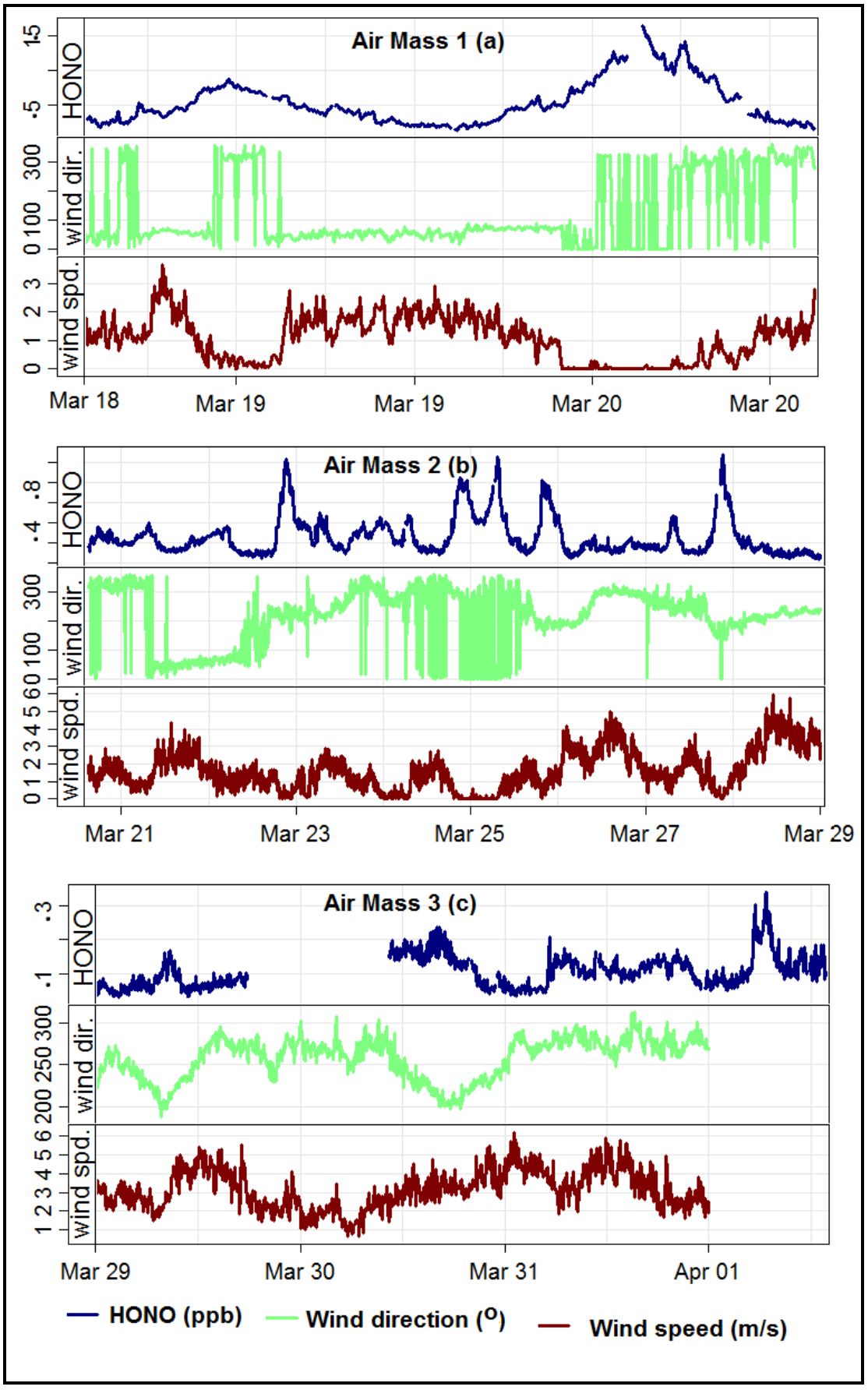

Figure 6.13 (a) Air mass 1 from 18th march 13:40pm to 20th march 15:00pm **(b)** Air mass 2 from 20th march 15:01pm to 28th march 03:00am, and **(c)** Air mass 3 from 28th march 03:01am to 1st April 14:00pm

Table 6.5 Wind conditions and HONO concentration during different air masses at Birmingham site

Label Air mass	Maximum HONO concentration (ppb)	Average HONO concentration (ppb)	Maximum wind speed (m/s)	Average wind speed (m/s)
1	1.65	0.52	4.6	1.058
2	1.08	0.27	6.476	1.38
3	0.38	0.10	8.964	3.233

Conclusions

An analysis was performed using four different data sets provided by campaign measurements to compare and contrast the concentrations of HONO at different geographical locations and seasons in order to investigate how HONO varies with meteorology, traffic emission and other sources. The observed mean HONO mixing ratio was largest in London during the winter season (1.18 ± 0.96 ppb), and lowest in York during summer season (0.19 ± 0.15 ppb).

Results show that HONO decreases with increasing wind speed, to an extent that varies by locations and seasons. This implies that HONO is emitted into the atmosphere rather than forming in the atmosphere. Diurnal profiles of HONO, NO_x and NO_2 showed two distinct peaks: one in the morning and another in the evening, corresponding to the rush hour traffic emission periods (though the York site appears to be the exception for the diurnal variation of HONO, due to the lack of an evening peak). It was found that NO_2 concentration aligns with morning peak during rush hour traffic, followed by decrease during the day. NO_2 falls primarily due to

photolysis during day, repartitioning NO_x to NO. NO_2 remains stable for the rest of the daytime until the evening rush hours. Morning peaks of HONO were one to two hours earlier than the NO_x due to the onset of HONO photolysis at sunrise.

$HONO/NO_x$ and $HONO/NO_2$ ratios were also analysed to explore the contribution from sources. It was observed that in Birmingham and London (winter) $HONO/NO_x$ ratios were higher between midnight and dawn when sunlight was absent and hence no photolysis. There is large decrease in the $HONO/NO_x$ ratio as the morning traffic begins followed by a stable period during the morning rush hours. However, the measurements observed differ in York and London (summer) as there are additional peaks that occur during the day. The observed higher $HONO/NO_x$ ratios suggest additional sources of HONO in the environment in addition to vehicular emissions. The daytime peak of $HONO/NO_x$ ratio at York and London (summer) suggests a significant additional (non-traffic) HONO source in the atmosphere. The highest $HONO/NO_2$ ratio was measured at night time, which is assumed to be due to conversion of NO_2 on humid surfaces in dark conditions. Similar positive correlations were found between HONO and NO_x & HONO and NO_2 at Birmingham and London during summer and winter. The poor correlation founded at York suggests a different source mix of HONO compared to the other sites. To explore potential sources of HONO at York, polar plots of HONO, NO_x and NO_2 were generated using CPF analysis, where high concentrations of HONO with low NO_2 and NO_x were observed in the south-east direction, where agricultural fields are located. At York, biological soil activities in this direction are likely a source of HONO and can be a potential source here in addition to vehicular emission sources.

A more detailed analysis was performed for Birmingham, where low wind speeds conditions led to a pollution event during the early days of the campaign, where elevated HONO concentrations were observed. The results showed that different air masses during the campaign exhibited differing influences on HONO concentrations, again suggesting that HONO is emitted into the atmosphere rather than forming in the atmosphere.

Chapter 7.0

Summary and future directions

7.1 Chapter overview

While detailed conclusions from the analyses are presented within each of the chapters, this section provides a summary of the important findings as a whole, together with limitations. It also includes recommendations for further/future research.

7.2 Summary and limitations

This thesis presents two distinct but related research topics, which investigate the influences of aerosol particle and trace gases on *(i)* visibility and *(ii)* tropospheric chemistry, using mathematical, chemical, analytical and modelling approaches.

7.2.1 Visibility

The present work explores both long and short term visibility, using data from various UK meteorological sites, by analysing the combined influence of atmospheric aerosol and meteorology.

7.2.1.1 Long term visibility trends

In this thesis, the long term trends in visibility for eight specific meteorological sites in the UK have been analysed from datasets over the last 60 years, where study locations include urban, rural and marine environments. Overall, visibility has improved at most of the stations through time. The greatest observed improvements are in urban areas, which are attributed to reductions in aerosol particle loadings and decreases in relative humidity (RH). Visibility was found to be lowest during winter and highest in the summer due to seasonal variations in RH and likely changes in the mixing height.

Bivariate polar plots of visibility, which account for the influence of wind speed and wind direction, explained the influence of wind on likely source areas of visibility reducing aerosols. Overall, an improved visibility at most of the stations in almost all directions was observed with notable improvements when the air masses moved over metropolitan areas (e.g. Greater Manchester and Greater London). At most sites, low visibility was observed when the direction of the air mass arrives from continental Europe which may indicate an influence of regional pollution events leading to visibility reductions. Significant changes in visibility were observed with changes in relative humidity, indicating a strong dependency of visibility on aerosol hygroscopicity. Many sites showed long term decreases in RH together with increase in air temperature when visibility was higher. Investigations showed that if the trends of decreasing RH continue, then the UK can expect further improvements in visibility for the same pollutant loading.

A light extinction model was developed to explain the dependency of visibility upon meteorology and aerosol characteristics. The model suggests that there have been significant changes in aerosol concentration over the last 60 years. The model incorporates parameterizations of aerosol hygroscopicity, particle concentration, particle scattering, and particle and gas absorption. It has been demonstrated that the model developed can be easily transferrable and applicable to other data sets worldwide (Chapter 3) and has the potential to generate historical air quality indications for locations with visibility records.

7.2.1.2 Short term visibility trends

In Chapter 4, the impact of fireworks and bonfire emissions on visibility and short term air quality is investigated using data from 34 meteorological stations in the UK. Overall, sharp reductions in nationwide visibility were observed on Guy Fawkes Night. However, this reduction is temporary, as average visibility returns to normal within two days owing to the dispersal of the additional PM loading. More detailed analysis on the data from a single urban area (Nottingham) showed that the effect of Guy Fawkes Night is even more pronounced when the effect of RH, through its influence on the extinction coefficient of PM, is taken into account. The reduction in visibility on Guy Fawkes Night is mainly caused by increases in atmospheric PM loading which is generated through bonfires and fireworks. With the UK becoming ever more multicultural the frequency of the use of fireworks may increase owing to the number of festivals (e.g. Diwali and Chinese New Year) celebrated. This may coincide with an increase in visibility reduction hotspots throughout the year.

The data and analysis shown through this research, indicates that the public should be made aware of the possibility of low visibility on Guy Fawkes Night which can be very localized. In particular, care should be taken when RH is predicted to be high and the atmosphere already has a high PM loading. Since firework displays are planned months in advance, weather and pollution forecasts of sufficient skill are unavailable to help in their planning. However, if forecasts subsequently suggest that the planned display will coincide with conditions likely to exacerbate poor visibility then the organizers and local authorities should be prepared to issue poor visibility warnings in advance. This precautionary step can help to increase

enjoyment, or at least prevent unnecessary accidents, during Guy Fawkes Night which is a much loved celebration.

7.2.2 Tropospheric chemistry

The variation in nitrous acid (HONO) concentration as a result of meteorological factors (temperature, RH, wind speed and direction), traffic emission and other sources was investigated. Additionally, the relationship between tropospheric HONO and other air pollutants including development of chemical kinetic models to estimate the influence of different source scales on HONO has been explored.

7.2.2.1 Nitrous acid during 2015 solar eclipse: Insight into potential sources and sinks

A total solar eclipse on 20 March 2015 provided a unique and natural opportunity to investigate how HONO, NO_x, O_3 and particle pollutants varied in response to rapid changes in the solar intensity. In general, the observed behaviour of O_3 and NO_x during the eclipse was as expected based upon known photochemistry. However, relatively little variation in HONO concentration was observed. The detailed analysis and results of the measured data have been presented in Chapter 5. Briefly, a chemical kinetic model was used, which investigated different scenarios to understand the changes in daytime HONO mixing ratios and its potential sources. Simulations clearly showed that a single source cannot explain the daytime HONO profile during the solar eclipse. From the simulations it was found that traffic related emissions during the eclipse influenced the measured HONO mixing ratio, however sources related to photolysis and NO_2.

7.2.2.2 Variation of nitrous acid at different urban sites: insights into sources

Investigations were carried out using observations provided by four measurement campaigns to compare and contrast the mixing ratios of HONO at different geographical locations and seasons. Influences such as meteorology, traffic emission and other sources were investigated to assess the variation of HONO mixing ratios and the results and discussions are presented in Chapter 6. Overall, mean HONO mixing ratios were highest in London during the winter season (1.18 ± 0.96 ppb), and lowest in York during the summer season (0.19 ± 0.15 ppb). It was observed that HONO decreased with increasing wind speed this varied by location and season, which suggests that HONO is emitted into the atmosphere rather than forming in the atmosphere. Diurnal profiles of HONO, NO_x and NO_2 showed two distinct peaks: one in the morning and another in the evening, corresponding to the rush hour traffic emission periods (though the York site appears to be the exception for the diurnal variation of HONO, due to the lack of an evening peak). It was found that NO_2 concentrations aligned with morning peaks during rush hour traffic, followed by decreases during the day. NO_2 falls primarily due to photolysis during day, repartitioning NO_x to NO. NO_2 remains stable for the rest of the daytime until the evening rush hours. Morning peaks of HONO were one to two hours earlier than the NO_x due to the onset of HONO photolysis at sunrise.

HONO/NO_x and HONO/NO_2 ratios were also analysed to explore the contribution from sources. It was observed that in Birmingham and London (winter) HONO/NO_x ratios were higher between midnight and dawn due to lack of photolysis. There is a large decrease in the HONO/NO_x ratio as the morning traffic begins followed by a stable period during the morning rush hours. However, the measurements observed

vary in York and London (summer) as there are additional peaks that occur during the day. The daytime peak of HONO/NO_x ratio at York and London (summer) suggests a significant additional (non-traffic) HONO source in the atmosphere. The largest HONO/NO_2 ratio was measured at night time, which is assumed to be due to conversion of NO_2 on humid surfaces in dark conditions. Potential sources of HONO at York were identified using polar plots of HONO, NO_x and NO_2 via CPF analysis. It was observed that high concentrations of HONO with low NO_2 and NO_x in the south-east direction, where agricultural fields are located. Hence, biological soil activities are likely to be a source of HONO in addition to vehicular emission sources at York.

A detailed analysis was performed for Birmingham, where low wind speed conditions led to a pollution event during the early days of the campaign, where elevated HONO concentrations were observed. The results also showed different broad air masses during the campaign which exhibited differing influences on HONO concentrations, again suggesting that HONO is emitted into the atmosphere rather than forming in the atmosphere.

7.3 Future works

This thesis has assessed combined impacts of aerosols and meteorology on tropospheric chemistry and visibility variations on both long and short term timescales. Two types of study are reported in this thesis in terms of visibility. In the first study, the long-term visibility-aerosol-weather relationship for the UK focused on different geographical environments (urban, rural and marine) was analysed. In the second study, the impact of fireworks and bonfires during Guy Fawkes Night on short term visibility was determined. A light extinction model was developed to

explain the long term trends and their dependence on aerosol and meteorology for the UK environment to fill the literature gap. In future, the light extinction model developed in this study could be applied for other geographical regions, especially high polluted areas/regions (such as India and China) to compare their variations and limitations for specific regions. The variation and relationship between visibility and different gases (SO_2, and NO_X), trace metals (Ca, Fe, Zn, and Pb) and particles (PM_1, $PM_{2.5}$, PM_{10}, and black carbon) pollutants in specific meteorological conditions could be analysed and compared during various UK festivals (owing to multiplicity of cultures) to improve UK air quality / fireworks legislations. The impacts of poor air quality during these festivals/ events on health could be studied to find out relative risks of mortality and morbidity.

This thesis also presented the HONO variations and constraints upon its sources during a solar eclipse under short term changes in light conditions. Understanding the contribution of different sources to HONO formation rates is very important as these mechanisms are little understood. Laboratory based studies designed to investigate HONO formation rate for different source scenarios such as biological soil activities and heterogeneous formation on humid surface, which are still poorly understood, could be potential future research. The present work also explored the HONO variations and sources at different geographical locations and seasons using observations provided by four measurement campaigns in urban environments. Future work could focus on measurements made in other environments, such as rural and marine in addition to urban environments to compare and contrast the mixing ratios of HONO in these different environments. In particular, formation

mechanism and transport phenomena in different environments still need to be understood.

Appendix A

Extinction model output parameters (*Vis (dry), βabs,* Gamma (γ) and *βsca)*

Station		Output parameters			
	Decade	*Vis(dry)* [m]	β_{abs} [m^{-1}]	Gamma (γ)	β_{sca} [m^{-1}]
Aldergrove	1950s	66168.94 ± 6406.58	1.91E-05 ± 2.07E-05	0.72 ± 0.13	0.000108 ± 0.000104
	1960s	67145.63 ± 6770.0	1.42E-05 ± 1.87E-05	0.78 ± 0.11	0.00013 ± 7.87E-05
	1970s	46450.98 ± 2542.37	5.54E-05 ± 1.25E-05	0.89 ± 0.11	9.93E-05 ± 5.27E-05
	1980s	60581.79 ± 3474.03	3.68E-05 ± 1.04E-05	0.91 ± 0.09	9.80E-05 ± 5.08E-05
	1990s	72645.1 ± 5414.83	4.30E-07 ± 1.77E-05	0.65 ± 0.09	0.000132 ± 4.29E-05
	2000s	33033.3 ± 2175.54	0 ± 6.14E-05	0.38 ± 0.11	0.0002 ± 2.86E-05
	2010s	27816.69 ± 1028.35	0.000134 ± 8.58E-06	1.05 ± 0.19	2.65E-05 ± 4.21E-05
Heathrow	1950s	30712.64 ± 1505.63	9.99E-05 ± 1.42E-05	1.28 ± 0.15	0.000104 ± 0.000161
	1960s	33724.2 ± 1690.38	8.65E-05 ± 1.32E-05	1.26 ± 0.13	7.87E-05 ± 0.000168
	1970s	29053.48 ± 1034.41	0.00011 ± 1.10E-05	1.26 ± 0.12	5.27E-05 ± 0.000127
	1980s	39380.87 ± 1684.78	6.63E-05 ± 1.23E-05	1.03 ± 0.11	5.08E-05 ± 0.000138
	1990s	47969.8 ± 1723.021	6.00E-05 ± 7.77E-06	1.17 ± 0.11	4.29E-05 ± 0.000109
	2000s	39486.93 ± 1182.31	7.14E-05 ± 8.96E-06	0.10 ± 0.10	2.86E-05 ± 0.000111
	2010s	29442.48 ±782.86	0.000127 ± 5.86E-06	1.40 ± 0.18	4.21E-05 ± 4.22E-05
Ringway	1950s	19009.64 ± 970.33	0.000165 ± 2.34E-05	1.22 ± 0.15	0.000222 ± 0.000104
	1960s	24280.22 ± 1312.52	9.83E-05 ± 2.43E-05	1.10 ± 0.12	0.000287 ± 7.87E-05
	1970s	28983.71 ± 1337.76	8.77E-05 ± 1.69E-05	1.09 ± 0.11	0.000215 ± 5.27E-05
	1980s	38266.72 ± 1971.32	4.22E-05 ± 1.91E-05	0.89 ± 0.10	0.000208 ± 5.08E-05
	1990s	50337.53 ± 2318.8	4.59E-05 ± 1.03E-05	1.06 ± 0.10	0.000139 ± 4.29E-05
	2000s	50433.99 ± 2835.64	5.67E-05 ± 1.07E-05	1.18 ± 0.15	0.000107 ± 2.86E-05
	2010s	----------	----------	----------	----------
Nottingham	1950s	23730.96 ±458.202	9.08E-05 ± 4.96E-05	1.10 ± 0.22	0.00034 ± 0.000104
	1960s	31058.79 ± 2110.9	7.17E-05 ± 2.07E-05	1.15 ± 0.11	0.000267 ± 7.87E-05
	1970s	35827.23 ± 1938.96	6.68E-05 ± 1.45E-05	1.11 ± 0.10	0.000197 ± 5.27E-05
	1980s	60996.37 ± 4725.79	7.06E-06 ± 1.72E-05	1.0 ± 0.10	0.000204 ± 5.08E-05
	1990s	39257.86 ± 1923.46	7.24E-05 ± 1.22E-05	1.10 ± 0.12	0.000127 ± 4.29E-05
	2000s	29994.36 ± 905.23	0.0001 ± 1.12E-05	0.80 ± 0.084	9.25E-05 ± 2.86E-05
	2010s	28622.94 ± 935.70	0.00013 ± 7.48E-06	1.21 ± 0.18	3.55E-05 ± 4.21E-05

Plymouth	1950s	37567.9 ± 2677.97	3.23E-05 ± 2.92E-05	0.73 ± 0.11	0.000197 ± 0.000104
	1960s	43782.5 ± 3244.77	3.92E-05 ± 1.89E-05	0.84 ± 0.10	0.000161 ± 7.87E-05
	1970s	46748.18 ± 2948.9	5.74E-05 ± 1.22E-05	1.06 ± 0.11	0.000114 ± 5.27E-05
	1980s	49226.96 ± 2903.94	4.95E-05 ± 1.20E-05	1.03 ± 0.11	0.000124 ± 5.08E-05
	1990s	38659.78 ± 1743.28	3.84E-05 ± 2.16E-05	0.56 ± 0.08	0.000137 ± 4.29E-05
	2000s	22827.89 ± 786.67	0.000115 ± 2.33E-05	0.53 ± 0.08	0.000118 ± 2.86E-05
	2010s	36199.28 ± 2242.56	5.56E-05 ± 2.63E-05	0.62 ± 0.12	0.000124 ± 4.21E-05
Tiree	1950s	91524.38 ± 22121.51	1.24E-05 ±3.19E-05	0.83 ± 0.27	9.62E-05 ± 0.00010
	1960s	95940.8 ± 9045.804	1.43E-05 ± 1.10E-05	0.79 ± 0.10	7.92E-05 ± 7.87E-05
	1970s	108150.7 ± 11993.07	1.69E-06 ± 1.28E-05	0.74 ± 0.09	9.58E-05 ± 5.27E-05
	1980s	79744.05 ± 5324.328	3.21E-05 ± 7.33E-06	1.02 ± 0.10	6.96E-05 ± 5.08E-05
	1990s	72533.1 ± 4859.271	3.85E-05 ± 7.47E-06	1.10 ± 0.11	7.08E-05 ± 4.29E-05
	2000s	40831.35 ± 2358.797	6.26E-05 ± 1.53E-05	0.73 ± 0.09	9.12E-05 ± 2.86E-05
	2010s	35281.66 ± 2462.969	7.74E-05 ± 2.19E-05	0.71 ± 0.13	8.96E-05 ±4.21E-05
Leuchars	1950s	68678.15 ± 8261.79	2.89E-05 ± 1.70E-05	1.22 ±0.18	0.000151 ± 0.000104
	1960s	91554.03 ± 5428.33	2.86E-05 ± 5.05E-06	1.43± 0.09	0.000103 ± 7.87E-05
	1970s	77735.19 ± 4208.63	2.93E-05 ± 6.50E-06	1.21 ± 0.09	0.000112± 5.27E-05
	1980s	66272.27 ± 2493.00	4.19E-05 ± 5.22E-06	1.18 ± 0.08	8.82E-05 ± 5.08E-05
	1990s	78279.2 ± 3279.53	2.56E-05 ± 6.22E-06	1.02 ± 0.08	9.99E-05 ± 4.29E-05
	2000s	62485.8 ± 1901.10	4.97E-05 ± 4.21E-06	1.18 ± 0.08	6.64E-05 ± 2.86E-05
	2010s	56086.63 ± 2125.58	6.11E-05 ± 4.97E-06	1.34 ± 0.13	5.56E-05 ± 4.21E-05
Waddington	1950s	36683.17 ± 2690.569	6.47E-05 ± 1.93E-05	1.12± 0.13	0.000198 ± 0.000104
	1960s	37699.07 ± 2375.559	6.34E-05 ± 1.62E-05	1.05 ± 0.10	0.000172 ± 7.87E-05
	1970s	39651.07 ± 1685.186	7.30E-05 ± 9.43E-06	1.14 ± 0.09	0.000125 ± 5.27E-05
	1980s	49441.39 ± 2317.583	5.18E-05 ± 9.29E-06	1.13 ± 0.09	0.00013 ± 5.08E-05
	1990s	45305.49 ± 1503.447	6.99E-05 ± 6.24E-06	1.28 ± 0.10	9.71E-05 ± 4.29E-05
	2000s	46205.36 ± 1299.249	6.84E-05 ± 5.59E-0	1.08 ± 0.09	7.29E-05 ± 2.86E-0
	2010s	44260.81 ± 1370.792	8.24E-05 ± 4.57E-06	1.47 ± 0.15	4.60E-05 ± 4.21E-05

References

Aas, E., 1996. Refractive index of phytoplankton derived from its metabolite composition. Journal of Plankton Research, 18(12): 2223-2249.

Abbey, D., Ostro, B., Fraser, G., Vancuren, T. and Burchette, R., 1994. Estimating fine particulates less than 2.5 microns in aerodynamic diameter (PM2. 5) from airport visibility data in California. Journal of Exposure Analysis and Environmental Epidemiology, 5(2): 161-180.

Acker, K., Febo, A., Trick, S., Perrino, C., Bruno, P., Wiesen, P., Möller, D., Wieprecht, W., Auel, R. and Giusto, M., 2006a. Nitrous acid in the urban area of Rome. Atmospheric Environment, 40(17): 3123-3133.

Acker, K. and Möller, D., 2007. Atmospheric variation of nitrous acid at different sites in Europe. Environmental Chemistry, 4(4): 242-255.

Acker, K., Möller, D., Wieprecht, W., Meixner, F.X., Bohn, B., Gilge, S., Plass-Dülmer, C. and Berresheim, H., 2006b. Strong daytime production of OH from HNO2 at a rural mountain site. Geophysical Research Letters, 33(2).

Ackermann-Liebrich, U., Leuenberger, P., Schwartz, J., Schindler, C., Monn, C., Bolognini, G., Bongard, J., Brändli, O., Domenighetti, G. and Elsasser, S., 1997. Lung function and long term exposure to air pollutants in Switzerland. Study on Air Pollution and Lung Diseases in Adults (SAPALDIA) Team. American journal of respiratory and critical care medicine, 155(1): 122-129.

Alam, M.S., Keyte, I.J., Yin, J., Stark, C., Jones, A.M. and Harrison, R.M., 2015. Diurnal variability of polycyclic aromatic compound (PAC) concentrations: Relationship with meteorological conditions and inferred sources. Atmospheric Environment, 122: 427-438.

Alicke, B., Geyer, A., Hofzumahaus, A., Holland, F., Konrad, S., Pätz, H., Schäfer, J., Stutz, J., Volz-Thomas, A. and Platt, U., 2003. OH formation by HONO photolysis during the BERLIOZ experiment. Journal of Geophysical Research: Atmospheres, 108(D4).

Allan, J., Williams, P., Morgan, W., Martin, C., Flynn, M., Lee, J., Nemitz, E., Phillips, G., Gallagher, M. and Coe, H., 2010. Contributions from transport,

solid fuel burning and cooking to primary organic aerosols in two UK cities. Atmospheric Chemistry and Physics, 10(2): 647-668.

Alshawa, A., Dopfer, O., Harmon, C.W., Nizkorodov, S.A. and Underwood, J.S., 2009. Hygroscopic growth and deliquescence of NaCl nanoparticles coated with surfactant AOT. The Journal of Physical Chemistry A, 113(26): 7678-7686.

Ammann, M., Kalberer, M., Jost, D., Tobler, L., Rössler, E., Piguet, D., Gäggeler, H. and Baltensperger, U., 1998. Heterogeneous production of nitrous acid on soot in polluted air masses. Nature, 395(6698): 157-160.

Appel, B., Tokiwa, Y., Hsu, J., Kothny, E. and Hahn, E., 1985. Visibility as related to atmospheric aerosol constituents. Atmospheric Environment (1967), 19(9): 1525-1534.

Arends, B., Baard, J. and Ten Brink, H., 1997. Trends in summer sulphate in Europe. Atmospheric Environment, 31(24): 4063-4072.

Arens, F., Ammann, M., Gutzwiller, L., Baltensperger, U. and Gäggeler, H., 2000. Formation of hono from the reaction of NO 2 with diesel soot. Journal of aerosol science, 31: 1035-1035.

Arya, S.P., 1999. Air pollution meteorology and dispersion.

Atkin, J.A., Burke, E.K., Greenwood, J.S. and Reeson, D., 2007. Hybrid metaheuristics to aid runway scheduling at London Heathrow airport. Transportation Science, 41(1): 90-106.

Attri, A.K., Kumar, U. and Jain, V., 2001. Microclimate: Formation of ozone by fireworks. Nature, 411(6841): 1015-1015.

Babisch, W., 2000. Traffic noise and cardiovascular disease: epidemiological review and synthesis. Noise and health, 2(8): 9.

Bach, W., Daniels, A., Dickinson, L., Hertlein, F., Morrows, J., Margolis, S. and Dinh, V.D., 1975. Fireworks pollution and health. International Journal of Environmental Studies, 7(3): 183-192.

Badri, A., 2016a. The Influence of Weather and Climate Change on Pedestrian Safety, University of Waterloo.

Badri, A., 2016b. The Influence of Weather and Climate Change on Pedestrian Safety.

Baergen, A.M., Styler, S.A., van Pinxteren, D., Müller, K., Herrmann, H. and Donaldson, D.J., 2015. Chemistry of Urban Grime: Inorganic Ion Composition of Grime vs Particles in Leipzig, Germany. Environmental science & technology, 49(21): 12688-12696.

Baik, N.-J., Kim, Y.P. and Moon, K.C., 1996. Visibility study in Seoul, 1993. Atmospheric Environment, 30(13): 2319-2328.

Barman, S., Singh, R., Negi, M. and Bhargava, S., 2008. Ambient air quality of Lucknow City (India) during use of fireworks on Diwali Festival. Environmental monitoring and assessment, 137(1-3): 495-504.

Barone, J., Cahill, T., Eldred, R., Flocchini, R., Shadoan, D. and Dietz, T., 1978. A multivariate statistical analysis of visibility degradation at four California cities. Atmospheric Environment (1967), 12(11): 2213-2221.

Barreca, A.I., 2012. Climate change, humidity, and mortality in the United States. Journal of Environmental Economics and Management, 63(1): 19-34.

Barrett, S.D., 2000. Airport competition in the deregulated European aviation market. Journal of Air Transport Management, 6(1): 13-27.

Bäumer, D., Vogel, B., Versick, S., Rinke, R., Möhler, O. and Schnaiter, M., 2008. Relationship of visibility, aerosol optical thickness and aerosol size distribution in an ageing air mass over South-West Germany. Atmospheric Environment, 42(5): 989-998.

Becker, J.M., Iskandrian, S. and Conkling, J., 2000. Fatal and near-fatal asthma in children exposed to fireworks. Annals of Allergy, Asthma & Immunology, 85(6): 512-513.

Beddows, D., Harrison, R.M., Green, D. and Fuller, G., 2015. Receptor modelling of both particle composition and size distribution from a background site in London, UK. Atmospheric Chemistry and Physics, 15(17): 10107-10125.

Beer, R., Glavich, T.A. and Rider, D.M., 2001. Tropospheric emission spectrometer for the Earth Observing System's Aura satellite. Applied optics, 40(15): 2356-2367.

Beig, G., Chate, D., Ghude, S.D., Ali, K., Satpute, T., Sahu, S., Parkhi, N. and Trimbake, H., 2013. Evaluating population exposure to environmental pollutants during Deepavali fireworks displays using air quality measurements of the SAFAR network. Chemosphere, 92(1): 116-124.

Bejan, I., El Aal, Y.A., Barnes, I., Benter, T., Bohn, B., Wiesen, P. and Kleffmann, J., 2006. The photolysis of ortho-nitrophenols: a new gas phase source of HONO. Physical Chemistry Chemical Physics, 8(17): 2028-2035.

Bennett, A., 2012. Introduction to atmospheric visibility estimation, Bristol Industrial and Research Associates Limited (Biral), Bristol, UK

Bian, H. and Zender, C.S., 2003. Mineral dust and global tropospheric chemistry: Relative roles of photolysis and heterogeneous uptake. Journal of Geophysical Research: Atmospheres, 108(D21).

Bigi, A. and Harrison, R.M., 2010. Analysis of the air pollution climate at a central urban background site. Atmospheric Environment, 44(16): 2004-2012.

Björkman, M. and Rylander, R., 1997. Maximum noise levels in city traffic. Journal of Sound and Vibration, 205(4): 513-516.

Bohn, B., Corlett, G.K., Gillmann, M., Sanghavi, S., Stange, G., Tensing, E., Vrekoussis, M., Bloss, W., Clapp, L. and Kortner, M., 2008. Photolysis frequency measurement techniques: results of a comparison within the ACCENT project. Atmospheric chemistry and physics, 8(17): 5373-5391.

Bohnenstengel, S., Belcher, S., Aiken, A., Allan, J., Allen, G., Bacak, A., Bannan, T., Barlow, J., Beddows, D. and Bloss, W., 2015. Meteorology, air quality, and health in London: The ClearfLo project. Bulletin of the American Meteorological Society, 96(5): 779-804.

Bond, T.C. and Bergstrom, R.W., 2006. Light absorption by carbonaceous particles: An investigative review. Aerosol science and technology, 40(1): 27-67.

Bressi, M., Sciare, J., Ghersi, V., Mihalopoulos, N., Petit, J.-E., Nicolas, J., Moukhtar, S., Rosso, A., Féron, A. and Bonnaire, N., 2014. Sources and geographical origins of fine aerosols in Paris (France). Atmospheric Chemistry and Physics, 14(16): 8813-8839.

Briggs, D., 2003. Environmental pollution and the global burden of disease. British Medical Bulletin, 68(1): 1-24.

Brimblecombe, P., 1987. The big smoke. Methuen London; New York.

Brimblecombe, P., 2006. The clean air act after 50 years. Weather, 61(11): 311-314.

Bröske, R., Kleffmann, J. and Wiesen, P., 2003. Heterogeneous conversion of NO 2 on secondary organic aerosol surfaces: A possible source of nitrous acid

(HONO) in the atmosphere? Atmospheric Chemistry and Physics, 3(3): 469-474.

Brumby, C.A., Crilley, L.R., Kramer, L.J., Bloss, W.J., Seakins, P.W., Lee, J.D. and Carpenter, L.J., 2016. HONO measurement by differential photolysis. Atmospheric Measurement Techniques, 9(6): 2483.

Brunekreef, B. and Holgate, S.T., 2002. Air pollution and health. The lancet, 360(9341): 1233-1242.

Butcher, L., 2012. Aviation: London Heathrow Airport. House of Commons Library.

Cahill, T., Ashbaugh, L. and Barone, J., 1977. Sources of visibility degradation in the Lake Tahoe Air Basin, California Univ., Davis (USA). Crocker Nuclear Lab.

Calvert, J., Yarwood, G. and Dunker, A., 1994. An evaluation of the mechanism of nitrous acid formation in the urban atmosphere. Research on Chemical Intermediates, 20(3-5): 463-502.

Camilleri, R. and Vella, A.J., 2010. Effect of fireworks on ambient air quality in Malta. Atmospheric Environment, 44(35): 4521-4527.

Cao, J.-j., Wang, Q.-y., Chow, J.C., Watson, J.G., Tie, X.-x., Shen, Z.-x., Wang, P. and An, Z.-s., 2012. Impacts of aerosol compositions on visibility impairment in Xi'an, China. Atmospheric Environment, 59: 559-566.

Carrico, C.M., Kreidenweis, S.M., Malm, W.C., Day, D.E., Lee, T., Carrillo, J., McMeeking, G.R. and Collett, J.L., 2005. Hygroscopic growth behavior of a carbon-dominated aerosol in Yosemite National Park. Atmospheric Environment, 39(8): 1393-1404.

Carslaw, D., 2015. The openair manual — open-source tools for analysing air pollution data. Manual for version 1.1-4, King's College London.

Carslaw, D.C. and Rhys-Tyler, G., 2013. New insights from comprehensive on-road measurements of NO x, NO 2 and NH 3 from vehicle emission remote sensing in London, UK. Atmospheric Environment, 81: 339-347.

Carslaw, D.C. and Ropkins, K., 2012. Openair—an R package for air quality data analysis. Environmental Modelling & Software, 27: 52-61.

Cathcart, S., Iversen, A., Murray, V. and Alves, B., 2007. Fireworks incident near Lewes, December 2006, Chemical Hazards and Poisons Report, Chemical Hazards and Poisons Division, London

Cazoir, D., Brigante, M., Ammar, R., D'Anna, B. and George, C., 2014. Heterogeneous photochemistry of gaseous NO 2 on solid fluoranthene films: A source of gaseous nitrous acid (HONO) in the urban environment. Journal of Photochemistry and Photobiology A: Chemistry, 273: 23-28.

Cesaroni, G., Forastiere, F., Stafoggia, M., Andersen, Z.J., Badaloni, C., Beelen, R., Caracciolo, B., de Faire, U., Erbel, R. and Eriksen, K.T., 2014. Long term exposure to ambient air pollution and incidence of acute coronary events: prospective cohort study and meta-analysis in 11 European cohorts from the ESCAPE Project. Bmj, 348: f7412.

Chan, C.K. and Yao, X., 2008. Air pollution in mega cities in China. Atmospheric environment, 42(1): 1-42.

Chan, H.-K., Eberl, S., Daviskas, E., Constable, C. and Young, I., 2002. Changes in lung deposition of aerosols due to hygroscopic growth: a fast SPECT study. Journal of aerosol medicine, 15(3): 307-311.

Chang, D., Song, Y. and Liu, B., 2009. Visibility trends in six megacities in China 1973–2007. Atmospheric Research, 94(2): 161-167.

Chang, S., Toossi, R. and Novakov, T., 1981. The importance of soot particles and nitrous acid in oxidizing SO 2 in atmospheric aqueous droplets. Atmospheric Environment (1967), 15(7): 1287-1292.

Charlson, R. and Pilat, M., 1969. Climate: The influence of aerosols. Journal of Applied Meteorology, 8(6): 1001-1002.

Charlson, R.J., Langner, J., Rodhe, H., Leovy, C. and Warren, S., 1991. Perturbation of the northern hemisphere radiative balance by backscattering from anthropogenic sulfate aerosols*. Tellus A, 43(4): 152-163.

Charlson, R.J. and Schwartz, S., 1992. Climate forcing by anthropogenic aerosols. Science, 255(5043): 423.

Charron, A., Birmili, W. and Harrison, R.M., 2007a. Factors influencing new particle formation at the rural site, Harwell, United Kingdom. Journal of Geophysical Research: Atmospheres, 112(D14).

Charron, A., Degrendele, C., Laongsri, B. and Harrison, R.M., 2013. Receptor modelling of secondary and carbonaceous particulate matter at a southern UK site. Atmospheric Chemistry and Physics, 13(4): 1879-1894.

Charron, A., Harrison, R.M. and Quincey, P., 2007b. What are the sources and conditions responsible for exceedences of the 24h PM 10 limit value (50μgm− 3) at a heavily trafficked London site? Atmospheric Environment, 41(9): 1960-1975.

Chatterjee, A., Sarkar, C., Adak, A., Mukherjee, U., Ghosh, S. and Raha, S., 2013. Ambient air quality during Diwali festival over Kolkata–a mega-city in India. Aerosol and Air Quality Research, 13(13): 1133-1144.

Che, H., Zhang, X., Li, Y., Zhou, Z. and Qu, J.J., 2007. Horizontal visibility trends in China 1981–2005. Geophysical Research Letters, 34(24).

Clark, P.A., Harcourt, S., Macpherson, B., Mathison, C., Cusack, S. and Naylor, M., 2008. Prediction of visibility and aerosol within the operational Met Office Unified Model. I: Model formulation and variational assimilation. Quarterly Journal of the Royal Meteorological Society, 134(636): 1801-1816.

Clarke, A., Gascoigne, M., Henderson-Sellers, A. and Williams, A., 1978. Modelling air pollution in Leeds (UK). International Journal of Environmental Studies, 12(2): 121-132.

Colbeck, I. and Harrison, R.M., 1984. Ozone—secondary aerosol—visibility relationships in North-West England. Science of the Total Environment, 34(1-2): 87-100.

Colvile, R., Hutchinson, E., Mindell, J. and Warren, R., 2001. The transport sector as a source of air pollution. Atmospheric environment, 35(9): 1537-1565.

Comrie, A.C., 1990. The climatology of surface ozone in rural areas: a conceptual model. Progress in Physical Geography, 14(3): 295-316.

Crilley, L., Kramer, L., Pope, F.D., Whalley, L.K., Cryer, D.R., Heard, D.E., Lee, J., Reed, C. and Bloss, W., 2016. On the interpretation of in situ HONO observations via photochemical steady state. Faraday Discussions.

Crilley, L.R., Bloss, W.J., Yin, J., Beddows, D.C., Harrison, R.M., Allan, J.D., Young, D.E., Flynn, M., Williams, P. and Zotter, P., 2015. Sources and contributions of wood smoke during winter in London: assessing local and regional influences. Atmospheric chemistry and physics, 15(6): 3149-3171.

D'Argenio, P., Cafaro, L., Santonastasi, F., Taggi, F. and Binkin, N., 1996. Capodanno Senza Danno: the effects of an intervention program on fireworks injuries in Naples. American journal of public health, 86(1): 84-86.

Dasch, J.M., 1982. Particulate and gaseous emissions from wood-burning fireplaces. Environmental Science & Technology, 16(10): 639-645.

Davis, R.E., 1991. A synoptic climatological analysis of winter visibility trends in the mideastern United States. Atmospheric Environment. Part B. Urban Atmosphere, 25(2): 165-175.

Day, J.A., 2005. Fog and Mist, Encyclopedia of World Climatology. Springer, pp. 379-380.

Dayan, U. and Levy, I., 2005. The influence of meteorological conditions and atmospheric circulation types on PM10 and visibility in Tel Aviv. Journal of Applied Meteorology, 44(5): 606-619.

DEFRA, 2016. Air Pollution in the UK 2015, A report prepared by AEA for Defra and the Devolved Administrations Department for Environment, Food and Rural Affairs, London.

Deng, J., Wang, T., Jiang, Z., Xie, M., Zhang, R., Huang, X. and Zhu, J., 2011. Characterization of visibility and its affecting factors over Nanjing, China. Atmospheric Research, 101(3): 681-691.

Dick van Steenis, M., 1997. INDUSTRIAL AIR POLLUTION AND ASTHMA.

Dominici, F., Peng, R.D., Bell, M.L., Pham, L., McDermott, A., Zeger, S.L. and Samet, J.M., 2006. Fine particulate air pollution and hospital admission for cardiovascular and respiratory diseases. Jama, 295(10): 1127-1134.

Donaldson, K., Stone, V., Clouter, A., Renwick, L. and MacNee, W., 2001. Ultrafine particles. Occupational and environmental medicine, 58(3): 211-216.

Doyle, M. and Dorling, S., 2002. Visibility trends in the UK 1950–1997. Atmospheric Environment, 36(19): 3161-3172.

Drewnick, F., Hings, S.S., Curtius, J., Eerdekens, G. and Williams, J., 2006. Measurement of fine particulate and gas-phase species during the New Year's fireworks 2005 in Mainz, Germany. Atmospheric Environment, 40(23): 4316-4327.

DTI, 2005. Fireworks Injury Survey 2005, Department of Trade and Industry, United Kingdom

Dui, W., Xueyan, B., Xuejiao, D., Fei, L., Haobo, T., Guolian, L. and Jian, H., 2007. Effect of Atmospheric Haze on the Deterioration of Visibility over the Pearl River Delta*. Acta Meteorologica Sinica, 21(2): 215.

Dyke, P., Coleman, P. and James, R., 1997. Dioxins in ambient air, bonfire night 1994. Chemosphere, 34(5): 1191-1201.

Dzubay, T.G., Stevens, R.K., Lewis, C.W., Hern, D.H., Courtney, W.J., Tesch, J.W. and Mason, M.A., 1982. Visibility and aerosol composition in Houston, Texas. Environmental Science & Technology, 16(8): 514-525.

Eder, B.K., Davis, J.M. and Bloomfield, P., 1994. An automated classification scheme designed to better elucidate the dependence of ozone on meteorology. Journal of Applied Meteorology, 33(10): 1182-1199.

EEA, 2015. Air quality in Europe — 2015 report. No 5/2015, European Environmental Agency Luxembourg.

Elshorbany, Y., Barnes, I., Becker, K.H., Kleffmann, J. and Wiesen, P., 2010. Sources and cycling of tropospheric hydroxyl radicals–an overview. Zeitschrift für Physikalische Chemie International journal of research in physical chemistry and chemical physics, 224(7-8): 967-987.

Elshorbany, Y., Kurtenbach, R., Wiesen, P., Lissi, E., Rubio, M., Villena, G., Gramsch, E., Rickard, A., Pilling, M. and Kleffmann, J., 2009. Oxidation capacity of the city air of Santiago, Chile. Atmospheric Chemistry and Physics, 9(6): 2257-2273.

Elshorbany, Y., Steil, B., Brühl, C. and Lelieveld, J., 2012. Impact of HONO on global atmospheric chemistry calculated with an empirical parameterization in the EMAC model. Atmospheric Chemistry and Physics, 12(20): 9977-10000.

Estellés, V., Smyth, T.J. and Campanelli, M., 2012. Columnar aerosol properties in a Northeastern Atlantic site (Plymouth, United Kingdom) by means of ground based skyradiometer data during years 2000–2008. Atmospheric environment, 61: 180-188.

Farias, F. and ApSimon, H., 2006. Relative contributions from traffic and aircraft NOx emissions to exposure in West London. Environmental Modelling & Software, 21(4): 477-485.

Febo, A., Perrino, C. and Allegrini, I., 1996. Measurement of nitrous acid in Milan, Italy, by DOAS and diffusion denuders. Atmospheric Environment, 30(21): 3599-3609.

Fenger, J., 1999. Urban air quality. Atmospheric environment, 33(29): 4877-4900.

Ferman, M.A., Wolff, G.T. and Kelly, N.A., 1981. An assessment of the gaseous pollutants and meteorological conditions associated with Denver's brown cloud. Journal of Environmental Science & Health Part A, 16(3): 315-339.

Finlayson-Pitts, B., Wingen, L., Sumner, A., Syomin, D. and Ramazan, K., 2003. The heterogeneous hydrolysis of NO 2 in laboratory systems and in outdoor and indoor atmospheres: an integrated mechanism. Physical Chemistry Chemical Physics, 5(2): 223-242.

Finlayson-Pitts, B.J. and Pitts, J.N., 1997. Tropospheric air pollution: ozone, airborne toxics, polycyclic aromatic hydrocarbons, and particles. Science, 276(5315): 1045-1051.

Finlayson-Pitts, B.J. and Pitts Jr, J.N., 2000. Chemistry of the upper and lower atmosphere: theory, experiments, and applications. Academic press.

Fitzgerald, J.W., 1975. Approximation formulas for the equilibrium size of an aerosol particle as a function of its dry size and composition and the ambient relative humidity. Journal of Applied Meteorology, 14(6): 1044-1049.

Flynn, T., 2008. Firework-related eye injury in the UK. Eye, 22(2): 319-320.

Fogarty, B. and Gordon, D., 1999. Firework related injury and legislation: the epidemiology of firework injuries and the effect of legislation in Northern Ireland. Burns, 25(1): 53-56.

Founda, D., Kazadzis, S., Mihalopoulos, N., Gerasopoulos, E., Lianou, M. and Raptis, P.I., 2016. Long-term visibility variation in Athens (1931–2013): a proxy for local and regional atmospheric aerosol loads. Atmospheric Chemistry and Physics, 16(17): 11219-11236.

Gaeggeler, K., Prevot, A.S., Dommen, J., Legreid, G., Reimann, S. and Baltensperger, U., 2008. Residential wood burning in an Alpine valley as a source for oxygenated volatile organic compounds, hydrocarbons and organic acids. Atmospheric Environment, 42(35): 8278-8287.

Galea, A. and Powles, O., 2010. A review of firework legislation and acute health effects. Chemical Hazards and Poisons Report: 32.

Gandolfo, A., Rouyer, L., Wortham, H. and Gligorovski, S., 2017. The influence of wall temperature on NO 2 removal and HONO levels released by indoor photocatalytic paints. Applied Catalysis B: Environmental.

Ganguly, N.D., 2009. Surface ozone pollution during the festival of Diwali, New Delhi, India. Earth Sci. India, 2(2).

Gaumet, J., Heinrich, J., Cluzeau, M., Pierrard, P. and Prieur, J., 1998. Cloud-base height measurements with a single-pulse erbium-glass laser ceilometer. Journal of Atmospheric and Oceanic Technology, 15(1): 37-45.

George, C., Strekowski, R., Kleffmann, J., Stemmler, K. and Ammann, M., 2005. Photoenhanced uptake of gaseous NO 2 on solid organic compounds: a photochemical source of HONO? Faraday discussions, 130: 195-210.

Gherman, T., Venables, D.S., Vaughan, S., Orphal, J. and Ruth, A.A., 2007. Incoherent broadband cavity-enhanced absorption spectroscopy in the near-ultraviolet: application to HONO and NO2. Environmental science & technology, 42(3): 890-895.

Ghim, Y.S., Moon, K.-C., Lee, S. and Kim, Y.P., 2005. Visibility trends in Korea during the past two decades. Journal of the Air & Waste Management Association, 55(1): 73-82.

Gill, S.E., Handley, J.F., Ennos, A.R. and Pauleit, S., 2007. Adapting cities for climate change: the role of the green infrastructure. Built environment, 33(1): 115-133.

Gjaevenes, K., Moseng, J. and Nordahl, T., 1974. Hearing loss in children caused by the impulsive noise of Chinese crackers. Scandinavian Audiology, 3(4): 153-156.

Godri, K.J., Green, D.C., Fuller, G.W., Dall'Osto, M., Beddows, D.C., Kelly, F.J., Harrison, R.M. and Mudway, I.S., 2010. Particulate oxidative burden associated with firework activity. Environmental science & technology, 44(21): 8295-8301.

Gomez, B. and Smith, C., 1984. Atmospheric pollution and fog frequency in Oxford, 1926–1980. Weather, 39(12): 379-384.

Gomez, B. and Smith, C., 1987. Visibility at Oxford, 1926–1985. Weather, 42(4): 98-106.

Gouder, C. and Montefort, S., 2014. Potential impact of fireworks on respiratory health. Lung India: official organ of Indian Chest Society, 31(4): 375.

Goyal, P., Kumar, A. and Mishra, D., 2014. The impact of air pollutants and meteorological variables on visibility in Delhi. Environmental Modeling & Assessment, 19(2): 127-138.

Groblicki, P.J., Wolff, G.T. and Countess, R.J., 1981. Visibility-reducing species in the Denver "brown cloud"—I. Relationships between extinction and chemical composition. Atmospheric Environment (1967), 15(12): 2473-2484.

Hadjimitsis, D., Retalis, A. and Clayton, C., 2002. The assessment of atmospheric pollution using satellite remote sensing technology in large cities in the vicinity of airports. Water, Air and Soil Pollution: Focus, 2(5-6): 631-640.

Hamad, S., Green, D. and Heo, J., 2016. Evaluation of health risk associated with fireworks activity at Central London. Air Quality, Atmosphere & Health, 9(7): 735-741.

Han, S., Bian, H., Zhang, Y., Wu, J., Wang, Y., Tie, X., Li, Y., Li, X. and Yao, Q., 2012. Effect of aerosols on visibility and radiation in spring 2009 in Tianjin, China. Aerosol Air Qual. Res, 12: 211-217.

Hand, J., Kreidenweis, S., Sherman, D.E., Collett, J., Hering, S., Day, D. and Malm, W., 2002. Aerosol size distributions and visibility estimates during the Big Bend regional aerosol and visibility observational (BRAVO) study. Atmospheric Environment, 36(32): 5043-5055.

Hänel, G., 1972. Computation of the extinction of visible radiation by atmospheric aerosol particles as a function of the relative humidity, based upon measured properties. Journal of Aerosol Science, 3(5): 377-386.

Hanna, E., Penman, J., Jónsson, T., Bigg, G.R., Björnsson, H., Sjúrðarson, S., Hansen, M.A., Cappelen, J. and Bryant, R.G., 2016. Meteorological effects of the solar eclipse of 20 March 2015: analysis of UK Met Office automatic weather station data and comparison with automatic weather station data from the Faroes and Iceland. Phil. Trans. R. Soc. A, 374(2077): 20150212.

Harris, B. and Smith, K., 1982. Cleaner air improves visibility in Glasgow. Geography, 67(2): 137-139.

Harrison, R.M. and Collins, G.M., 1998. Measurements of reaction coefficients of NO2 and HONO on aerosol particles. Journal of atmospheric chemistry, 30(3): 397-406.

Harrison, R.M., Jones, A.M. and Lawrence, R.G., 2004. Major component composition of PM 10 and PM 2.5 from roadside and urban background sites. Atmospheric Environment, 38(27): 4531-4538.

Harrison, R.M. and Kitto, A.-M.N., 1994. Evidence for a surface source of atmospheric nitrous acid. Atmospheric Environment, 28(6): 1089-1094.

Harrison, R.M., Pope, F.D. and Shi, Z., 2015. Trends in Local Air Quality 1970–2014, Still Only One Earth: Progress in the 40 Years Since the First UN Conference on the Environment. Royal Society of Chemistry, pp. 58-106.

Hautière, N., Babari, R., Dumont, E., Du Chatelet, J.P. and Paparoditis, N., 2013. Measurements and Observations of Meteorological Visibility at ITS Stations.

Haywood, J. and Boucher, O., 2000. Estimates of the direct and indirect radiative forcing due to tropospheric aerosols: A review. Reviews of geophysics, 38(4): 513-543.

He, K., Yang, F., Ma, Y., Zhang, Q., Yao, X., Chan, C.K., Cadle, S., Chan, T. and Mulawa, P., 2001. The characteristics of PM 2.5 in Beijing, China. Atmospheric Environment, 35(29): 4959-4970.

Heathrow, 2016. Climate Change Adaptation and Resilience Progress Report Heathrow Airport Limited Heathrow.

HEI, H., 2013. review panel on ultrafine particles. Understanding the health effects of ambient ultrafine particles. HEI Perspectives 3Health Effects Institute, Boston, MA: 122.

Heland, J., Kleffmann, J., Kurtenbach, R. and Wiesen, P., 2001. A new instrument to measure gaseous nitrous acid (HONO) in the atmosphere. Environmental science & technology, 35(15): 3207-3212.

Hirai, K., Yamazaki, Y., Okada, K., FURUTA, S. and KUBO, K., 2000. Acute eosinophilic pneumonia associated with smoke from fireworks. Internal medicine, 39(5): 401-403.

HMSO, 1997. The fireworks (safety) regulations 1997. No. 2294, Her Majesty's Stationery Office, London

HMSO, 2004. The Fireworks Regulations 2004. No. 1836, Her Majesty's Stationery Office, London.

Holgate, S.T., Koren, H.S., Samet, J.M. and Maynard, R.L., 1999. Air pollution and health. Academic Press.

Holliday, J., 2004. Winds of Change "An exhibition about the history of Tiree's weather station and early flights to the island", An Iodhlann Scarinish, Isle of Tiree.

Horvath, H., 1995. Estimation of the average visibility in central Europe. Atmospheric Environment, 29(2): 241-246.

Horvath, H., 1996. Spectral extinction coefficients of rural aerosol in southern Italy-A case study of cause and effect of variability of atmospheric aerosol. Journal of Aerosol Science, 27(3): 437-453.

Huang, W., Tan, J., Kan, H., Zhao, N., Song, W., Song, G., Chen, G., Jiang, L., Jiang, C. and Chen, R., 2009. Visibility, air quality and daily mortality in Shanghai, China. Science of the Total Environment, 407(10): 3295-3300.

Hueglin, C., Gehrig, R., Baltensperger, U., Gysel, M., Monn, C. and Vonmont, H., 2005. Chemical characterisation of PM2. 5, PM10 and coarse particles at urban, near-city and rural sites in Switzerland. Atmospheric Environment, 39(4): 637-651.

Hyslop, N.P., 2009. Impaired visibility: the air pollution people see. Atmospheric Environment, 43(1): 182-195.

Ising, H., Dienel, D., Günther, T. and Markert, B., 1980. Health effects of traffic noise. International archives of occupational and environmental health, 47(2): 179-190.

Janeiro, F.M., Wagner, F., Ramos, P.M. and Silva, A.M., 2007. Automated atmospheric visibibility measurements using a digital camera and image registration, 1st Symposium on Environmental Instrumentation and Measurements, Iasi, ROMANIA.

Jayamurugan, R., Kumaravel, B., Palanivelraja, S. and Chockalingam, M., 2013. Influence of temperature, relative humidity and seasonal variability on ambient air quality in a coastal urban area. International Journal of Atmospheric Sciences, doi:10.1155/2013/264046.

Jebson, S., 2008. Fact sheet number 17: Weather observations.

Jenkins, G.J., 2007. The climate of the United Kingdom and recent trends. Exeter: Met Office Hadley Centre.

Jiang, Q., Sun, Y., Wang, Z. and Yin, Y., 2015. Aerosol composition and sources during the Chinese Spring Festival: fireworks, secondary aerosol, and holiday effects. Atmospheric Chemistry and Physics, 15(11): 6023-6034.

Jinhuan, Q. and Liquan, Y., 2000. Variation characteristics of atmospheric aerosol optical depths and visibility in North China during 1980–1994. Atmospheric Environment, 34(4): 603-609.

Jiusto, J.E., 1969. 11. SOME PRINCIPLES OF FOG MODIFICATION WITH HYGROSCOPIC NUCLEI. PROGRESS OF ASA RESEARCH ON WAR FOG PR 0 D I FIC AT1: 24.

Joly, A., Smargiassi, A., Kosatsky, T., Fournier, M., Dabek-Zlotorzynska, E., Celo, V., Servrancikx, R., D'Amours, R., Malo, A. and Brook, J., 2008. Characterisation of particulate exposure during fireworks displays. Epidemiology, 19(6): S218.

Jones, A.P., 1999. Indoor air quality and health. Atmospheric environment, 33(28): 4535-4564.

Kalberer, M., Ammann, M., Arens, F., Gäggeler, H. and Baltensperger, U., 1999. Heterogeneous formation of nitrous acid (HONO) on soot aerosol particles. Journal of Geophysical Research: Atmospheres, 104(D11): 13825-13832.

Kampa, M. and Castanas, E., 2008. Human health effects of air pollution. Environmental pollution, 151(2): 362-367.

Kim, E. and Hopke, P.K., 2004. Comparison between conditional probability function and nonparametric regression for fine particle source directions. Atmospheric Environment, 38(28): 4667-4673.

Kim, J., Yoon, S.-C., Jefferson, A. and Kim, S.-W., 2006a. Aerosol hygroscopic properties during Asian dust, pollution, and biomass burning episodes at Gosan, Korea in April 2001. Atmospheric Environment, 40(8): 1550-1560.

Kim, Y.J., Kim, K.W., Kim, S.D., Lee, B.K. and Han, J.S., 2006b. Fine particulate matter characteristics and its impact on visibility impairment at two urban sites in Korea: Seoul and Incheon. Atmospheric environment, 40: 593-605.

Kirchstetter, T.W., Harley, R.A. and Littlejohn, D., 1996. Measurement of nitrous acid in motor vehicle exhaust. Environmental science & technology, 30(9): 2843-2849.

Kleffmann, J., 2007. Daytime sources of nitrous acid (HONO) in the atmospheric boundary layer. ChemPhysChem, 8(8): 1137-1144.

Kleffmann, J., Becker, K.H., Lackhoff, M. and Wiesen, P., 1999. Heterogeneous conversion of NO 2 on carbonaceous surfaces. Physical Chemistry Chemical Physics, 1(24): 5443-5450.

Kleffmann, J., Gavriloaiei, T., Hofzumahaus, A., Holland, F., Koppmann, R., Rupp, L., Schlosser, E., Siese, M. and Wahner, A., 2005. Daytime formation of nitrous acid: A major source of OH radicals in a forest. Geophysical Research Letters, 32(5).

Kleffmann, J., Heland, J., Kurtenbach, R., Lorzer, J. and Wiesen, P., 2002. A new instrument (LOPAP) for the detection of nitrous acid (HONO). Environmental Science and Pollution Research: 48-54.

Kleffmann, J., Kurtenbach, R., Lörzer, J., Wiesen, P., Kalthoff, N., Vogel, B. and Vogel, H., 2003. Measured and simulated vertical profiles of nitrous acid—Part I: Field measurements. Atmospheric Environment, 37(21): 2949-2955.

Kleffmann, J., Lörzer, J., Wiesen, P., Kern, C., Trick, S., Volkamer, R., Rodenas, M. and Wirtz, K., 2006. Intercomparison of the DOAS and LOPAP techniques for the detection of nitrous acid (HONO). Atmospheric Environment, 40(20): 3640-3652.

Kleffmann, J. and Wiesen, P., 2008. Technical Note: Quantification of interferences of wet chemical HONO LOPAP measurements under simulated polar conditions. Atmospheric Chemistry and Physics, 8(22): 6813-6822.

Knox, F., Chan, W., Jackson, A., Foot, B., Sharkey, J. and McGinnity, F., 2008. A British Ophthalmological Surveillance Unit study on serious ocular injuries from fireworks in the UK. Eye, 22(7): 944-947.

Koch, D., Bond, T.C., Streets, D., Unger, N. and Van der Werf, G.R., 2007. Global impacts of aerosols from particular source regions and sectors. Journal of Geophysical Research: Atmospheres, 112(D2).

Kong, S., Li, L., Li, X., Yin, Y., Chen, K., Liu, D., Yuan, L., Zhang, Y., Shan, Y. and Ji, Y., 2015. The impacts of firework burning at the Chinese Spring Festival on air quality: insights of tracers, source evolution and aging processes. Atmospheric Chemistry and Physics, 15(4): 2167-2184.

Koschmieder, H., 1924. Theorie der horizontalen Sichtweite. Beitr. Phys. Freien. Atmos., 12: 33-55.

Kotchmar, D.J., Garner, J., Gardner, D. and Comfort, B., 1996. Air Quality Criteria for Oxides of Nitrogen. Diane Publishing.

Kuhn, F., Morris, R., Witherspoon, C.D., Mann, L., Mester, V., Módis, L., Berta, A. and Bearden, W., 2000. Serious fireworks-related eye injuries. Ophthalmic epidemiology, 7(2): 139-148.

Kulmala, M., Korhonen, P., Vesala, T., Hansson, H.-C., Noone, K. and Svenningsson, B., 1996. The effect of hygroscopicity on cloud droplet formation. Tellus B, 48(3): 347-360.

Kulmala, M., Suni, T., Lehtinen, K., Maso, M.D., Boy, M., Reissell, A., Rannik, Ü., Aalto, P., Keronen, P. and Hakola, H., 2004. A new feedback mechanism linking forests, aerosols, and climate. Atmospheric Chemistry and Physics, 4(2): 557-562.

Kulshrestha, U., Rao, T.N., Azhaguvel, S. and Kulshrestha, M., 2004. Emissions and accumulation of metals in the atmosphere due to crackers and sparkles during Diwali festival in India. Atmospheric Environment, 38(27): 4421-4425.

Kumar, P., Morawska, L., Birmili, W., Paasonen, P., Hu, M., Kulmala, M., Harrison, R.M., Norford, L. and Britter, R., 2014. Ultrafine particles in cities. Environment international, 66: 1-10.

Künzli, N., Kaiser, R., Medina, S., Studnicka, M., Chanel, O., Filliger, P., Herry, M., Horak, F., Puybonnieux-Texier, V. and Quénel, P., 2000. Public-health impact of outdoor and traffic-related air pollution: a European assessment. The Lancet, 356(9232): 795-801.

Kuo, C.-Y., Cheng, F.-C., Chang, S.-Y., Lin, C.-Y., Chou, C.C., Chou, C.-H. and Lin, Y.-R., 2013. Analysis of the major factors affecting the visibility degradation in two stations. Journal of the Air & Waste Management Association, 63(4): 433-441.

Kurtenbach, R., Becker, K., Gomes, J., Kleffmann, J., Lörzer, J., Spittler, M., Wiesen, P., Ackermann, R., Geyer, A. and Platt, U., 2001. Investigations of emissions and heterogeneous formation of HONO in a road traffic tunnel. Atmospheric Environment, 35(20): 3385-3394.

Lack, D. and Cappa, C., 2010. Impact of brown and clear carbon on light absorption enhancement, single scatter albedo and absorption wavelength dependence of black carbon. Atmospheric Chemistry and Physics, 10(9): 4207-4220.

LaFranchi, B., Wolfe, G., Thornton, J., Harrold, S., Browne, E., Min, K., Wooldridge, P., Gilman, J., Kuster, W. and Goldan, P., 2009. Closing the peroxy acetyl nitrate budget: observations of acyl peroxy nitrates (PAN, PPN, and MPAN) during BEARPEX 2007. Atmospheric Chemistry and Physics, 9(19): 7623-7641.

Lal, S., Naja, M. and Subbaraya, B., 2000. Seasonal variations in surface ozone and its precursors over an urban site in India. Atmospheric Environment, 34(17): 2713-2724.

Laskin, D., 2006. The great London smog. Weatherwise, 59(6): 42-45.

Lawton, C., 2014. Benchmarking the Economy and Labour Market of Nottingham, Division of Economics, Nottingham Business School.

Lee, B.H., Wood, E.C., Zahniser, M.S., McManus, J.B., Nelson, D.D., Herndon, S.C., Santoni, G., Wofsy, S.C. and Munger, J.W., 2011. Simultaneous measurements of atmospheric HONO and NO 2 via absorption spectroscopy using tunable mid-infrared continuous-wave quantum cascade lasers. Applied Physics B: Lasers and Optics, 102(2): 417-423.

Lee, C.-G., Yuan, C.-S., Chang, J.-C. and Yuan, C., 2005. Effects of aerosol species on atmospheric visibility in Kaohsiung city, Taiwan. Journal of the Air & Waste Management Association, 55(7): 1031-1041.

Lee, D., 1983. Trends in summer visibility in London and southern England 1962–1979. Atmospheric Environment (1967), 17(1): 151-159.

Lee, D., 1985. A preliminary analysis of long-term visibility trends in central scotland. Journal of climatology, 5(6): 673-680.

Lee, D., 1994. Regional Variations in Longterm Visibility Trends in the UK, 1962—1990. Geography: 108-121.

Lee, D.O., 1990. The influence of wind direction, circulation type and air pollution emissions on summer visibility trends in southern England. Atmospheric Environment. Part A. General Topics, 24(1): 195-201.

Lee, J., Whalley, L., Heard, D., Stone, D., Dunmore, R., Hamilton, J., Young, D., Allan, J., Laufs, S. and Kleffmann, J., 2016. Detailed budget analysis of

HONO in central London reveals a missing daytime source. Atmospheric Chemistry and Physics, 16(5): 2747-2764.

Lee, J.D., Lewis, A.C., Monks, P.S., Jacob, M., Hamilton, J.F., Hopkins, J.R., Watson, N.M., Saxton, J.E., Ennis, C. and Carpenter, L.J., 2006. Ozone photochemistry and elevated isoprene during the UK heatwave of August 2003. Atmospheric Environment, 40(39): 7598-7613.

Lee, K., Xue, J., Geyh, A.S., Ozkaynak, H., Leaderer, B.P., Weschler, C.J. and Spengler, J.D., 2002. Nitrous acid, nitrogen dioxide, and ozone concentrations in residential environments. Environmental health perspectives, 110(2): 145.

Lelieveld, J. and Dentener, F.J., 2000. What controls tropospheric ozone? Journal of Geophysical Research: Atmospheres, 105(D3): 3531-3551.

Li, X., Brauers, T., Häseler, R., Bohn, B., Fuchs, H., Hofzumahaus, A., Holland, F., Lou, S., Lu, K. and Rohrer, F., 2012. Exploring the atmospheric chemistry of nitrous acid (HONO) at a rural site in Southern China. Atmospheric Chemistry and Physics, 12(3): 1497-1513.

Li, Y., Leung, G.M., Tang, J., Yang, X., Chao, C.Y.H., Lin, J.Z., Lu, J., Nielsen, P.V., Niu, J. and Qian, H., 2007. Role of ventilation in airborne transmission of infectious agents in the built environment–a multidisciplinary systematic review. Indoor air, 17(1): 2-18.

Liang, Y., Zha, Q., Wang, W., Cui, L., Lui, K.H., Ho, K.F., Wang, Z., Lee, S.-c. and Wang, T., 2017. Revisiting Nitrous Acid (HONO) Emission from On-road Vehicles: A Tunnel Study with a Mixed Fleet. Journal of the Air & Waste Management Association(just-accepted).

Liepert, B.G. and Kukla, G.J., 1997. Decline in global solar radiation with increased horizontal visibility in Germany between 1964 and 1990. Journal of Climate, 10(9): 2391-2401.

Liu, X., Zhang, Y., Cheng, Y., Hu, M. and Han, T., 2012. Aerosol hygroscopicity and its impact on atmospheric visibility and radiative forcing in Guangzhou during the 2006 PRIDE-PRD campaign. Atmospheric environment, 60: 59-67.

Liu, Y. and Daum, P.H., 2000. The effect of refractive index on size distributions and light scattering coefficients derived from optical particle counters. Journal of Aerosol Science, 31(8): 945-957.

Logan, J.A., 1985. Tropospheric ozone: Seasonal behavior, trends, and anthropogenic influence. Journal of Geophysical Research: Atmospheres, 90(D6): 10463-10482.

Lohmann, R., Northcott, G.L. and Jones, K.C., 2000. Assessing the contribution of diffuse domestic burning as a source of PCDD/Fs, PCBs, and PAHs to the UK atmosphere. Environmental science & technology, 34(14): 2892-2899.

Longfellow, C.A., Ravishankara, A. and Hanson, D.R., 1999. Reactive uptake on hydrocarbon soot: Focus on.

Lu, G.Y. and Wong, D.W., 2008. An adaptive inverse-distance weighting spatial interpolation technique. Computers & Geosciences, 34(9): 1044-1055.

Lv, G., Song, C.l., Pan, S.z., Gao, J.h. and Cao, X.f., 2014. Comparison of number, surface area and volume distributions of particles emitted from a multipoint port fuel injection car and a gasoline direct injection car. Atmospheric Pollution Research, 5(4): 753-758.

Madronich, S., Flocke, S., Zeng, J., Petropavlovskikh, I. and Lee-Taylor, J., 2003. Tropospheric Ultraviolet and Visible (TUV) Radiation Model.

Maglieri, D.J. and Henderson, H.R., 1973. Noise from aerial bursts of fireworks. The Journal of the Acoustical Society of America, 54(5): 1224-1227.

Majewski, G., Czechowski, P.O., Badyda, A. and Brandyk, A., 2014. Effect of air pollution on visibility in urban conditions. Warsaw Case Study. Environment Protection Engineering, 40(2): 47--64.

Malm, W.C. and Pitchford, M.L., 1997. Comparison of calculated sulfate scattering efficiencies as estimated from size-resolved particle measurements at three national locations. Atmospheric Environment, 31(9): 1315-1325.

Malm, W.C., Sisler, J.F., Huffman, D., Eldred, R.A. and Cahill, T.A., 1994. Spatial and seasonal trends in particle concentration and optical extinction in the United States. Journal of Geophysical Research: Atmospheres, 99(D1): 1347-1370.

Malm, W.C., Walther, E.G., O'Dell, K. and Kleine, M., 1981. Visibility in the southwestern United States from summer 1978 to spring 1979. Atmospheric Environment (1967), 15(10): 2031-2042.

Mandal, R., Sen, B. and Sen, S., 1997. Impact of fireworks on our environment. Indian Journal of Environmental Protection, 17(11): 850-853.

Mathai, C. and Tombach, I., 1987. A critical assessment of atmospheric visibility and aerosol measurements in the eastern United States. JAPCA, 37(6): 700-707.

McDonald, J.D., Zielinska, B., Fujita, E.M., Sagebiel, J.C., Chow, J.C. and Watson, J.G., 2000. Fine particle and gaseous emission rates from residential wood combustion. Environmental Science & Technology, 34(11): 2080-2091.

McFarland, L.V., Harris, J.R., Kobayashi, J.M. and Dicker, R.C., 1984. Risk factors for fireworks-related injury in Washington State. JAMA, 251(24): 3251-3254.

McInnes, L., Bergin, M. and Ogren, J., 1998. Apportionment of light scattering and hygroscopic growth. Geophysical Research Letters, 25(4): 513-516.

Meier, J., Wehner, B., Massling, A., Birmili, W., Nowak, A., Gnauk, T., Brüggemann, E., Herrmann, H., Min, H. and Wiedensohler, A., 2009. Hygroscopic growth of urban aerosol particles in Beijing (China) during wintertime: a comparison of three experimental methods. Atmospheric Chemistry and Physics, 9(18): 6865-6880.

Meusel, H., Kuhn, U., Reiffs, A., Mallik, C., Harder, H., Martinez, M., Schuladen, J., Bohn, B., Parchatka, U. and Crowley, J.N., 2016. Daytime formation of nitrous acid at a coastal remote site in Cyprus indicating a common ground source of atmospheric HONO and NO. Atmospheric Chemistry and Physics, 16(22): 14475-14493.

Michoud, V., Colomb, A., Borbon, A., Miet, K., Beekmann, M., Camredon, M., Aumont, B., Perrier, S., Zapf, P. and Siour, G., 2014. Study of the unknown HONO daytime source at a European suburban site during the MEGAPOLI summer and winter field campaigns. Atmospheric Chemistry and Physics, 14(6): 2805-2822.

Michoud, V., Kukui, A., Camredon, M., Colomb, A., Borbon, A., Miet, K., Aumont, B., Beekmann, M., Durand-Jolibois, R. and Perrier, S., 2012. Radical budget analysis in a suburban European site during the MEGAPOLI summer field campaign. Atmospheric Chemistry and Physics, 12(24): 11951-11974.

Middleton, J.T., Kendrick Jr, J. and Schwalm, H., 1950. Injury to herbaceous plants by smog or air pollution. Plant Dis.;(United States), 34(9).

Middleton, W., 1957. Vision through the atmosphere, Geophysik II/Geophysics II. Springer, pp. 254-287.

Mie, G., 1908. Beiträge zur Optik trüber Medien, speziell kolloidaler Metallösungen. Annalen der physik, 330(3): 377-445.

Mikhailov, E., Vlasenko, S., Rose, D. and Pöschl, U., 2013. Mass-based hygroscopicity parameter interaction model and measurement of atmospheric aerosol water uptake. Atmospheric Chemistry and Physics, 13(2): 717-740.

Miyoshi, C. and Mason, K.J., 2013. The damage cost of carbon dioxide emissions produced by passengers on airport surface access: the case of Manchester Airport. Journal of Transport Geography, 28: 137-143.

Mohan, M. and Payra, S., 2009. Influence of aerosol spectrum and air pollutants on fog formation in urban environment of megacity Delhi, India. Environmental monitoring and assessment, 151(1-4): 265-277.

Molnár, A., Mészáros, E., Imre, K. and Rüll, A., 2008. Trends in visibility over Hungary between 1996 and 2002. Atmospheric Environment, 42(11): 2621-2629.

Morawska, L., Thomas, S., Jamriska, M. and Johnson, G., 1999. The modality of particle size distributions of environmental aerosols. Atmospheric Environment, 33(27): 4401-4411.

Moreno, T., Querol, X., Alastuey, A., Minguillón, M.C., Pey, J., Rodriguez, S., Miró, J.V., Felis, C. and Gibbons, W., 2007. Recreational atmospheric pollution episodes: inhalable metalliferous particles from firework displays. Atmospheric Environment, 41(5): 913-922.

Myhre, G., Shindell, D., Bréon, F., Collins, W., Fuglestvedt, J., Huang, J., Koch, D., Lamarque, J., Lee, D., Mendoza, B., Nakajima, T., Robock, A., Stephens, G., Takemura, T. and Zhang, H., 2013. Anthropogenic and Natural Radiative Forcing. In: T. Stocker, D. Qin, G. Plattner, M. Tignor, S. Allen, J. Boschung, A. Nauels, Y. Xia, V. Bex and P. Midgley (Editors), The Physical Science Basis. Contribution of Working Group I to the Fifth Assessment Report of the Intergovernmental Panel on Climate Change. Cambridge University Press, Cambridge, United Kingdom and New York, NY, USA.

NAPAP, 1990. Visibility Existing and Historical Conditions – Causes and Effects, National Acid Precipitation Assessment Program (NAPAP), Washington, DC, Report 24.

Nasir, U. and Brahmaiah, D., 2015. Impact of fireworks on ambient air quality: a case study. International Journal of Environmental Science and Technology, 12(4): 1379-1386.

Navarro-González, R., McKay, C.P. and Mvondo, D.N., 2001. A possible nitrogen crisis for Archaean life due to reduced nitrogen fixation by lightning. Nature, 412(6842): 61-64.

Nel, A., 2005. Air pollution-related illness: effects of particles. Science, 308(5723): 804-806.

Nishanth, T., Praseed, K., Rathnakaran, K., Kumar, M.S., Krishna, R.R. and Valsaraj, K., 2012. Atmospheric pollution in a semi-urban, coastal region in India following festival seasons. Atmospheric environment, 47: 295-306.

Noll, K.E., Mueller, P.K. and Imada, M., 1968. Visibility and aerosol concentration in urban air. Atmospheric Environment (1967), 2(5): 465-475.

Ogden, R., 1998. The Meteorological Forecasting Office at Heathrow. Royal Meteorological Society, Specialist Group for the History of Meteorology and Physical Oceanography.

ONS, 2014. Estimates of the Economic Importance of Tourism 2008-2013, Office for National Statistics UK.

Oswald, R., Behrendt, T., Ermel, M., Wu, D., Su, H., Cheng, Y., Breuninger, C., Moravek, A., Mougin, E. and Delon, C., 2013. HONO emissions from soil bacteria as a major source of atmospheric reactive nitrogen. Science, 341(6151): 1233-1235.

Pandis, S.N., Wexler, A.S. and Seinfeld, J.H., 1995. Dynamics of tropospheric aerosols. The Journal of Physical Chemistry, 99(24): 9646-9659.

Parker, J., 1971. Air Pollution at Heathrow Airport, London: April-September, 1970. 0148-7191, SAE Technical Paper.

Pathak, B., Bharali, C., Biswas, J. and Bhuyan, P.K., 2013. Firework induced large increase in trace gases and black carbon at Dibrugarh, India. Journal of Earth Science and Engineering, 3(8): 540.

Paulrud, S. and Nilsson, C., 2004. The effects of particle characteristics on emissions from burning wood fuel powder. Fuel, 83(7): 813-821.

Penner, J.E., Dong, X. and Chen, Y., 2004. Observational evidence of a change in radiative forcing due to the indirect aerosol effect. Nature, 427(6971): 231-234.

Perner, D. and Platt, U., 1979. Detection of nitrous acid in the atmosphere by differential optical absorption. Geophysical Research Letters, 6(12): 917-920.

Perry, A.H. and Symons, L., 1991. Highway meteorology. Taylor & Francis.

Perry, K.D., 1999. Effects of outdoor pyrotechnic displays on the regional air quality of Western Washington State. Journal of the Air & Waste Management Association, 49(2): 146-155.

Pitchford, M., Tombach, I., Barna, M., Gebhart, K., Green, M., Knipping, E., Kumar, N., Malm, W., Pun, B. and Schichtel, B., 2004. Big bend regional aerosol and visibility observational study (BRAVO); final report. US Environmental Protection Agency Region VI, Dallas, TX.

Poirot, R.L. and Wishinski, P.R., 1986. Visibility, sulfate and air mass history associated with the summertime aerosol in northern Vermont. Atmospheric Environment (1967), 20(7): 1457-1469.

Pope, F.D., Dennis-Smither, B.J., Griffiths, P.T., Clegg, S.L. and Cox, R.A., 2010. Studies of single aerosol particles containing malonic acid, glutaric acid, and their mixtures with sodium chloride. I. Hygroscopic growth. The Journal of Physical Chemistry A, 114(16): 5335-5341.

Pope III, C.A., Burnett, R.T., Thun, M.J., Calle, E.E., Krewski, D., Ito, K. and Thurston, G.D., 2002. Lung cancer, cardiopulmonary mortality, and long-term exposure to fine particulate air pollution. Jama, 287(9): 1132-1141.

Pope III, C.A. and Dockery, D.W., 2006. Health effects of fine particulate air pollution: lines that connect. Journal of the air & waste management association, 56(6): 709-742.

Pöschl, U., 2005. Atmospheric aerosols: composition, transformation, climate and health effects. Angewandte Chemie International Edition, 44(46): 7520-7540.

Pozzoli, L., Bey, I., Rast, S., Schultz, M., Stier, P. and Feichter, J., 2008. Trace gas and aerosol interactions in the fully coupled model of aerosol-chemistry-climate ECHAM5-HAMMOZ: 2. Impact of heterogeneous chemistry on the global aerosol distributions. Journal of Geophysical Research: Atmospheres, 113(D7).

Prentice, R.A., 2010. Aviation Weather Services Handbook. Skyhorse Publishing Inc.

Prince, A.P., Wade, J., Grassian, V., Kleiber, P. and Young, M., 2002. Heterogeneous reactions of soot aerosols with nitrogen dioxide and nitric acid: atmospheric chamber and Knudsen cell studies. Atmospheric Environment, 36(36): 5729-5740.

Public Health, 2014. The Plymouth Report 2014, Public Health, Office of the Director of Public Health, Plymouth City Council, Windsor House, Plymouth.

Pusede, S., Gentner, D., Wooldridge, P., Browne, E., Rollins, A., Min, K.-E., Russell, A., Thomas, J., Zhang, L. and Brune, W., 2014. On the temperature dependence of organic reactivity, nitrogen oxides, ozone production, and the impact of emission controls in San Joaquin Valley, California. Atmospheric Chemistry and Physics, 14(7): 3373-3395.

Pyatt, F. and Haywood, W., 1989. Air borne particulate distributions and their accumulation in tree canopies, Nottingham, UK. Environmentalist, 9(4): 291-298.

Qin, M., Xie, P., Su, H., Gu, J., Peng, F., Li, S., Zeng, L., Liu, J., Liu, W. and Zhang, Y., 2009. An observational study of the HONO–NO 2 coupling at an urban site in Guangzhou City, South China. Atmospheric Environment, 43(36): 5731-5742.

Raes, F., Van Dingenen, R., Vignati, E., Wilson, J., Putaud, J.-P., Seinfeld, J.H. and Adams, P., 2000. Formation and cycling of aerosols in the global troposphere. Atmospheric environment, 34(25): 4215-4240.

RAF, 2014. A Report on an environmental noise survey of aircraft activity at RAF Leuchars, Occupational and Environmental Medicine Wing, Noise and Vibration Division, Royal Air Force Centre of Aviation Medicine Leuchars

Ramanathan, V., Crutzen, P., Kiehl, J. and Rosenfeld, D., 2001. Aerosols, climate, and the hydrological cycle. science, 294(5549): 2119-2124.

Rappenglück, B., Ackermann, L., Alvarez, S., Golovko, J., Buhr, M., Field, R., Soltis, J., Montague, D.C., Hauze, B. and Adamson, S., 2014. Strong wintertime ozone events in the Upper Green River basin, Wyoming. Atmospheric Chemistry and Physics, 14(10): 4909-4934.

Rappenglück, B., Lubertino, G., Alvarez, S., Golovko, J., Czader, B. and Ackermann, L., 2013. Radical precursors and related species from traffic as observed and modeled at an urban highway junction. Journal of the Air & Waste Management Association, 63(11): 1270-1286.

Ravindra, K., Mittal, A.K. and Van Grieken, R., 2001. Health risk assessment of urban suspended particulate matter with special reference to polycyclic aromatic hydrocarbons: a review. Reviews on environmental health, 16(3): 169-189.

Ravindra, K., Mor, S. and Kaushik, C., 2003. Short-term variation in air quality associated with firework events: A case study. Journal of Environmental Monitoring, 5(2): 260-264.

Ren, X., Gao, H., Zhou, X., Crounse, J., Wennberg, P., Browne, E., LaFranchi, B., Cohen, R., McKay, M. and Goldstein, A., 2010. Measurement of atmospheric nitrous acid at Bodgett Forest during BEARPEX2007. Atmospheric Chemistry and Physics, 10(13): 6283-6294.

Ren, X., Harder, H., Martinez, M., Lesher, R.L., Oliger, A., Simpas, J.B., Brune, W.H., Schwab, J.J., Demerjian, K.L. and He, Y., 2003. OH and HO 2 chemistry in the urban atmosphere of New York City. Atmospheric Environment, 37(26): 3639-3651.

Ren, X., Sanders, J., Rajendran, A., Weber, R., Goldstein, A., Pusede, S., Browne, E., Min, K.-E. and Cohen, R., 2011. A relaxed eddy accumulation system for measuring vertical fluxes of nitrous acid. Atmospheric Measurement Techniques, 4(10): 2093-2103.

Renner, E., Schröder, W., Theiss, D. and Wolke, R., 2004. The Black Triangle Area–Fit for Europe?, Air Pollution Modeling and Its Application XV. Springer, pp. 515-516.

Rhodes, C., 2016. Tourism: statistics and policy. 06022, House of Commons Library.

Roach, W., 1994. Back to basics: Fog: Part 1—Definitions and basic physics. Weather, 49(12): 411-415.

Roberts, J.M., Veres, P., Warneke, C., Neuman, J., Washenfelder, R., Brown, S., Baasandorj, M., Burkholder, J., Burling, I. and Johnson, T.J., 2010. Measurement of HONO, HNCO, and other inorganic acids by negative-ion

proton-transfer chemical-ionization mass spectrometry (NI-PT-CIMS): Application to biomass burning emissions. Atmospheric Measurement Techniques, 3: 981.

Roberts, J.W. and Dickey, P., 1995. Exposure of children to pollutants in house dust and indoor air, Reviews of environmental contamination and toxicology. Springer, pp. 59-78.

Rose, M., 2014. Report on Prevent future deaths (1) in category of Road (Highways Safety) related deaths. Ref. 2014–0654, Courts and Tribunals Judiciary.

Rosenfeld, J., 1996. Cars vs. the weather: a century of progress. Weatherwise, 49(5): 14-23.

Saha, U., Talukdar, S., Jana, S. and Maitra, A., 2014. Effects of air pollution on meteorological parameters during Deepawali festival over an Indian urban metropolis. Atmospheric Environment, 98: 530-539.

Samoli, E., Atkinson, R.W., Analitis, A., Fuller, G.W., Beddows, D., Green, D.C., Mudway, I.S., Harrison, R.M., Anderson, H.R. and Kelly, F.J., 2016. Differential health effects of short-term exposure to source-specific particles in London, UK. Environment International, 97: 246-253.

Sanderson, J.B., 1961. The National Smoke Abatement Society and the Clean Air Act (1956). Political Studies, 9(3): 236-253.

Sarkar, S., Khillare, P.S., Jyethi, D.S., Hasan, A. and Parween, M., 2010. Chemical speciation of respirable suspended particulate matter during a major firework festival in India. Journal of Hazardous Materials, 184(1): 321-330.

Satheesh, S. and Srinivasan, J., 2006. A method to estimate aerosol radiative forcing from spectral optical depths. Journal of the atmospheric sciences, 63(3): 1082-1092.

Sati, A.P. and Mohan, M., 2014. Analysis of air pollution during a severe smog episode of November 2012 and the Diwali Festival over Delhi, India. International Journal of Remote Sensing, 35(19): 6940-6954.

Schichtel, B.A., Gebhart, K.A., Malm, W.C., Barna, M.G., Pitchford, M.L., Knipping, E.M. and Tombach, I.H., 2005. Reconciliation and Interpretation of Big Bend National Park Particulate Sulfur Source Apportionment: Results from the Big Bend Regional Aerosol and Visibility Observational Study—Part I. Journal of the Air & Waste Management Association, 55(11): 1709-1725.

Schichtel, B.A., Husar, R.B., Falke, S.R. and Wilson, W.E., 2001. Haze trends over the United States, 1980–1995. Atmospheric Environment, 35(30): 5205-5210.

Schmid, P., Bogdal, C., Wang, Z., Azara, V., Haag, R. and von Arx, U., 2014. Releases of chlorobenzenes, chlorophenols and dioxins during fireworks. Chemosphere, 114: 158-164.

Schroeter, J.D., Musante, C.J., Hwang, D., Burton, R., Guilmette, R. and Martonen, T.B., 2001. Hygroscopic growth and deposition of inhaled secondary cigarette smoke in human nasal pathways. Aerosol Science & Technology, 34(1): 137-143.

Seibert, P., Beyrich, F., Gryning, S.-E., Joffre, S., Rasmussen, A. and Tercier, P., 2000. Review and intercomparison of operational methods for the determination of the mixing height. Atmospheric environment, 34(7): 1001-1027.

Seidel, D.J. and Birnbaum, A.N., 2015. Effects of Independence Day fireworks on atmospheric concentrations of fine particulate matter in the United States. Atmospheric Environment, 115: 192-198.

Seinfeld, J. and Pandis, S., 1998. Atmospheric chemistry and physics. J. Wiley Interscience, New York.

Seinfeld, J.H., Pandis, S.N. and Noone, K., 1998. Atmospheric chemistry and physics: from air pollution to climate change. AIP.

Semb, A., 2001. 10. Sulphur dioxide: from protection of human lungs to remote lake restoration. Late lessons from early warnings: the precautionary principle 1896–2000: 101.

Sequeira, R. and Lai, K.-H., 1998. The effect of meteorological parameters and aerosol constituents on visibility in urban Hong Kong. Atmospheric Environment, 32(16): 2865-2871.

Shepard, D., 1968. A two-dimensional interpolation function for irregularly-spaced data, Proceedings of the 1968 23rd ACM national conference. ACM, pp. 517-524.

Shi, Y., Zhang, N., Gao, J., Li, X. and Cai, Y., 2011. Effect of fireworks display on perchlorate in air aerosols during the Spring Festival. Atmospheric Environment, 45(6): 1323-1327.

Siddiqui, N., Chu, X. and Guttenplan, M., 2006. Crossing locations, light conditions, and pedestrian injury severity. Transportation Research Record: Journal of the Transportation Research Board(1982): 141-149.

Simpson, W.T., 2007. Importance of relative humidity and temperature control in conditioning wood products. Wood and Fiber Science, 14(2): 94-103.

Singh, A., Bloss, W.J. and Pope, F.D., 2015. Remember, remember the 5th of November; gunpowder, particles and smog. Weather, 70(11): 320-324.

Singh, A., Bloss, W.J. and Pope, F.D., 2017. 60 years of UK visibility measurements: impact of meteorology and atmospheric pollutants on visibility. Atmospheric Chemistry and Physics, 17(3): 2085-2101.

Singh, A. and Dey, S., 2012. Influence of aerosol composition on visibility in megacity Delhi. Atmospheric Environment, 62: 367-373.

Singh, D.V., Sharma, Y.R. and Azad, R.V., 2005. Visual outcome after fireworks injuries. Journal of Trauma and Acute Care Surgery, 59(1): 109-111.

Singh, T., Khillare, P., Shridhar, V. and Agarwal, T., 2008. Visibility impairing aerosols in the urban atmosphere of Delhi. Environmental monitoring and assessment, 141(1-3): 67-77.

Sisler, J.F. and Malm, W.C., 1994. The relative importance of soluble aerosols to spatial and seasonal trends of impaired visibility in the United States. Atmospheric environment, 28(5): 851-862.

Sloane, C.S., 1983. Summertime visibility declines: meteorological influences. Atmospheric Environment (1967), 17(4): 763-774.

Sloane, C.S., 1984. Meteorologically adjusted air quality trends: visibility. Atmospheric Environment (1967), 18(6): 1217-1229.

Sloane, C.S. and Wolff, G.T., 1985. Prediction of ambient light scattering using a physical model responsive to relative humidity: Validation with measurements from Detroit. Atmospheric Environment (1967), 19(4): 669-680.

Soeteman, J.H., 2009. Health problems of Enschede residents in the aftermath of the fireworks disaster: a longitudinal study with a pre-disaster assessment in general practice.

Sörgel, M., Regelin, E., Bozem, H., Diesch, J., Drewnick, F., Fischer, H., Harder, H., Held, A., Hosaynali-Beygi, Z. and Martinez, M., 2011. Quantification of the

unknown HONO daytime source and its relation to NO2. Atmos. Chem. Phys, 11(20): 10433-10447.

Sorooshian, A., Murphy, S.M., Hersey, S., Bahreini, R., Jonsson, H., Flagan, R.C. and Seinfeld, J.H., 2010. Constraining the contribution of organic acids and AMS m/z 44 to the organic aerosol budget: On the importance of meteorology, aerosol hygroscopicity, and region. Geophysical Research Letters, 37(21).

Sottong John, BROOMFIELD MARK, MACCARTHY JOANNA, MISRA ANNE, THISTLETHWAITE GLEN and JOHN, W., 2015. "Global Atmosphere – Greenhouse Gases" Still Only One Earth: Progress in the 40 Years Since the First UN Conference on the Environment. Royal Society of Chemistry, 40: 34-57.

Spataro, F. and Ianniello, A., 2014. Sources of atmospheric nitrous acid: state of the science, current research needs, and future prospects. Journal of the Air & Waste Management Association, 64(11): 1232-1250.

Squizzato, S., Masiol, M., Visin, F., Canal, A., Rampazzo, G. and Pavoni, B., 2014. The PM 2.5 chemical composition in an industrial zone included in a large urban settlement: main sources and local background. Environmental Science: Processes & Impacts, 16(8): 1913-1922.

Stebbings, T., Simms, K. and Crimes, S., 1999. Air Quality Management for a Large International Airport the Experience at Heathrow, Proceedings of 2nd International Conference, pp. 81-82.

Steinhauser, G., Sterba, J.H., Foster, M., Grass, F. and Bichler, M., 2008. Heavy metals from pyrotechnics in New Years Eve snow. Atmospheric Environment, 42(37): 8616-8622.

Stemmler, K., Ammann, M., Donders, C., Kleffmann, J. and George, C., 2006. Photosensitized reduction of nitrogen dioxide on humic acid as a source of nitrous acid. Nature, 440(7081): 195-198.

Stier, P., Seinfeld, J.H., Kinne, S. and Boucher, O., 2007. Aerosol absorption and radiative forcing. Atmospheric Chemistry and Physics, 7(19): 5237-5261.

Stjern, C.W., Stohl, A. and Kristjánsson, J.E., 2011. Have aerosols affected trends in visibility and precipitation in Europe? Journal of Geophysical Research: Atmospheres, 116(D2).

Stockwell, W.R. and Calvert, J.G., 1983. The Mechanism of NO3 and HONO formation in the nighttime chemistry of the urban atmosphere. Journal of Geophysical Research: Oceans, 88(C11): 6673-6682.

Stutz, J., Alicke, B., Ackermann, R., Geyer, A., Wang, S., White, A.B., Williams, E.J., Spicer, C.W. and Fast, J.D., 2004. Relative humidity dependence of HONO chemistry in urban areas. Journal of Geophysical Research: Atmospheres, 109(D3).

Stutz, J., Alicke, B. and Neftel, A., 2002. Nitrous acid formation in the urban atmosphere: Gradient measurements of NO2 and HONO over grass in Milan, Italy. Journal of Geophysical Research: Atmospheres, 107(D22).

Su, H., Cheng, Y., Oswald, R., Behrendt, T., Trebs, I., Meixner, F.X., Andreae, M.O., Cheng, P., Zhang, Y. and Pöschl, U., 2011. Soil nitrite as a source of atmospheric HONO and OH radicals. Science, 333(6049): 1616-1618.

Su, H., Cheng, Y.F., Shao, M., Gao, D.F., Yu, Z.Y., Zeng, L.M., Slanina, J., Zhang, Y.H. and Wiedensohler, A., 2008. Nitrous acid (HONO) and its daytime sources at a rural site during the 2004 PRIDE-PRD experiment in China. Journal of Geophysical Research: Atmospheres, 113(D14).

Sullare, V.A., Khan, A.U. and Gour, B., 2013. Analysis of visibility and temperature patterns of Indian cities and it's clustering to identify the effect of presence of aerosol particles in the atmosphere, Wireless and Optical Communications Networks (WOCN), 2013 Tenth International Conference on. IEEE, pp. 1-3.

Svenningsson, B., Rissler, J., Swietlicki, E., Mircea, M., Bilde, M., Facchini, M., Decesari, S., Fuzzi, S., Zhou, J. and Mønster, J., 2006. Hygroscopic growth and critical supersaturations for mixed aerosol particles of inorganic and organic compounds of atmospheric relevance. Atmospheric Chemistry and Physics, 6(7): 1937-1952.

Svenningsson, I., Hansson, H.C., Wiedensohler, A., Ogren, J., Noone, K. and Hallberg, A., 1992. Hygroscopic growth of aerosol particles in the Po Valley. Tellus B, 44(5): 556-569.

Tang, I.N., 1996. Chemical and size effects of hygroscopic aerosols on light scattering coefficients. Journal of Geophysical Research: Atmospheres, 101(D14): 19245-19250.

Tiao, G., Box, G. and Hamming, W., 1975. Analysis of Los Angeles photochemical smog data: a statistical overview. Journal of the Air Pollution Control Association, 25(3): 260-268.

Tie, X., Brasseur, G., Emmons, L., Horowitz, L. and Kinnison, D., 2001. Effects of aerosols on tropospheric oxidants: A global model study. Journal of Geophysical Research: Atmospheres, 106(D19): 22931-22964.

Tie, X. and Cao, J., 2009. Aerosol pollution in China: Present and future impact on environment. Particuology, 7(6): 426-431.

Tie, X., Madronich, S., Walters, S., Edwards, D.P., Ginoux, P., Mahowald, N., Zhang, R., Lou, C. and Brasseur, G., 2005. Assessment of the global impact of aerosols on tropospheric oxidants. Journal of Geophysical Research: Atmospheres, 110(D3).

Titos, G., Jefferson, A., Sheridan, P., Andrews, E., Lyamani, H., Alados-Arboledas, L. and Ogren, J., 2014. Aerosol light-scattering enhancement due to water uptake during the TCAP campaign. Atmospheric Chemistry and Physics, 14(13): 7031-7043.

Tiwari, S., Payra, S., Mohan, M., Verma, S. and Bisht, D.S., 2011. Visibility degradation during foggy period due to anthropogenic urban aerosol at Delhi, India. Atmospheric Pollution Research, 2(1): 116-120.

Tiwari, S., Srivastava, A.K., Bisht, D.S., Bano, T., Singh, S., Behura, S., Srivastava, M.K., Chate, D. and Padmanabhamurty, B., 2009. Black carbon and chemical characteristics of PM10 and PM2. 5 at an urban site of North India. Journal of Atmospheric Chemistry, 62(3): 193-209.

Tong, S., Hou, S., Zhang, Y., Chu, B., Liu, Y., He, H., Zhao, P. and Ge, M., 2015. FDATMOS16 Exploring the nitrous acid (HONO) formation mechanism in winter Beijing: direct emissions and heterogeneous production in urban and suburban areas. Faraday Discussions.

Trijonis, J., 1982. Visibility in California. Journal of the Air Pollution Control Association, 32(2): 165-169.

Tsai, H.-H., Chien, L.-H., Yuan, C.-S., Lin, Y.-C., Jen, Y.-H. and Ie, I.-R., 2012. Influences of fireworks on chemical characteristics of atmospheric fine and coarse particles during Taiwan's Lantern Festival. Atmospheric environment, 62: 256-264.

Tsai, Y.I. and Cheng, M.T., 1999. Visibility and aerosol chemical compositions near the coastal area in central Taiwan. Science of the total environment, 231(1): 37-51.

UKCAA, 2011. Airport Statistics, UK Civil Aviation Authority, London.

UKMO, 1994. Handbook of Aviation Meteorology, 3rd Edition, United Kingdom Meteorological Office (UKMO), Her Majesty's Stationery Office (HMSO) London.

Van Donkelaar, A., Martin, R.V. and Park, R.J., 2006. Estimating ground-level PM2. 5 using aerosol optical depth determined from satellite remote sensing. Journal of Geophysical Research: Atmospheres, 111(D21).

Van Kamp, I., Van der Velden, P.G., Stellato, R.K., Roorda, J., Van Loon, J., Kleber, R.J., Gersons, B.B. and Lebret, E., 2006. Physical and mental health shortly after a disaster: first results from the Enschede firework disaster study. The European Journal of Public Health, 16(3): 252-258.

Vassilia, K., Eleni, P. and Dimitrios, T., 2004. Firework-related childhood injuries in Greece: a national problem. Burns, 30(2): 151-153.

Vautard, R., Yiou, P. and van Oldenborgh, G.J., 2009. Decline of fog, mist and haze in Europe over the past 30 years. Nature Geoscience, 2(2): 115-119.

Vecchi, R., Bernardoni, V., Cricchio, D., D'Alessandro, A., Fermo, P., Lucarelli, F., Nava, S., Piazzalunga, A. and Valli, G., 2008. The impact of fireworks on airborne particles. Atmospheric Environment, 42(6): 1121-1132.

Vecera, Z. and Dasgupta, P., 1994. Indoor nitrous acid levels. Production of nitrous acid from open-flame sources. International journal of environmental analytical chemistry, 56(4): 311-316.

Venkataraman, C., Reddy, C.K., Josson, S. and Reddy, M.S., 2002. Aerosol size and chemical characteristics at Mumbai, India, during the INDOEX-IFP (1999). Atmospheric Environment, 36(12): 1979-1991.

Verma, C. and Deshmukh, D.K., 2014. The ambient air and noise quality in India during diwali festival: A Review. Recent Research in Science and Technology, 6(1).

Vernon, S., 1988. Fireworks and the eye. Journal of the Royal Society of Medicine, 81(10): 569-571.

Vidal Bastías, M. and Cloutier, A., 2005. Evaluation of wood sorption models for high temperatures. Maderas. Ciencia y tecnología, 7(3): 145-158.

Villena, G., Kleffmann, J., Kurtenbach, R., Wiesen, P., Lissi, E., Rubio, M.A., Croxatto, G. and Rappenglück, B., 2011a. Vertical gradients of HONO, NO x and O 3 in Santiago de Chile. Atmospheric Environment, 45(23): 3867-3873.

Villena, G., Wiesen, P., Cantrell, C., Flocke, F., Fried, A., Hall, S., Hornbrook, R., Knapp, D., Kosciuch, E. and Mauldin, R., 2011b. Nitrous acid (HONO) during polar spring in Barrow, Alaska: A net source of OH radicals? Journal of Geophysical Research: Atmospheres, 116(D14).

Wang, J. and Ogawa, S., 2015. Effects of meteorological conditions on PM2. 5 concentrations in Nagasaki, Japan. International journal of environmental research and public health, 12(8): 9089-9101.

Wang, J., Zhang, X., Guo, J., Wang, Z. and Zhang, M., 2017. Observation of nitrous acid (HONO) in Beijing, China: Seasonal variation, nocturnal formation and daytime budget. Science of The Total Environment.

Wang, K., Dickinson, R.E. and Liang, S., 2009. Clear sky visibility has decreased over land globally from 1973 to 2007. Science, 323(5920): 1468-1470.

Wang, M., Beelen, R., Stafoggia, M., Raaschou-Nielsen, O., Andersen, Z.J., Hoffmann, B., Fischer, P., Houthuijs, D., Nieuwenhuijsen, M. and Weinmayr, G., 2014. Long-term exposure to elemental constituents of particulate matter and cardiovascular mortality in 19 European cohorts: results from the ESCAPE and TRANSPHORM projects. Environment international, 66: 97-106.

Wang, Y., Zhuang, G., Xu, C. and An, Z., 2007. The air pollution caused by the burning of fireworks during the lantern festival in Beijing. Atmospheric Environment, 41(2): 417-431.

Webster, F., 1984. The climatological station at London's Heathrow Airport. Weather, 39(10): 311-315.

Weihanl, S., Qiupengl, Z., Wenzhil, S., Chaol, L. and Jiwenz, Y., 1990. Effect of the air pollution on atmospheric visibility in Beijing~ Tianjin area. Journal of Environmental Sciences, 2(1): 75-82.

Weingartner, E., Burtscher, H. and Baltensperger, U., 1997. Hygroscopic properties of carbon and diesel soot particles. Atmospheric Environment, 31(15): 2311-2327.

Weitkamp, C., 2006. Lidar: range-resolved optical remote sensing of the atmosphere, 102. Springer Science & Business.

Whiffen, B., Delannoy, P. and Siok, S., 2004. Fog: Impact on road transportation and mitigation options, National Highway Visibility Conference, Madison, Wisconsin, USA.

White, W. and Roberts, P., 1977. On the nature and origins of visibility-reducing aerosols in the Los Angeles air basin. Atmospheric Environment (1967), 11(9): 803-812.

White, W.H., 1976. Reduction of visibility by sulphates in photochemical smog.

Whiteaker, J.R., Suess, D.T. and Prather, K.A., 2002. Effects of meteorological conditions on aerosol composition and mixing state in Bakersfield, CA. Environmental science & technology, 36(11): 2345-2353.

WHO, 2004. Road safety - Visibility, World Health Organization

WHO, 2016. WHO's Urban Ambient Air Pollution Database–Update 2016. World Health Organization, Geneva.

Wickham, H. and Wickham, M.H., 2007. The ggplot package.

Wilkins, E., 1954. Air pollution and the London fog of December, 1952. Journal of the Royal Sanitary Institute, 74(1): 1-15.

Willett, K., Dunn, R., Thorne, P., Bell, S., De Podesta, M., Parker, D., Jones, P. and Williams Jr, C., 2014. HadISDH land surface multi-variable humidity and temperature record for climate monitoring. Climate of the Past, 10(6): 1983-2006.

Williams, M., 2004. Air pollution and policy—1952–2002. Science of the total environment, 334: 15-20.

Wise, E.K., 2008. Meteorologically influenced wildfire impacts on urban particulate matter and visibility in Tucson, Arizona, USA. International journal of wildland fire, 17(2): 214-223.

Witsaman, R.J., Comstock, R.D. and Smith, G.A., 2006. Pediatric fireworks-related injuries in the United States: 1990–2003. Pediatrics, 118(1): 296-303.

WMO, 1992. International Meteorological Vocabulary, World Meteorological Organization, Geneva.

WMO, 2008. Guide to Meteorological Instruments and Methods of Observation, 7th edition, World Meteorological Organization, Geneva.

WMO, 2015. Manual on the Global Observing System, Volume I – Global Aspects, World Meteorological Organization, WMO-No. 544, Geneva.

Wojtal, P., Halla, J. and McLaren, R., 2011. Pseudo steady states of HONO measured in the nocturnal marine boundary layer: a conceptual model for HONO formation on aqueous surfaces. Atmospheric Chemistry and Physics, 11(7): 3243-3261.

Wong, K., Tsai, C., Lefer, B., Haman, C., Grossberg, N., Brune, W., Ren, X., Luke, W. and Stutz, J., 2012. Daytime HONO vertical gradients during SHARP 2009 in Houston, TX. Atmospheric Chemistry and Physics, 12(2): 635-652.

Wu, D., Tie, X., Li, C., Ying, Z., Lau, A.K.-H., Huang, J., Deng, X. and Bi, X., 2005. An extremely low visibility event over the Guangzhou region: A case study. Atmospheric Environment, 39(35): 6568-6577.

Wu, J., Fu, C., Zhang, L. and Tang, J., 2012. Trends of visibility on sunny days in China in the recent 50 years. Atmospheric environment, 55: 339-346.

Xiaoye, Z., 2007. Aerosol over China and their climate effect. Adv. Earth Sci, 22(1): 12-16.

Xu, Z., Wang, T., Wu, J., Xue, L., Chan, J., Zha, Q., Zhou, S., Louie, P.K. and Luk, C.W., 2015. Nitrous acid (HONO) in a polluted subtropical atmosphere: Seasonal variability, direct vehicle emissions and heterogeneous production at ground surface. Atmospheric Environment, 106: 100-109.

Yang, L.-x., Wang, D.-c., Cheng, S.-h., Wang, Z., Zhou, Y., Zhou, X.-h. and Wang, W.-x., 2007. Influence of meteorological conditions and particulate matter on visual range impairment in Jinan, China. Science of the Total Environment, 383(1): 164-173.

Yang, L., Zhou, X., Wang, Z., Zhou, Y., Cheng, S., Xu, P., Gao, X., Nie, W., Wang, X. and Wang, W., 2012. Airborne fine particulate pollution in Jinan, China: concentrations, chemical compositions and influence on visibility impairment. Atmospheric environment, 55: 506-514.

Ye, B., Ji, X., Yang, H., Yao, X., Chan, C.K., Cadle, S.H., Chan, T. and Mulawa, P.A., 2003. Concentration and chemical composition of PM 2.5 in Shanghai for a 1-year period. Atmospheric Environment, 37(4): 499-510.

Yerramsetti, V.S., Sharma, A.R., Navlur, N.G., Rapolu, V., Dhulipala, N.C. and Sinha, P., 2013. The impact assessment of Diwali fireworks emissions on the air quality of a tropical urban site, Hyderabad, India, during three consecutive years. Environmental monitoring and assessment, 185(9): 7309-7325.

Yokelson, R.J., Crounse, J., DeCarlo, P., Karl, T., Urbanski, S., Atlas, E., Campos, T., Shinozuka, Y., Kasputin, V. and Clarke, A., 2009. Emissions from biomass burning in the Yucatan. Atmospheric Chemistry and Physics, 9: 5785.

Yu, Y., Galle, B., Panday, A., Hodson, E., Prinn, R. and Wang, S., 2009. Observations of high rates of NO 2-HONO conversion in the nocturnal atmospheric boundary layer in Kathmandu, Nepal. Atmospheric Chemistry and Physics, 9(17): 6401-6415.

Yuan, C.-S., Lee, C.-G., Liu, S.-H., Chang, J.-c., Yuan, C. and Yang, H.-Y., 2006. Correlation of atmospheric visibility with chemical composition of Kaohsiung aerosols. Atmospheric Research, 82(3): 663-679.

Zhang, M., Wang, X., Chen, J., Cheng, T., Wang, T., Yang, X., Gong, Y., Geng, F. and Chen, C., 2010. Physical characterization of aerosol particles during the Chinese New Year's firework events. Atmospheric Environment, 44(39): 5191-5198.

Zhang, Q., Quan, J., Tie, X., Li, X., Liu, Q., Gao, Y. and Zhao, D., 2015. Effects of meteorology and secondary particle formation on visibility during heavy haze events in Beijing, China. Science of the Total Environment, 502: 578-584.

Zhang, R., Tie, X. and Bond, D.W., 2003. Impacts of anthropogenic and natural NOx sources over the US on tropospheric chemistry. Proceedings of the National Academy of Sciences, 100(4): 1505-1509.

Zhang, Y.-h., Shao, M. and Cheng, C.-l., 2006. Quantitative relationship between visibility and mass concentration of PM2. 5 in Beijing. Journal of Environmental Sciences, 18(3): 475-481.

Zhao, H., Che, H., Zhang, X., Ma, Y., Wang, Y., Wang, H. and Wang, Y., 2013. Characteristics of visibility and particulate matter (PM) in an urban area of Northeast China. Atmospheric Pollution Research, 4(4): 427-434.

Zhao, P., Zhang, X., Xu, X. and Zhao, X., 2011. Long-term visibility trends and characteristics in the region of Beijing, Tianjin, and Hebei, China. Atmospheric Research, 101(3): 711-718.

Zhou, X., Civerolo, K., Dai, H., Huang, G., Schwab, J. and Demerjian, K., 2002. Summertime nitrous acid chemistry in the atmospheric boundary layer at a rural site in New York State. Journal of Geophysical Research: Atmospheres, 107(D21).

Zhou, X., Gao, H., He, Y., Huang, G., Bertman, S.B., Civerolo, K. and Schwab, J., 2003. Nitric acid photolysis on surfaces in low-NOx environments: Significant atmospheric implications. Geophysical Research Letters, 30(23).

List of published peer reviewed journal papers, short articles, conference presentations, talks and media coverages during PhD study

Peer reviewed papers (Published)

1. Ilyinskay E., Schmidt A., Mather T.A., Pope f., Witham c., Baxter P.J., Johansson t., Barsotti S., Pfeffer M., **Singh A.,** Sanderson P., Bergsson B., Kilbride B.M., Donovan A., Peters N.J., Oppenheimer c., and Edmonds M., **2017**, Understanding the environmental impacts of large fissure eruptions: Aerosol and gas emissions from the 2014-2015 Holuhraun eruption (Iceland), *Earth and Planetary Science Letters,* 474, 309-322.

2. **Singh, A.,** Bloss, W.J. and Pope, F.D., **2017**. 60 years of UK visibility measurements: impact of meteorology and atmospheric pollutants on visibility. *Atmospheric Chemistry and Physics*, 17(3): 2085-2101.

3. **Singh, A.,** Bloss, W.J. and Pope, F.D., **2015**. Remember, remember the 5th of November; gunpowder, particles and smog. *Weather*, 70(11): 320-324.

Peer reviewed papers (Under review)

1. **Singh, A.,** Crilley R.L., Bloss, W.J. and Pope, F.D., Measurments of HONO during 2015 solar eclipse: Insight into potential sources and sinks. *Geophysical Reaserch Letters.*

Peer reviewed papers (In preparation)

1. **Singh, A.,** Crilley R.L., Bloss, W.J. and Pope, F.D., Intercomparison of atmopsheric HONO at a number of urban background sites: insights into sources.

2. **Singh, A.,** Pant P., W.J. and Pope, F.D., Impacts of firworks associated aerosols during different festivals and celebrations: A review

Short article (Published)

1. **Singh, A., 2014.** Urban air pollution and its effect on fog occurrence: a view from Northern Indian, *ClimateSnack.*

Conference presentations and talks

1. Long-term visibility trends in the UK and India, *National Environmental Engineering Research Institute (NEERI), Government of India,* 3 Dec 2016- Invited talk

   Link:http://www.rsc.org/events/download/Document/a21ab3a2-2122-447e-8eaa-faa5de4f0e4c
2. Long-term visibility data in the UK-how does visibility vary with meteorological and pollutant parameters?, *European Geosciences Union,* 17-22 April 2016.

   Link: http://meetingorganizer.copernicus.org/EGU2016/EGU2016-874-3.pdf
3. 60 years of visibility data in the UK-how does visibility vary with meteorological and pollutant parameters?, *American Geophysical Union,* 14-18 Dec 2015.

   Link: https://agu.confex.com/agu/fm15/webprogram/Paper63394.html

4. Are aerosol particles a source of HONO in the atmosphere?, *Aerosol Society Conference,* Birmingham,12 Nov 2015.
   Link:https://aerosol-soc.com/abstracts/aerosol-particles-source-hono-atmosphere
5. Atmospheric photochemical pollution measurement during 2015 solar eclipse, *Royal Meteorological Society,* July 2015.
   Link:https://www.rmets.org/sites/default/files/event_documents/6/Master%20Abstract%20Book%20V3_0.pdf
6. Impact of changing PM concentration on UK visibility, *ACCENT Plus-2014, Urbino-Italy,* 22-29 June 2014.
7. Role of aerosol and metrological parameters in visibility change: A view from the United Kingdom, *Aerosol Society Conference, Birmingham,* 27 Dec 2014.
   Link: http://aerosol-soc.org.uk/files/AjitSingh.PodiumAbstract.AASC14.pdf
8. Long term visibility trends with effects of changing atmospheric particles and meteorological parameters over the UK, *ASCITES networking meeting,* York, 1-3 December 2014

Research in Media/News

1. The Indian Express "UK, Indian scientists investigating air-pollution causes" November 3, 2016 (**Link**)

2. University of Birmingham press "Birmingham and Indian scientists investigating air-pollution causes" November 3, 2016 (**Link**)

3. Daily mail "Fireworks can cut visibility by a QUARTER: Motorists are advised to be more alert when driving on Bonfire Night" November 6, 2015 (**Link**)

4. University of Birmingham press "Fireworks are fun but can reduce visibility" November 3, 2015 (**Link**)

5. Red brick news "No smoke without fireworks" November 5, 2015 (**Link**)

6. Science Daily "Fireworks are fun but can reduce visibility" November 2, 2015 (**Link**)

5. Nature World News "Firework and Bonfire Celebrations Reduce Visibility, Especially When Humidity Is High" November 3, 2015 (**Link**)

7. Air Quality News "Bonfire night pollution bring poor visibility warning" November 5, 2015 (**Link**)

8. Improbable Research "Diminished British Visibility Due to Guy Fawkes Night Bonfires" October 30, 2015 (**Link**)

9. EurekAlert "Fireworks are fun but can reduce visibility" November 2, 2015 (**Link**)

10. NVS24 "Fireworks are fun but can reduce visibility" November 2, 2015 (**Link**)

11. GIZMODO "Remember, Remember: There's a Downside to All Those Guy Fawkes Bonfires" November 5, 2015 (**Link**)

12. University GEES Bulletin "Remember, remember the 5th of November; gunpowder, particles and smog" Issue 276, November 6, 2015.

13. University GEES Bulletin "Air pollution measurements during the Eclipse" Issue 252, March 27, 2015.

14. University GEES Bulletin "Field campaign measuring the Holuhraun eruption plume in Iceland" Issue 246, February 6, 2015.